NASA CONTRACTOR REPORT

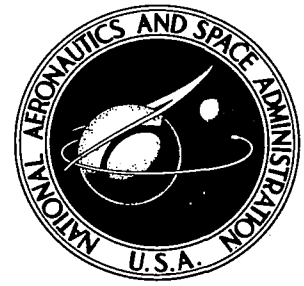

NASA CR-1750

THEORETICAL STUDY OF CORRUGATED PLATES: SHEARING OF A TRAPEZOIDALLY CORRUGATED PLATE WITH TROUGH LINES PERMITTED TO CURVE

by Chuan-jui Lin and Charles Libove

Prepared by
SYRACUSE UNIVERSITY RESEARCH INSTITUTE
Syracuse, N. Y.
for Langley Research Center

NATIONAL AERONAUTICS AND SPACE ADMINISTRATION • WASHINGTON, D. C. • DECEMBER 1971

1. Report No.	2. Government Accession No.	3. Recipient's Catalog No.
NASA CR-1750		

4. Title and Subtitle	5. Report Date
THEORETICAL STUDY OF CORRUGATED PLATES: SHEARING OF A TRAPEZOIDALLY CORRUGATED PLATE WITH TROUGH LINES PERMITTED TO CURVE	December 1971
	6. Performing Organization Code

7. Author(s)	8. Performing Organization Report No.
Chuan-jui Lin and Charles Libove	MAE 1833-T2
	10. Work Unit No. 722-02-10-03

9. Performing Organization Name and Address	11. Contract or Grant No.
Syracuse University Research Institute Department of Mechanical and Aerospace Engineering Syracuse, New York 13210	NGR 33-022-115
	13. Type of Report and Period Covered: Contractor Report

12. Sponsoring Agency Name and Address	14. Sponsoring Agency Code
National Aeronautics and Space Administration Washington, D. C. 20546	

15. Supplementary Notes

16. Abstract

A theoretical analysis is presented of the elastic shearing of a trapezoidally corrugated plate with discrete attachments at the ends of the corrugations. Numerical results on effective shear stiffness, stresses, and displacements are presented for selected geometries and end-attachment conditions. It is shown that the frame-like deformation of the cross-sections, which results from the absence of continuous end attachments, can lead to large transverse bending stresses and large reductions in shearing stiffness.

17. Key Words (Suggested by Author(s))	18. Distribution Statement
Corrugated plate Shear stress Shear deformation	Unclassified - Unlimited

19. Security Classif. (of this report)	20. Security Classif. (of this page)	21. No. of Pages	22. Price*
Unclassified	Unclassified	162	$3.00

*For sale by the National Technical Information Service, Springfield, Virginia 22151

THEORETICAL STUDY OF CORRUGATED PLATES:

SHEARING OF A TRAPEZOIDALLY CORRUGATED PLATE WITH

TROUGH LINES PERMITTED TO CURVE

By Chuan-jui Lin* and Charles Libove**
Syracuse University

SUMMARY

A theoretical analysis is presented of the elastic shearing of a trapezoidally corrugated plate with discrete attachments at the ends of the corrugations. Numerical results on effective shear stiffness, stresses, and displacements are presented for selected geometries and end-attachment conditions. It is shown that the frame-like deformation of the cross-sections, which results from the absence of continuous end attachments, can lead to large transverse bending stresses and large reductions in shearing stiffness.

INTRODUCTION

In a previous report (ref. 1) a theoretical analysis was presented of the elastic shearing of a trapezoidally corrugated plate with discrete attachment at the corrugation ends on the assumption that the trough lines (mn in fig. 1) are held straight. This assumption limited the applicability of reference 1 mainly to the case in which the corrugated plate is attached to a flat plate along its trough lines.

The present report analyzes again the elastic shearing of a trapezoidally corrugated plate but removes the assumption that the trough lines are held straight. Thus the present analysis is applicable to a corrugated plate alone, rather than to a corrugated plate which is attached to a flat plate. The removal of this constraint reduces, of course, the effective shearing stiffness and alters the nature of the stresses and displacements.

The analysis of reference 1 considered two kinds of conditions along the trough lines: (a) complete freedom of rotation and (b) complete suppression of rotation. In the present analysis only the first of these conditions is considered, as that is the only meaningful condition for a corrugated plate alone.

*NDEA Fellow

**Professor of Mechanical and Aerospace Engineering

As in reference 1, three different types of discrete attachment at the ends of the corrugation are considered. These are illustrated in figure 2 and may be described as follows:

(i) Point attachments at the ends of the trough lines only (fig. 2(a)), the attachments being considered as mathematical points, providing restraint against displacement but not against rotation.

(ii) Point attachments at the ends of both the trough lines and the crest lines (fig. 2(b)), the attachments again being considered as mathematical points.

(iii) Very wide attachments at the ends of the trough lines only, as shown in figure 2(c). This kind of attachment is approximated in the analysis by means of the idealization shown in figure 2(d), i.e. by adding, to the end constraints of figure 2(a), end constraints against vertical displacement (but not against longitudinal displacement) at the junctions of the trough plate elements and the adjacent sloping plate elements.

In cases (i) and (ii) no consideration is given to the possibility that the member to which a corrugation end is attached will interfere with the deformation of the corrugation.

The analysis is based on the method of stationary total potential energy. Each cross section is assumed to have certain degrees of freedom for deformation in and out of the plane of the cross section. By equating to zero the first variation of the total potential energy, differential equations and boundary conditions are obtained for these degrees of freedom as functions of the longitudinal coordinate (z in fig. 1). Solution of these equations leads to all the desired information.

Numerical results on shearing stiffness, stresses and deformations for selected families of geometries are presented and discussed.

SYMBOLS

A_{11}, A_{12}, etc.	defined by equations (13b)
$\bar{A}_1$, $\bar{A}_3$	coefficients in the displacement equations (C39)
$\bar{\bar{A}}_1$, $\bar{\bar{A}}_4$, $\bar{\bar{A}}_5$, $\bar{\bar{A}}_8$	coefficients in equations (B50a) through (B50e) for displacements; obtained by solving equations (B52), (B53) or (B54), depending on the type of attachments at the ends of the corrugations
A_1^*, A_3^*, A_5^*, A_7^*	coefficients in equations (B42) for displacements
$\tilde{A}_1$, $\tilde{A}_4$, $\tilde{A}_5$, $\tilde{A}_8$	defined by the first four of equations (30)
$\tilde{A}_1'$, $\tilde{A}_2'$, $\tilde{A}_3'$, $\tilde{A}_4'$	coefficients in equations (C33) for displacements
$\tilde{A}_6'$	coefficient in displacement equation (C39)
$\tilde{A}_{11}$, $\tilde{A}_{22}$, $\tilde{A}_{12}$	defined by equations (C8b)
a_1, a_2, a_3	defined by equations (40)
a_{11}, a_{12}, a_{22}	coefficients in expression for U_b (see eqs. (11) and (12))
$\hat{a}$	defined by equation (B7)
a_{11}^*, a_{12}^*, a_{22}^*	defined by equations (B25)
$\tilde{a}_{11}$, $\tilde{a}_{12}$, $\tilde{a}_{22}$	defined by equations (C7)
a_{22}'	defined by the first of equations (C14)
$\tilde{a}_{22}^*$	defined by the first of equations (C22)
$\bar{a}_{22}$	defined by equation (D6)
$\bar{a}_{22}^*$	defined by the first of equations (D17)
B_j/A_j (j=1,2,..,8)	obtained by solving equations (B23)
B_1^*, B_3^*	coefficients in equations (D34) for displacements
$\hat{B}_6$	coefficient in equations (D34) for displacements

b	one-half the length of the corrugations (see fig. 1(b))
b_1, b_2, b_3	defined by equations (40)
b_{11}, b_{12}, b_{22}	coefficients in expression for U_{ext} (see eqs. (2) and (3))
$\hat{b}$	defined by equation (B7)
b^*_{11}, b^*_{12}, b^*_{22}	defined by equations (B26)
C_j/A_j $(j=1,2,\ldots,8)$	obtained by solving equations (B23)
c	characteristic length (taken as pitch p in numerical work)
c_{00}, c_{01}, etc.	coefficients in expression for U_{sh} (see eqs. (5) and (6a))
$\hat{c}$	defined by equation (B7)
c^*_{11}, c^*_{12}, c^*_{22}	defined by equations (B27)
c_U, c_X	defined by equations (32)
$\hat{c}_v$, $\hat{c}_y$	defined by equations (B60)
$\bar{c}_{00} = Gt/k$	
D	frame flexural stiffness; see equation (14)
D_j/A_j $(j=1,2,\ldots,8)$	obtained by solving equations (B23)
$\hat{D}_j/\hat{B}_j$ $(j=1,2,3,4)$	defined by equations (D23) and (D24)
$\tilde{D}'_j/\tilde{A}'_j$ $(j=1,2,3,4)$	defined by equations (C28) and (C29)
d_{00}, d_{11}, etc.	coefficients in expression for U_{sh} (see eqs. (5) and (6b))
d^*_{10}, d^*_{11}, d^*_{21}, etc.	defined by equations (B28)

$\tilde{d}_{11}$, $\tilde{d}_{21}$	defined by equations (B62)
$\hat{d}_1$, $\hat{d}_2$, etc.	defined by equations (B8)
E	Young's modulus associated with frame bending of the cross sections
E'	Young's modulus associated with longitudinal extension
E_{10}	coefficient in equations (B42), (B50a), (B50b) and (B50e) for displacements
$\tilde{E}_{10}$	defined by the last of equations (30)
e	one-half the width of the trough plate element (see fig. 1(a))
e_{00}, e_{11}, etc.	defined by equations (A2)
$\bar{e}_{11}$, $\bar{e}_{12}$, $\bar{e}_{22}$	coefficients in expression for U_{tw} (see eqs. (9) and (10))
e^*_{00}, e^*_{11}, etc.	coefficient in expression for U_{sh} (see eqs. (5) and (6c))
$\hat{e}$	defined by equation (B7)
$\hat{e}_{00}$	defined by equation (D5)
$\bar{e}^*_{11}$, $\bar{e}^*_{12}$, $\bar{e}^*_{22}$	defined by equations (B30)
e^{**}_{00}, e^{**}_{11}, etc.	defined by equations (B29)
$\hat{e}^{**}_{00}$	defined by equation (D17)
$\tilde{e}_{11}$, $\tilde{e}_{12}$, $\tilde{e}_{22}$, $\tilde{e}_{10}$, $\tilde{e}_{20}$	defined by equations (B62)
e''_{11}, e''_{12}, e''_{22}	defined by equations (C6)
$\tilde{e}'_{00}$, $\tilde{e}'_{10}$, $\tilde{e}'_{11}$, $\tilde{e}'_{12}$, $\tilde{e}'_{22}$	defined by equations (C10)
e'_{22}	defined by equation (C14)

$\tilde{e}^*_{00}$, $\tilde{e}^*_{10}$, $\tilde{e}^*_{22}$	defined by equations (C22)
F	shear force (see fig. 1(b))
f	width of the crest plate element (see fig. 1(a))
$\hat{f}$	defined by equation (B7)
$\bar{f}_{ss}$, $\bar{f}_{sc}$, etc.	functions of z defined by equations (31)
$\tilde{f}_{ss}$, $\tilde{f}_{sc}$, etc.	functions of z defined by equations (31)
G	shear modulus associated with middle surface shear of the plate elements
G'	shear modulus associated with torsion of the plate elements
g_{21}, g_{22}, g_{31}, g_{32}	defined by equations (39)
$\hat{g}$	defined by equation (B7)
h	height of corrugation (see fig. 1(a))
$\hat{h}$	defined by equation (B7)
$i = \sqrt{-1}$	
J_1, J_2, J_3	torsion constants of plate elements 01, 12, 23 respectively (see eqs. (7) and (8))
$\hat{j}$	defined by equation (B7)
k	width of the inclined plate element (see fig. 1(a))
k_0, k_2, etc.	coefficients in characteristic equations (B12) and (B20); defined by equations (B13)
$\hat{k}$	defined by equation (B7)
$\tilde{k}_{02}$, $\tilde{k}_{20}$, etc.	defined by equations (C21)
$\hat{k}_{02}$, $\hat{k}_{20}$, etc.	defined by equations (D16)

L_{11}, L_{12}, etc.	defined by equations (B24)
$\tilde{L}_{11}$, $\tilde{L}_{12}$, etc.	defined by equations (C27)
$\hat{L}_{11}$, $\hat{L}_{12}$, etc.	defined by equations (D22)
$\hat{m}$	defined by equation (B7)
N_4, N_5	defined by equations (B56)
N_{11}, N_{12}, etc.	defined by equations (B55a) through (B55d)
$\overline{N}_5$	defined by equation (B58)
$\overline{N}_{41}$, $\overline{N}_{42}$, $\overline{N}_{43}$, $\overline{N}_{44}$	defined by equations (B57a)
$\overline{N}_{51}$, $\overline{N}_{52}$, $\overline{N}_{53}$, $\overline{N}_{54}$, $\overline{N}_{55}$	defined by equations (B57b)
$\overline{\overline{N}}_{41}$, $\overline{\overline{N}}_{42}$, $\overline{\overline{N}}_{43}$, $\overline{\overline{N}}_{44}$	defined by equations (B59)
$\hat{n}_1$, $\hat{n}_2$, $\hat{n}_3$, $\hat{n}_4$	defined by equations (B9)
P^B, P^C, P^D, P^E	real numbers defined by equations (B46) through (B49); obtained by solving equations (B23) with j = 1 and 5 and noting equations (B31)
P_3	defined by equation (C41b)
P_{11}, P_{12}, etc.	defined by equations (C41a)
p	pitch of corrugation (see fig. 1(a))
p'	developed width of one corrugation, 2e + 2k + f
$\hat{p}_1$, $\hat{p}_2$, ..., $\hat{p}_8$	defined by equations (B10)
Q^B, Q^C, Q^D, Q^E	real numbers defined by equations (B46) through (B49); obtained by solving equations (B23) with j = 1 and 5 and noting equations (B31)
Q^3	defined by equation (D37)
Q_{11}, Q_{12}, etc.	defined by equations (D36)

$\hat{q}_1, \hat{q}_2, \hat{q}_3, \hat{q}_4$	defined by equations (B11)
R	variable in characteristic equation (B20)
$R_j (j=1,2,\ldots,10)$	roots of characteristic equation (B20)
R_1^*	complex conjugate of R_1
R_5^*	complex conjugate of R_5
$\tilde{R}$	variable in characteristic equation (C19)
$\tilde{R}_j (j=1,2,\ldots,6)$	roots of characteristic equation (C19)
$\hat{R}$	variable in characteristic equation (D14)
$\hat{R}_j (j=1,2,\ldots,6)$	roots of characteristic equation (D14)
$r \equiv R/c$	variable in characteristic equation (B12)
$r_j \equiv R_j/c \ (j=1,2,\ldots,10)$	
$\tilde{r} = \tilde{R}/c$	
$\hat{r} = \hat{R}/c$	
S^B, S^C, S^D, S^E	real numbers defined by equations (B46) through (B49); obtained by solving equations (B23) with $j = 1$ and 5 and noting equations (B31)
s_1, s_2, s_3	transverse coordinates along the cross-sectional centerline (see fig. 3(a))
Ω_{sv}, Ω_{sy}	defined by equations (B60)
TPE	total potential energy of a single corrugation
T^B, T^C, T^D, T^E	real numbers defined by equations (B46) through (B49); obtained by solving equations (B23) with $j = 1$ and 5 and noting equations (B31)
t	thickness of corrugation (see fig. 1(a))
Ω_{tu}, Ω_{tx}	defined by equations (B60)

U	strain energy of an entire corrugation (see eq. (15)); also real part of R_1 and R_2 when R_1 and R_2 are complex (see eqs. (B44))
U_b	strain energy per unit length of corrugation associated with frame bending of the cross sections (see eq. (11))
U_{ext}	strain energy per unit length of corrugation associated with longitudinal extension (see eq. (2))
U_{sh}	strain energy per unit length of corrugation associated with middle surface shear (see eq. (5))
U_{tw}	strain energy per unit length of corrugation associated with torsion (see eq. (9))
u	longitudinal displacement
u_0	one-half the relative shearing displacement of two adjacent trough lines (see fig. 3(b))
u_1	longitudinal displacement (function of z) along junction line (1) (see fig. 3(b))
u_2	longitudinal displacement (function of z) along junction line (2) (see fig. 3(b))
V	imaginary part of R_1, negative of imaginary part of R_2 when R_1 and R_2 are complex (see eqs. (B44))
$\tilde{V}_0$, $\tilde{V}_1$, $\tilde{V}_2$	functions of z defined by equations (33)
v_0, v_1, v_2	parameters defining the deformation of the cross section in its own plane (functions of z) (see fig. 3(c))
W	function of z defined by equation (C48)
$\overline{W}$	function of z defined by equation (D44)
X	real part of R_5 and R_6 when R_5 and R_6 are complex (see eqs. (B44))

x	transverse coordinate (see fig. 1(b))
Y	imaginary part of R_5, negative of imaginary part of R_6 when R_5 and R_6 are complex (see eqs. (B44))
z	longitudinal coordinate (see fig. 1(b))
α_1^B, α_2^B, etc.	defined by equations (B61)
β	defined by equation (13a)
β_1^C, β_2^C, etc.	defined by equations (B61)
β_1^D, β_2^D, etc.	defined by equations (B61)
β_1^E, β_2^E, etc.	defined by equations (B61)
$\tilde{\beta}$	defined by equation (C8a)
γ	shear strain
γ_1, γ_2, γ_3	shear strain in plate elements 01, 12, 23 respectively
$\gamma_j^B = B_j/A_j$ $\gamma_j^C = C_j/A_j$ $\gamma_j^D = D_j/A_j$ $\gamma_j^E = E_j/A_j$	computed from equation (B23) and (B32); representable by equations (B46) through (B49) when R_1, R_2, ..., R_8 are complex
γ_1^{B*}, γ_1^{C*}, γ_1^{D*}, γ_1^{E*}	complex conjugates of γ_1^B, γ_1^C, γ_1^D, γ_1^E respectively
γ_5^{B*}, γ_5^{C*}, γ_5^{D*}, γ_5^{E*}	complex conjugates of γ_5^B, γ_5^C, γ_5^D, γ_5^E respectively
$\tilde{\gamma}_j^D$, $\tilde{\gamma}_j^E$ (j=1,2,3,4)	defined by equations (C29)
$\hat{\gamma}_j^D$, $\hat{\gamma}_j^E$ (j=1,2,3,4)	defined by equations (D24)
ε	longitudinal strain
ε_1, ε_2, ε_3	longitudinal strain in plate elements 01, 12, 23 respectively

ζ_1, ζ_2	defined by equations (B2)
θ	angle between sides of corrugation and horizontal (see fig. 1(a))
λ_1, λ_2, ..., λ_{21}	defined by equations (B14) through (B18)
ν	Poisson's ratio, taken as .3 for numerical work
ξ_1, ξ_2	defined by equations (B40)
$\overline{\xi}$	defined by equation (C37)
$\hat{\xi}$	defined by equation (D32)
σ	cross-sectional normal stress
$\sigma_{①}$, $\sigma_{②}$	cross-sectional normal stresses (functions of z) along junctions ① and ② respectively
$\sigma'_{①}$, $\sigma'_{②}$	extreme-fiber bending stresses (functions of z) at junctions ① and ② respectively, resulting from frame bending of the cross sections
τ	middle-surface shear stress
τ_{01}, τ_{12}, τ_{23}	middle-surface shear stresses in plate elements 01, 12, 23 respectively
τ'_{01}, τ'_{12}, τ'_{23}	extreme-fiber shear stresses due to twisting of the plate elements 01, 12, 23 respectively
ϕ	rate of twist
ϕ_1, ϕ_2, ϕ_3	rate of twist of plate elements 01, 12, 23 respectively
ψ	factor in shear-stiffness equations (29) and (B63a); defined by equation (B63b)
$\tilde{\psi}$	factor in equation (C42) for shear stiffness; defined by equation (C43)
$\hat{\psi}$	factor in equation (D38) for shear stiffness; defined by equation (D39)
Ω	relative shearing stiffness, i.e. the ratio of shear stiffness of the actual corrugation to that of an identical corrugation with uniform middle-surface shear strain

ANALYSIS

The plate is assumed to be composed of infinitely many identical corrugations, all deforming in an identical way, and the analysis may therefore be based on a single corrugation. The form of the corrugation is shown in figure 1. A single corrugation is considered to be that portion between adjacent trough lines (lines labeled mn in fig. 1). The numbering system for the salient points of the cross section of a single corrugation is shown in figure 3(a). The notation for the geometry of the corrugation and coordinate systems is shown in figures 1 and 3(a).

Considering a single corrugation, the shearing of this corrugation is imagined to be effected by a longitudinal shift of the trough line at station ⓪ through a distance u_0 in the positive-z direction and a similar shift of the trough line at station ⑤ in the negative-z direction, as shown in figure 3(b). Thus the total shearing displacement of one trough line with respect to the other is $2u_0$. The end-points of the trough lines (points m and n in fig. 1) are moved only longitudinally. However, the rest of the points of a trough line are permitted to move both longitudinally and laterally, subject to certain constraints arising from the symmetry of the corrugation with respect to a vertical plane through the crest line (m'n' in fig. 1), the antisymmetry of the imposed displacements with respect to this plane, the requirement of continuity between adjacent corrugations, and the requirement that all corrugations deform identically. These considerations and requirements lead to the following constraints on the deformations of the trough lines:

(a) The longitudinal strain is zero everywhere along a trough line.

(b) The vertical displacement is zero everywhere along a trough line.

(c) The trough lines at stations ⓪ and ⑤ curve into identical shapes.

Certain deductions can also be made regarding the mutual internal reaction acting along the common trough line between two adjacent corrugations. These lead to the conclusion that, while there are an unknown longitudinal shear flow distribution and an unknown vertical shear distribution along the trough lines at stations ⓪ and ⑤, there is no horizontal running tension nor any bending moment transferred from one corrugation to the next across a trough line.

Figure 4 shows schematically the type of linkage system that can be imagined to exist along the edges of an isolated corrugation in order that the isolated corrugation satisfy the above conditions and represent a single one of the infinitely many corrugations of the corrugated plate.

Assumption regarding longitudinal displacements. - The longitudinal (z-wise) displacements at stations ⓪ and ⑤ of any cross section are $+u_0$ and $-u_0$, as already discussed. The longitudinal displacements of the other middle-surface points of the cross section are assumed to

vary linearly between stations. These longitudinal displacements are shown in figure 3(b), which also shows their assumed antisymmetrical nature consistent with the antisymmetrical nature of the presecribed displacements at stations ⓪ and ⑤ . Therefore the longitudinal displacements of all middle-surface points of the corrugation are defined by one prescribed displacement parameter u_0 and two unknown functions of z : $u_1(z)$ and $u_2(z)$. If the resultant longitudinal shearing force F (see fig. 1(b)) is regard as prescribed instead of u_0 , the latter will become an additional unknown.

Assumptions regarding displacements in the plane of the cross section. - Especially near the ends, the cross sections can be expected to undergo significant flexural deformations in their own planes, somewhat in the manner of a rigid-jointed frame. Therefore the deformations of a cross section in its own plane will be assumed to be inextensional, as is done in frame analysis. Certain degrees of freedom will be assumed for the displacements of stations ① through ⑤ , consistent with the expected antisymmetry of the deformation pattern, and the displacements between stations will be assumed identical with those of the corresponding rigid-jointed frame, hinged at stations ⓪ and ⑤ .

Three degrees of freedom are sufficient for this purpose, and figure 3(c) shows the three selected, as viewed from the positive end of the z-axis. The first two of these degrees of freedom are the same as employed in reference 1. The third is a rigid-body translation, of amount $v_0(z)$, required because in the present analysis the trough lines are permitted to curve in the horizontal (xz) plane. Thus the displacements in the plane of the cross section are completely defined by three unknown functions of z : $v_1(z)$, $v_2(z)$ and $v_0(z)$.

Middle-surface extensional strains. - Referring to the foregoing assumptions regarding longitudinal displacements, and using the coordinate system of figure 3(a), the longitudinal displacements u for all points of the middle surface can be expressed in terms of u_0 , $u_1(z)$ and $u_2(z)$. The expressions for these longitudinal displacements are given in the second column of table 1. The corresponding extensional strains ε are obtained by differentiating these displacements with respect to z , and the resulting expressions are given in the last column of table 1. Because the longitudinal strains are antisymmetrical with respect to the crest line, it suffices to consider explicitly only the three plate elements listed in table 1.

TABLE 1. - LONGITUDINAL DISPLACEMENTS AND STRAINS

Plate element	Displacement, u	Strain, ε
01	$u_0 + \frac{s_1}{e}(u_1 - u_0)$	$\frac{s_1}{e}\frac{du_1}{dz} = \varepsilon_1$
12	$u_1 + \frac{s_2}{k}(u_2 - u_1)$	$\frac{du_1}{dz} + \frac{s_2}{k}\left(\frac{du_2}{dz} - \frac{du_1}{dz}\right) \equiv \varepsilon_2$
23	$u_2\left(1 - \frac{2s_3}{f}\right)$	$\frac{du_2}{dz}\left(1 - \frac{2s_3}{f}\right) \equiv \varepsilon_3$

Middle-surface shear strains. - The shear strains γ of the middle surface of the plate elements of the corrugation, obtained from both the longitudinal displacements and the displacements in the plane of the cross section, are given in table 2. It is seen that they are constant across the width of any plate element (i.e., independent of s_1, s_2, and s_3), as a result of the assumptions that u varies linearly between stations and the cross-sectional deformation is inextensional.

TABLE 2. - SHEAR STRAINS

Plate element	Shear strain, γ
01	$\frac{u_1 - u_0}{e} - \frac{dv_0}{dz} \equiv \gamma_1$
12	$\frac{u_2 - u_1}{k} - \frac{d}{dz}(v_0\cos\theta) + \frac{d}{dz}(v_1\sin\theta) \equiv \gamma_2$
23	$-\frac{2u_2}{f} - \frac{dv_0}{dz} + \frac{d}{dz}(v_1\sin\theta\cos\theta) + \frac{d}{dz}(v_2\sin\theta) \equiv \gamma_3$

Rate of twist of the plate elements. - If the corrugation length (2b) is several times the pitch (p), it can be argued that the torsional strain energy will be a small fraction of the strain energy due to the flexural (frame-like) deformations of the cross sections.* Therefore, in computing the torsional strain energy of a plate element, it is probably sufficiently accurate to assume a constant rate of twist across the width of the element rather than to consider the detailed variation of rate of twist across the width. This constant rate of twist will be taken as the overall rate of twist corresponding to the displacements of the longitudinal edges of the plate element. For example, the rate of twist of the plate element 01 will be taken as $\frac{d}{dz}\left(\frac{v_1}{e}\right)$, in accordance with the edge displacements shown in figure 3(c) for this plate element. The rates of twist ϕ obtained in this manner are given in table 3.

*The numerical results of reference 1 are consistent with this deduction. The same deduction is arrived at in reference 2.

TABLE 3. - RATES OF TWIST

Plate element	Rate of twist, ϕ
01	$\frac{d}{dz}\left(\frac{v_1}{e}\right) \equiv \phi_1$
12	$-\frac{d}{dz}\left(\frac{v_2}{k}\right) - \frac{d}{dz}\left(\frac{v_1\cos\theta}{k}\right) \equiv \phi_2$
23	$-\frac{d}{dz}\left(\frac{2v_1\sin^2\theta}{f}\right) + \frac{d}{dz}\left(\frac{2v_2\cos\theta}{f}\right) \equiv \phi_3$

Strain energy components. - As in reference 1, the strain energy of the corrugation is assumed to arise from the following four sources: (a) middle-surface extension of the plate elements in the longitudinal direction, (b) middle-surface shear of the plate elements, (c) twisting of the plate elements, and (d) frame-like bending of the cross sections. Expressions are developed below for the density (i.e. strain energy per unit length of corrugation) due to each of these sources. In developing these expressions, use is made of the fact that plate elements 34 and 45 contribute the same strain energy as plate elements 12 and 01 respectively.

(a) Strain energy due to middle-surface extension: The strain energy, per unit length of corrugation, due to the longitudinal strains of the middle surface is

$$U_{ext} = E't\left[\int_0^e \varepsilon_1^2 ds_1 + \int_0^k \varepsilon_2^2 ds_2 + \frac{1}{2}\int_0^f \varepsilon_3^2 ds_3\right] \tag{1}$$

where E' is the Young's modulus associated with longitudinal extension, $\varepsilon_1, \varepsilon_2, \varepsilon_3$ are defined in table 1, and s_1, s_2, s_3 are coordinate shown in figure 3(a). In writing equation (1), middle surface normal stresses in the transverse direction have been assumed negligible. The prime on the Young's modulus symbol is a tracer to distinguish this Young's modulus from the Young's modulus associated with frame bending.

Substituting the expressions for ε_1, ε_2, and ε_3 from table 1 and performing the integrations, one obtains

$$U_{ext} = b_{11}\left(\frac{du_1}{dz}\right)^2 + 2b_{12}\frac{du_1}{dz}\frac{du_2}{dz} + b_{22}\left(\frac{du_2}{dz}\right)^2 \tag{2}$$

where

$$\left.\begin{aligned} b_{11} &= \frac{1}{3} E'te\left(1 + \frac{k}{e}\right) \\ b_{12} &= \frac{1}{6} E'tk \\ b_{22} &= \frac{1}{6} E't(2k + f) \end{aligned}\right\} \quad (3)$$

(b) Strain energy due to middle-surface shear: The strain energy, per unit length of corrugation, due to the middle-surface shear strain is

$$U_{sh} = Gt(\gamma_1^2 e + \gamma_2^2 k + \frac{1}{2}\gamma_3^2 f) \quad (4)$$

where G is the shear modulus associated with middle-surface shear and γ_1, γ_2, γ_3 are the plate-element shear strains given in table 2. Substituting for the strains their expressions from table 2, one obtains

$$\begin{aligned} U_{sh} = {} & c_{00}u_0^2 + c_{11}u_1^2 + c_{22}u_2^2 + 2c_{01}u_0u_1 + 2c_{12}u_1u_2 \\ & + d_{00}u_0\frac{dv_0}{dz} + d_{10}u_1\frac{dv_0}{dz} + d_{20}u_2\frac{dv_0}{dz} \\ & + d_{11}u_1\frac{dv_1}{dz} + d_{21}u_2\frac{dv_1}{dz} + d_{22}u_2\frac{dv_2}{dz} \\ & + e^*_{00}\left(\frac{dv_0}{dz}\right)^2 + e^*_{11}\left(\frac{dv_1}{dz}\right)^2 + e^*_{22}\left(\frac{dv_2}{dz}\right)^2 \\ & + 2e^*_{10}\frac{dv_1}{dz}\frac{dv_0}{dz} + 2e^*_{20}\frac{dv_2}{dz}\frac{dv_0}{dz} + 2e^*_{12}\frac{dv_1}{dz}\frac{dv_2}{dz} \end{aligned} \quad (5)$$

where

$$\left.\begin{aligned} c_{00} &= G\frac{t}{e} & c_{11} &= G\frac{t}{e}\left(1 + \frac{e}{k}\right) \\ c_{22} &= G\left(\frac{t}{k} + 2\frac{t}{f}\right) & & \\ c_{01} &= -G\frac{t}{e} & c_{12} &= -G\frac{t}{k} \end{aligned}\right\} \quad (6a)$$

$$d_{00} = 2Gt \qquad d_{10} = -2Gt(1 - \cos\theta)$$

$$d_{20} = 2Gt(1 - \cos\theta) \qquad d_{11} = d_{22} = -2Gt \sin\theta \qquad (6b)$$

$$d_{21} = 2Gt \sin\theta(1 - \cos\theta)$$

$$e^*_{00} = Gt(e + k \cos^2\theta + \tfrac{f}{2})$$

$$e^*_{11} = Gt \sin^2\theta(k + \tfrac{f}{2} \cos^2\theta)$$

$$e^*_{22} = \tfrac{1}{2} Gtf \sin^2\theta$$

$$e^*_{10} = -\tfrac{1}{2} Gt(2k + f)\sin\theta\cos\theta \qquad (6c)$$

$$e^*_{20} = -\tfrac{1}{2} Gtf \sin\theta$$

$$e^*_{12} = \tfrac{1}{2} Gtf \sin^2\theta \cos\theta$$

(c) Strain energy due to twisting of the plate elements: The strain energy, per unit length of corrugation, due to twisting of the plate elements is

$$U_{tw} = G'(J_1\phi_1^2 + J_2\phi_2^2 + \tfrac{1}{2}J_3\phi_3^2) \qquad (7)$$

where G' is the shear modulus associated with torsion (the prime being a tracer to distinguish it from the shear modulus G associated with middle-surface shear); J_1, J_2, J_3 are the torsion constants of plate elements 01, 12 and 23 respectively, considered as bars of narrow rectangular cross section; and ϕ_1, ϕ_2, ϕ_3 are the rates of twist given in table 3. Substituting the expressions from table 3 for the rates of twist and

$$J_1 = \tfrac{1}{3} et^3 \qquad J_2 = \tfrac{1}{3} kt^3 \qquad J_3 = \tfrac{1}{3} ft^3 \qquad (8)$$

for the torsion constants, one obtains

$$U_{tw} = \bar{e}_{11}\left(\frac{dv_1}{dz}\right)^2 + \bar{e}_{22}\left(\frac{dv_2}{dz}\right)^2 + 2\bar{e}_{12}\frac{dv_1}{dz}\frac{dv_2}{dz} \qquad (9)$$

in which

$$\left.\begin{aligned}
\bar{e}_{11} &= G'\left(\frac{J_1}{e^2} + \frac{J_2}{k^2}\cos^2\theta + \frac{2J_3}{f^2}\sin^4\theta\right) \\
\bar{e}_{22} &= G'\left(\frac{J_2}{k^2} + \frac{2J_3}{f^2}\cos^2\theta\right) \\
\bar{e}_{12} &= G'\left(\frac{J_2}{k^2}\cos\theta - \frac{2J_3}{f^2}\sin^2\theta\cos\theta\right)
\end{aligned}\right\} \quad (10)$$

(d) Strain energy due to frame bending of the cross sections: Considering a unit length of corrugation to be a rigid-jointed frame whose joint displacements are a superposition of the three modes shown in figure 3(c), while the joints are permitted to rotate freely, one obtains for the strain energy a quadratic expression in v_1 and v_2. (v_0 is absent from this expression because it represents a rigid body translation.)

The derivation of this expression is given in appendix A of reference 1 and will not be repeated here. In that derivation a parameter α is used which has the value 0 or 1 according to whether joints ⓪ and ⑤ are hinged or clamped. Only the case $\alpha = 0$ is pertinent to the present analysis. Setting α equal to zero gives the following expression for the strain energy, per unit length of corrugation, due to frame-like bending of the cross sections:

$$U_b = a_{11}v_1^2 + 2a_{12}v_1v_2 + a_{22}v_2^2 \quad (11)$$

where

$$\left.\begin{aligned}
a_{11} &= \frac{D}{\beta^2 e^3}\left[A_{11} + A_{22}\left(\frac{e}{k}\right)^2\cos^2\theta + 4A_{33}\left(\frac{e}{f}\right)^2\sin^4\theta\right. \\
&\qquad \left. - A_{12}\frac{e}{k}\cos\theta + 2A_{23}\frac{e}{k}\frac{e}{f}\sin^2\theta\cos\theta - 2A_{13}\frac{e}{f}\sin^2\theta\right] \\
a_{12} &= \frac{D}{\beta^2 e^3}\left[A_{22}\left(\frac{e}{k}\right)^2\cos\theta - 4A_{33}\left(\frac{e}{f}\right)^2\sin^2\theta\cos\theta\right. \\
&\qquad \left. - \frac{1}{2}A_{12}\frac{e}{k} - A_{23}\frac{e}{k}\frac{e}{f}(\cos^2\theta - \sin^2\theta) + A_{13}\frac{e}{f}\cos\theta\right] \\
a_{22} &= \frac{D}{\beta^2 e^3}\left[A_{22}\left(\frac{e}{k}\right)^2 + 4A_{33}\left(\frac{e}{f}\right)^2\cos^2\theta - 2A_{23}\frac{e}{k}\frac{e}{f}\cos\theta\right]
\end{aligned}\right\} \quad (12)$$

with

$$\beta = 12\,\frac{e}{k}\left(1 + \frac{e}{k}\right) + 6\,\frac{e}{f}\left(3 + 4\,\frac{e}{k}\right) \tag{13a}$$

$$\left.\begin{aligned}
A_{11} &= 216\,\frac{e}{k}\left(\frac{e}{k} + 2\,\frac{e}{f}\right)\left(2\,\frac{e}{k} + 3\,\frac{e}{f}\right) + 432\left(\frac{e}{k}\right)^2\left(\frac{e}{k} + 2\,\frac{e}{f}\right)^2 \\
A_{22} &= 216\,\frac{e}{k}\left(\frac{e}{k} + 6\,\frac{e}{f}\right)\left(2\,\frac{e}{k} + 3\,\frac{e}{f}\right) + 144\left(\frac{e}{k}\right)^2\left[3\left(\frac{e}{k}\right)^2 + 30\,\frac{e}{k}\,\frac{e}{f} + 45\left(\frac{e}{f}\right)^2\right] \\
&\quad + 864\left(\frac{e}{k}\right)^3\frac{e}{f}\left(\frac{e}{k} + 2\,\frac{e}{f}\right) \\
A_{33} &= 432\,\frac{e}{k}\,\frac{e}{f}\left(2\,\frac{e}{k} + 3\,\frac{e}{f}\right) + 144\left(\frac{e}{k}\right)^2\frac{e}{f}\left(12\,\frac{e}{k} + 21\,\frac{e}{f}\right) \\
&\quad + 864\left(\frac{e}{k}\right)^3\frac{e}{f}\left(\frac{e}{k} + 2\,\frac{e}{f}\right) \\
A_{12} &= -\,432\,\frac{e}{k}\left(\frac{e}{k} + 3\,\frac{e}{f}\right)\left(2\,\frac{e}{k} + 3\,\frac{e}{f}\right) \\
&\quad - 864\left(\frac{e}{k}\right)^2\left(\frac{e}{k} + 3\,\frac{e}{f}\right)\left(\frac{e}{k} + 2\,\frac{e}{f}\right) \\
A_{13} &= 432\,\frac{e}{k}\,\frac{e}{f}\left(2\,\frac{e}{k} + 3\,\frac{e}{f}\right) + 864\left(\frac{e}{k}\right)^2\frac{e}{f}\left(\frac{e}{k} + 2\,\frac{e}{f}\right) \\
A_{23} &= -\,1296\,\frac{e}{k}\,\frac{e}{f}\left(2\,\frac{e}{k} + 3\,\frac{e}{f}\right) - 288\left(\frac{e}{k}\right)^2\frac{e}{f}\left(15\,\frac{e}{k} + 27\,\frac{e}{f}\right) \\
&\quad - 1728\left(\frac{e}{k}\right)^3\frac{e}{f}\left(\frac{e}{k} + 2\,\frac{e}{f}\right)
\end{aligned}\right\} \tag{13b}$$

The symbol D appearing in equations (12) represents the frame flexural stiffness of the corrugation per unit width of frame, i.e. per unit length of corrugation. A detailed discussion of the symbol D has been given in reference 1, where it is concluded that an appropriate value for D is the plate flexural stiffness, i.e.

$$D = \frac{Et^3}{12(1 - \nu^2)} \tag{14}$$

where E and ν are Young's modulus and Poisson's ratio, respectively.

Total strain energy. - The total strain energy U of a single corrugation can be obtained by integrating the sum of the foregoing strain energy densities over the entire length of the corrugation. I.e.,

$$U = \int_{-b}^{b} (U_{ext} + U_{sh} + U_{tw} + U_b)dz \tag{15}$$

where U_{ext}, U_{sh}, U_{tw}, U_b are defined by equations (2), (5), (9) and (11) respectively.

Total potential energy. - The potential energy of the prescribed shearing forces F along the sides of a corrugation, whose relative longitudinal displacement is $2u_0$, equals $-2Fu_0$. Adding this to the above strain energy U gives the total potential energy (TPE) of a single corrugation as

$$TPE = -2Fu_0 + U \tag{16}$$

Minimization of the TPE. - The TPE as defined by equation (16) is a functional of u_0, $u_1(z)$, $u_2(z)$, $v_0(z)$, $v_1(z)$, $v_2(z)$. In accordance with the method of minimum total potential energy (ref. 3) the "best" values of these quantities will be those which minimize the TPE. To obtain these "best" values, the technique of variational calculus may be used to form the first variation of TPE due to variations in u_0, $u_1(z)$, $u_2(z)$, $v_0(z)$, $v_1(z)$, $v_2(z)$ and equate it to zero. This will lead to a system of field equations (primarily differential equations) and boundary conditions defining u_0, $u_1(z)$, ..., $v_2(z)$.

The detailed execution of this procedure is given in appendix A. The resulting field equations, equations (A12) and (A11) of appendix A, are repeated here for convenience:

$$\left.\begin{aligned}
&b_{11}\frac{d^2u_1}{dz^2} + b_{12}\frac{d^2u_2}{dz^2} - \frac{1}{2}d_{10}\frac{dv_0}{dz} - \frac{1}{2}d_{11}\frac{dv_1}{dz} - c_{11}u_1 - c_{12}u_2 = c_{01}u_0 \\
&b_{12}\frac{d^2u_1}{dz^2} + b_{22}\frac{d^2u_2}{dz^2} - \frac{1}{2}d_{20}\frac{dv_0}{dz} - \frac{1}{2}d_{21}\frac{dv_1}{dz} - \frac{1}{2}d_{22}\frac{dv_2}{dz} - c_{12}u_1 - c_{22}u_2 = 0 \\
&e_{00}\frac{d^2v_0}{dz^2} + e_{10}\frac{d^2v_1}{dz^2} + e_{20}\frac{d^2v_2}{dz^2} + \frac{1}{2}d_{10}\frac{du_1}{dz} + \frac{1}{2}d_{20}\frac{du_2}{dz} = 0 \\
&e_{10}\frac{d^2v_0}{dz^2} + e_{11}\frac{d^2v_1}{dz^2} + e_{12}\frac{d^2v_2}{dz^2} + \frac{1}{2}d_{11}\frac{du_1}{dz} + \frac{1}{2}d_{21}\frac{du_2}{dz} - a_{11}v_1 - a_{12}v_2 = 0 \\
&e_{20}\frac{d^2v_0}{dz^2} + e_{12}\frac{d^2v_1}{dz^2} + e_{22}\frac{d^2v_2}{dz^2} + \frac{1}{2}d_{22}\frac{du_2}{dz} - a_{12}v_1 - a_{22}v_2 = 0
\end{aligned}\right\} \tag{17}$$

and

$$2c_{00}u_0 b + c_{01}\int_{-b}^{b} u_1 dz = F \tag{18}$$

Different sets of boundary conditions are obtained in appendix A, depending on the nature of the end attachments. If there are point attachments at the ends of trough lines only (fig. 2(a)) the boundary conditions at $z = \pm b$ are

$$\frac{du_1}{dz} = 0 \quad , \quad \frac{du_2}{dz} = 0 \tag{19}$$

$$v_0 = 0 \tag{20}$$

$$\left.\begin{aligned} 2e_{10}\frac{dv_0}{dz} + 2e_{11}\frac{dv_1}{dz} + 2e_{12}\frac{dv_2}{dz} + d_{11}u_1 + d_{21}u_2 &= 0 \\ 2e_{20}\frac{dv_0}{dz} + 2e_{12}\frac{dv_1}{dz} + 2e_{22}\frac{dv_2}{dz} + d_{22}u_2 &= 0 \end{aligned}\right\} \tag{21}$$

If the attachments at the ends of the trough lines are wide as idealized in figure 2(d), it is only necessary to replace the first of equations (21) by the condition

$$v_1 = 0 \tag{22}$$

Finally, if the attachments are as shown in figure 2(b), namely point attachments at the ends of both the crest lines and the trough lines, the boundary conditions are

$$\frac{du_1}{dz} = 0 \quad , \quad \frac{du_2}{dz} = 0 \tag{23}$$

$$v_0 = 0 \tag{24}$$

$$v_1\cos\theta + v_2 = 0 \tag{25}$$

$$2(e_{10} - e_{20}\cos\theta)\frac{dv_0}{dz} + 2(e_{11} - e_{12}\cos\theta)\frac{dv_1}{dz} + 2(e_{12} - e_{22}\cos\theta)\frac{dv_2}{dz}$$

$$+ d_{11}u_1 + (d_{21} - d_{22}\cos\theta)u_2 = 0 \tag{26}$$

The physical meaning of these boundary conditions is discussed in appendix A.

Solution of equations. - Essentially, the basic solution of the problem consists of solving equations (17) for $u_1(z)$, $u_2(z)$, $v_0(z)$, $v_1(z)$, $v_2(z)$ in terms of u_0, subject to appropriate set of boundary conditions. The solution for $u_1(z)$ is then substituted in equation (18), which then gives u_0 in terms of F or F in terms of u_0.

The system of simultaneous differential equations (17) is linear with constant coefficients, and it can therefore be solved in a straight-forward manner. The full details of the solution are in appendix B, and only the main features of the solution (those needed for computational purpose) will be cited here.

The numerical realization of the solution requires that equation (B20) be solved for its eight non-zero roots, R_1, R_2, ..., R_8. In equation (B20) c is any characteristic length (c was taken equal to the pitch p in the subsequent calculations) and the coefficients k_0, k_2, etc. are functions of the ratios of the elastic constants and of the parameters defining the basic shape of the cross section, i.e. θ, t/c, e/c, k/c and f/c. These coefficients are defined by equations (B13). Because only even powers of R appear in equation (B20), four of these roots are the negatives of the other four, as stated in equations (B21a).

For most cross-sectional geometries of interest R_1 through R_8 are complex, and therefore the further description of the solution will pertain to that case. For a description of the solution procedure in the general case the reader is referred to appendix B.

When R_1 through R_8 are complex, they come in conjugate pairs, and therefore four of them have the representation shown in equations (B44) with U, V, X and Y real numbers. Equations (B44) and (B21a) provide a complete representation of all eight roots.

With U, V, X and Y known, the displacement ratios $u_1(z)/u_0$, etc. can be computed from equations (B50) in which ζ_1 and ζ_2 are defined by equations (B2); ξ_1 and ξ_2 are defined by equations (B40); $P^{B,C,D,E}$, $Q^{B,C,D,E}$, $S^{B,C,D,E}$ and $T^{B,C,D,E}$ are obtained by solving equations (B23) for $j = 1$ and 5 and noting equations (B31) and (B46) through (B49); and $\overline{\overline{A}}_1/u_0$, $\overline{\overline{A}}_4/u_0$, $\overline{\overline{A}}_5/u_0$, $\overline{\overline{A}}_7/u_0$, E_{10}/u_0 are obtained by solving equations (B52), (B53) or (B54), depending on the type of end attachments.

Relationship between F and u_0. - Equations (B50) give the displacements due to a prescribed value of u_0, i.e. a prescribed value of half the relative shearing displacement of the two sides of a corrugation. For determining the displacements produced by a prescribed shearing force F, one needs the relationship between F and u_0. This relationship is given by equations (B63) when R_1 through R_8 are complex. The symbols $\overset{\frown}{sv}$, $\overset{\frown}{sy}$, etc. in equations (B63b) are defined by equations (B60).

Equation (B63a) gives the overall shearing stiffness $F/2u_0$ of a single corrugation. One can define a dimensionless shearing stiffness parameter Ω as the ratio of the actual shearing stiffness of a single corrugation to that of an identical corrugation having continuous end attachment producing uniform shear strain throughout the corrugation. The uniform shear strain of the latter corrugation due to the relative shearing displacement $2u_0$ of its sides is $2u_0$ divided by the developed width $p' = 2e + 2k + f$. The shear force F' required to maintain the relative shearing displacement $2u_0$ is therefore $Gt \cdot 2b \cdot 2u_0/p'$, which implies the following shear stiffness for the continuously attached corrugation:

$$\frac{F'}{2u_0} = \frac{Gt \cdot 2b}{p'} \tag{27}$$

The relative shearing stiffness of the given corrugation is defined as

$$\Omega = \frac{F/2u_0}{F'/2u_0} \tag{28}$$

Eliminating numerator and denominator of this expression via equations (B63a) and (27) respectively, one obtains

$$\Omega = \frac{p'\psi}{2e} = (1 + \frac{k}{e} + \frac{1}{2}\frac{f}{e})\psi \tag{29}$$

Stresses. - With the displacements $u_1(z)$, $u_2(z)$, etc. determined, the stresses in the corrugation can also be obtained. Expressions for the various stresses will now be given, again restricted to the case in which the non-zero roots of the characteristic equation are complex. In order to avoid lengthy equations, the following short-hand notations will be employed:

$$\left.\begin{aligned}
\tilde{A}_1 &\equiv \frac{\bar{\bar{A}}_1}{u_0}\cosh\frac{Ub}{c} \\
\tilde{A}_4 &\equiv \frac{\bar{\bar{A}}_4}{u_0}\cosh\frac{Ub}{c} \\
\tilde{A}_5 &\equiv \frac{\bar{\bar{A}}_5}{u_0}\cosh\frac{Xb}{c} \\
\tilde{A}_8 &\equiv \frac{\bar{\bar{A}}_8}{u_0}\cosh\frac{Xb}{c} \\
\tilde{E}_{10} &\equiv \frac{E_{10}}{u_0}
\end{aligned}\right\} \tag{30}$$

$$\left.\begin{aligned}
\bar{f}_{ss}(z) &\equiv \sinh\frac{Uz}{c}\sin\frac{Vz}{c} & \tilde{f}_{ss}(z) &\equiv \sinh\frac{Xz}{c}\sin\frac{Yz}{c} \\
\bar{f}_{sc}(z) &\equiv \sinh\frac{Uz}{c}\cos\frac{Vz}{c} & \tilde{f}_{sc}(z) &\equiv \sinh\frac{Xz}{c}\cos\frac{Yz}{c} \\
\bar{f}_{cs}(z) &\equiv \cosh\frac{Uz}{c}\sin\frac{Vz}{c} & \tilde{f}_{cs}(z) &\equiv \cosh\frac{Xz}{c}\sin\frac{Yz}{c} \\
\bar{f}_{cc}(z) &\equiv \cosh\frac{Uz}{c}\cos\frac{Vz}{c} & \tilde{f}_{cc}(z) &\equiv \cosh\frac{Xz}{c}\cos\frac{Yz}{c}
\end{aligned}\right. \tag{31}$$

$$c_U \equiv \cosh \frac{Ub}{c}$$

$$c_X \equiv \cosh \frac{Xb}{c} \qquad (32)$$

$$\tilde{V}_1(z) \equiv (\tilde{A}_4 P^C - \tilde{A}_1 Q^C) \frac{U \bar{f}_{ss} + V \bar{f}_{cc}}{c_U} + (\tilde{A}_1 P^C + \tilde{A}_4 Q^C) \frac{U \bar{f}_{cc} - V \bar{f}_{ss}}{c_U}$$

$$+ (\tilde{A}_8 S^C - \tilde{A}_5 T^C) \frac{X \tilde{f}_{ss} + Y \tilde{f}_{cc}}{c_X} + (\tilde{A}_5 S^C + \tilde{A}_8 T^C) \frac{X \tilde{f}_{cc} - Y \tilde{f}_{ss}}{c_X}$$

$$\tilde{V}_2(z) \equiv (\tilde{A}_4 P^D - \tilde{A}_1 Q^D) \frac{U \bar{f}_{ss} + V \bar{f}_{cc}}{c_U} + (\tilde{A}_1 P^D + \tilde{A}_4 Q^D) \frac{U \bar{f}_{cc} - V \bar{f}_{ss}}{c_U}$$

$$+ (\tilde{A}_8 S^D - \tilde{A}_5 T^D) \frac{X \tilde{f}_{ss} + Y \tilde{f}_{cc}}{c_X} + (\tilde{A}_5 S^D + \tilde{A}_8 T^D) \frac{X \tilde{f}_{cc} - Y \tilde{f}_{ss}}{c_X} \qquad (33)$$

$$\tilde{V}_0(z) \equiv (\tilde{A}_4 P^E - \tilde{A}_1 Q^E) \frac{U \bar{f}_{ss} + V \bar{f}_{cc}}{c_U} + (\tilde{A}_1 P^E + \tilde{A}_4 Q^E) \frac{U \bar{f}_{cc} - V \bar{f}_{ss}}{c_U}$$

$$+ (\tilde{A}_8 S^E - \tilde{A}_5 T^E) \frac{X \tilde{f}_{ss} + Y \tilde{f}_{cc}}{c_X} + (\tilde{A}_5 S^E + \tilde{A}_8 T^E) \frac{X \tilde{f}_{cc} - Y \tilde{f}_{ss}}{c_X}$$

$$+ \tilde{E}_{10}$$

The longitudinal normal stresses $\sigma_{①}$ and $\sigma_{②}$, along junctions ① and ② (see fig. 3(a)) are given by

$$\sigma_{①} = E' \frac{du_1}{dz} \quad \text{and} \quad \sigma_{②} = E' \frac{du_2}{dz} \qquad (34)$$

Substituting for u_1 and u_2 their expressions (eqs. (B50a) and (B50b)) gives

$$\frac{\sigma_{①}^{c}}{E'u_0} = \tilde{A}_1 \frac{U\,\overline{f}_{sc} - U\,\overline{f}_{cs}}{c_U} + \tilde{A}_4 \frac{U\,\overline{f}_{cs} + V\,\overline{f}_{sc}}{c_U} + \tilde{A}_5 \frac{X\,\tilde{f}_{sc} - Y\,\tilde{f}_{cs}}{c_X}$$

$$+ \tilde{A}_8 \frac{X\,\tilde{f}_{cs} + Y\,\tilde{f}_{sc}}{c_X} \qquad (35a)$$

$$\frac{\sigma_{②}^{c}}{E'u_0} = (\tilde{A}_1 P^B + \tilde{A}_4 Q^B) \frac{U\,\overline{f}_{sc} - V\,\overline{f}_{cs}}{c_U} + (\tilde{A}_4 P^B - \tilde{A}_1 Q^B) \frac{U\,\overline{f}_{cs} + V\,\overline{f}_{sc}}{s_U}$$

$$+ (\tilde{A}_5 S^B + \tilde{A}_8 T^B) \frac{X\,\tilde{f}_{sc} - Y\,\tilde{f}_{cs}}{c_X} + (\tilde{A}_8 S^B - \tilde{A}_5 T^B) \frac{X\,\tilde{f}_{cs} + Y\,\tilde{f}_{sc}}{c_X} \qquad (35b)$$

These stresses are positive if tensile.

The middle-surface shear stresses in the plate elements making up the corrugation can be determined from the shear strains of table 2 and the displacement equations (B50). These shear stresses will be denoted by τ_{01}, τ_{12} and τ_{23} respectively. The following expressions are obtained for them:

$$\frac{\tau_{01}^{c}}{Gu_0} = \frac{c}{e}\left[\zeta_1 - 1 + \tilde{A}_1 \frac{\overline{f}_{cc}}{c_U} + \tilde{A}_4 \frac{\overline{f}_{ss}}{c_U} + \tilde{A}_5 \frac{\tilde{f}_{cc}}{c_X} + \tilde{A}_8 \frac{\tilde{f}_{ss}}{c_X} + \xi_1 \tilde{E}_{10}\right] - \tilde{V}_0 \qquad (36a)$$

$$\frac{\tau_{12}^{c}}{Gu_0} = \frac{c}{k}\{\zeta_2 - \zeta_1 + [\tilde{A}_1(P^B - 1) + \tilde{A}_4 Q^B]\frac{\overline{f}_{cc}}{c_U}$$

$$+ [\tilde{A}_4(P^B - 1) - \tilde{A}_1 Q^B]\frac{\overline{f}_{ss}}{c_U} + [\tilde{A}_5(S^B - 1) + \tilde{A}_8 T^B]\frac{\tilde{f}_{cc}}{c_X}$$

$$+ [\tilde{A}_8(S^B - 1) - \tilde{A}_5 T^B]\frac{\tilde{f}_{ss}}{c_X} + (\xi_2 - \xi_1)\tilde{E}_{10}\} + \tilde{V}_1 \sin\theta - \tilde{V}_0 \cos\theta \qquad (36b)$$

$$\frac{\tau_{23}^{c}}{Gu_0} = -2\frac{c}{f}\{\zeta_2 + (\tilde{A}_1 P^B + \tilde{A}_4 Q^B)\frac{\overline{f}_{cc}}{c_U} + (\tilde{A}_4 P^B - \tilde{A}_1 Q^B)\frac{\overline{f}_{ss}}{c_U}$$

$$+ (\tilde{A}_5 S^B + \tilde{A}_8 T^B)\frac{\tilde{f}_{cc}}{c_X} + (\tilde{A}_8 S^B - \tilde{A}_5 T^B)\frac{\tilde{f}_{ss}}{c_X} + \xi_2 \tilde{E}_{10}\}$$

$$+ \tilde{V}_2 \sin\theta + \tilde{V}_1 \sin\theta\cos\theta - \tilde{V}_0 \qquad (36c)$$

The positive sense of τ_{01} is shown in figure 5. The positive senses of the other two shearing stresses are the same as that of τ_{01} .

The extreme-fiber shear stresses due to torsion will be denoted by τ'_{01}, τ'_{12} and τ'_{23} for plate elements 01, 12 and 23 respectively. They can be obtained by multiplying the rates of twist in table 3 by G't (ref. 4) and substituting equations (B50) for the displacements. The resulting expressions are

$$\frac{\tau'^{c}_{01}}{G'u_0} = \frac{t}{e}\tilde{V}_1 \qquad (37a)$$

$$\frac{\tau'^{c}_{12}}{G'u_0} = -\frac{t}{k}(\tilde{V}_2 + \tilde{V}_1\cos\theta) \qquad (37b)$$

$$\frac{\tau'^{c}_{23}}{G'u_0} = -2\frac{t}{f}(\tilde{V}_1\sin^2\theta - \tilde{V}_2\cos\theta) \qquad (37c)$$

The positive sense of τ'_{01} is shown in figure 5 as an example to indicate the positive senses of all three torsional shearing stresses.

Due to frame-like deformation of the cross sections transverse bending moments are developed which vary linearly between stations and are zero at stations ⓪ and ⑤ . The transverse bending moment (per unit length of corrugation) at any station other than ⓪ and ⑤ is a linear function of $v_1(z)$ and $v_2(z)$ (v_0 playing no role because it represents a rigid-body translation of the cross section). The associated extreme-fiber bending stress, obtained by multiplying the bending moment by $6/t^2$, will also be a linear function of v_1 and v_2 . The extreme-fiber transverse bending stresses at

stations ① and ② will be denoted by $\sigma'_{①}$ and $\sigma'_{②}$ and will be considered positive if they are tensile in the lower fibers (see fig. 5). Expressions for these stresses in terms of v_1 and v_2 can be obtained directly from equations (56) of reference 1 with the parameter α therein set equal to zero. The resulting expressions are

$$\begin{bmatrix} \dfrac{\sigma'^{c}_{①}}{Eu_0} \\ \\ \dfrac{\sigma'^{c}_{②}}{Eu_0} \end{bmatrix} = \frac{1}{1-\nu^2}\frac{t}{e}\frac{c}{e} \begin{bmatrix} g_{21} & g_{22} \\ \\ g_{31} & g_{32} \end{bmatrix} \begin{bmatrix} v_1/u_0 \\ \\ v_2/u_0 \end{bmatrix} \tag{38}$$

where v_1/u_0 and v_2/u_0 are now given by equations (B50c) and (B50d), and the g_{ij} matrix elements are defined as follows:

$$\left.\begin{aligned} g_{21} &= \frac{1}{\beta}\frac{e}{k}\left[2a_1 + b_1 - (2a_2 + b_2)\frac{e}{k}\cos\theta - (4a_3 + 2b_3)\frac{e}{f}\sin^2\theta\right] \\ &\quad - 3\left(\frac{e}{k}\right)^2\cos\theta \\ g_{22} &= \frac{1}{\beta}\frac{e}{k}\left[-(2a_2 + b_2)\frac{e}{k} + (4a_3 + 2b_3)\frac{e}{f}\cos\theta\right] - 3\left(\frac{e}{k}\right)^2 \\ g_{31} &= \frac{3}{\beta}\frac{e}{f}\left(b_1 - b_2\frac{e}{k}\cos\theta - 2b_3\frac{e}{f}\sin^2\theta\right) - 6\left(\frac{e}{f}\right)^2\sin^2\theta \\ g_{32} &= \frac{3}{\beta}\frac{e}{f}\left(-b_2\frac{e}{k} + 2b_3\frac{e}{f}\cos\theta\right) + 6\left(\frac{e}{f}\right)^2\cos\theta \end{aligned}\right\} \tag{39}$$

with

$$\left.\begin{aligned} a_1 &\equiv -6\left(2\frac{e}{k} + 3\frac{e}{f}\right) \\ a_2 &\equiv -12\frac{e}{k}\left(\frac{e}{k} + 3\frac{e}{f}\right) \\ a_3 &\equiv 12\frac{e}{k}\frac{e}{f} \\ b_1 &\equiv 6\frac{e}{k} \\ b_2 &\equiv -6\frac{e}{k}\left(2\frac{e}{k} + 3\right) \\ b_3 &\equiv -6\frac{e}{f}\left(4\frac{e}{k} + 3\right) \end{aligned}\right\} \tag{40}$$

Special cases. - The above results apply to the general case in which none of the dimensions e, f, and k is zero (fig. 6(a)). Analyses for the special cases $f = 0$ (fig. 6(b)) and $e = 0$ (fig. 6(c)) are contained in appendixes C and D respectively. In these appendixes only the end conditions of figure 2(a) needed consideration. Those of figure 2(b) are equivalent to continuous attachment when e or f approaches zero, because of the resulting complete suppression of the deformation of the end cross sections in their own planes. The end conditions of figure 2(d) are similarly equivalent to continuous attachment if f approaches zero, or to those of figure 2(a) if e approaches zero.

The main results from appendixes C and D will now be cited.

The special case $f = 0$ leads to a sixth degree (rather than a tenth degree) characteristic equation, (C19), with six roots in the form (C23) and (C24). The numerical computation of the four non-zero roots can be done by means of the quadratic formula. With the roots determined, the relationship between the arbitrary constant ($\tilde{A}'_j$, $\tilde{D}'_j$, and $\tilde{E}'_j$) can be obtained from equations (C28) and (C29). Equations (C39), with $\overline{A}_1$, $\overline{A}_3$, and A'_6 defined by (C40), then give the displacements $u_1(z)$, $v_2(z)$ and $v_0(z)$. Equations (C42) and (C43) give the basic shearing stiffness, and equations (C45) through (C49) give the stresses.

The special case $e = 0$ also leads to a sixth degree characteristic equation, (D14), which has six roots ($\hat{R}_1$, ..., $\hat{R}_6$) with the properties shown in equations (D18) and (D19). The four non-zero roots can be easily determined from the quadratic factor of equation (D14). With the roots known, the relationship between the arbitrary constants ($\hat{B}_j$, $\hat{D}_j$ and $\hat{E}_j$) can be obtained from equations (D21), (D23) and (D24). Equations (D34), with B^*_1, B^*_3, and $\hat{B}_6$ defined by (D35), then give the displacements $u_2(z)$, $v_2(z)$, and $v_0(z)$. Equations (D38) and (D40) give the absolute shearing stiffness and the relative shearing stiffness respectively, and equations (D41) through (D45) give the stresses.

NUMERICAL RESULTS AND DISCUSSION

The foregoing analysis was used to determine numerical results on shear stiffness, stresses and deformations for selected cross-sectional geometries and end-attachment conditions. Poisson's ratio ν was taken as 0.3, G was taken as $E/[2(1 + \nu)]$, and no distinction was made between E and E', or G and G'. In order to keep the number of computations within reasonable bounds, the numerical studies were limited to the case of the so-called symmetrical corrugation, that is the case in which the trough and the crest plate elements have equal width ($2e = f$).

The numerical results were obtained by means of the equations discussed in the previous section. For determining the non-zero roots of the characteristic equation (B20), subroutine PØLRT of the IBM 360 Scientific Subroutine Package was employed. This subroutine can handle complex as well as real roots. The characteristic length c was taken equal to the pitch p.

For the sake of maximum generality the stiffness, stresses, and deformations are represented by dimensionless parameters. For a given basic shape of cross-sectional centerline — i.e., for given values of h/p, e/p and f/p, there are two additional dimensionless parameters needed to define completely the geometry of the corrugation (except for its absolute size). The most obvious choices for these parameters are b/p (semi-length divided by pitch) and t/p (thickness divided by pitch). It was found, however, that the use of $(b/p)\cdot(t/p)^{3/2}$ is preferable to b/p alone as the choice for the first parameter; for then the dimensionless stiffness, stresses and deformations turn out to be relatively insensitive to the second parameter, t/p . A similar result was observed in the case of trough lines held straight (ref. 1), but in that case bt/p^2 was the significant parameter corresponding to $(b/p)(t/p)^{3/2}$ of the present case.

Shear stiffness. - Figures 7 through 9 give the basic numerical results for shear stiffness. The results are given in terms of the relative shear stiffness parameter Ω , defined as the ratio of the absolute shear stiffness $F/2u_0$ of the actual corrugation to that of an identical corrugation with continuous end attachment producing a state of uniform shear (eq. (27)). To convert the relative shear stiffness Ω to the absolute shear stiffness $F/2u_0$, it is only necessary to multiply Ω by $2\,Gtb/p'$, in accordance with equations (28) and (27). That is

$$\frac{F}{2u_0} = \frac{Gt \cdot 2b}{p'}\,\Omega = \frac{Gtb}{e + k + \frac{1}{2}f}\,\Omega \qquad (41)$$

In these figures Ω is given as a function of $(b/p)\cdot(t/p)^{3/2}$ for the following range of cross-sectional geometries:

$h/p = .1, .2, .3, .4, .5$

$f/p(=2e/p) = .1, .2, .3, .5$

$t/p = .005$ and $.015$

Figure 7 is for the case of point attachments at the ends of the trough lines only (fig. 2(a)), figure 8 for the case of point attachments at the ends of both the crest lines and the trough lines (fig. 2(b)), and figure 9 for the case of wide attachments at the ends of the trough lines only (fig. 2(d)).

Figures 10, 11 and 12 present the same kind of information as figure 7, 8 and 9 respectively, but use log-log scales rather than semi-log scales in order to show more clearly the relationship between Ω and $(b/p)\cdot(t/p)^{3/2}$ in the regions of very low Ω (close to zero) and very

high Ω (close to unity). In figures 10, 11 and 12 the curves generally have a kink at $\Omega = .5$. To the left of the kink each curve gives Ω as a function of $(b/p)\cdot(t/p)^{3/2}$; to the right of the kink it gives $1 - \Omega$ as a function of $(b/p)\cdot(t/p)^{3/2}$.

The range of geometrical parameters covered in figures 10, 11 and 12 is as follows:

$$h/p = .2 \text{ and } .4$$

$$f/p(= 2e/p) = .1, .2, .3, .5$$

for $t/p = .005$ and $.015$; and

$$h/p = .2 \text{ and } .4$$

$$f/p(= 2e/p) = .2, .3, .5$$

for $t/p = .050$.

The curves for $t/p = .005$ and $.015$ duplicate the information given in parts (b) and (d) of figures 7, 8 and 9. However the curves for $t/p = .050$ give information which is not contained in figures 7, 8 and 9.

The closeness of the solid and non-solid curves in figures 7 through 12 shows that Ω is virtually a function of $(b/p)\cdot(t/p)^{3/2}$ alone, i.e. relatively insensitive to t/p, except in the region of very low (perhaps impractically low) values of $(b/p)\cdot(t/p)^{3/2}$.

Comparison of figures 7 and 8 (or 10 and 11) shows that a significant increase of shear stiffness results from having point attachments at the ends of the crest lines in addition to point attachments at the ends of the trough lines. (In the case of trough lines held straight (ref. 1) the increase of stiffness due to the additional set of attachments was much less significant.)

Comparison of figures 7 and 9 (or 10 and 12) shows that a much larger increase of shear stiffness is obtained by changing from point attachments to wide attachments at the ends of the trough lines. This increase is also an upper limit to the increase that can be expected as a result of one-sided interference, like that shown in figure 3 of reference 5 (also reproduced as figure 5 of ref. 1), between the troughs and the end member to which they are attached.

As is to be expected, figures 7 to 12 show that, all other things remaining constant, an increase of h or f will lead to a reduction of the relative shear stiffness Ω . Since increasing h or f implies increase of the developed width p' , equation (41) shows that the

absolute shear stiffness $F/2u_0$ will experience an even greater percentage reduction than the relative shear stiffness Ω .

It is of interest to compare the shear stiffness obtained in the present case with that obtained in the case of trough lines held straight (ref. 1). Figure 13, 14 and 15 present such a comparison for a particular shape of cross-sectional centerline ($h/p = f/p = 2e/p = .2$) and two values of thickness parameter: $t/p = .005$ and .020. In these figures Ω is plotted as a function of the length-to-pitch ratio ($2b/p$). The dashed curves are for the case of trough lines held straight, the solid curves for trough lines permitted to curve. It is seen that the shear stiffness in the latter case is appreciably lower than in the former, except for the very short and very long corrugations (i.e. very small or very large values of $2b/p$) and for the case of wide attachments at the ends of the trough lines (fig. 15). The lowering of the stiffness due to allowing the trough lines to curve is more pronounced for the thinner corrugation ($t/p = .005$) than for the thicker one ($t/p = .020$).

The above-discussed differences in Ω , between the case of trough lines held straight and trough lines permitted to curve, suggest that analyses which make the simplifying assumption that the trough lines (along with all other generators) remain straight* (e.g., refs. 6, 7 and 2), may be appreciably in error for some ranges of geometries if the plate does not actually have some external constraint which forces the trough lines to remain straight.

Displacement and stress patterns for a particular geometry. - The manner in which the displacements and stresses vary along the length of the corrugation for one particular geometry is shown in figures 16, 17 and 18, one figure for each of the three end-attachment conditions considered in the present analysis. The geometry is defined by the following numerical values:

$$h/p = .4$$

$$f/p = 2e/p = .4$$

$$t/p = .015$$

$$(b/p)(t/p)^{3/2} = .02$$

These imply a length-to-pitch ratio, $2b/p$, of approximately 21.8 and a θ value of 76°. Those quantities selected for plotting in figures 16,

*The assumption of straightness of the generators is usually present implicitly as a by-product of the assumption of inextensional deformation of the middle surface.

17 and 18 are dimensionless measures of the longitudinal displacements u_1 and u_2; the displacements v_0, v_1 and v_2 in the plane of the cross section; the middle-surface shear stresses τ_{01}, τ_{12} and τ_{23}; the extreme-fiber torsional shear stresses τ'_{01}, τ'_{12} and τ'_{23}; the longitudinal normal stresses $\sigma_{①}$ and $\sigma_{②}$ at stations ① and ②; and the transverse extreme-fiber stresses $\sigma'_{①}$ and $\sigma'_{②}$ at stations ① and ② due to frame-like bending of the cross sections.

These figures show a number of things, the main one being that stresses and deformations are far from uniform along the length of the corrugation — i.e., "end effects" due to the discrete nature of the end attachments can penetrate an appreciable distance in toward the central portion of the corrugation. These figures also indicate that the major stresses are likely to be bending stresses associated with frame bending of the end cross sections. The peaking of the τ_{01} shear stress near the end, to a value much higher than its average value, indicates that local buckling of the trough plate element due to shear near the end of the corrugation may need to be considered in the proportioning of the corrugation. The longitudinal normal stresses $\sigma_{①}$ and $\sigma_{②}$, though smaller than the maximum normal stress due to flexure of the cross section, are much larger than the longitudinal stresses obtained in the case of trough lines held straight (ref. 1), and they therefore show that the assumption of inextensible generators would be less valid in the present case than it would be in the case of reference 1. Due to the longitudinal normal stresses $\sigma_{⓪} = 0$, $\sigma_{①}$, $\sigma_{②}$, $\sigma_{③} = -\sigma_{②}$, $\sigma_{④} = -\sigma_{①}$, and $\sigma_{⑤} = 0$ at junctions ⓪ through ⑤, the crest and trough plate elements are in a state of bending in their own planes and the inclined plate elements may be in a state of combined compression and bending in their own planes. Figures 16, 17 and 18 show that these stresses reach peak values near (but not at) the ends. Local buckling due to them may also be a factor requiring consideration in the design of the corrugation. The graphs of v_0, v_1 and v_2 show that the displacements in the plane of the cross section are an order of magnitude larger than the longitudinal displacements, and the nonlinearity of these graphs contradicts the frequently used simplifying assumption that the generators of the corrugation remain straight lines.

Figure 17 provides a partial check on the correctness of the analysis and calculations. With $f = 2e$ and point attachments at the ends of both the crest lines and the trough lines, an additional element of symmetry is introduced which, on physical grounds, should lead to the following characteristics for the stresses and displacements:

$$\tau_{01} = \tau_{23} \qquad \tau'_{01} = -\tau'_{23} \qquad \tau'_{12} = 0$$

$$\sigma'_{①} = \sigma'_{②} \qquad \sigma_{①} = -\sigma_{②}$$

$$u_2 = u_0 - u_1$$

$$v_1 \cos\theta + v_2 = 0$$

(The conditions $\tau'_{12} = 0$ and $v_1\cos\theta + v_2 = 0$ express the fact that the inclined plate elements, of width k, undergo zero rotation at every cross section.) Examination of figure 17 shows that all of these characteristics except the first ($\tau_{01} = \tau_{23}$) are satisfied very well by the numerical results. The curves of τ_{01} and τ_{23}, which should coincide, differ in ordinate by a few percent in the region $z/b = .4$ to 1.0. This discrepancy may be due to round-off errors in the rather lengthy calculation of τ_{23}.

Maximum stresses. - Figures 16, 17 and 18 and similar results (not shown) for other geometries provided an indication of what kinds of stresses are significant and where their maximums occur. These maximums were then computed for a much larger range of geometries, and the results are presented in figures 19, 20 and 21, one figure for each of the three kinds of end conditions. These results were obtained for the case $t/p = .015$; however the dimensionless parameters used as ordinate and abscissa in each graph were so selected as to make the curves virtually independent of t/p. Figures 19, 20 and 21 may therefore be used for values of t/p other than .015.

The range of geometries covered in figures 19 and 20 (point attachments at the ends of the trough lines only or at the ends of both the trough lines and the crest lines) is as follows:

$$h/p = .1, .3, .5$$

$$f/p = .1, .2, .3, .5$$

$$(b/p)(t/p)^{3/2} = .00035 \text{ to } 2.5$$

Figure 21 (wide attachments at the ends of the trough lines) covers the same range plus $h/p = .2$.

The stress maximums selected for plotting in figures 19 and 20 are the end values (at $z = b$) of the following stresses: (I) the extreme-fiber frame bending stress $\sigma'_{\textcircled{1}}$, (II) the middle-surface shear stress τ_{01}, and (III) the magnitude of the maximum resultant extreme-fiber shear stress in plate element 01, i.e. $|\tau_{01}| + |\tau'_{01}|$.

For the case of wide attachments at the ends of the trough lines, the frame bending stress $\sigma'_{\textcircled{2}}$ was found to be generally larger than $\sigma'_{\textcircled{1}}$, and figure 21 therefore gives the end value of $\sigma'_{\textcircled{2}}$ rather than $\sigma'_{\textcircled{1}}$. Similarly, $|\tau_{12}| + |\tau'_{12}|$ can be larger than $|\tau_{01}| + |\tau'_{01}|$; figure 21 therefore gives the former sum instead of the latter. Because there was found to be very little twisting of plate element 01 in the case of wide attachments, the latter sum essentially equals $|\tau_{01}|$ alone.

An extensive survey of the peak values of the longitudinal normal stresses $\sigma_{\textcircled{1}}$ and $\sigma_{\textcircled{2}}$ would have required much more calculation than the other maximum stresses, because the values of z/b at which the peak longitudinal stresses occur cannot be specified in advance. Therefore no graphical data are presented for them. The isolated numerical results in table 4 may, however, be of some interest. Table 4 gives, for selected geometries and end conditions, the peak values of the dimensionless longitudinal normal stress parameters and the location (z/b) of these peak values.

COMPARISON WITH EXPERIMENT AND WITH ROTHWELL'S THEORY

Rothwell in reference 2 cites some experimental data on shear stiffness of trapezoidally corrugated plates given by Horsfall in reference 8. The following test-specimen dimensions are given by Rothwell: $h = .373"$ $p = 3.55"$, $2e = f = .75"$, $\theta = 20^{\circ}$, length $= 2b = 18"$. The attachments consisted of 1/4-inch diameter bolts at the ends of both the trough lines and the crest lines.

The results of the experiments, as given by Rothwell, are represented by the circles in figure 22. The lower curve in figure 22 is the theoretical prediction of the present theory, assuming point attachments at the ends of both the crest lines and the trough lines and assuming an isotropic material with Poisson's ratio of 0.3. The upper curve is the theoretical prediction given by Rothwell, based on his theory, which assumes inextensional deformation for the middle surface (thereby implying that the generators remain straight lines) but makes an approximate correction for the shear strain of the middle surface.

As is to be expected, the present theory, with its more degrees of freedom, predicts lower shear stiffnesses than Rothwell's, but it also predicts lower shear stiffnesses than those obtained experimentally. This may be due to the finite width of the bolt heads used in the end attachments or perhaps to interference between the deformation of the crest and trough plate elements and the member to which the attachment is made. There is not enough detail in reference 2 about the experiment to permit a more definite assessment of the cause of the discrepancy, and the original source, reference 8, is not available at the time of this writing.

CONCLUDING REMARKS

A theoretical analysis (based on the method of minimum potential energy) and numerical results have been presented for the elastic shearing of a trapezoidally corrugated plate with discontinuous attachments at the ends of the corrugations. The present work is an extension of previous work (ref. 1) in which the same problem was considered but with the trough lines assumed to be held straight. Thus the present work is more nearly applicable to a corrugated plate by itself, while the previous work was more pertinent to a corrugated plate fastened to a flat plate.

TABLE 4. - PEAK VALUES OF $\sigma_{(1)}p/Eu_0$ AND $\sigma_{(2)}p/Eu_0$

End Condition	$\frac{h}{p} = \frac{f}{p} = \frac{2e}{p}$	$\frac{b}{p}\left(\frac{t}{p}\right)^{3/2}$	$\frac{t}{p}$	$\frac{2b}{p}$	$\frac{\sigma_{(1)}p}{Eu_0}$	$\frac{\sigma_{(2)}p}{Eu_0}$	$\frac{z}{b}$
Fig. 2(a)	.2	.002	.005	11.3	0.8317	-0.3166	0.83
			.015	2.18	0.4458	-0.1640	0.65
			.050	.358	0.0400	-0.0087	0.55
		.02	.005	113	3.9844	-1.5150	0.99
			.015	21.8	2.1597	-0.7854	0.96
			.050	3.58	0.8962	-0.2957	0.88
	.4	.002	.005	11.3	0.1680	-0.0565	0.65
			.015	2.18	0.0175	-0.0056	0.60
			.050	.358	0.00086	-0.00019	0.60
		.02	.005	113	1.3673	-0.4595	0.96
			.015	21.8	0.7722	-0.2583	0.88
			.050	3.58	0.3740	-0.1234	0.65
Fig. 2(b)	.2	.002	.005	11.3	0.7942	-0.7879	0.88
			.015	2.18	0.4288	-0.4179	0.65
			.050	.358	0.0347	-0.0327	0.60
		.02	.005	113	3.1623	-3.1381	0.99
			.015	21.8	1.6835	-1.6466	0.96
			.050	3.58	0.6462	-0.6122	0.88
	.4	.002	.005	11.3	0.1661	-0.1659	0.65
			.015	2.18	0.0174	-0.1736	0.60
			.050	.358	0.00085	-0.00085	0.60
		.02	.005	113	1.2289	-1.2280	0.96
			.015	21.8	0.6955	-0.6941	0.88
			.050	3.58	0.3398	-0.3375	0.65
Fig. 2(d)	.2	.002	.005	11.3	0.2158	0.8906	0.88
			.015	2.18	0.1049	0.4532	0.65
			.050	3.58	0.0138	0.0349	0.60
		.02	.005	113	0.2720	0.1120	0.99
			.015	21.8	0.1368	0.5781	0.97
			.050	3.58	0.0508	0.2051	0.88
	.4	.002	.005	11.3	0.1502	0.2258	0.65
			.015	2.18	0.0165	0.0248	0.60
			.050	.358	0.0008	0.0012	0.60
		.02	.005	113	0.7261	1.0910	0.96
			.015	21.8	0.4066	0.6127	0.88
			.050	3.58	0.1916	0.2914	0.65

Three different kinds of end-attachment conditions have been assumed in the present work, as in reference 1: (a) Point attachments at the ends of the trough lines only, (b) point attachments at the ends of the trough lines and the crest lines, and (c) wide attachments at the ends of the trough lines only, the width of the attachment being the full width of the plate element at the trough.

Based on the analysis, numerical results have been presented for the effective shearing stiffness and certain maximum stresses for a wide range of geometries. A knowledge of these quantities is felt to be of importance in the design and stress analysis of trapezoidally corrugated plates intended as shear webs.

The numerical results confirm the by now well known fact that the absence of continuous attachment at the ends of the corrugations can cause a marked lowering of the effective shear stiffness, even for corrugation lengths many times larger than the pitch. This lowering of the shear stiffness results from the large frame-like flexural deformations of the cross sections permitted by the discontinuous end attachment. Of the three kinds of end conditions considered, point attachments at the ends of the trough lines gave the lowest shear stiffness, as was to be expected. A moderate increase in stiffness was obtained for the case of point attachments at the ends of the crest lines and the trough lines, but a very marked increase was obtained by having wide attachments at the ends of the trough lines only. The case of wide attachments represents an upper limit to the constraint provided by point attachments at the ends of the trough lines plus one-sided interference between the troughs and the member to which the troughs are attached.

Because of the discreteness of the end attachments, the stresses can be quite non-uniform along the length of the corrugation. In particular, the middle-surface shear stress in the trough plate element was observed to peak significantly at the ends of the corrugation. The most significant stress, from the point of view of magnitude, was found to be an extreme-fiber bending stress associated with the flexural deformation of the end cross section. However, data have also been presented for the maximum middle-surface shear stress and the maximum extreme-fiber shear stress (combination of middle-surface and torsional shear stress). A limited amount of numerical data (table 4) was presented on the maximum longitudinal normal stresses. The longitudinal normal stresses vanish at the ends but in the interior reach peak values which may exceed the maximum shear stress.

For a given basic shape of cross-sectional centerline, two additional dimensionless parameters are required to completely define the geometry of the corrugations to within a scale factor, e.g. a thickness parameter t/p and a length parameter $2b/p$. The numerical work revealed, however, that if a certain combination of length and thickness were used as one of the parameters, then the dimensionless shear stiffness and dimensionless stresses would be virtually independent of the second parameter. The combination parameter that serves this purpose was found to be $(b/p)(t/p)^{3/2}$. (The analogous parameter when trough lines are held straight (ref. 1) was bt/p^2 .)

Except for the very small or very large length-to-pitch ratios and except for the case of wide attachments a significant difference in shear stiffness was found to exist between the case of trough lines held straight (ref. 1) and the present case of trough lines which are permitted to curve. This suggests that the assumption frequently made (or implied) in the shearing analysis of corrugated plates, that the generators remain straight lines, may be questionable in some cases and for some range of geometries.

In reference 1, it was found that the analytical results taking into account the torsional stiffness of the plate elements making up the corrugation were only very slightly different from those obtained neglecting the torsional stiffness. Calculations, the results of which have not been presented, show that the same phenomenon is true in the present case, thus tending to justify the simplified manner in which the torsional strain energy was included in the total potential energy expression — i.e. by the use of an average rate of twist across the width of each plate element rather than the detailed pointwise rate of twist.

Inasmuch as the present analysis is based on the method of minimum potential energy, one could claim that it over estimates the shear stiffness were it not for the approximate treatment of the torsional strain energy and the assumed absence of interaction between the frame bending moments and the longitudinal curvatures. Because of these simplifications one can only claim that the shear stiffness is <u>probably</u> over-estimated.

It would appear that worth-while avenues of future analytical work on the shearing of corrugated plates should include the extension of the present approach to (a) the case of one-sided interference between the corrugation ends and the member to which the ends are attached and (b) the case of curvilinear (e.g., circular arc) corrugation. The shearing of the circular-arc corrugation has been studied by McKenzie (ref. 6), but on the basis of the assumption that the generators remain straight and inextensible. As already noted, such an assumption may not be appropriate in all cases.

APPENDIX A

VARIATION OF THE TPE

Equation (16) in expanded form is

$$
\begin{aligned}
TPE = & \int_{-b.}^{b} \left[b_{11}\left(\frac{du_1}{dz}\right)^2 + 2b_{12}\frac{du_1}{dz}\frac{du_2}{dz} + b_{22}\left(\frac{du_2}{dz}\right)^2 \right] dz \\
& + \int_{-b}^{b} (c_{00}u_0^2 + c_{11}u_1^2 + c_{22}u_2^2 + 2c_{01}u_0u_1 + 2c_{12}u_1u_2) dz \\
& + \int_{-b}^{b} \left(d_{00}u_0\frac{dv_0}{dz} + d_{10}u_1\frac{dv_0}{dz} + d_{20}u_2\frac{dv_0}{dz} + d_{11}u_1\frac{dv_1}{dz} \right. \\
& \left. + d_{21}u_2\frac{dv_1}{dz} + d_{22}u_2\frac{dv_2}{dz} \right) dz \\
& + \int_{-b}^{b} \left[e_{00}\left(\frac{dv_0}{dz}\right)^2 + e_{11}\left(\frac{dv_1}{dz}\right)^2 + e_{22}\left(\frac{dv_2}{dz}\right)^2 \right. \\
& \left. + 2e_{10}\frac{dv_1}{dz}\frac{dv_0}{dz} + 2e_{20}\frac{dv_2}{dz}\frac{dv_0}{dz} + 2e_{12}\frac{dv_1}{dz}\frac{dv_2}{dz} \right] dz \\
& + \int_{-b}^{b} (a_{11}v_1^2 + 2a_{12}v_1v_2 + a_{22}v_2^2) dz - 2\,F\,u_0 \qquad \text{(A1)}
\end{aligned}
$$

where

$$
\left.
\begin{aligned}
e_{00} &\equiv e^*_{00} & e_{10} &\equiv e^*_{10} \\
e_{11} &\equiv e^*_{11} + \bar{e}_{11} & e_{20} &\equiv e^*_{20} \\
e_{22} &\equiv e^*_{22} + \bar{e}_{22} & e_{12} &\equiv e^*_{12} + \bar{e}_{12}
\end{aligned}
\right\} \qquad \text{(A2)}
$$

The first variation of the TPE due to the small variations δu_0, $\delta u_1(z)$, $\delta u_2(z)$, $\delta v_0(z)$, $\delta v_1(z)$, $\delta v_2(z)$ in the displacements u_0, $u_1(z)$, ..., $v_2(z)$ is

$$
\begin{aligned}
\delta(\mathrm{TPE}) = {} & 2\int_{-b}^{b}\left\{b_{11}\frac{du_1}{dz}\frac{d(\delta u_1)}{dz} + b_{12}\left[\frac{du_1}{dz}\frac{d(\delta u_2)}{dz} + \frac{du_2}{dz}\frac{d(\delta u_1)}{dz}\right]\right. \\
& \left. + b_{22}\frac{du_2}{dz}\frac{d(\delta u_2)}{dz}\right\}dz \\
& + 2\int_{-b}^{b}\left[c_{00}u_0\delta u_0 + c_{11}u_1\delta u_1 + c_{22}u_2\delta u_2 + c_{01}(u_0\delta u_1 + u_1\delta u_0)\right. \\
& \left. + c_{12}(u_1\delta u_2 + u_2\delta u_1)\right]dz \\
& + \int_{-b}^{b}\left\{d_{00}\left[u_0\frac{d(\delta v_0)}{dz} + \frac{dv_0}{dz}\delta u_0\right] + d_{10}\left[u_1\frac{d(\delta v_0)}{dz} + \frac{dv_0}{dz}\delta u_1\right]\right. \\
& + d_{20}\left[u_2\frac{d(\delta v_0)}{dz} + \frac{dv_0}{dz}\delta u_2\right] + d_{11}\left[u_1\frac{d(\delta v_1)}{dz} + \frac{dv_1}{dz}\delta u_1\right] \\
& \left. + d_{21}\left[u_2\frac{d(\delta v_1)}{dz} + \frac{dv_1}{dz}\delta u_2\right] + d_{22}\left[u_2\frac{d(\delta v_2)}{dz} + \frac{dv_2}{dz}\delta u_2\right]\right\}dz \\
& + 2\int_{-b}^{b}\left\{e_{00}\frac{dv_0}{dz}\frac{d(\delta v_0)}{dz} + e_{11}\frac{dv_1}{dz}\frac{d(\delta v_1)}{dz} + e_{22}\frac{dv_2}{dz}\frac{d(\delta v_2)}{dz}\right. \\
& + e_{10}\left[\frac{dv_1}{dz}\frac{d(\delta v_0)}{dz} + \frac{dv_0}{dz}\frac{d(\delta v_1)}{dz}\right] + e_{20}\left[\frac{dv_2}{dz}\frac{d(\delta v_0)}{dz} + \frac{dv_0}{dz}\frac{d(\delta v_2)}{dz}\right] \\
& \left. + e_{12}\left[\frac{dv_1}{dz}\frac{d(\delta v_2)}{dz} + \frac{dv_2}{dz}\frac{d(\delta v_1)}{dz}\right]\right\}dz \\
& + 2\int_{-b}^{b}\left[a_{11}v_1\delta v_1 + a_{12}(v_1\delta v_2 + v_2\delta v_1) + a_{22}v_2\delta v_2\right]dz - 2F\cdot\delta u_0
\end{aligned}
\tag{A3}
$$

Where the derivative of a variation appears in the integrand of equation (A3), integration by parts will transform such a term so that the integrand involves the variation itself, rather than the derivative of the variation, and will also introduce boundary terms. Using the first term as an example,

$$\int_{-b}^{b} \frac{du_1}{dz} \frac{d(\delta u_1)}{dz}\, dz = \frac{du_1}{dz}\, \delta u_1 \Big|_{-b}^{b} - \int_{-b}^{b} \frac{d^2 u_1}{dz^2}\, \delta u_1 dz$$

Reducing all integrands in this fashion wherever possible, and utilizing the boundary condition

$$v_0(\pm b) = 0 \quad , \quad \delta v_0(\pm b) = 0 \tag{A4}$$

which applies to all three types of end conditions shown in figure 2, one obtains

$$\begin{aligned}
\delta(\mathrm{TPE}) = {} & (\delta u_0) \cdot \int_{-b}^{b} (2c_{00}u_0 + 2c_{01}u_1 - \frac{F}{b}) dz \\
& + 2 \int_{-b}^{b} \left(-b_{11} \frac{d^2 u_1}{dz^2} - b_{12} \frac{d^2 u_2}{dz^2} + c_{01}u_0 + c_{11}u_1 + c_{12}u_2 \right. \\
& \left. + \frac{1}{2} d_{10} \frac{dv_0}{dz} + \frac{1}{2} d_{11} \frac{dv_1}{dz} \right) (\delta u_1) dz \\
& + 2 \int_{-b}^{b} \left(-b_{12} \frac{d^2 u_1}{dz^2} - b_{22} \frac{d^2 u_2}{dz^2} + c_{12}u_1 + c_{22}u_2 + \frac{1}{2} d_{20} \frac{dv_0}{dz} \right. \\
& \left. + \frac{1}{2} d_{21} \frac{dv_1}{dz} + \frac{1}{2} d_{22} \frac{dv_2}{dz} \right) (\delta u_2) dz \\
& - 2 \int_{-b}^{b} \left(\frac{1}{2} d_{10} \frac{du_1}{dz} + \frac{1}{2} d_{20} \frac{du_2}{dz} + e_{00} \frac{d^2 v_0}{dz^2} + e_{10} \frac{d^2 v_1}{dz^2} + e_{20} \frac{d^2 v_2}{dz^2} \right) (\delta v_0) dz \\
& + 2 \int_{-b}^{b} \left(a_{11}v_1 + a_{12}v_2 - \frac{1}{2} d_{11} \frac{du_1}{dz} - \frac{1}{2} d_{21} \frac{du_2}{dz} - e_{10} \frac{d^2 v_0}{dz^2} \right. \\
& \left. - e_{11} \frac{d^2 v_1}{dz^2} - e_{12} \frac{d^2 v_2}{dz^2} \right) (\delta v_1) dz
\end{aligned}$$

(equation continued on next page)

$$+ 2 \int_{-b}^{b} \left(a_{12} v_1 + a_{22} v_2 - \frac{1}{2} d_{22} \frac{du_2}{dz} - e_{20} \frac{d^2 v_0}{dz^2} - e_{12} \frac{d^2 v_1}{dz^2} \right.$$

$$\left. - e_{22} \frac{d^2 v_2}{dz^2} \right) (\delta v_2) dz + 2 \left[\left(b_{11} \frac{du_1}{dz} + b_{12} \frac{du_2}{dz} \right) (\delta u_1) \right] \Bigg|_{-b}^{b}$$

$$+ 2 \left[\left(b_{12} \frac{du_1}{dz} + b_{22} \frac{du_2}{dz} \right) (\delta u_2) \right] \Bigg|_{-b}^{b} + \left[d_{11} u_1 + d_{21} u_2 + 2e_{10} \frac{dv_0}{dz} \right.$$

$$\left. + 2e_{11} \frac{dv_1}{dz} + 2e_{12} \frac{dv_2}{dz} \right] (\delta v_1) \Bigg|_{-b}^{b} + \left[d_{22} u_2 + 2e_{20} \frac{dv_0}{dz} \right.$$

$$\left. + 2e_{12} \frac{dv_1}{dz} + 2e_{22} \frac{dv_2}{dz} \right] (\delta v_2) \Bigg|_{-b}^{b} \qquad \text{(A5)}$$

Equation (A5) is valid as it stands for the case in which there are point attachments at the ends of the trough lines only (fig. 2(a)). If the attachment is one of the other two types shown in figure 2, equation (A5) must be modified to take into account the implied constraints on δv_1 and δv_2 at $z = \pm b$.

Thus, if there are wide attachments at the ends of the trough lines (fig. 2(d)), it follows that

$$(\delta v_1)_{z=\pm b} = 0 \qquad \text{(A6)}$$

and the next-to-the last term in equation (A5) must therefore be omitted. If there are point attachments at the ends of the crest lines as well as the trough lines (fig. 2(b)), the resulting constraint against horizontal displacement of the crest attachment point is expressible as

$$[(v_1 \sin\theta)\cos\theta + v_2 \sin\theta - v_0]_{z=\pm b} = 0 \qquad \text{(A7)}$$

Taking into account equation (A4) and considering that $\sin\theta \neq 0$, this becomes

$$(v_1 \cos\theta + v_2)_{z=\pm b} = 0 \qquad \text{(A8)}$$

or, in variational form,

$$(\delta v_1 \cos\theta + \delta v_2)_{z=\pm b} = 0 \qquad \text{(A9)}$$

Thus, for the type of end attachment shown in figure 2(b), δv_2 in the last term of equation (A5) should be replaced by $-\delta v_1 \cos\theta$. The last two terms of equation (A5) can then be combined, leading to the following form of the equation for $\delta(\text{TPE})$:

$$\begin{aligned}
\delta(\text{TPE}) \;=\; & (\delta u_0)\cdot\int_{-b}^{b}(\ldots)dz + 2\int_{-b}^{b}(\ldots)(\delta u_1)dz \\
& + 2\int_{-b}^{b}(\ldots)(\delta u_2)dz - 2\int_{-b}^{b}(\ldots)(\delta v_0)dz \\
& + 2\int_{-b}^{b}(\ldots)(\delta v_1)dz + 2\int_{-b}^{b}(\ldots)(\delta v_2)dz \\
& + 2\left[\left(b_{11}\frac{du_1}{dz} + b_{12}\frac{du_2}{dz}\right)(\delta u_1)\right]\Bigg|_{-b}^{b} \\
& + 2\left[\left(b_{12}\frac{du_1}{dz} + b_{22}\frac{du_2}{dz}\right)(\delta u_2)\right]\Bigg|_{-b}^{b} \\
& + \left\{\left[d_{11}u_1 + d_{21}u_2 + 2e_{10}\frac{dv_0}{dz} + 2e_{11}\frac{dv_1}{dz} + 2e_{12}\frac{dv_2}{dz}\right.\right. \\
& \left.\left. - \left(d_{22}u_2 + 2e_{20}\frac{dv_0}{dz} + 2e_{12}\frac{dv_1}{dz} + 2e_{22}\frac{dv_2}{dz}\right)\cos\theta\right](\delta v_1)\right\}\Bigg|_{-b}^{b}
\end{aligned} \tag{A10}$$

in which the symbol (...) has been used to represent terms that are identical to the corresponding terms in expression (A5).

Differential equations. - In order for the TPE to be a minimum, $\delta(\text{TPE})$ must vanish for all possible values of δu_0, δu_1, δu_2, δv_0, δv_1, δv_2 consistent with the constraints. Thus the coefficients of the latter five quantities in the various integrands of equation (A5) must individually vanish, as well as the entire integral coefficient of δu_0 . This leads to the following system of one integral equation and five differential equations, which apply regardless of the type of end attachment:

$$4c_{00}u_0 b + 2c_{01}\int_{-b}^{b} u_1 dz - 2F = 0 \tag{A11}$$

$$
\left.
\begin{aligned}
&-b_{11}\frac{d^2u_1}{dz^2} - b_{12}\frac{d^2u_2}{dz^2} + c_{01}u_0 + c_{11}u_1 + c_{12}u_2 + \tfrac{1}{2}d_{10}\frac{dv_0}{dz} + \tfrac{1}{2}d_{11}\frac{dv_1}{dz} = 0\\
&-b_{12}\frac{d^2u_1}{dz^2} - b_{22}\frac{d^2u_2}{dz^2} + c_{12}u_1 + c_{22}u_2 + \tfrac{1}{2}d_{20}\frac{dv_0}{dz} + \tfrac{1}{2}d_{21}\frac{dv_1}{dz} + \tfrac{1}{2}d_{22}\frac{dv_2}{dz} = 0\\
&\tfrac{1}{2}d_{10}\frac{du_1}{dz} + \tfrac{1}{2}d_{20}\frac{du_2}{dz} + e_{00}\frac{d^2v_0}{dz^2} + e_{10}\frac{d^2v_1}{dz^2} + e_{20}\frac{d^2v_2}{dz^2} = 0\\
&a_{11}v_1 + a_{12}v_2 - \tfrac{1}{2}d_{11}\frac{du_1}{dz} - \tfrac{1}{2}d_{21}\frac{du_2}{dz} - e_{10}\frac{d^2v_0}{dz^2} - e_{11}\frac{d^2v_1}{dz^2} - e_{12}\frac{d^2v_2}{dz^2} = 0\\
&a_{12}v_1 + a_{22}v_2 - \tfrac{1}{2}d_{22}\frac{du_2}{dz} - e_{20}\frac{d^2v_0}{dz^2} - e_{12}\frac{d^2v_1}{dz^2} - e_{22}\frac{d^2v_2}{dz^2} = 0
\end{aligned}
\right\} \quad (A12)
$$

Boundary conditions. - The vanishing of $\delta(TPE)$ also requires that the boundary terms of the $\delta(TPE)$ expression vanish identically for all variations in v_1, v_2, u_1 and u_2 at $z = \pm b$ consistent with the constraints. Referring to equation (A5), which applies to the case of point attachments at the ends of the trough lines only, it is seen that this requirement leads to the following boundary conditions:

$$
\left.
\begin{aligned}
&b_{11}\frac{du_1}{dz} + b_{12}\frac{du_2}{dz} = 0\\
&b_{12}\frac{du_1}{dz} + b_{22}\frac{du_2}{dz} = 0\\
&d_{11}u_1 + d_{21}u_2 + 2e_{10}\frac{dv_0}{dz} + 2e_{11}\frac{dv_1}{dz} + 2e_{12}\frac{dv_2}{dz} = 0\\
&d_{22}u_2 + 2e_{20}\frac{dv_0}{dz} + 2e_{12}\frac{dv_1}{dz} + 2e_{22}\frac{dv_2}{dz} = 0
\end{aligned}
\right\} \quad (A13)
$$

at $z = \pm b$. Inasmuch as $b_{11}b_{22} - b_{12}^2$ does not vanish, the first two of these equations may be replaced by

$$
\frac{du_1}{dz} = 0 \quad \text{and} \quad \frac{du_2}{dz} = 0 \qquad (A14)
$$

at $z = \pm b$. Thus, the complete set of boundary conditions corresponding to the case of point attachments at the ends of the trough lines only (fig. 2(a)) consists of equations (A13), (A14) and

$$v_0(\pm b) = 0 \tag{A15}$$

which is the first of equations (A4).

For the case of wide attachments at the ends of the trough lines (fig. 2(d)), expression (A5) applies but with the next-to-the-last term excluded. As a result, the first of equations (A13) is non-existent, and the condition

$$v_1(\pm b) = 0 \tag{A16}$$

is used in its stead. Otherwise the boundary conditions are the same as for the previous case.

For the third case, in which there are point attachments at the ends of the crest lines as well as the trough lines (fig. 2(b)), equation (A8) constitutes one of the boundary conditions, and equation (A15) a second. The remaining three boundary conditions, implied by the vanishing of the boundary terms of expression (A10), are equations (A14) and the following:

$$d_{11}u_1 + d_{21}u_2 + 2e_{10}\frac{dv_0}{dz} + 2e_{11}\frac{dv_1}{dz} + 2e_{12}\frac{dv_2}{dz}$$

$$- \left(d_{22}u_2 + 2e_{20}\frac{dv_0}{dz} + 2e_{12}\frac{dv_1}{dz} + 2e_{22}\frac{dv_2}{dz}\right)\cos\theta = 0 \tag{A17}$$

at $z = \pm b$.

Equations (A14) in conjunction with the fact that $du_0/dz = 0$, are readily interpreted to mean that the longitudinal normal stress acting at the corrugation ends vanishes.

Following the procedure of appendix B of reference 1, equations (A13) and (A17) can be shown to be equivalent to the requirement that certain effective in-plane shears at the ends of the plate elements vanish.

APPENDIX B

SOLUTION OF THE EQUATIONS FOR BASIC UNKNOWNS

Equations (17) and (18) are the field equations of the physical problem. In this appendix equations (17) will be solved for $u_1(z)$, $u_2(z)$, $v_0(z)$, $v_1(z)$ and $v_2(z)$ in terms of u_0, subject to boundary conditions of equations (19), (20) and (21); or equations (19), (20), (22) and the second of equations (21); or equations (23), (24), (25) and (26). Then the relationship between the shearing force F and the total relative shearing displacement $2u_0$ of one side of the corrugation with respect to the other can be obtained from equation (18). Physical arguments can be used to show that u_1 and u_2 should be even functions of z and v_0, v_1 and v_2 odd functions of z. The subsequent work will be simplified by considering only that solution of equations (17) which satisfies these conditions.

Particular integral. - A particular integral of equations (17) will be sought in the following form, consistent with the even-ness of u_1 and u_2 and the oddness of v_0, v_1, v_2 :

$$u_1 = \text{constant} \quad , \quad u_2 = \text{constant} \quad , \quad v_0 = 0 \quad , \quad v_1 = 0 \quad , \quad v_2 = 0$$

For this form of particular integral the last three of equations (17) are identically satisfied while the first two reduce to

$$c_{11}u_1 + c_{12}u_2 = -c_{01}u_0$$

$$c_{12}u_1 + c_{22}u_2 = 0$$

whence

$$\left.\begin{aligned} u_1 &= \zeta_1 u_0 \\ u_2 &= \zeta_2 u_0 \end{aligned}\right\} \quad \text{(B1)}$$

with

$$\left.\begin{aligned} \zeta_1 &\equiv \frac{-c_{01}c_{22}}{c_{11}c_{22} - c_{12}^2} \\ \zeta_2 &\equiv \frac{c_{01}c_{12}}{c_{11}c_{22} - c_{12}^2} \end{aligned}\right\} \quad \text{(B2)}$$

Thus a particular solution of equations (17) is

$$\begin{aligned} u_1 &= \zeta_1 u_0 \\ u_2 &= \zeta_2 u_0 \\ v_0 &= 0 \\ v_1 &= 0 \\ v_2 &= 0 \end{aligned} \tag{B3}$$

Characteristic equation for complementary solutions. - The complete solution of equations (17) consists of two parts: (i) the particular integral, equations (B3), and (ii) the complementary solutions, i.e. all the linearly independent solutions of the homogeneous system obtained by setting u_0 equal to zero . Solutions of this homogeneous system will first be sought in the following form:

$$\begin{aligned} u_1 &= Ae^{rz} \\ u_2 &= Be^{rz} \\ v_1 &= Ce^{rz} \\ v_2 &= De^{rz} \\ v_0 &= Ee^{rz} \end{aligned} \tag{B4}$$

Substituting these assumptions in equations (17) with u_0 set equal to zero leads to the following restrictions on A, B, C, D, E and r :

$$\begin{bmatrix} b_{11}r^2-c_{11} & b_{12}r^2-c_{12} & -\frac{1}{2}d_{11}r & 0 & -\frac{1}{2}d_{10}r \\ b_{12}r^2-c_{12} & b_{22}r^2-c_{22} & -\frac{1}{2}d_{21}r & -\frac{1}{2}d_{22}r & -\frac{1}{2}d_{20}r \\ -\frac{1}{2}d_{11}r & -\frac{1}{2}d_{21}r & a_{11}-e_{11}r^2 & a_{12}-e_{12}r^2 & -e_{10}r^2 \\ 0 & -\frac{1}{2}d_{22}r & a_{12}-e_{12}r^2 & a_{22}-e_{22}r^2 & -e_{20}r^2 \\ -\frac{1}{2}d_{10}r & -\frac{1}{2}d_{20}r & -e_{10}r^2 & -e_{20}r^2 & -e_{00}r^2 \end{bmatrix} \begin{bmatrix} A \\ B \\ C \\ D \\ E \end{bmatrix} = \begin{bmatrix} 0 \\ 0 \\ 0 \\ 0 \\ 0 \end{bmatrix} \tag{B5}$$

Thus, for non-trival solutions of the form of equations (B4), r must satisfy the following characteristic equation:

$$\begin{vmatrix} b_{11}r^2-c_{11} & b_{12}r^2-c_{12} & -\frac{1}{2}d_{11}r & 0 & -\frac{1}{2}d_{10}r \\ b_{12}r^2-c_{12} & b_{22}r^2-c_{22} & -\frac{1}{2}d_{21}r & -\frac{1}{2}d_{22}r & -\frac{1}{2}d_{20}r \\ -\frac{1}{2}d_{11}r & -\frac{1}{2}d_{21}r & a_{11}-e_{11}r^2 & a_{12}-e_{12}r^2 & -e_{10}r^2 \\ 0 & -\frac{1}{2}d_{22}r & a_{12}-e_{12}r^2 & a_{22}-e_{22}r^2 & -e_{20}r^2 \\ -\frac{1}{2}d_{10}r & -\frac{1}{2}d_{20}r & -e_{10}r^2 & -e_{20}r^2 & -e_{00}r^2 \end{vmatrix} = 0 \qquad \text{(B6)}$$

Expanding the determinant by cofactors based upon the fifth column, multiplying through by -32 for convenience, and introducing the shorthand notation

$$\left.\begin{aligned} \hat{a} &\equiv a_{11}a_{22} - a_{12}^2 & \hat{g} &\equiv 2a_{12}e_{12} - a_{11}e_{22} - a_{22}e_{11} \\ \hat{b} &\equiv b_{11}b_{22} - b_{12}^2 & \hat{h} &\equiv a_{12}d_{22} - a_{22}d_{21} \\ \hat{c} &\equiv c_{11}c_{22} - c_{12}^2 & \hat{j} &\equiv a_{11}d_{22} - a_{12}d_{21} \\ \hat{e} &\equiv e_{11}e_{22} - e_{12}^2 & \hat{k} &\equiv d_{21}e_{22} - d_{22}e_{12} \\ \hat{f} &\equiv 2b_{12}c_{12} - b_{11}c_{22} - b_{22}c_{11} & \hat{m} &\equiv d_{21}e_{12} - d_{22}e_{11} \end{aligned}\right\} \qquad \text{(B7)}$$

$$\left.\begin{aligned} \hat{d}_1 &\equiv b_{22}d_{10} - b_{12}d_{20} & \hat{d}_6 &\equiv 4a_{12}b_{22} - d_{21}d_{22} + 4c_{22}e_{12} \\ \hat{d}_2 &\equiv c_{12}d_{20} - c_{22}d_{10} & \hat{d}_7 &\equiv 4a_{22}b_{22} + 4c_{22}e_{22} - d_{22}^2 \\ \hat{d}_3 &\equiv 8c_{12}e_{20} - 2d_{10}d_{22} & \hat{d}_8 &\equiv a_{22}e_{10} - a_{12}e_{20} \\ \hat{d}_4 &\equiv c_{11}d_{20} - c_{22}d_{10} & \hat{d}_9 &\equiv 2d_{10}d_{21} - 2d_{11}d_{20} - 8c_{12}e_{10} \\ \hat{d}_5 &\equiv e_{12}e_{20} - e_{10}e_{22} \end{aligned}\right\} \qquad \text{(B8)}$$

$$\hat{n}_1 \equiv b_{12}d_{10} - b_{11}d_{20} \qquad \hat{n}_3 \equiv 2d_{10}d_{11} - 8c_{11}e_{10}$$
$$\hat{n}_2 \equiv c_{11}d_{20} - c_{12}d_{10} \qquad \hat{n}_4 \equiv a_{22}e_{10} - a_{12}e_{20} \tag{B9}$$

$$\hat{p}_1 \equiv e_{11}e_{20} - e_{10}e_{12} \qquad \hat{p}_5 \equiv 4a_{12}b_{12} + 4c_{12}e_{12} - d_{11}d_{22}$$
$$\hat{p}_2 \equiv 4a_{11}b_{22} + 4c_{22}e_{11} - d_{21}^2 \qquad \hat{p}_6 \equiv b_{12}d_{10} - b_{11}d_{20}$$
$$\hat{p}_3 \equiv 4a_{11}b_{12} + 4c_{12}e_{11} - d_{11}d_{21} \qquad \hat{p}_7 \equiv c_{12}d_{20} - c_{22}d_{10} \tag{B10}$$
$$\hat{p}_4 \equiv 4a_{12}b_{22} + 4c_{22}e_{12} - d_{22}d_{21} \qquad \hat{p}_8 \equiv a_{12}e_{10} - a_{11}e_{20}$$

$$\hat{q}_1 \equiv 2b_{12}c_{12} - b_{11}c_{22} - b_{22}c_{11} \qquad \hat{q}_3 \equiv b_{11}d_{21} - b_{12}d_{11}$$
$$\hat{q}_2 \equiv d_{22}e_{20} - d_{20}e_{22} \qquad \hat{q}_4 \equiv d_{22}e_{10} - d_{20}e_{12} \tag{B11}$$

one converts equation (B6) to

$$(k_0 + k_2r^2 + k_4r^4 + k_6r^6 + k_8r^8)r^2 = 0 \tag{B12}$$

where

$$\begin{aligned}
k_0 &= 2e_{00}\lambda_5 + d_{10}\lambda_9 - d_{20}\lambda_{13} \\
k_2 &= 2e_{00}\lambda_4 + d_{10}\lambda_8 - d_{20}\lambda_{12} - 2e_{20}\lambda_{17} + 2e_{10}\lambda_{21} \\
k_4 &= 2e_{00}\lambda_3 + d_{10}\lambda_7 - d_{20}\lambda_{11} - 2e_{20}\lambda_{16} + 2e_{10}\lambda_{20} \\
k_6 &= 2e_{00}\lambda_2 + d_{10}\lambda_6 - d_{20}\lambda_{10} - 2e_{20}\lambda_{15} + 2e_{10}\lambda_{19} \\
k_8 &= 2e_{00}\lambda_1 - 2e_{20}\lambda_{14} + 2e_{10}\lambda_{18}
\end{aligned} \tag{B13}$$

with

$$\left.\begin{aligned}
\lambda_1 &= 16\hat{b}\hat{e} \\
\lambda_2 &= 16(\hat{b}\hat{g} + \hat{e}\hat{f}) + 4\hat{k}(b_{11}d_{21} - 2b_{12}d_{11}) - 4b_{11}d_{22}\hat{m} \\
&\quad + 4b_{22}d_{11}^2 e_{22} \\
\lambda_3 &= 16(\hat{a}\hat{b} + \hat{c}\hat{e} + \hat{f}\hat{g}) + 4b_{11}(d_{21}\hat{h} - d_{22}\hat{j}) + 4c_{11}(d_{22}\hat{m} - d_{21}\hat{k}) \\
&\quad + 8d_{11}(c_{12}\hat{k} - b_{12}\hat{h}) + d_{11}^2(d_{22}^2 - 4a_{22}b_{22} \quad 4c_{22}e_{22}) \\
\lambda_4 &= 16(\hat{a}\hat{f} + \hat{c}\hat{g}) + 4\hat{h}(2c_{12}d_{11} - c_{11}d_{21}) + 4(c_{11}d_{22}\hat{j} + a_{22}c_{22}d_{11}^2)
\end{aligned}\right\} \quad (B14)$$

$$\left.\begin{aligned}
\lambda_5 &= 16\hat{a}\hat{c} \\
\lambda_6 &= 8\hat{e}\hat{d}_1 + 8b_{12}(e_{10}\hat{k} - e_{20}\hat{m}) + 8b_{22}d_{11}\hat{d}_5 \\
\lambda_7 &= 8\hat{g}\hat{d}_1 + 8\hat{e}\hat{d}_2 + 8b_{12}(e_{10}\hat{h} - e_{20}\hat{j}) + \hat{m}\hat{d}_3 + \hat{k}\hat{d}_9 + 2d_{11}(e_{10}\hat{d}_7 - e_{20}\hat{d}_6) \\
\lambda_8 &= 8\hat{a}\hat{d}_1 + 8\hat{g}\hat{d}_4 + \hat{j}\hat{d}_3 + \hat{h}\hat{d}_9 - 8d_{11}c_{22}\hat{d}_8 \\
\lambda_9 &= 8\hat{a}\hat{d}_2
\end{aligned}\right\} \quad (B15)$$

$$\left.\begin{aligned}
\lambda_{10} &= 8\hat{e}\hat{n}_1 + 8b_{11}(e_{10}\hat{k} - e_{20}\hat{m}) + 8b_{12}d_{11}\hat{d}_5 \\
\lambda_{11} &= 8\hat{e}\hat{n}_2 + 8\hat{g}\hat{n}_1 + 8b_{11}(e_{10}\hat{h} - e_{20}\hat{j}) + \hat{k}\hat{n}_3 + 8c_{11}e_{20}\hat{m} \\
&\quad + 8d_{11}b_{12}\hat{n}_4 + 8d_{11}c_{12}(e_{22}e_{10} - e_{12}e_{20}) \\
\lambda_{12} &= 8\hat{a}\hat{n}_1 + 8\hat{g}\hat{n}_2 + 8c_{11}e_{20}\hat{j} + \hat{h}\hat{n}_3 - 8c_{12}d_{11}\hat{n}_4 + 2a_{22}d_{11}^2 d_{20} \\
\lambda_{13} &= 8\hat{a}\hat{n}_2
\end{aligned}\right\} \quad (B16)$$

$$\lambda_{14} = 16\hat{b}\hat{p}_1$$

$$\lambda_{15} = 4\hat{m}\hat{p}_6 + 16(b_{12}c_{12} - c_{11}b_{22})\hat{p}_1 - 4b_{11}e_{20}\hat{p}_2$$
$$+ 4b_{12}e_{20}\hat{p}_3 - 4d_{11}e_{12}\hat{d}_1 + 4d_{11}e_{20}(b_{22}d_{11} - b_{12}d_{21})$$
$$+ 4e_{10}(b_{11}\hat{p}_4 - b_{12}\hat{p}_5)$$

$$\lambda_{16} = 4\hat{m}\hat{n}_2 + 4\hat{j}\hat{p}_6 + 4e_{20}(c_{11}\hat{p}_2 - c_{12}\hat{p}_3) + 16(b_{12}c_{12} - b_{11}c_{22})\hat{p}_8$$
$$+ (d_{11}d_{10} - 4c_{11}e_{10})\hat{p}_4 + (4c_{12}e_{10} - d_{11}d_{20})\hat{p}_5$$
$$+ 4d_{11}e_{20}(c_{12}d_{21} - c_{22}d_{11})$$

$$\lambda_{17} = 4\hat{j}\hat{n}_2 + 16\hat{c}\hat{p}_8 + 4a_{12}d_{11}\hat{p}_7$$

(B17)

$$\lambda_{18} = 16\hat{b}\hat{d}_5$$

$$\lambda_{19} = 16\hat{b}\hat{d}_8 + 16\hat{d}_5\hat{q}_1 + 4\hat{q}_2\hat{q}_3 - 4b_{11}d_{22}\hat{q}_4$$
$$+ 4b_{12}d_{10}(d_{21}e_{22} - d_{22}e_{12}) - 4b_{22}d_{10}d_{11}e_{22}$$

$$\lambda_{20} = 16\hat{d}_5\hat{c} + 16\hat{d}_8\hat{q}_1 + 4(c_{12}d_{11} - c_{11}d_{21})\hat{q}_2$$
$$+ 4a_{22}d_{20}\hat{q}_3 + 4c_{11}d_{22}\hat{q}_4 + 4b_{12}d_{10}\hat{h}$$
$$+ d_{10}d_{11}\hat{d}_7 - 4a_{12}b_{11}d_{20}d_{22}$$

$$\lambda_{21} = 16\hat{c}\hat{n}_4 + 4\hat{h}\hat{d}_4 + 4a_{22}d_{11}\hat{p}_7$$

(B18)

From equation (B4) it is evident that the quantity r appearing as the unknown in the characteristic equation (B12) has the dimension of $(\text{length})^{-1}$. For computational purposes one should convert the characteristic equation to an alternate form in which the unknown is dimensionless. This can be done by introducing any characteristic length c (e.g., c could be taken equal to the pitch p) and defining a dimensionless variable R as follows:

$$R = cr \tag{B19}$$

In terms of R equation (B12) becomes

$$(k_0 + \frac{k_2}{c^2} R^2 + \frac{k_4}{c^4} R^4 + \frac{k_6}{c^6} R^6 + \frac{k_8}{c^8} R^8)R^2 = 0 \tag{B20}$$

The roots of equation (B12) will be denoted by $r_1, r_2, \ldots, r_{10}$, those of equation (B20) by $R_1, R_2, \ldots, R_{10}$, and these two sets of roots have the following relationship, in accordance with equation (B19):

$$R_j = cr_j \qquad (j = 1,2,\ldots,10) \tag{B19'}$$

The nature of the roots of the characteristic equation. - Because equation (B20) contains only even powers of R and has R^2 as a factor, the following properties can be postulated for the R_j :

$$\begin{aligned} R_4 &= -R_1 \qquad R_8 = -R_5 \\ R_3 &= -R_2 \qquad R_7 = -R_6 \end{aligned} \tag{B21a}$$

$$\begin{aligned} R_9 &= 0 \\ R_{10} &= 0 \end{aligned} \tag{B21b}$$

Examination of equation (B20) shows that for a given cross-sectional shape (i.e. fixed values of θ, e/c, k/c, and f/c) and fixed ratios of the elastic constants to each other, the R_j are functions of t/c only.

The non-zero roots, R_1 through R_8 , may be real or complex, and for most geometries of interest they are generally complex. In that case the following additional properties may be ascribed to the R_j :

$$R_2 = R_1^* \qquad R_6 = R_5^* \tag{B22}$$

where R_i^* denotes the complex conjugate of R_i .

Complementary solutions associated with $R_1, R_2, \ldots R_8$. - The values of A, B, C, D, and E in equations (B4) associated with the particular non-zero root $r = r_j$ $(j = 1, 2, \ldots, 8)$ will be denoted by A_j, B_j, C_j, D_j, and E_j. The relationships existing among these five coefficients can be obtained by substituting $r = r_j$ into equations (B5) and solving the last four of these equations for the ratios of B, C D and E to A. These equations can be written as follows:

$$\begin{bmatrix} L_{11} & L_{12} & L_{13} & L_{14} \\ L_{12} & L_{22} & L_{23} & L_{24} \\ L_{13} & L_{23} & L_{33} & L_{34} \\ L_{14} & L_{24} & L_{34} & L_{44} \end{bmatrix} \begin{bmatrix} B_j/A_j \\ C_j/A_j \\ D_j/A_j \\ E_j/A_j \end{bmatrix} = \begin{bmatrix} \frac{G}{E} c_{12}^* - \frac{E'}{E} b_{12}^* R_j^2 \\ \frac{1}{2}\frac{G}{E} d_{11}^* R_j \\ 0 \\ \frac{1}{2}\frac{G}{E} d_{10}^* R_j \end{bmatrix} \tag{B23}$$

where

$$\left.\begin{aligned}
L_{11} &= \frac{E'}{E} b_{22}^* R_j^2 - \frac{G}{E} c_{22}^* \\
L_{12} &= -\frac{1}{2}\frac{G}{E} d_{21}^* R_j \\
L_{13} &= -\frac{1}{2}\frac{G}{E} d_{22}^* R_j \\
L_{14} &= -\frac{1}{2}\frac{G}{E} d_{20}^* R_j \\
L_{22} &= a_{11}^* \left(\frac{t}{c}\right)^2 - \left[\frac{G}{E} e_{11}^{**} + \frac{G'}{E}\left(\frac{t}{c}\right)^2 \bar{e}_{11}^*\right] R_j^2 \\
L_{23} &= a_{12}^* \left(\frac{t}{c}\right)^2 - \left[\frac{G}{E} e_{12}^{**} + \frac{G'}{E}\left(\frac{t}{c}\right)^2 \bar{e}_{12}^*\right] R_j^2 \\
L_{24} &= -\frac{G}{E} e_{10}^{**} R_j^2 \\
L_{33} &= a_{22}\left(\frac{t}{c}\right)^2 - \left[\frac{G}{E} e_{22}^{**} + \frac{G'}{E}\left(\frac{t}{c}\right)^2 \bar{e}_{22}^*\right] R_j^2 \\
L_{34} &= -\frac{G}{E} e_{20}^{**} R_j^2 \\
L_{44} &= -\frac{G}{E} e_{00}^{**} R_j^2
\end{aligned}\right\} \tag{B24}$$

with

$$
\left.
\begin{aligned}
a_{11}^{*} &= \frac{(c/e)^3}{12(1-\nu^2)\beta^2}\left[A_{11} + A_{22}\left(\frac{e}{k}\right)^2 \cos^2\theta + 4A_{33}\left(\frac{e}{f}\right)^2 \sin^4\theta \right. \\
&\qquad \left. - A_{12}\,\frac{e}{k}\cos\theta + 2A_{23}\,\frac{e}{k}\,\frac{e}{f}\sin^2\theta\cos\theta - 2A_{13}\,\frac{e}{f}\sin^2\theta\right] \\
a_{12}^{*} &= \frac{(c/e)^3}{12(1-\nu^2)\beta^2}\left[A_{22}\left(\frac{e}{k}\right)^2 \cos\theta - 4A_{33}\left(\frac{e}{f}\right)^2 \sin^2\theta\cos\theta \right. \\
&\qquad \left. - \frac{1}{2}\,A_{12}\,\frac{e}{k} - A_{23}\,\frac{e}{k}\,\frac{e}{f}(\cos^2\theta - \sin^2\theta) + A_{13}\,\frac{e}{f}\cos\theta\right] \\
a_{22}^{*} &= \frac{(c/e)^3}{12(1-\nu^2)\beta^2}\left[A_{22}\left(\frac{e}{k}\right)^2 + 4A_{33}\left(\frac{e}{f}\right)^2 \cos^2\theta - 2A_{23}\,\frac{e}{k}\,\frac{e}{f}\cos\theta\right]
\end{aligned}
\right\} \quad \text{(B25)}
$$

$$
\left.
\begin{aligned}
b_{11}^{*} &= \frac{1}{3}\left(\frac{e}{c} + \frac{k}{c}\right) \\
b_{12}^{*} &= \frac{1}{6}\,\frac{k}{c} \\
b_{22}^{*} &= \frac{1}{6}\left(2\,\frac{k}{c} + \frac{f}{c}\right)
\end{aligned}
\right\} \quad \text{(B26)}
$$

$$
\left.
\begin{aligned}
c_{11}^{*} &= \frac{c}{e} + \frac{c}{k} \\
c_{12}^{*} &= -\frac{c}{k} \\
c_{22}^{*} &= \frac{c}{k} + 2\,\frac{c}{f}
\end{aligned}
\right\} \quad \text{(B27)}
$$

$$
\left.
\begin{aligned}
d_{11}^{*} &= d_{22}^{*} = -2\sin\theta \\
d_{21}^{*} &= 2\sin\theta(1-\cos\theta) \\
d_{10}^{*} &= -2(1-\cos\theta) \\
d_{20}^{*} &= 2(1-\cos\theta)
\end{aligned}
\right\} \quad \text{(B28)}
$$

$$
\left.
\begin{aligned}
e_{00}^{**} &= \frac{e}{c} + \frac{k}{c}\cos^2\theta + \frac{1}{2}\frac{f}{c} \\
e_{11}^{**} &= \sin^2\theta\left(\frac{k}{c} + \frac{1}{2}\frac{f}{c}\cos^2\theta\right) \\
e_{22}^{**} &= \frac{1}{2}\frac{f}{c}\sin^2\theta \\
e_{10}^{**} &= -\frac{1}{2}\left(2\frac{k}{c} + \frac{f}{c}\right)\sin\theta\cos\theta \\
e_{20}^{**} &= -\frac{1}{2}\frac{f}{c}\sin\theta \\
e_{12}^{**} &= \frac{1}{2}\frac{f}{c}\sin^2\theta\cos\theta
\end{aligned}
\right\} \quad \text{(B29)}
$$

$$
\left.
\begin{aligned}
\overline{e}_{11}^{*} &= \frac{1}{3}\left(\frac{c}{e} + \frac{c}{k}\cos^2\theta + 2\frac{c}{f}\sin^4\theta\right) \\
\overline{e}_{22}^{*} &= \frac{1}{3}\left(\frac{c}{k} + 2\frac{c}{f}\cos^2\theta\right) \\
\overline{e}_{12}^{*} &= \frac{1}{3}\left(\frac{c}{k} - 2\frac{c}{f}\sin^2\theta\right)\cos\theta
\end{aligned}
\right\} \quad \text{(B30)}
$$

The solution of equations (B23) will be denoted as follows:

$$
\begin{bmatrix} B_j/A_j \\ C_j/A_j \\ D_j/A_j \\ E_j/A_j \end{bmatrix} = \begin{bmatrix} \gamma_j^B \\ \gamma_j^C \\ \gamma_j^D \\ \gamma_j^E \end{bmatrix} \quad \text{(B31)}
$$

From the last four of equations (B5), it is seen that if r is replaced by its negative, B/A remains unchanged while C/A, D/A and E/A merely change sign. From this property and equations (B21a) it follows that

$$\left.\begin{array}{llll} \gamma_4^B = \gamma_1^B & \gamma_4^C = -\gamma_1^C & \gamma_4^D = -\gamma_1^D & \gamma_4^E = -\gamma_1^E \\ \gamma_3^B = \gamma_2^B & \gamma_3^C = -\gamma_2^C & \gamma_3^D = -\gamma_2^D & \gamma_3^E = -\gamma_2^E \\ \gamma_8^B = \gamma_5^B & \gamma_8^C = -\gamma_5^C & \gamma_8^D = -\gamma_5^D & \gamma_8^E = -\gamma_5^E \\ \gamma_7^B = \gamma_6^B & \gamma_7^C = -\gamma_6^C & \gamma_7^D = -\gamma_6^D & \gamma_7^E = -\gamma_6^E \end{array}\right\} \quad \text{(B32)}$$

By summing the eight solutions of the form of equations (B4) corresponding to $r = r_1$ through $r = r_8$, expressing each exponential in terms of hyperbolic functions, discarding those terms not having the proper even-ness or oddness in z, and taking into account equations (B32), one arrives at the following part of the complementary solution:

$$\left.\begin{aligned} u_1 &= A_1^* \cosh \frac{R_1 z}{c} + A_3^* \cosh \frac{R_2 z}{c} + A_5^* \cosh \frac{R_5 z}{c} + A_7^* \cosh \frac{R_6 z}{c} \\ u_2 &= A_1^* \gamma_1^B \cosh \frac{R_1 z}{c} + A_3^* \gamma_2^B \cosh \frac{R_2 z}{c} + A_5^* \gamma_5^B \cosh \frac{R_5 z}{c} + A_7^* \gamma_6^B \cosh \frac{R_6 z}{c} \\ v_1 &= A_1^* \gamma_1^C \sinh \frac{R_1 z}{c} + A_3^* \gamma_2^C \sinh \frac{R_2 z}{c} + A_5^* \gamma_5^C \sinh \frac{R_5 z}{c} + A_7^* \gamma_6^C \sinh \frac{R_6 z}{c} \\ v_2 &= A_1^* \gamma_1^D \sinh \frac{R_1 z}{c} + A_3^* \gamma_2^D \sinh \frac{R_2 z}{c} + A_5^* \gamma_5^D \sinh \frac{R_5 z}{c} + A_7^* \gamma_6^D \sinh \frac{R_6 z}{c} \\ v_0 &= A_1^* \gamma_1^E \sinh \frac{R_1 z}{c} + A_3^* \gamma_2^E \sinh \frac{R_2 z}{c} + A_5^* \gamma_5^E \sinh \frac{R_5 z}{c} + A_7^* \gamma_6^E \sinh \frac{R_6 z}{c} \end{aligned}\right\} \quad \text{(B33)}$$

where A_1^*, A_3^*, A_5^*, A_7^* are certain linear combinations of the A_j's and may be regarded as new arbitrary constants.

Complementary solution associated with the root $R = R_9 = 0$. - Substitution of $r = r_9 = 0$ into equations (B5) gives the following relations which the coefficients A_9, B_9, ..., E_9 must satisfy:

$$\begin{bmatrix} -c_{11} & -c_{12} & 0 & 0 & 0 \\ -c_{12} & -c_{22} & 0 & 0 & 0 \\ 0 & 0 & a_{11} & a_{12} & 0 \\ 0 & 0 & a_{12} & a_{22} & 0 \\ 0 & 0 & 0 & 0 & 0 \end{bmatrix} \begin{bmatrix} A_9 \\ B_9 \\ C_9 \\ D_9 \\ E_9 \end{bmatrix} = \begin{bmatrix} 0 \\ 0 \\ 0 \\ 0 \\ 0 \end{bmatrix} \tag{B34}$$

Since $c_{11}c_{22} - c_{12}^2$ and $a_{11}a_{22} - a_{12}^2$ are not zero, these equations have the solution

$$\left.\begin{aligned} A_9 = B_9 = C_9 = D_9 = 0 \\ E_9 = \text{indeterminate} \end{aligned}\right\} \tag{B35}$$

Substitution of these values, together with $r = r_9 = 0$, into equations (B4) gives the following complementary solution:

$$\left.\begin{aligned} u_1 = u_2 = v_1 = v_2 = 0 \\ v_0 = E_9 \end{aligned}\right\} \tag{B36}$$

where E_9 is an arbitrary constant.

This solution gives v_0 even in z rather than odd. The constant E_9 may therefore be equated to zero. Thus the root $R = R_9 = 0$ makes no constribution to the complementary solutions.

Additional complementary solution not of the form of equations (B4). - The presence of a repeated root (see eqs. (B21b)) of the characteristic equation indicates that there exists a complementary solution that is not of the form of equations (B4). This complementary solution can be found by inspection if one assumes the following form for it:

$$\begin{aligned} u_1 &= A_{10} \\ u_2 &= B_{10} \\ v_1 &= C_{10}z/c \\ v_2 &= D_{10}z/c \\ v_0 &= E_{10}z/c \end{aligned} \tag{B37}$$

where $A_{10}, B_{10}, \ldots, E_{10}$ are constants. Equations (B37) satisfy the symmetry and antisymmetry requirements with respect to z. Substituting equations (B37) into the original differential equations (17) (with the u_0 term omitted) leads to the following conditions on $A_{10}, B_{10}, \ldots, E_{10}$:

$$\begin{bmatrix} -2c_{11} & -2c_{12} & -\frac{a_{10}}{c} & -\frac{d_{11}}{c} & 0 \\ -2c_{12} & -2c_{22} & -\frac{d_{20}}{c} & -\frac{d_{21}}{c} & -\frac{d_{22}}{c} \\ 0 & 0 & 0 & 0 & 0 \\ 0 & 0 & 0 & a_{11} & a_{12} \\ 0 & 0 & 0 & a_{12} & a_{22} \end{bmatrix} \begin{bmatrix} A_{10} \\ B_{10} \\ E_{10} \\ C_{10} \\ D_{10} \end{bmatrix} = \begin{bmatrix} 0 \\ 0 \\ 0 \\ 0 \\ 0 \end{bmatrix} \tag{B38}$$

whence

$$\left.\begin{aligned} C_{10} &= D_{10} = 0 \\ E_{10} &= \text{indeterminate} \\ A_{10} &= \xi_1 E_{10} \\ B_{10} &= \xi_2 E_{10} \end{aligned}\right\} \tag{B39}$$

where

$$\xi_1 = \frac{c_{12}d_{20} - c_{22}d_{10}}{2c(c_{11}c_{22} - c_{12}^2)} \tag{B40}$$

$$\xi_2 = \frac{c_{12}d_{10} - c_{11}d_{20}}{2c(c_{11}c_{22} - c_{12}^2)}$$

Thus the complementary solution of the form of equations (B37) is

$$\begin{aligned} u_1 &= \xi_1 E_{10} \\ u_2 &= \xi_2 E_{10} \\ v_1 &= 0 \\ v_2 &= 0 \\ v_0 &= E_{10} z/c \end{aligned} \tag{B41}$$

where E_{10} is an arbitrary constant.

Complete solution. - The complete solution of the differential equations (17) (satisfying the symmetry and antisymmetry requirements), obtained by adding together the particular integral (B3) and the complementary solutions (B33) and (B41), is

$$\left.\begin{aligned} u_1 &= \zeta_1 u_0 + A_1^* \cosh \frac{R_1 z}{c} + A_3^* \cosh \frac{R_2 z}{c} + A_5^* \cosh \frac{R_5 z}{c} \\ &\quad + A_7^* \cosh \frac{R_6 z}{c} + \xi_1 E_{10} \\ u_2 &= \zeta_2 u_0 + A_1^* \gamma_1^B \cosh \frac{R_1 z}{c} + A_3^* \gamma_2^B \cosh \frac{R_2 z}{c} + A_5^* \gamma_5^B \cosh \frac{R_5 z}{c} \\ &\quad + A_7^* \gamma_6^B \cosh \frac{R_6 z}{c} + \xi_2 E_{10} \\ v_1 &= A_1^* \gamma_1^C \sinh \frac{R_1 z}{c} + A_3^* \gamma_2^C \sinh \frac{R_2 z}{c} + A_5^* \gamma_5^C \sinh \frac{R_5 z}{c} + A_7^* \gamma_6^C \sinh \frac{R_6 z}{c} \\ v_2 &= A_1^* \gamma_1^D \sinh \frac{R_1 z}{c} + A_3^* \gamma_2^D \sinh \frac{R_2 z}{c} + A_5^* \gamma_5^D \sinh \frac{R_5 z}{c} + A_7^* \gamma_6^D \sinh \frac{R_6 z}{c} \\ v_0 &= A_1^* \gamma_1^E \sinh \frac{R_1 z}{c} + A_3^* \gamma_2^E \sinh \frac{R_2 z}{c} + A_5^* \gamma_5^E \sinh \frac{R_5 z}{c} \\ &\quad + A_7^* \gamma_6^E \sinh \frac{R_6 z}{c} + E_{10} \frac{z}{c} \end{aligned}\right\} \tag{B42}$$

The unknown constants A_1^*, A_3^*, A_5^*, A_7^* and E_{10} are determined in terms of u_0 through the boundary conditions, which are: equations (19), (20) and (21) for the case of point attachments at the ends of the trough lines only; (23) through (26) in the case of point attachments at the ends of the trough lines and the crest lines; and (19), (20), (22) and the second of equations (21) in the case of wide attachments at the ends of the trough lines.

Substitution of the expression for $u_1(z)$ from equations (B42) into equation (18) gives

$$(c_{00} + c_{01}\zeta_1)b + c_{01}\left(\frac{A_1^*}{u_0}\frac{c}{R_1}\sinh\frac{R_1 b}{c} + \frac{A_3^*}{u_0}\frac{c}{R_2}\sinh\frac{R_2 b}{c} + \frac{A_5^*}{u_0}\frac{c}{R_5}\sinh\frac{R_5 b}{c} + \frac{A_7^*}{u_0}\frac{c}{R_6}\sinh\frac{R_6 b}{c} + \frac{E_{10}}{u_0}\xi_1 b\right) = \frac{F}{2u_0} \tag{B43}$$

With A_1^*/u_0, etc. determined through the boundary conditions, equation (B43) yields the effective overall shearing stiffness $F/2u_0$ of a single corrugation.

Special form of solution when R_1 through R_8 are complex. - The procedure described above is quite general; it applies regardless of whether the eight non-zero roots of the characteristic equation (B20) are real or complex. For almost all cross-sectional geometries of interest, however, the eight non-zero roots of this equation turn out to be complex. It is therefore worth-while to investigate the special form taken on by equations (B42) and the boundary condition equations in that case.

Considering the case of complex roots, and taking into account equations (B22), one can represent R_1, R_2, R_5 and R_6 in the form

$$\begin{aligned} R_1 &= U + iV & R_5 &= X + iY \\ R_2 &= U - iV & R_6 &= X - iY \end{aligned} \tag{B44}$$

where U, V, X and Y are real numbers. Furthermore, from the last four equations of (B5) it is evident that if r is replaced by its complex conjugate then B/A, C/A, D/A and E/A are also changed to their complex conjugates. Applying this to the complex conjugate pairs r_1, r_2 and r_5, r_6, and taking into account equations (B31), it follows that

$$\begin{aligned} \gamma_2^B &= \gamma_1^{B*} & \gamma_2^C &= \gamma_1^{C*} & \gamma_2^D &= \gamma_1^{D*} & \gamma_2^E &= \gamma_1^{E*} \\ \gamma_6^B &= \gamma_5^{B*} & \gamma_6^C &= \gamma_5^{C*} & \gamma_6^D &= \gamma_5^{D*} & \gamma_6^E &= \gamma_5^{E*} \end{aligned} \tag{B45}$$

Thus the $\gamma_j^{B,C,D,E}$ which appear in equations (B42) have the following representation:

$$\left.\begin{aligned} \gamma_1^B &= P^B + iQ^B & \gamma_5^B &= S^B + iT^B \\ \gamma_2^B &= P^B - iQ^B & \gamma_6^B &= S^B - iT^B \end{aligned}\right\} \quad (B46)$$

$$\left.\begin{aligned} \gamma_1^C &= P^C + iQ^C & \gamma_5^C &= S^C + iT^C \\ \gamma_2^C &= P^C - iQ^C & \gamma_6^C &= S^C - iT^C \end{aligned}\right\} \quad (B47)$$

$$\left.\begin{aligned} \gamma_1^D &= P^D + iQ^D & \gamma_5^D &= S^D + iT^D \\ \gamma_2^D &= P^D - iQ^D & \gamma_6^D &= S^D - iT^D \end{aligned}\right\} \quad (B48)$$

$$\left.\begin{aligned} \gamma_1^E &= P^E + iQ^E & \gamma_5^E &= S^E + iT^E \\ \gamma_2^E &= P^E - iQ^E & \gamma_6^E &= S^E - iT^E \end{aligned}\right\} \quad (B49)$$

where P^B, Q^B, etc. are real numbers.

Substituting expressions (B44) and (B46) through (B49) into equations (B42) gives the following form of the complete solution, applicable to the case in which the eight non-zero roots of the characteristic equation are complex:

$$\frac{u_1(z)}{u_0} = \zeta_1 + \frac{\overline{\overline{A}}_1}{u_0} \cosh \frac{Uz}{c} \cos \frac{Vz}{c} + \frac{\overline{\overline{A}}_4}{u_0} \sinh \frac{Uz}{c} \sin \frac{Vz}{c}$$

$$+ \frac{\overline{\overline{A}}_5}{u_0} \cosh \frac{Xz}{c} \cos \frac{Yz}{c} + \frac{\overline{\overline{A}}_8}{u_0} \sinh \frac{Xz}{c} \sin \frac{Yz}{c} + \frac{E_{10}}{u_0} \xi_1 \qquad (B50a)$$

$$\frac{u_2(z)}{u_0} = \zeta_2 + \left(\frac{\bar{\bar{A}}_1}{u_0} P^B + \frac{\bar{\bar{A}}_4}{u_0} Q^R\right) \cosh \frac{Uz}{c} \cos \frac{Vz}{c}$$

$$+ \left(\frac{\bar{\bar{A}}_4}{u_0} \rho^B - \frac{\bar{\bar{A}}_1}{u_0} Q^B\right) \sinh \frac{Uz}{c} \sin \frac{Vz}{c} + \left(\frac{\bar{\bar{A}}_5}{u_0} S^B + \frac{\bar{\bar{A}}_8}{u_0} T^B\right) \cosh \frac{Xz}{c} \cos \frac{Yz}{c}$$

$$+ \left(\frac{\bar{\bar{A}}_8}{u_0} S^B - \frac{\bar{\bar{A}}_5}{u_0} T^B\right) \sinh \frac{Xz}{c} \text{ sir } \frac{Yz}{c} + \frac{E_{10}}{u_0} \xi_2 \qquad \text{(B50b)}$$

$$\frac{v_1(z)}{u_0} = \left(\frac{\bar{\bar{A}}_4}{u_0} P^C - \frac{\bar{\bar{A}}_1}{u_0} Q^C\right) \cosh \frac{Uz}{c} \sin \frac{Vz}{c} + \left(\frac{\bar{\bar{A}}_1}{u_0} P^C + \frac{\bar{\bar{A}}_4}{u_0} Q^C\right) \sinh \frac{Uz}{c} \cos \frac{Vz}{c}$$

$$+ \left(\frac{\bar{\bar{A}}_8}{u_0} S^C - \frac{\bar{\bar{A}}_5}{u_0} T^C\right) \cosh \frac{Xz}{c} \sin \frac{Yz}{c} + \left(\frac{\bar{\bar{A}}_5}{u_0} S^C + \frac{\bar{\bar{A}}_8}{u_0} T^C\right) \sinh \frac{Xz}{c} \cos \frac{Yz}{c}$$

(B50c)

$$\frac{v_2(z)}{u_0} = \left(\frac{\bar{\bar{A}}_4}{u_0} P^D - \frac{\bar{\bar{A}}_1}{u_0} Q^D\right) \cosh \frac{Uz}{c} \sin \frac{Vz}{c} + \left(\frac{\bar{\bar{A}}_1}{u_0} P^D + \frac{\bar{\bar{A}}_4}{u_0} Q^D\right) \sinh \frac{Uz}{c} \cos \frac{Vz}{c}$$

$$+ \left(\frac{\bar{\bar{A}}_8}{u_0} S^D - \frac{\bar{\bar{A}}_5}{u_0} T^D\right) \cosh \frac{Xz}{c} \sin \frac{Yz}{c} + \left(\frac{\bar{\bar{A}}_5}{u_0} S^D + \frac{\bar{\bar{A}}_8}{u_0} T^D\right) \sinh \frac{Xz}{c} \cos \frac{Yz}{c}$$

(B50d)

$$\frac{v_0(z)}{u_0} = \left(\frac{\bar{\bar{A}}_4}{u_0} P^E - \frac{\bar{\bar{A}}_1}{u_0} Q^E\right) \cosh \frac{Uz}{c} \sin \frac{Vz}{c} + \left(\frac{\bar{\bar{A}}_1}{u_0} P^E + \frac{\bar{\bar{A}}_4}{u_0} Q^E\right) \sinh \frac{Uz}{c} \cos \frac{Vz}{c}$$

$$+ \left(\frac{\bar{\bar{A}}_8}{u_0} S^E - \frac{\bar{\bar{A}}_5}{u_0} T^E\right) \cosh \frac{Xz}{c} \sin \frac{Yz}{c} + \left(\frac{\bar{\bar{A}}_5}{u_0} S^E + \frac{\bar{\bar{A}}_8}{u_0} T^E\right) \sinh \frac{Xz}{c} \cos \frac{Yz}{c}$$

$$+ \frac{E_{10}}{u_0} \frac{z}{c} \qquad \text{(B50e)}$$

where $\bar{\bar{A}}_1$, $\bar{\bar{A}}_4$, $\bar{\bar{A}}_5$ and $\bar{\bar{A}}_8$ are new arbitrary constants related as follows to the previous ones:

$$\bar{\bar{A}}_1 = A_1^* + A_3^* \qquad \bar{\bar{A}}_5 = A_5^* + A_7^*$$
$$\bar{\bar{A}}_4 = i(A_1^* - A_3^*) \qquad \bar{\bar{A}}_8 = i(A_5^* - A_7^*) \tag{B51}$$

These four arbitrary constants and the fifth one, E_{10}, are to be evaluated from the boundary condition equations listed in the previous section after equations (B42). These lead to the following sets of simultaneous equations for $\frac{\bar{\bar{A}}_1}{u_0}\cosh\frac{Ub}{c}$, $\frac{\bar{\bar{A}}_4}{u_0}\cosh\frac{Ub}{c}$, $\frac{\bar{\bar{A}}_5}{u_0}\cosh\frac{Xb}{c}$, $\frac{\bar{\bar{A}}_8}{u_0}\cosh\frac{Xb}{c}$ and $\frac{E_{10}}{u_0}$:

$$\begin{bmatrix} N_{11} & N_{12} & N_{13} & N_{14} & 0 \\ N_{21} & N_{22} & N_{23} & N_{24} & 0 \\ N_{31} & N_{32} & N_{33} & N_{34} & N_{35} \\ N_{41} & N_{42} & N_{43} & N_{44} & N_{45} \\ N_{51} & N_{52} & N_{53} & N_{54} & N_{55} \end{bmatrix} \begin{bmatrix} \frac{\bar{\bar{A}}_1}{u_0}\cosh\frac{Ub}{c} \\ \frac{\bar{\bar{A}}_4}{u_0}\cosh\frac{Ub}{c} \\ \frac{\bar{\bar{A}}_5}{u_0}\cosh\frac{Xb}{c} \\ \frac{\bar{\bar{A}}_8}{u_0}\cosh\frac{Xb}{c} \\ \frac{E_{10}}{u_0} \end{bmatrix} = \begin{bmatrix} 0 \\ 0 \\ 0 \\ N_4 \\ N_5 \end{bmatrix} \tag{B52}$$

for the case of point attachments at the ends of the trough lines only (fig. 2(a));

$$\begin{bmatrix} N_{11} & N_{12} & N_{13} & N_{14} & 0 \\ N_{21} & N_{22} & N_{23} & N_{24} & 0 \\ N_{31} & N_{32} & N_{33} & N_{34} & N_{35} \\ \bar{N}_{41} & \bar{N}_{42} & \bar{N}_{43} & \bar{N}_{44} & 0 \\ \bar{N}_{51} & \bar{N}_{52} & \bar{N}_{53} & \bar{N}_{54} & \bar{N}_{55} \end{bmatrix} \begin{bmatrix} \frac{\bar{\bar{A}}_1}{u_0} \cosh \frac{Ub}{c} \\ \frac{\bar{\bar{A}}_4}{u_0} \cosh \frac{Ub}{c} \\ \frac{\bar{\bar{A}}_5}{u_0} \cosh \frac{Xb}{c} \\ \frac{\bar{\bar{A}}_8}{u_0} \cosh \frac{Xb}{c} \\ \frac{E_{10}}{u_0} \end{bmatrix} = \begin{bmatrix} 0 \\ 0 \\ 0 \\ 0 \\ \bar{N}_5 \end{bmatrix} \tag{B53}$$

for the case of point attachments at the ends of the trough lines and the crest lines (fig. 2(b)); and

$$\begin{bmatrix} N_{11} & N_{12} & N_{13} & N_{14} & 0 \\ N_{21} & N_{22} & N_{23} & N_{24} & 0 \\ N_{31} & N_{32} & N_{33} & N_{34} & N_{35} \\ \bar{\bar{N}}_{41} & \bar{\bar{N}}_{42} & \bar{\bar{N}}_{43} & \bar{\bar{N}}_{44} & 0 \\ N_{51} & N_{52} & N_{53} & N_{54} & N_{55} \end{bmatrix} \begin{bmatrix} \frac{\bar{\bar{A}}_1}{u_0} \cosh \frac{Ub}{c} \\ \frac{\bar{\bar{A}}_4}{u_0} \cosh \frac{Ub}{c} \\ \frac{\bar{\bar{A}}_5}{u_0} \cosh \frac{Xb}{c} \\ \frac{\bar{\bar{A}}_8}{u_0} \cosh \frac{Xb}{c} \\ \frac{E_{10}}{u_0} \end{bmatrix} = \begin{bmatrix} 0 \\ 0 \\ 0 \\ 0 \\ N_5 \end{bmatrix} \tag{B54}$$

for the case of wide attachments at the ends of the trough lines (fig. 2(c) or (d)).

The matrix elements in these equations are defined as follows:

$$N_{11} = U\,\widehat{tu}\,\widehat{cv} - V\,\widehat{sv} \qquad N_{21} = P^B N_{11} - Q^B N_{12}$$

$$N_{12} = U\,\widehat{sv} + V\,\widehat{tu}\,\widehat{cv} \qquad N_{22} = P^B N_{12} + Q^B N_{11}$$

$$N_{13} = X\,\widehat{tx}\,\widehat{cy} - Y\,\widehat{sy} \qquad N_{23} = S^B N_{13} - T^B N_{14}$$

$$N_{14} = X\,\widehat{sy} + Y\,\widehat{tx}\,\widehat{cy} \qquad N_{24} = S^B N_{14} + T^B N_{13} \qquad \text{(B55a)}$$

$$N_{31} = P^E\,\widehat{tu}\,\widehat{cv} - Q^E\,\widehat{sv}$$

$$N_{32} = P^E\,\widehat{sv} + Q^E\,\widehat{tu}\,\widehat{cv}$$

$$N_{33} = S^E\,\widehat{tx}\,\widehat{cy} - T^E\,\widehat{sy}$$

$$N_{34} = S^E\,\widehat{sy} + T^E\,\widehat{tx}\,\widehat{cy} \qquad \text{(B55b)}$$

$$N_{35} = b/c$$

$$N_{41} = \tilde{d}_{11}\widehat{cv} + \tilde{d}_{21}\alpha_1^B + \tilde{e}_{11}\beta_1^C + \tilde{e}_{12}\beta_1^D + \tilde{e}_{10}\beta_1^E$$

$$N_{42} = \tilde{d}_{11}\widehat{tu}\,\widehat{sv} + \tilde{d}_{21}\alpha_2^B + \tilde{e}_{11}\beta_2^C + \tilde{e}_{12}\beta_2^D + \tilde{e}_{10}\beta_2^E$$

$$N_{43} = \tilde{d}_{11}\widehat{cy} + \tilde{d}_{21}\alpha_3^B + \tilde{e}_{11}\beta_3^C + \tilde{e}_{12}\beta_3^D + \tilde{e}_{10}\beta_3^E \qquad \text{(B55c)}$$

$$N_{44} = \tilde{d}_{11}\widehat{tx}\,\widehat{sy} + \tilde{d}_{21}\alpha_4^B + \tilde{e}_{11}\beta_4^C + \tilde{e}_{12}\beta_4^D + \tilde{e}_{10}\beta_4^E$$

$$N_{45} = \tilde{d}_{11}\xi_1 + \tilde{d}_{21}\xi_2 + \tilde{e}_{10}$$

$$N_{51} = \tilde{d}_{22}\alpha_1^B + \tilde{e}_{12}\beta_1^C + \tilde{e}_{22}\beta_1^D + \tilde{e}_{20}\beta_1^E$$

$$N_{52} = \tilde{d}_{22}\alpha_2^B + \tilde{e}_{12}\beta_2^C + \tilde{e}_{22}\beta_2^D + \tilde{e}_{20}\beta_2^E$$

$$N_{53} = \tilde{d}_{22}\alpha_3^B + \tilde{e}_{12}\beta_3^C + \tilde{e}_{22}\beta_3^D + \tilde{e}_{20}\beta_3^E \qquad \text{(B55d)}$$

(equation continued on next page)

$$N_{54} = \tilde{d}_{22}\alpha_4^B + \tilde{e}_{12}\beta_4^C + \tilde{e}_{22}\beta_4^D + \tilde{e}_{20}\beta_4^E$$

$$N_{55} = \tilde{d}_{22}\xi_2 + \tilde{e}_{20}$$

$$N_4 = -\zeta_1\tilde{d}_{11} - \zeta_2\tilde{d}_{21} \qquad N_5 = -\zeta_2\tilde{d}_{22} \tag{B56}$$

$$\begin{aligned}
\bar{N}_{41} &= (P^C \widehat{tu}\,\widehat{cv} - Q^C \widehat{sv})\cos\theta + (P^D \widehat{tu}\,\widehat{cv} - Q^D \widehat{sv}) \\
\bar{N}_{42} &= (P^C \widehat{sv} + Q^C \widehat{tu}\,\widehat{cv})\cos\theta + (P^D \widehat{sv} + Q^D \widehat{tu}\,\widehat{cv}) \\
\bar{N}_{43} &= (S^C \widehat{tu}\,\widehat{cv} - T^C \widehat{sc})\cos\theta + (S^D \widehat{tu}\,\widehat{cv} - T^D \widehat{sv}) \\
\bar{N}_{44} &= (S^C \widehat{sv} + T^C \widehat{tu}\,\widehat{cv})\cos\theta + (S^D \widehat{sv} + Q^D \widehat{tu}\,\widehat{cv})
\end{aligned} \tag{B57a}$$

$$\begin{aligned}
\bar{\bar{N}}_{51} &= N_{41} - N_{51}\cos\theta \\
\bar{\bar{N}}_{52} &= N_{42} - N_{52}\cos\theta \\
\bar{\bar{N}}_{53} &= N_{43} - N_{53}\cos\theta \\
\bar{\bar{N}}_{54} &= N_{44} - N_{54}\cos\theta \\
\bar{\bar{N}}_{55} &= N_{45} - N_{55}\cos\theta
\end{aligned} \tag{B57b}$$

$$\bar{\bar{N}}_5 = N_4 - N_5\cos\theta \tag{B58}$$

$$\begin{aligned}
\bar{\bar{\bar{N}}}_{41} &= P^C \widehat{tu}\,\widehat{cv} - Q^C \widehat{sv} \\
\bar{\bar{\bar{N}}}_{42} &= P^C \widehat{sv} + Q^C \widehat{tu}\,\widehat{cv} \\
\bar{\bar{\bar{N}}}_{43} &= S^C \widehat{tx}\,\widehat{cy} - T^C \widehat{sy} \\
\bar{\bar{\bar{N}}}_{44} &= S^C \widehat{sy} + T^C \widehat{tx}\,\widehat{cy}
\end{aligned} \tag{B59}$$

where

$$\left.\begin{aligned} \widehat{sv} &\equiv \sin\frac{Vb}{c} \\ \widehat{sy} &\equiv \sin\frac{Yb}{c} \\ \widehat{cv} &\equiv \cos\frac{Vb}{c} \\ \widehat{cy} &\equiv \cos\frac{Yb}{c} \\ \widehat{tu} &\equiv \tanh\frac{Ub}{c} \\ \widehat{tx} &\equiv \tanh\frac{Xb}{c} \end{aligned}\right\} \quad \text{(B60)}$$

and

$$\left.\begin{aligned} \alpha_1^B &= P^B\,\widehat{cv} - Q^B\,\widehat{tu}\,\widehat{sv} \\ \alpha_2^B &= P^B\,\widehat{tu}\,\widehat{sv} + Q^B\,\widehat{cv} \\ \alpha_3^B &= S^B\,\widehat{cy} - T^B\,\widehat{tx}\,\widehat{sy} \\ \alpha_4^B &= S^B\,\widehat{tx}\,\widehat{sy} + T^B\,\widehat{cy} \\ \beta_1^C &= U(P^C\,\widehat{cv} - Q^C\,\widehat{tu}\,\widehat{sv}) - V(P^C\,\widehat{tu}\,\widehat{sv} + Q^C\,\widehat{cv}) \\ \beta_2^C &= U(P^C\,\widehat{tu}\,\widehat{sv} + Q^C\,\widehat{cv}) + V(P^C\,\widehat{cv} - Q^C\,\widehat{tu}\,\widehat{sv}) \\ \beta_3^C &= X(S^C\,\widehat{cy} - T^C\,\widehat{tx}\,\widehat{sy}) - Y(S^C\,\widehat{tx}\,\widehat{sy} + T^C\,\widehat{cy}) \\ \beta_4^C &= X(S^C\,\widehat{tx}\,\widehat{sy} + T^C\,\widehat{cy}) + Y(S^C\,\widehat{cy} - T^C\,\widehat{tx}\,\widehat{sy}) \\ \beta_1^D &= U(P^D\,\widehat{cv} - Q^D\,\widehat{tu}\,\widehat{sv}) - V(P^D\,\widehat{tu}\,\widehat{sv} + Q^D\,\widehat{cv}) \\ \beta_2^D &= U(P^D\,\widehat{tu}\,\widehat{sv} + Q^D\,\widehat{cv}) + V(P^D\,\widehat{cv} - Q^D\,\widehat{tu}\,\widehat{sv}) \end{aligned}\right\} \quad \text{(B61)}$$

67

(equation continued on next page)

$$
\begin{aligned}
\beta_3^D &= X(S^D \widehat{cy} - T^D \widehat{tx}\,\widehat{sy}) - Y(S^D \widehat{tx}\,\widehat{sy} + T^D \widehat{cy}) \\
\beta_4^D &= X(S^D \widehat{tx}\,\widehat{sy} + T^C \widehat{cy}) + Y(S^D \widehat{cy} - T^D \widehat{tx}\,\widehat{sy}) \\
\beta_1^E &= U(P^E \widehat{cv} - Q^E \widehat{tu}\,\widehat{sv}) - V(P^E \widehat{tu}\,\widehat{sv} + Q^E \widehat{cv}) \\
\beta_2^E &= U(P^E \widehat{tu}\,\widehat{sv} + Q^E \widehat{cv}) + V(P^E \widehat{cv} - Q^E \widehat{tu}\,\widehat{sv}) \\
\beta_3^E &= X(S^E \widehat{cy} - T^E \widehat{tx}\,\widehat{sy}) - Y(S^E \widehat{tx}\,\widehat{sy} + T^E \widehat{cy}) \\
\beta_4^E &= X(S^E \widehat{tx}\,\widehat{sy} + T^E \widehat{cy}) + Y(S^E \widehat{cy} - T^E \widehat{tx}\,\widehat{sy})
\end{aligned}
$$

and

$$
\begin{aligned}
\tilde{d}_{11} &= \tilde{d}_{22} = -\sin\theta \\
\tilde{d}_{21} &= \sin\theta(1 - \cos\theta) \\
\tilde{e}_{11} &= \sin^2\theta\left(\frac{k}{c} + \frac{1}{2}\frac{f}{c}\cos^2\theta\right) + \frac{1}{3}\frac{G'}{G}\left(\frac{t}{c}\right)^2\left(\frac{c}{e} + \frac{c}{k}\cos^2\theta + 2\frac{c}{f}\sin^4\theta\right) \\
\tilde{e}_{22} &= \frac{1}{2}\frac{f}{c}\sin^2\theta + \frac{1}{3}\frac{G'}{G}\left(\frac{t}{c}\right)^2\left(\frac{c}{k} + 2\frac{c}{f}\cos^2\theta\right) \\
\tilde{e}_{12} &= \frac{1}{2}\frac{f}{c}\sin^2\theta\cos\theta + \frac{1}{3}\frac{G'}{G}\left(\frac{t}{c}\right)^2\left(\frac{c}{k}\cos\theta - 2\frac{c}{f}\sin^2\theta\cos\theta\right) \\
\tilde{e}_{10} &= -\frac{1}{2}\left(2\frac{k}{c} + \frac{f}{c}\right)\sin\theta\cos\theta \\
\tilde{e}_{20} &= -\frac{1}{2}\frac{f}{c}\sin\theta
\end{aligned}
\qquad \text{(B62)}
$$

Substituting expressions (B44) into (B43), and making use of (B51) and the definitions of c_{00} and c_{01} (eqs. (6a)), one obtains the following formula for computing the shearing stiffness $F/2u_0$ of a single corrugation in the case of the non-zero roots being complex:

$$
\frac{F}{2u_0} = \frac{Gtb}{e}\,\psi \qquad \text{(B63a)}
$$

where

$$\psi = 1 - \zeta_1 - \frac{E_{10}}{u_0}\xi_1 - \frac{c}{b}\left[\left(\frac{\bar{\bar{A}}_1}{u_0}\cosh\frac{Ub}{c}\right)\frac{U\,\hat{tu}\,\hat{cv} + V\,\hat{sv}}{U^2+V^2} + \left(\frac{\bar{\bar{A}}_4}{u_0}\cosh\frac{Ub}{c}\right)\frac{U\,\hat{sv} - V\,\hat{tu}\,\hat{cv}}{U^2+V^2} + \left(\frac{\bar{\bar{A}}_5}{u_0}\cosh\frac{Xb}{c}\right)\frac{X\,\hat{tx}\,\hat{cy} + Y\,\hat{sy}}{X^2+Y^2} + \left(\frac{\bar{\bar{A}}_8}{u_0}\cosh\frac{Xb}{c}\right)\frac{X\,\hat{sy} - Y\,\hat{tx}\,\hat{cy}}{X^2+Y^2}\right] \qquad \text{(B63b)}$$

It will be noted that in equations (B51), (B52) and (B53) the combinations $\frac{\bar{\bar{A}}_1}{u_0}\cosh\frac{Ub}{c}$, etc. are regarded as the unknowns rather than $\frac{\bar{\bar{A}}_1}{u_0}$, etc. alone. This is done in order to avoid having extremely large matrix elements in the simultaneous equations when b/c is large.

APPENDIX C

SPECIAL CASE: f = 0

In this appendix the special case $f = 0$ will be considered, in which junctions lines ② and ③ coincide and form a line of points of inflection of the cross sections (see fig. 6(b)). Only the end-attachment conditions of figure 2(a) (i.e. point attachments at the trough line ends only) need be considered in conjunction with the case $f = 0$, for any of the other two types of end attachment would completely prevent cross-sectional deformation and therefore be tantamount to continuous attachment.

Along the common junction line formed by junction ② and ③ when $f = 0$ the longitudinal deformation must vanish, and the vertical displacement must also vanish. These constraints can be expressed as follows:

$$u_2(z) = 0 \tag{C1}$$

and

$$[v_1(z)\sin\theta]\sin\theta - [v_2(z)]\cos\theta = 0 \tag{C2}$$

The variational form of these equations is

$$\delta u_2 = 0 \tag{C3}$$

$$\delta v_1 = \delta v_2 \cos\theta/\sin^2\theta \tag{C4}$$

Introducing the foregoing conditions into equation (A5) gives the following expression for the first variation of the TPE:

$$\begin{aligned}\delta(\text{TPE}) = {} & (\delta u_0)\int_{-b}^{b}(2c_{00}u_0 + 2c_{01}u_1 - \frac{F}{b})dz \\ & + 2\int_{-b}^{b}\left(-b_{11}\frac{d^2u_1}{dz^2} + c_{01}u_0 + c_{11}u_1 + \frac{1}{2}d_{10}\frac{dv_0}{dz}\right. \\ & \left. + \frac{1}{2}d_{11}\frac{dv_2}{dz}\frac{\cos}{\sin^2}\right)(\delta u_1)dz \\ & - 2\int_{-b}^{b}\left[\frac{1}{2}d_{10}\frac{du_1}{dz} + e_{00}\frac{d^2v_0}{dz^2} + (e_{10}\frac{\cos\theta}{\sin^2\theta} + e_{20})\frac{d^2v_2}{dz^2}\right](\delta v_0)dz\end{aligned}$$

(equation continued on next page)

$$+ 2 \int_{-b}^{b} \left[\left(a_{11} \frac{\cos^2\theta}{\sin^4\theta} + 2a_{12} \frac{\cos\theta}{\sin^2\theta} + a_{22} \right) v_2 \right.$$

$$- \frac{1}{2} d_{11} \frac{du_1}{dz} \frac{\cos\theta}{\sin^2\theta} - \left(e_{10} \frac{\cos\theta}{\sin^2\theta} + e_{20} \right) \frac{d^2 v_0}{dz^2}$$

$$\left. - \left(e''_{11} \frac{\cos^2\theta}{\sin^4\theta} + 2e''_{12} \frac{\cos\theta}{\sin^2\theta} + e''_{22} \right) \frac{d^2 v_2}{dz^2} \right] (\delta v_2) dz$$

$$+ \left(2 b_{11} \frac{du_1}{dz} \delta u_1 \right) \Big|_{-b}^{b}$$

$$+ \left[d_{11} u_1 \frac{\cos\theta}{\sin^2\theta} + 2 \left(e_{10} \frac{\cos\theta}{\sin^2\theta} + e_{20} \right) \frac{dv_0}{dz} \right.$$

$$\left. + 2 \left(e''_{11} \frac{\cos^2\theta}{\sin^4\theta} + 2e''_{12} \frac{\cos\theta}{\sin^2\theta} + e''_{22} \right) \frac{dv_2}{dz} \right] (\delta v_2) \Big|_{-b}^{b} \qquad \text{(C5)}$$

where

$$\left.
\begin{aligned}
e_{00} &= Gt\left(e + k\cos^2\theta + \frac{f}{2}\right) \\
e_{10} &= -\frac{1}{2} Gt(2k + f)\sin\theta \cos\theta \\
e_{20} &= -\frac{1}{2} Gtf \sin\theta \\
e''_{11} &= Gt \sin^2\theta \left(k + \frac{f}{2} \cos^2\theta\right) + G'\left(\frac{J_1}{e^2} + \frac{J_2}{k^2} \cos^2\theta\right) \\
e''_{22} &= \frac{1}{2} Gtf \sin^2\theta + G'\frac{J_2}{k^2} \\
e''_{12} &= \frac{1}{2} Gtf \sin^2\theta \cos\theta + G' \frac{J_2}{k^2} \cos\theta
\end{aligned}
\right\} \qquad \text{(C6)}$$

At this stage the vanishing of f has not yet been introduced into equation (C5). In order to incorporate this condition, f may be allowed to approach zero in all terms of equation (C5) except those associated with frame bending, that is a_{11}, a_{12} and a_{22}. The strain energy of frame bending for the case $f = 0$ cannot be obtained correctly by letting $f \to 0$ in the equations for a_{11}, a_{12} and a_{22} — equations (12) and (13). The reason for this is that if condition (C2) is first imposed (as it has been) to prevent vertical displacements of stations (2) and (3), the subsequent imposition of the condition

$f \to 0$ will lead to clamping (zero rotation) at the vertex formed by stations (2) and (3) as they meet, rather than to the condition of free rotation corresponding to the point of inflection (zero moment) which should be present at this vertex. In order to obtain correctly the zero moment condition existing at the vertex, f must be allowed to approach infinity, rather than zero, in those terms of equation (C5) which arise from strain energy of frame bending, namely a_{11}, a_{12}, and a_{22}. Doing this, one obtains the following limiting values of a_{11}, a_{12}, and a_{22} for use in equation (C5):

$$\left.\begin{aligned} a_{11} &\to \frac{D}{\tilde{\beta}^2 e^3}\left[\tilde{A}_{11} + \tilde{A}_{22}\left(\frac{e}{k}\right)^2 \cos^2\theta - \tilde{A}_{12}\left(\frac{e}{k}\right)\cos\theta\right] \equiv \tilde{a}_{11} \\ a_{12} &\to \frac{D}{\tilde{\beta}^2 e^3}\left[\tilde{A}_{22}\left(\frac{e}{k}\right)^2 \cos\theta - \frac{1}{2}\tilde{A}_{12}\frac{e}{k}\right] \equiv \tilde{a}_{12} \\ a_{22} &\to \frac{D}{\tilde{\beta}^2 e^3}\tilde{A}_{22}\left(\frac{e}{k}\right)^2 \equiv \tilde{a}_{22} \end{aligned}\right\} \quad (C7)$$

where

$$\tilde{\beta} \equiv 12\frac{e}{k}\left(1 + \frac{e}{k}\right) \quad (C8a)$$

$$\left.\begin{aligned} \tilde{A}_{11} &\equiv 432\left(\frac{e}{k}\right)^3\left(1 + \frac{e}{k}\right) \\ \tilde{A}_{22} &\equiv 432\left(\frac{e}{k}\right)^3\left(1 + \frac{e}{k}\right) \\ \tilde{A}_{12} &\equiv -864\left(\frac{e}{k}\right)^3\left(1 + \frac{e}{k}\right) \end{aligned}\right\} \quad (C8b)$$

Incorporating the above limiting values of a_{11}, a_{12}, and a_{22} into equation (C5) and letting f approach zero in equations (C6) leads to the following expression for $\delta(TPE)$:

$$\delta(TPE) = (\delta u_0)\int_{-b}^{b}(2c_{00}u_0 + 2c_{01}u_1 - \frac{F}{b})dz$$

$$+ 2\int_{-b}^{b}\left(-b_{11}\frac{d^2u_1}{dz^2} + c_{01}u_0 + c_{11}u_1 + \frac{1}{2}d_{10}\frac{dv_0}{dz}\right.$$

$$\left. + \frac{1}{2}d_{11}\frac{\cos\theta}{\sin^2\theta}\frac{dv_2}{dz}\right)(\delta u_1)dz$$

(equation continued on next page)

$$
\begin{aligned}
&- 2\int_{-b}^{b}\left(\frac{1}{2}\,d_{10}\,\frac{du_1}{dz} + \tilde{e}'_{00}\,\frac{d^2v_0}{dz^2} + \tilde{e}'_{10}\,\frac{\cos\theta}{\sin^2\theta}\,\frac{d^2v_2}{dz^2}\right)(\delta v_0)\,dz \\
&+ 2\int_{-b}^{b}\Bigg[\left(\tilde{a}_{11}\,\frac{\cos^2\theta}{\sin^4\theta} + 2\tilde{a}_{12}\,\frac{\cos\theta}{\sin^2\theta} + \tilde{a}_{22}\right)v_2 \\
&\qquad - \frac{1}{2}\,d_{11}\,\frac{du_1}{dz}\,\frac{\cos\theta}{\sin^2\theta} - \tilde{e}'_{10}\,\frac{\cos\theta}{\sin^2\theta}\,\frac{d^2v_0}{dz^2} \\
&\qquad - \left(\tilde{e}'_{11}\,\frac{\cos^2\theta}{\sin^4\theta} + 2\tilde{e}'_{12}\,\frac{\cos\theta}{\sin^2\theta} + \tilde{e}'_{22}\right)\frac{d^2v_2}{dz^2}\Bigg](\delta v_2)\,dz \\
&+ \left(2b_{11}\,\frac{du_1}{dz}\,\delta u_1\right)\Big|_{-b}^{b} \\
&+ \Bigg[d_{11}u_1\,\frac{\cos\theta}{\sin^2\theta} + 2\tilde{e}'_{10}\,\frac{\cos\theta}{\sin^2\theta}\,\frac{dv_0}{dz} \\
&\qquad + 2\left(\tilde{e}'_{11}\,\frac{\cos^2\theta}{\sin^4\theta} + 2\tilde{e}'_{12}\,\frac{\cos\theta}{\sin^2\theta} + \tilde{e}'_{22}\right)\frac{dv_2}{dz}\Bigg](\delta v_2)\Big|_{-b}^{b}
\end{aligned}
\tag{C9}
$$

where

$$
\left.
\begin{aligned}
\tilde{e}'_{00} &= Gt(e + k\cos^2\theta) \\
\tilde{e}'_{10} &= -Gtk\sin\theta\cos\theta \\
\tilde{e}'_{11} &= Gtk\sin^2\theta + G'\left(\frac{J_1}{e^2} + \frac{J_2}{k^2}\cos^2\theta\right) \\
\tilde{e}'_{22} &= G'\,\frac{J_2}{k^2} \\
\tilde{e}'_{12} &= G'\,\frac{J_2}{k^2}\cos\theta
\end{aligned}
\right\} \tag{C10}
$$

Differential equations and boundary conditions. - The vanishing of $\delta(\mathrm{TPE})$, equation (C9), provides the following equations governing $u_1(z)$, $v_0(z)$, $v_2(z)$ and F :

$$4c_{00}u_0 b + 2c_{01}\int_{-b}^{b} u_1 dz - 2F = 0 \tag{C11}$$

$$\left.\begin{aligned} &-b_{11}\frac{d^2u_1}{dz^2} + c_{01}u_0 + c_{11}u_1 + \frac{1}{2}d_{10}\frac{dv_0}{dz} + \frac{1}{2}d_{11}\frac{\cos\theta}{\sin^2\theta}\frac{dv_2}{dz} = 0 \\ &\frac{1}{2}d_{10}\frac{du_1}{dz} + \tilde{e}'_{00}\frac{d^2v_0}{dz^2} + \tilde{e}'_{10}\frac{\cos\theta}{\sin^2\theta}\frac{d^2v_2}{dz^2} = 0 \\ &a'_{22}v_2 - \frac{1}{2}d_{11}\frac{\cos\theta}{\sin^2\theta}\frac{du_1}{dz} - \tilde{e}'_{10}\frac{\cos\theta}{\sin^2\theta}\frac{d^2v_0}{dz^2} - e'_{22}\frac{d^2v_2}{dz^2} = 0 \end{aligned}\right\} \tag{C12}$$

$$\left.\begin{aligned} &\left(\frac{du_1}{dz}\right)_{z=\pm b} = 0 \\ &\left(d_{11}\frac{\cos\theta}{\sin^2\theta}u_1 + 2\tilde{e}'_{10}\frac{\cos\theta}{\sin^2\theta}\frac{dv_0}{dz} + 2e'_{22}\frac{dv_2}{dz}\right)_{z=\pm b} = 0 \end{aligned}\right\} \tag{C13a}$$

where

$$\left.\begin{aligned} a'_{22} &\equiv \tilde{a}_{11}\frac{\cos^2\theta}{\sin^4\theta} + 2\tilde{a}_{12}\frac{\cos\theta}{\sin^2\theta} + \tilde{a}_{22} \\ e'_{22} &\equiv \tilde{e}'_{11}\frac{\cos^2\theta}{\sin^4\theta} + 2\tilde{e}'_{12}\frac{\cos\theta}{\sin^2\theta} + \tilde{e}'_{22} \end{aligned}\right\} \tag{C14}$$

Besides equations (C13a), the boundary condition

$$v_0(\pm b) = 0 \tag{C13b}$$

of the general case applies also to the present case.

Particular solution of the differential equations. - A particular solution of equations (C12) having the proper parity with respect to z is

$$\left.\begin{aligned} u_1 &= -\frac{c_{01}}{c_{11}} u_0 \\ v_2 &= 0 \\ v_0 &= 0 \end{aligned}\right\} \tag{C15}$$

Complementary solutions of exponential form. - The complementary solution, which is the solution of the homogeneous system obtained by omitting the term $c_{01}u_0$ from equations (C12), is first assumed in the form

$$\left.\begin{aligned} u_1 &= \tilde{A}' e^{\tilde{r}z} \\ v_2 &= \tilde{D}' e^{\tilde{r}z} \\ v_0 &= \tilde{E}' e^{\tilde{r}z} \end{aligned}\right\} \tag{C16}$$

Substituting these expressions into equations (C12) with the u_0 term excluded, one obtains the following conditions on $\tilde{A}'$, $\tilde{D}'$, $\tilde{E}'$ and $\tilde{r}$:

$$\begin{bmatrix} b_{11}\tilde{r}^2 - c_{11} & -\frac{1}{2} d_{11} \frac{\cos\theta}{\sin^2\theta} \tilde{r} & -\frac{1}{2} d_{10}\tilde{r} \\ -\frac{1}{2} d_{11} \frac{\cos\theta}{\sin^2\theta} \tilde{r} & a'_{22} - e'_{22}\tilde{r}^2 & -\tilde{e}'_{10} \frac{\cos\theta}{\sin^2\theta} \tilde{r}^2 \\ -\frac{1}{2} d_{10}\tilde{r} & -\tilde{e}'_{10} \frac{\cos\theta}{\sin^2\theta} \tilde{r}^2 & -\tilde{e}'_{00} \tilde{r}^2 \end{bmatrix} \begin{bmatrix} \tilde{A}' \\ \tilde{D}' \\ \tilde{E}' \end{bmatrix} = \begin{bmatrix} 0 \\ 0 \\ 0 \end{bmatrix} \tag{C17}$$

which lead to the following characteristic equation for $\tilde{r}$:

$$\begin{vmatrix} b_{11}\tilde{r}^2 - c_{11} & -\frac{1}{2}d_{11}\frac{\cos\theta}{\sin^2\theta}\tilde{r} & -\frac{1}{2}d_{10}\tilde{r} \\ -\frac{1}{2}d_{11}\frac{\cos\theta}{\sin^2\theta}\tilde{r} & a'_{22} - e'_{22}\tilde{r}^2 & -\tilde{e}'_{10}\frac{\cos\theta}{\sin^2\theta}\tilde{r}^2 \\ -\frac{1}{2}d_{10}\tilde{r} & -\tilde{e}'_{10}\frac{\cos\theta}{\sin^2\theta}\tilde{r}^2 & -\tilde{e}'_{00}\tilde{r}^2 \end{vmatrix} = 0 \qquad \text{(C18)}$$

Equations (C18) when expanded becomes

$$\left\{\left[\tilde{k}_{02}\left(\frac{t}{c}\right)^2\right] + \left[\tilde{k}_{20} + \tilde{k}_{22}\left(\frac{t}{c}\right)^2\right]\tilde{R}^2 + \left[\tilde{k}_{40} + \tilde{k}_{42}\left(\frac{t}{c}\right)^2\right]\tilde{R}^4\right\}\tilde{R}^2 = 0 \qquad \text{(C19)}$$

where

$$\tilde{R} \equiv c\tilde{r} \qquad \text{(C20)}$$

$$\left.\begin{aligned}
\tilde{k}_{02} &= \frac{G^2}{E^2}\tilde{a}^*_{22}\left[c^*_{11}\tilde{e}^*_{00} - \frac{1}{4}(d^*_{10})^2\right] \\
\tilde{k}_{20} &= \frac{G^3}{E^3}\frac{\cos^2\theta}{\sin^4\theta}\left\{\frac{k}{c}\left[\frac{1}{4}(d^*_{10})^2 - c^*_{11}\tilde{e}^*_{00}\right]\sin^2\theta \right. \\
&\qquad \left. + \left[c^*_{11}(\tilde{e}^*_{10})^2 + \frac{1}{4}(d^*_{11})^2\tilde{e}^*_{00} - \frac{1}{2}d^*_{11}d^*_{10}\tilde{e}^*_{10}\right]\right\} \\
\tilde{k}_{22} &= -\frac{E'}{E}\frac{G}{E}b^*_{11}\tilde{a}^*_{22}\tilde{e}^*_{00} - \frac{G^2}{E^2}\tilde{e}^*_{22}\left[c^*_{11}\tilde{e}^*_{00} - \frac{1}{4}(d^*_{10})^2\right] \\
\tilde{k}_{40} &= \frac{E'}{E}\left(\frac{G}{E}\right)^2 b^*_{11}\left[\tilde{e}^*_{00}\frac{k}{c}\sin^2\theta - (\tilde{e}^*_{10})^2\right]\frac{\cos^2\theta}{\sin^4\theta} \\
\tilde{k}_{42} &= \frac{E'}{E}\left(\frac{G}{E}\right)b^*_{11}\tilde{e}^*_{00}\tilde{e}^*_{22}
\end{aligned}\right\} \qquad \text{(C21)}$$

with

$$\left.\begin{aligned}
\tilde{a}^{*}_{22} &= \frac{(c/e)^3}{12(1-\nu^2)\tilde{\beta}^2\sin^4\theta}\left[\tilde{A}_{11}\cos^2\theta - \tilde{A}_{12}\frac{e}{k}\cos\theta + \tilde{A}_{22}\left(\frac{e}{k}\right)^2\right] \\
\tilde{e}^{*}_{00} &= \frac{e}{c} + \frac{k}{c}\cos^2\theta \\
\tilde{e}^{*}_{10} &= -\frac{k}{c}\sin\theta\cos\theta \\
\tilde{e}^{*}_{22} &= \frac{1}{3}\frac{G'}{E}\frac{1}{\sin^4\theta}\left(\frac{c}{e}\cos^2\theta + \frac{c}{k}\right)
\end{aligned}\right\} \qquad (C22)$$

Denoting the roots of equation (C19) by $\tilde{R}_1, \tilde{R}_2, \ldots, \tilde{R}_6$, the following properties may be postulated for them:

$$\tilde{R}_2 = -\tilde{R}_1 \qquad \tilde{R}_4 = -\tilde{R}_3 \qquad (C23)$$

$$\tilde{R}_5 = \tilde{R}_6 = 0 \qquad (C24)$$

The corresponding values of $\tilde{r}$ will be denoted by $\tilde{r}_1, \tilde{r}_2, \ldots, \tilde{r}_6$.

Thus, five solutions of the homogeneous system having the form of equations (C16) exist, corresponding to the five different roots of equation (C19). For each such solution the relationships which must exist among the coefficients $\tilde{A}'$, $\tilde{D}'$, and $\tilde{E}'$ can be obtained by substituting the particular value of $\tilde{r}$ into equations (C17). Denoting by $\tilde{A}'_j$, $\tilde{D}'_j$, and $\tilde{E}'_j$ the values of the coefficients associated with the particular root $r = \tilde{r}_j$, the following relationships are implied by the last two of equations (C17) for $j = 1,2,3$ or 4 :

$$\begin{bmatrix} a'_{22}c^2 - e'_{22}(c\tilde{r}_j)^2 & -\tilde{e}'_{10}\dfrac{\cos\theta}{\sin^2\theta}(c\tilde{r}_j)^2 \\ -\tilde{e}'_{10}\dfrac{\cos\theta}{\sin^2\theta}(c\tilde{r}_j)^2 & -\tilde{e}'_{00}(c\tilde{r}_j)^2 \end{bmatrix} \begin{bmatrix} \tilde{D}'_j/\tilde{A}'_j \\ \tilde{E}'_j/\tilde{A}'_j \end{bmatrix} = \begin{bmatrix} \frac{1}{2}d_{11}c\dfrac{\cos\theta}{\sin^2\theta}(c\tilde{r}_j) \\ \frac{1}{2}d_{10}c(c\tilde{r}_j) \end{bmatrix} \qquad (C25)$$

Substituting for a'_{22}, $\tilde{e}'_{00}$, $\tilde{e}'_{10}$, $\tilde{e}'_{22}$, d_{10} and d_{11} their definitions from equations (C14), (C10), and (6b), one converts equation (C25) to

$$\begin{bmatrix} \tilde{L}_{11} & \tilde{L}_{12} \\ \tilde{L}_{12} & \tilde{L}_{22} \end{bmatrix} \begin{bmatrix} \tilde{D}'_j/\tilde{A}'_j \\ \tilde{E}'_j/\tilde{A}'_j \end{bmatrix} = \begin{bmatrix} \frac{1}{2}\frac{G}{E}\frac{\cos\theta}{\sin^2\theta} d^*_{11}\tilde{R}_j \\ \frac{1}{2}\frac{G}{E} d^*_{10}\tilde{R}_j \end{bmatrix} \tag{C26}$$

where

$$\left.\begin{aligned} \tilde{L}_{11} &= \left(\frac{t}{c}\right)^2(\tilde{a}^*_{22} - \tilde{e}^*_{22}\tilde{R}_j^2) - \frac{G}{E}\frac{k}{c}\frac{\cos^2\theta}{\sin^2\theta}\tilde{R}_j^2 \\ \tilde{L}_{12} &= -\frac{G}{E}\frac{\cos\theta}{\sin^2\theta}\tilde{e}^*_{10}\tilde{R}_j^2 \\ \tilde{L}_{22} &= -\frac{G}{E}e^*_{00}R_j^2 \end{aligned}\right\} \tag{C27}$$

The solution of equations (C26) is

$$\begin{bmatrix} \tilde{D}'_j/\tilde{A}'_j \\ \tilde{E}'_j/\tilde{A}'_j \end{bmatrix} = \begin{bmatrix} \tilde{\gamma}^D_j \\ \tilde{\gamma}^E_j \end{bmatrix} \tag{C28}$$

where

$$\left.\begin{aligned} \tilde{\gamma}^D_j &= \frac{1}{2}\tilde{R}_j\frac{G}{E}(\tilde{L}_{22}\frac{\cos\theta}{\sin^2\theta}d^*_{11} - \tilde{L}_{12}d^*_{10})/(\tilde{L}_{11}\tilde{L}_{22} - \tilde{L}_{12}^2) \\ \tilde{\gamma}^E_j &= \frac{1}{2}\tilde{R}_j\frac{G}{E}(\tilde{L}_{11}d^*_{10} - \tilde{L}_{12}\frac{\cos\theta}{\sin^2\theta}d^*_{11})/(\tilde{L}_{11}\tilde{L}_{22} - \tilde{L}_{12}^2) \end{aligned}\right\} \tag{C29}$$

From equations (C29) and (C23) it is evident that

$$\tilde{\gamma}_2^D = -\tilde{\gamma}_1^D \ , \quad \tilde{\gamma}_4^D = -\tilde{\gamma}_3^D \ , \quad \tilde{\gamma}_2^E = -\tilde{\gamma}_1^E \ , \quad \tilde{\gamma}_4^E = -\tilde{\gamma}_3^E \tag{C30}$$

For $j = 5$ $(\tilde{r} = \tilde{r}_5 = 0)$ equations (C17) give

$$\begin{bmatrix} -c_{11} & 0 & 0 \\ 0 & a'_{22} & 0 \\ 0 & 0 & 0 \end{bmatrix} \begin{bmatrix} \tilde{A}'_5 \\ \tilde{D}'_5 \\ \tilde{E}'_5 \end{bmatrix} = \begin{bmatrix} 0 \\ 0 \\ 0 \end{bmatrix} \tag{C31}$$

whence

$$\tilde{A}'_5 = \tilde{D}'_5 = 0 \ , \quad \tilde{E}'_5 = \text{indeterminate} \tag{C32}$$

Summing the four solutions of the form (C16) corresponding to $\tilde{r} = \tilde{r}_1$ through $\tilde{r}_4$ and making use of equations (C28) and (C30), one obtains

$$\begin{bmatrix} u_1 \\ v_2 \\ v_0 \end{bmatrix} = \begin{bmatrix} 1 & 1 & 1 & 1 \\ \tilde{\gamma}_1^D & -\tilde{\gamma}_1^D & \tilde{\gamma}_3^D & -\tilde{\gamma}_3^D \\ \tilde{\gamma}_1^E & -\tilde{\gamma}_1^E & \tilde{\gamma}_3^E & -\tilde{\gamma}_3^E \end{bmatrix} \begin{bmatrix} \tilde{A}'_1 e^{\tilde{R}_1 \frac{z}{c}} \\ \tilde{A}'_2 e^{-\tilde{R}_1 \frac{z}{c}} \\ \tilde{A}'_3 e^{\tilde{R}_3 \frac{z}{c}} \\ \tilde{A}'_4 e^{-\tilde{R}_3 \frac{z}{c}} \end{bmatrix} \tag{C33}$$

Expressing the exponential functions in terms of hyperbolic functions and discarding the terms which do not have the proper symmetry (in the case of u_1) or antisymmetry (in the case of v_2 and v_0) with respect to z, one converts equations (C33) to

$$
\begin{aligned}
u_1 &= \bar{A}_1 \cosh \frac{\tilde{R}_1 z}{c} + \bar{A}_3 \cosh \frac{\tilde{R}_3 z}{c} \\
v_2 &= \tilde{\gamma}_1^D \bar{A}_1 \sinh \frac{\tilde{R}_1 z}{c} + \tilde{\gamma}_3^D \bar{A}_3 \sinh \frac{\tilde{R}_3 z}{c} \\
v_0 &= \tilde{\gamma}_1^E \bar{A}_1 \sinh \frac{\tilde{R}_1 z}{c} + \tilde{\gamma}_3^E \bar{A}_3 \sinh \frac{\tilde{R}_3 z}{c}
\end{aligned}
\tag{C34}
$$

where $\bar{A}_1$ and $\bar{A}_3$ are new arbitrary constants arising from certain linear combinations of the previous ones.

From equations (C32) and (C16) the following solution corresponding to $\tilde{r} = r_5 = 0$ is obtained:

$$
\begin{aligned}
u_1 &= 0 \\
v_2 &= 0 \\
v_0 &= \tilde{E}_5'
\end{aligned}
$$

Since $v_0 = \tilde{E}_5' =$ constant is even in z, rather than odd, the constant $\tilde{E}_5'$ may be equated to zero. Thus the pertinent solution contributed by the root $\tilde{r} = \tilde{r}_5 = 0$ is identically zero.

Complementary solution not of exponential form. - The existence of a repeated root (see eq. (C24)) indicates that the homogeneous system has an additional solution that is not of the form of equations (C16). This additional solution can be obtained by inspection if one postulates that it has the following form consistent with the evenness of u_1 and the oddness of v_2 and v_0

$$
\begin{aligned}
u_1 &= \tilde{A}_6' \\
v_2 &= \tilde{D}_6' \, z/c \\
v_0 &= \tilde{E}_6' \, z/c
\end{aligned}
\tag{C35}
$$

Substitution of this assumption into equations (C12) with the u_0 term omitted shows that equations (C35) are indeed a solution of the homogeneous system provided that

$$\tilde{D}'_6 = 0$$
$$\tilde{E}'_6 = \bar{\xi}\,\tilde{A}'_6 \tag{C36}$$

where

$$\bar{\xi} \equiv -2cc_{11}/d_{10} \tag{C37}$$

Thus the following additional solution of the homogeneous system is obtained:

$$u_1 = \tilde{A}'_6$$
$$v_2 = 0 \tag{C38}$$
$$v_0 = \bar{\xi}\,\tilde{A}'_6\, z/c$$

Complete solution of the differential equations (C12). - Summing the particular integral (C15) and the various solutions (C34) and (C38) of the homogeneous system, one obtains the following complete solution of equations (C12) having the pertinent symmetry and antisymmetry properties:

$$u_1 = -\frac{c_{01}}{c_{11}}u_0 + \bar{A}_1 \cosh\frac{\tilde{R}_1 z}{c} + \bar{A}_3 \cosh\frac{\tilde{R}_3 z}{c} + \tilde{A}'_6$$
$$v_2 = \tilde{\gamma}^D_1 \bar{A}_1 \sinh\frac{\tilde{R}_1 z}{c} + \tilde{\gamma}^D_3 \bar{A}_3 \sinh\frac{\tilde{R}_3 z}{c} \tag{C39}$$
$$v_0 = \tilde{\gamma}^E_1 \bar{A}_1 \sinh\frac{\tilde{R}_1 z}{c} + \tilde{\gamma}^E_3 \bar{A}_3 \sinh\frac{\tilde{R}_3 z}{c} + \bar{\xi}\,\tilde{A}'_6\,\frac{z}{c}$$

Evaluation of the arbitrary constants. - The three arbitrary constants $\bar{A}_1$, $\bar{A}_3$ and $\tilde{A}'_6$ can be determined from the boundary conditions, equations (C13a) and (C13b). The following equations are obtained which can be solved simultaneously for the three constants:

$$\begin{bmatrix} P_{11} & P_{12} & 0 \\ P_{21} & P_{22} & P_{23} \\ P_{31} & P_{32} & P_{33} \end{bmatrix} \begin{bmatrix} \frac{\bar{A}_1}{u_0} \sinh \frac{\tilde{R}_1 b}{c} \\ \frac{\bar{A}_3}{u_0} \sinh \frac{\tilde{R}_3 b}{c} \\ \tilde{A}_6'/u_0 \end{bmatrix} = \begin{bmatrix} 0 \\ 0 \\ P_3 \end{bmatrix} \tag{C40}$$

where

$$\left.\begin{aligned}
P_{11} &= \tilde{R}_1 \\
P_{12} &= \tilde{R}_3 \\
P_{21} &= \tilde{\gamma}_1^E \\
P_{22} &= \tilde{\gamma}_3^E \\
P_{23} &= \bar{\xi} \frac{b}{c} \\
P_{31} &= \left\{ d_{11}^* \frac{\cos\theta}{\sin^2\theta} + 2\tilde{R}_1 \left[\tilde{\gamma}_1^D \left\langle \frac{k}{c} \frac{\cos^2\theta}{\sin^2\theta} + \frac{E}{G} \tilde{e}_{22}^* \left(\frac{t}{c}\right)^2 \right\rangle + \tilde{\gamma}_1^E \tilde{e}_{10}^* \frac{\cos\theta}{\sin^2\theta} \right] \right\} \coth \frac{\tilde{R}_1 b}{c} \\
P_{32} &= \left\{ d_{11}^* \frac{\cos\theta}{\sin^2\theta} + 2\tilde{R}_3 \left[\tilde{\gamma}_3^D \left\langle \frac{k}{c} \frac{\cos^2\theta}{\sin^2\theta} + \frac{E}{G} \tilde{e}_{22}^* \left(\frac{t}{c}\right)^2 \right\rangle + \tilde{\gamma}_3^E \tilde{e}_{10}^* \frac{\cos\theta}{\sin^2\theta} \right] \right\} \coth \frac{\tilde{R}_3 b}{c} \\
P_{33} &= d_{11}^* \frac{\cos\theta}{\sin^2\theta} + 2\tilde{e}_{10}^* \bar{\xi} \frac{\cos\theta}{\sin^2\theta}
\end{aligned}\right\} \tag{C41a}$$

$$P_3 = d_{11}^* \frac{\cos\theta/\sin^2\theta}{1 + e/k} \tag{C41b}$$

Relationship between F and u_0. - With $u_1(z)$ determined in terms of u_0 (the first of eqs. (C39)), equation (C11) can be used to obtain the following relationship between F and u_0 :

$$\frac{F}{2u_0} = \frac{Gtb}{e}\tilde{\psi} \tag{C42}$$

where

$$\tilde{\psi} = 1 - \frac{1}{1+\frac{e}{k}} - \left(\frac{\bar{A}_1}{u_0}\sinh\frac{\tilde{R}_1 b}{c}\right)\frac{c}{\tilde{R}_1 b} - \left(\frac{\bar{A}_3}{u_0}\sinh\frac{\tilde{R}_3 b}{c}\right)\frac{c}{\tilde{R}_3 b} - \frac{\tilde{A}'_6}{u_0} \tag{C43}$$

A relative shear stiffness Ω can be defined the same way as in the general case. Equation (29) of the main body of the paper applies with f set equal to zero and ψ replaced by $\tilde{\psi}$.

Stresses. - The longitudinal normal stresses are identically zero at stations ⓪, ②, ③ and ⑤ . The non-zero longitudinal normal stresses $\sigma_{①}$ along junction ① are obtained from the equation

$$\sigma_{①} = E'\frac{du_1}{dz} \tag{C44}$$

Eliminating u_1 through the first of equations (C39), one obtains the following expression for the dimensionless stress parameter $\sigma_{①}c/E'u_0$:

$$\frac{\sigma_{①}c}{E'u_0} = \frac{\bar{A}_1}{u_0}\tilde{R}_1\sinh\frac{\tilde{R}_1 z}{c} + \frac{\bar{A}_3}{u_0}\tilde{R}_3\sinh\frac{\tilde{R}_3 z}{c} \tag{C45}$$

The dimensionless middle-surface shear stresses, as obtained from table 2 and equations (C39), are

$$\left.\begin{aligned}
\frac{\tau_{01}{}^{c}}{Gu_0} &= -\frac{c}{e}\frac{1}{1+k/e} + \frac{\bar{A}_1}{u_0}\left(\frac{c}{e} - \tilde{\gamma}_1^{E}\,\tilde{R}_1\right)\cosh\frac{\tilde{R}_1 z}{c} \\
&\quad + \frac{\bar{A}_3}{u_0}\left(\frac{c}{e} - \tilde{\gamma}_3^{E}\,\tilde{R}_3\right)\cosh\frac{\tilde{R}_3 z}{c} + \frac{A'_6}{u_0}\left(\frac{c}{e} - \bar{\xi}\right) \\
\frac{\tau_{12}{}^{c}}{Gu_0} &= -\frac{c/k}{1+e/k} + \frac{\bar{A}_1}{u_0}\left(\tilde{\gamma}_1^{D}\,\tilde{R}_1\cot\theta - \frac{c}{k} - \tilde{\gamma}_1^{E}\,\tilde{R}_1\cos\theta\right)\cosh\frac{\tilde{R}_1 z}{c} \\
&\quad + \frac{\bar{A}_3}{u_0}\left(\tilde{\gamma}_3^{D}\,\tilde{R}_3\cot\theta - \frac{c}{k} - \tilde{\gamma}_3^{E}\,\tilde{R}_3\cos\theta\right)\cosh\frac{\tilde{R}_3 z}{c} \\
&\quad - \frac{\tilde{A}'_6}{u_0}\left(\frac{c}{k} + \bar{\xi}\cos\theta\right)
\end{aligned}\right\} \qquad (C46)$$

where the subscripts 01 and 12 stand for the plate elements 01 and 12 respectively.

From the rates of twist in table 3 and the displacement expressions (C39) the following expressions are obtained for the extreme-fiber shearing stresses due to the twisting of plate elements 01 and 12 respectively:

$$\begin{aligned}
\frac{\tau'_{01}{}^{c}}{G'u_0} &= \frac{t}{e}\frac{\cos\theta}{\sin^2\theta}\,W(z) \\
\frac{\tau'_{12}{}^{c}}{G'u_0} &= -\frac{t}{k}\frac{1}{\sin^2\theta}\,W(z)
\end{aligned} \qquad (C47)$$

where

$$W(z) = \frac{\bar{A}_1}{u_0}\,\tilde{\gamma}_1^{D}\,\tilde{R}_1\cosh\frac{\tilde{R}_1 z}{c} + \frac{\bar{A}_3}{u_0}\,\tilde{\gamma}_3^{D}\,\tilde{R}_3\cosh\frac{\tilde{R}_3 z}{c} \qquad (C48)$$

The frame bending moments and associated extreme fiber bending stresses are zero at stations ⓪ , ② , ③ and ⑤ . Referring to equations (D44) of reference 1, one obtains the following dimensionless expression for the extreme fiber transverse bending stresses $\sigma'_{①}$ along junction ① :

$$\frac{\sigma_{①}{}'^{c}}{Eu_0} = -\frac{6}{1-\nu^2}\frac{t}{k}\frac{c}{e}\frac{1}{\tilde{\beta}\sin^2\theta}\left[3\frac{e}{k}\cos\theta + 3\left(\frac{e}{k}\right)^2\right]\frac{v_2}{u_0} \qquad \text{(C49)}$$

in which $\sigma_{①}{}'$ is positive for compression in the upper fibers, tension in the lower fibers (see fig. 5).

APPENDIX D

SPECIAL CASE: e = 0

Figure 6(c) shows the special case $e = 0$, in which the plate elements at the troughs are of zero width, with the result that the two adjacent inclined plate elements meet to form a vertex along the trough line.

This special case can be obtained from the general case (appendix A) by first imposing along the junction line (1) the same displacement conditions as exist along the junction line (0), namely

$$u_1(z) = u_0 \tag{D1}$$

$$v_1(z) = 0 \tag{D2}$$

and introducing these conditions (and their variational forms $\delta u_1 = \delta u_0$, $\delta v_1 = 0$) into the $\delta(TPE)$ expression, equation (A5). This will eliminate from the $\delta(TPE)$ those terms arising from longitudinal extension and twisting of plate elements 01 and 45.

In order to eliminate the terms associated with middle-surface shearing of these plate elements, the condition $e \to 0$ should then be introduced into all the remaining coefficients except those associated with the strain energy of frame bending (a_{11}, a_{12}, a_{22}).

The condition $e \to 0$ will not lead to the correct strain energy of frame bending because this condition, imposed after condition (D2), implies clamping (zero rotation) rather than free rotation along the trough lines in the limiting case. In order to obtain correctly the zero moment condition existing along the trough lines the condition $e \to \infty$ must be imposed instead in those terms (a_{11}, a_{12}, a_{22}) associated with frame bending of the cross sections.

Applying the above procedure to equation (A5) gives the following expression for $\delta(TPE)$:

$$\delta(TPE) = (\delta u_0)\int_{-b}^{b}(2\bar{c}_{00}u_0 + 2c_{12}u_2 - \frac{F}{b})dz$$

$$+ 2\int_{-b}^{b}\left(-b_{22}\frac{d^2u_2}{dz^2} + c_{12}u_0 + c_{22}u_2 + \frac{1}{2}d_{20}\frac{dv_0}{dz}\right.$$

$$\left. + \frac{1}{2}d_{22}\frac{dv_2}{dz}\right)(\delta u_2)dz$$

(equation continued on next page)

$$- 2 \int_{-b}^{b} \left(\frac{1}{2} d_{20} \frac{du_2}{dz} + \hat{e}_{00} \frac{d^2 v_0}{dz^2} + e_{20} \frac{d^2 v_2}{dz^2} \right) (\delta v_0) dz$$

$$+ 2 \int_{-b}^{b} \left(\bar{a}_{22} v_2 - \frac{1}{2} d_{22} \frac{du_2}{dz} - e_{20} \frac{d^2 v_0}{dz^2} - e_{22} \frac{d^2 v_2}{dz^2} \right) (\delta v_2) dz$$

$$+ \left[2b_{22} \frac{du_2}{dz} (\delta u_2) \right] \Bigg|_{-b}^{b}$$

$$+ \left[\left(d_{22} u_2 + 2e_{20} \frac{dv_0}{dz} + 2e_{22} \frac{dv_2}{dz} \right) (\delta v_2) \right] \Bigg|_{-b}^{b} \qquad \text{(D3)}$$

where

$$\bar{c}_{00} = Gt/k \qquad \text{(D4)}$$

$$\hat{e}_{00} = Gt\left(k \cos^2 \theta + \frac{f}{2}\right) \qquad \text{(D5)}$$

$$\bar{a}_{22} = \frac{E}{2(1 - \nu^2)} \left(\frac{t}{k} \right)^3 \frac{\frac{k}{f}\left(1 + 2 \frac{k}{f} \cos \theta\right)^2}{1 + 2 \frac{k}{f}} \qquad \text{(D6)}$$

Differential equations and boundary conditions. - From the vanishing of $\delta(\text{TPE})$, equation (D3), the following equations governing u_2, v_0 and v_2 are obtained:

$$4\bar{c}_{00} u_0 b + 2c_{12} \int_{-b}^{b} u_2 dz - 2F = 0 \qquad \text{(D7)}$$

$$\left.
\begin{aligned}
& - b_{22} \frac{d^2 u_2}{dz^2} + c_{12} u_0 + c_{22} u_2 + \frac{1}{2} d_{20} \frac{dv_0}{dz} + \frac{1}{2} d_{22} \frac{dv_2}{dz} = 0 \\
& \frac{1}{2} d_{20} \frac{du_2}{dz} + \hat{e}_{00} \frac{d^2 v_0}{dz^2} + e_{20} \frac{d^2 v_2}{dz^2} = 0 \\
& \bar{a}_{22} v_2 - \frac{1}{2} d_{22} \frac{du_2}{dz} - e_{20} \frac{d^2 v_0}{dz^2} - e_{22} \frac{d^2 v_2}{dz^2} = 0
\end{aligned}
\right\} \qquad \text{(D8)}$$

$$\left(\frac{du_2}{dz}\right)_{z=\pm b} = 0$$

$$\left(d_{22}u_2 + 2e_{20}\frac{dv_0}{dz} + 2e_{22}\frac{dv_2}{dz}\right)_{z=\pm b} = 0 \qquad \text{(D9a)}$$

Besides equations (D9a), the boundary condition

$$v_0(\pm b) = 0 \qquad \text{(D9b)}$$

of the general case applies also to the present special case.

The above development is for the case of point attachments at the ends of the trough lines only (fig. 2(a) or 2(d)). When e = 0 the presence of additional attachments at the ends of the crest lines (fig. 2(b)) would completely prevent cross-sectional deformation and therefore be tantamount to continuous attachment.

Particular solution of the differential equations. - A particular solution of equation (D8) having the proper parity with respect to z is

$$\left.\begin{aligned} u_2 &= -\frac{c_{12}}{c_{22}}u_0 \\ v_0 &= 0 \\ v_2 &= 0 \end{aligned}\right\} \qquad \text{(D10)}$$

Complementary solutions of exponential form. - The complementary solution, which is the solution of the homogeneous system obtained by omitting the term $c_{12}u_0$ from equations (D8), is first assumed in the form

$$\left.\begin{aligned} u_2 &= \hat{B}e^{\hat{r}z} \\ v_2 &= \hat{D}e^{\hat{r}z} \\ v_0 &= \hat{E}e^{\hat{r}z} \end{aligned}\right\} \qquad \text{(D11)}$$

Substitution of these expressions into equations (D8) with the $c_{12}u_0$ term omitted leads to the following conditions on $\hat{B}$, $\hat{D}$, $\hat{E}$ and $\hat{f}$:

$$\begin{bmatrix} b_{22}\hat{r}^2 - c_{22} & -\frac{1}{2}d_{22}\hat{r} & -\frac{1}{2}d_{20}\hat{r} \\ -\frac{1}{2}d_{22}\hat{r} & \bar{a}_{22} - e_{22}\hat{r}^2 & -e_{20}\hat{r}^2 \\ -\frac{1}{2}d_{20}\hat{r} & -e_{20}\hat{r}^2 & -e_{00}\hat{r}^2 \end{bmatrix} \begin{bmatrix} \hat{B} \\ \hat{D} \\ \hat{E} \end{bmatrix} = \begin{bmatrix} 0 \\ 0 \\ 0 \end{bmatrix} \qquad \text{(D12)}$$

from which arises the following characteristic equation for $\hat{r}$:

$$\begin{vmatrix} b_{22}\hat{r}^2 - c_{22} & -\frac{1}{2}d_{22}\hat{r} & -\frac{1}{2}d_{20}\hat{r} \\ -\frac{1}{2}d_{22}\hat{r} & \bar{a}_{22} - e_{22}\hat{r}^2 & -e_{20}\hat{r}^2 \\ -\frac{1}{2}d_{20}\hat{r} & -e_{20}\hat{r}^2 & -e_{00}\hat{r}^2 \end{vmatrix} = 0 \qquad \text{(D13)}$$

Equation (D13) when expanded becomes

$$\left\{\left[\hat{k}_{02}\left(\frac{t}{c}\right)^2\right] + \left[\hat{k}_{20} + \hat{k}_{22}\left(\frac{t}{c}\right)^2\right]\hat{R}^2 + \left[\hat{k}_{40} + \hat{k}_{42}\left(\frac{t}{c}\right)^2\right]\hat{R}^4\right\}\hat{R}^2 = 0 \qquad \text{(D14)}$$

where

$$\hat{R} \equiv c\hat{r} \qquad \text{(D15)}$$

$$\hat{k}_{02} = \left(\frac{G}{E}\right)^2 \bar{a}^*_{22}\left[c^*_{22}\hat{e}^{**}_{00} - \frac{1}{4}(d^*_{20})^2\right]$$

$$\hat{k}_{20} = \left(\frac{G}{E}\right)^3\left[\frac{1}{4}(d^*_{20})^2 e^{**}_{22} - \frac{1}{2}\, d^*_{20}d^*_{11}e^{**}_{20} + c^*_{22}(e^{**}_{20})^2 - c^*_{22}\hat{e}^{**}_{00}e^{**}_{22} + \frac{1}{4}(d^*_{11})^2\, \hat{e}^{**}_{00}\right] \tag{D16}$$

$$\hat{k}_{22} = \left(\frac{G}{E}\right)^2 \frac{G'}{E}\left[\frac{1}{4}(d^*_{20})^2\, \bar{e}^*_{22} - c^*_{22}\bar{e}^*_{22}\hat{e}^{**}_{00}\right] - \frac{E'}{E}\,\frac{G}{E}\,\bar{a}^*_{22}b^*_{22}\hat{e}^{**}_{00}$$

$$\hat{k}_{40} = \frac{E'}{E}\left(\frac{G}{E}\right)^2 b^*_{22}[\hat{e}^{**}_{00}e^{**}_{22} - (e^{**}_{20})^2]$$

$$\hat{k}_{42} = \frac{E'}{E}\,\frac{G}{E}\,\frac{G'}{E}\, b^*_{22}\hat{e}^{**}_{00}\bar{e}^*_{22}$$

with

$$\bar{a}^*_{22} = \frac{\left(\frac{c}{k}\right)^2 \frac{c}{f}(1 + 2\,\frac{k}{f}\cos\theta)^2}{2(1 - \nu^2)(1 + 2\,\frac{k}{f})} \tag{D17}$$

$$\hat{e}^{**}_{00} = \frac{k}{c}\cos^2\theta + \frac{1}{2}\,\frac{f}{c}$$

Denoting the roots of equation (D14) by $\hat{R}_1, \hat{R}_2, \ldots, \hat{R}_6$, the following properties may be postulated for them:

$$\hat{R}_2 = -\hat{R}_1 \qquad \hat{R}_4 = -\hat{R}_3 \tag{D18}$$

$$\hat{R}_5 = \hat{R}_6 = 0 \tag{D19}$$

The corresponding values of $\hat{r}$ will be denoted by $\hat{r}_1, \hat{r}_2, \ldots, \hat{r}_6$.

Thus, there exist five solutions of the homogeneous system having the form of equations (D11). For each such solution the relationships which must exist among the coefficients $\hat{B}$, $\hat{D}$, and $\hat{E}$ can be obtained by substituting the specific value of $\hat{r}$ into equations (D12). Letting $\hat{B}_j$, $\hat{D}_j$, and $\hat{E}_j$ denote the values of $\hat{B}$, $\hat{D}$, and $\hat{E}$ associated with the root $\hat{r} = \hat{r}_j$, the following relationships are implied by the last two of equations (D12) for $j = 1, 2, 3, 4$:

$$\begin{bmatrix} \bar{a}_{22}c^2 - e_{22}(c\hat{r}_j)^2 & - e_{20}(c\hat{r}_j)^2 \\ - e_{20}(c\hat{r}_j)^2 & - \hat{e}_{00}(c\hat{r}_j)^2 \end{bmatrix} \begin{bmatrix} \hat{D}_j/\hat{B}_j \\ \hat{E}_j/\hat{B}_j \end{bmatrix} = \begin{bmatrix} \frac{1}{2} d_{22}c(c\hat{r}_j) \\ \frac{1}{2} d_{20}c(c\hat{r}_j) \end{bmatrix} \tag{D20}$$

Substituting for $\bar{a}_{22}$, e_{22}, e_{20}, $\hat{e}_{00}$, d_{22} and d_{20} their definitions from equations (D5), (D6), (6b) and (A2), one converts equations (D20) to

$$\begin{bmatrix} \hat{L}_{11} & \hat{L}_{12} \\ \hat{L}_{12} & \hat{L}_{22} \end{bmatrix} \begin{bmatrix} \hat{D}_j/\hat{B}_j \\ \hat{E}_j/\hat{B}_j \end{bmatrix} = \begin{bmatrix} \frac{1}{2} \frac{G}{E} d^*_{11}\hat{R}_j \\ \frac{1}{2} \frac{G}{E} d^*_{20}\hat{R}_j \end{bmatrix} \tag{D21}$$

where

$$\begin{aligned} \hat{L}_{11} &= \left(\frac{t}{c}\right)^2\left[\bar{a}^*_{22} - \frac{G'}{E}\bar{e}^*_{22}\hat{R}_j^2\right] - \frac{G}{E} e^{**}_{22}\hat{R}_j^2 \\ \hat{L}_{12} &= - \frac{G}{E} e^{**}_{20}\hat{R}_j^2 \\ \hat{L}_{22} &= - \frac{G}{E} \hat{e}^{**}_{00}\hat{R}_j^2 \end{aligned} \tag{D22}$$

The solution of equations (D21) is

$$\begin{bmatrix} \hat{D}_j/\hat{B}_j \\ \hat{E}_j/\hat{B}_j \end{bmatrix} = \begin{bmatrix} \hat{\gamma}^D_j \\ \hat{\gamma}^E_j \end{bmatrix} \tag{D23}$$

where

$$\hat{\gamma}_j^D = \frac{1}{2}\hat{R}_j \frac{G}{E}(\hat{L}_{22}d_{11}^* - \hat{L}_{12}d_{20}^*)/(\hat{L}_{11}\hat{L}_{22} - \hat{L}_{12}^2)$$

$$\hat{\gamma}_j^E = \frac{1}{2}\hat{R}_j \frac{G}{E}(\hat{L}_{11}d_{20}^* - \hat{L}_{12}d_{11}^*)/(\hat{L}_{11}\hat{L}_{22} - \hat{L}_{12}^2) \qquad \text{(D24)}$$

From equations (D24) and (D18) it is evident that

$$\hat{\gamma}_2^D = -\hat{\gamma}_1^D\,, \quad \hat{\gamma}_4^D = -\hat{\gamma}_3^D\,, \quad \hat{\gamma}_2^E = -\hat{\gamma}_1^E\,, \quad \hat{\gamma}_4^E = -\hat{\gamma}_3^E \qquad \text{(D25)}$$

For $j = 5$ $(\hat{r} = \hat{r}_5 = 0)$ equations (D12) give

$$\begin{bmatrix} -c_{22} & 0 & 0 \\ 0 & \bar{a}_{22} & 0 \\ 0 & 0 & 0 \end{bmatrix} \begin{bmatrix} \hat{B}_5 \\ \hat{D}_5 \\ \hat{E}_5 \end{bmatrix} = \begin{bmatrix} 0 \\ 0 \\ 0 \end{bmatrix} \qquad \text{(D26)}$$

whence

$$\hat{B}_5 = \hat{D}_5 = 0\,, \quad \hat{E}_5 = \text{indeterminate} \qquad \text{(D27)}$$

Summing the four solutions of the form of equations (D11) corresponding to $\hat{r} = \hat{r}_1$ through $\hat{r}_4$ and making use of equations (D23) and (D25), one obtains

$$\begin{bmatrix} u_2 \\ v_2 \\ v_0 \end{bmatrix} = \begin{bmatrix} 1 & 1 & 1 & 1 \\ \hat{\gamma}_1^D & -\hat{\gamma}_1^D & \hat{\gamma}_3^D & -\hat{\gamma}_3^D \\ \hat{\gamma}_1^E & -\hat{\gamma}_1^E & \hat{\gamma}_3^E & -\hat{\gamma}_3^E \end{bmatrix} \begin{bmatrix} \hat{B}_1 e^{\hat{R}_1 \frac{z}{c}} \\ \hat{B}_2 e^{-\hat{R}_1 \frac{z}{c}} \\ \hat{B}_3 e^{\hat{R}_3 \frac{z}{c}} \\ \hat{B}_4 e^{-\hat{R}_3 \frac{z}{c}} \end{bmatrix} \qquad \text{(D28)}$$

Expressing the exponential functions in terms of hyperbolic functions, and taking into account the fact that u_2 must be even in z, v_2 and v_0 odd in z, one converts equations (D28) to

$$\left.\begin{aligned} u_2 &= B_1^* \cosh \frac{\hat{R}_1 z}{c} + B_3^* \cosh \frac{\hat{R}_3 z}{c} \\ v_2 &= \hat{\gamma}_1^D B_1^* \sinh \frac{\hat{R}_1 z}{c} + \hat{\gamma}_3^D B_3^* \sinh \frac{\hat{R}_3 z}{c} \\ v_0 &= \hat{\gamma}_1^E B_1^* \sinh \frac{\hat{R}_1 z}{c} + \hat{\gamma}_3^E B_3^* \sinh \frac{\hat{R}_3 z}{c} \end{aligned}\right\} \quad \text{(D29)}$$

where B_1^* and B_3^* are new arbitrary constants arising from certain linear combinations of the previous ones.

From equations (D27) and (D11) the following solution corresponding to $\hat{r} = \hat{r}_5 = 0$ is obtained:

$$u_2 = 0$$

$$v_2 = 0$$

$$v_0 = \hat{E}_5$$

Since $v_0 = \hat{E}_5 =$ constant is even in z, rather than odd, the constant $\hat{E}_5$ may be equated to zero. Thus the pertinent solution contributed by the root $\hat{r} = \hat{r}_5 = 0$ is identically zero.

Complementary solution not of exponential form. - The existence of a repeated root (see eq. (D19)) indicates that the homogeneous system has an additional solution that is not of the form of equations (D11). This additional solution can be obtained by inspection if one postulates that it has the following form consistent with the evenness of u_2 and the oddness of v_2 and v_0 :

$$\left.\begin{aligned} u_2 &= \hat{B}_6 \\ v_2 &= \hat{D}_6 z/c \\ v_0 &= \hat{E}_6 z/c \end{aligned}\right\} \quad \text{(D30)}$$

Substituting this assumption into the system of differential equations (D8) with the $c_{12}u_0$ term omitted shows that equations (D30) are indeed a solution of the homogeneous system provided that

$$\left.\begin{aligned} \hat{D}_6 &= 0 \\ \hat{E}_6 &= \hat{\xi}\hat{B}_6 \end{aligned}\right\} \quad (D31)$$

where

$$\hat{\xi} = -2\, c \cdot c_{22}/d_{20} \quad (D32)$$

Therefore the additional solution of the homogeneous system is

$$\left.\begin{aligned} u_2 &= \hat{B}_6 \\ v_2 &= 0 \\ v_0 &= \hat{\xi}\hat{B}_6 z/c \end{aligned}\right\} \quad (D33)$$

Complete solution of the differential equations (D8). - Summing the particular solution (D10) and the various solutions (D29) and (D33) of the homogeneous system, one obtains the following complete solution of the differential equations (D8) having the pertinent symmetry and antisymmetry properties:

$$\left.\begin{aligned} u_2 &= -\frac{c_{12}}{c_{22}} u_0 + B_1^* \cosh \frac{\hat{R}_1 z}{c} + B_3^* \cosh \frac{\hat{R}_3 z}{c} + \hat{B}_6 \\ v_2 &= \hat{\gamma}_1^D B_1^* \sinh \frac{\hat{R}_1 z}{c} + \hat{\gamma}_3^D B_3^* \sinh \frac{\hat{R}_3 z}{c} \\ v_0 &= \hat{\gamma}_1^E B_1^* \sinh \frac{\hat{R}_1 z}{c} + \hat{\gamma}_3^E B_3^* \sinh \frac{\hat{R}_3 z}{c} + \hat{\xi}\hat{B}_6 z/c \end{aligned}\right\} \quad (D34)$$

Evaluation of the arbitrary constants. - The three arbitrary constants B_1^*, B_3^*, and $\hat{B}_6$ can be determined from the boundary conditions, equations (D9a) and (D9b). These boundary conditions lead to the following equations defining B_1^*, B_3^*, and $\hat{B}_6$:

$$\begin{bmatrix} Q_{11} & Q_{12} & 0 \\ Q_{21} & Q_{22} & Q_{23} \\ Q_{31} & Q_{32} & Q_{33} \end{bmatrix} \begin{bmatrix} \frac{B_1^*}{u_0} \sinh \frac{\hat{R}_1 b}{c} \\ \frac{B_3^*}{u_0} \sinh \frac{\hat{R}_3 b}{c} \\ \hat{B}_6/u_0 \end{bmatrix} = \begin{bmatrix} 0 \\ 0 \\ Q_3 \end{bmatrix} \tag{D35}$$

where

$$\left.\begin{aligned} Q_{11} &= \hat{R}_1 \\ Q_{12} &= \hat{R}_3 \\ Q_{21} &= \hat{\gamma}_1^E \\ Q_{22} &= \hat{\gamma}_3^E \\ Q_{23} &= \hat{\xi}\, b/c \\ Q_{31} &= \{d_{11}^* + 2\hat{R}_1[(e_{22}^{**} + \frac{G'}{G}\frac{t^2}{c^2}\bar{e}_{22}^*)\hat{\gamma}_1^D + e_{20}^{**}\hat{\gamma}_1^E]\}\coth\frac{\hat{R}_1 b}{c} \\ Q_{32} &= \{d_{11}^* + 2\hat{R}_3[(e_{22}^{**} + \frac{G'}{G}\frac{t^2}{c^2}\bar{e}_{22}^*)\hat{\gamma}_3^D + e_{20}^{**}\hat{\gamma}_3^E]\}\coth\frac{\hat{R}_3 b}{c} \\ Q_{33} &= d_{11}^* + 2e_{20}^{**}\hat{\xi} \end{aligned}\right\} \tag{D36}$$

$$Q_3 = \frac{2\sin\theta}{1 + 2\frac{k}{f}} \tag{D37}$$

Relationship between F and u_0. - With $u_2(z)$ known in terms of u_0 (the first of eqs. (D34)), equation (D7) yields the following relationship between the shearing force F and the relative shearing displacement $2u_0$:

$$\frac{F}{2u_0} = \frac{Gtb}{k}\hat{\psi} \tag{D38}$$

where

$$\hat{\psi} = 1 - \frac{1}{1 + 2\frac{k}{f}} - \left(\frac{B_1^*}{u_0}\sinh\frac{\hat{R}_1 b}{c}\right)\frac{c}{\hat{R}_1 b}$$

$$- \left(\frac{B_3^*}{u_0}\sinh\frac{\hat{R}_3 b}{c}\right)\frac{c}{\hat{R}_3 b} - \frac{\hat{B}_6}{u_0} \tag{D39}$$

Equation (D38) can be used to compute the overall shearing stiffness of a single corrugation.

A relative shearing stiffness Ω, the ratio of the shearing stiffness (D38) to that of the same corrugation with continuous end attachment producing uniform middle-surface shear strain throughout the sheet, is given by

$$\Omega = (1 + \frac{1}{2}\frac{f}{k})\hat{\psi} \tag{D40}$$

Stresses. - The longitudinal normal stresses are identically zero at stations ⓪, ①, ④ and ⑤. The non-vanishing longitudinal normal stresses $\sigma_{②}$ along junction line ②, obtained from the strains du_2/dz, are given in dimensionless form by

$$\frac{\sigma_{②}^{c}}{E'u_0} = \frac{B_1^*}{u_0}\hat{R}_1\sinh\frac{\hat{R}_1 z}{c} + \frac{B_3^*}{u_0}\hat{R}_3\sinh\frac{\hat{R}_3 z}{c} \tag{D41}$$

The dimensionless middle-surface shear stresses, as obtained from table 2 and equations (D34), are given by

$$\left.\begin{aligned}
\frac{\tau_{12}{}^{c}}{Gu_0} &= \left(\frac{u_2(z)}{u_0} - 1\right)\frac{c}{k} \\
&\quad - \cos\theta\left(\hat{\gamma}_1^E \frac{B_1^*}{u_0}\hat{R}_1 \cosh\frac{\hat{R}_1 z}{c} + \hat{\gamma}_3^E \frac{B_3^*}{u_0}\hat{R}_3 \cosh\frac{\hat{R}_3 z}{c} + \hat{\xi}\frac{\hat{B}_6}{u_0}\right) \\
\frac{\tau_{23}{}^{c}}{Gu_0} &= -2\frac{c}{f}\frac{u_2(z)}{u_0} - \left(\hat{\gamma}_1^E \frac{B_1^*}{u_0}\hat{R}_1 \cosh\frac{\hat{R}_1 z}{c} + \hat{\gamma}_3^E \frac{B_3^*}{u_0}\hat{R}_3 \cosh\frac{\hat{R}_3 z}{c}\right. \\
&\quad \left. + \hat{\xi}\frac{\hat{B}_6}{u_0}\right) + \sin\theta\left(\hat{\gamma}_1^D \frac{B_1^*}{u_0}\hat{R}_1 \cosh\frac{\hat{R}_1 z}{c} + \hat{\gamma}_3^D \frac{B_3^*}{u_0}\hat{R}_3 \cosh\frac{\hat{R}_3 z}{c}\right)
\end{aligned}\right\} \quad (D42)$$

where the subscripts 12 and 23 represent the plate elements 12 and 23 respectively.

From the rates of twist in table 3 and the displacement expressions (D34) the following expressions are obtained for the extreme-fiber shearing stresses due to the twisting of plate elements 12 and 23 respectively:

$$\left.\begin{aligned}
\frac{\tau'_{12}{}^{c}}{G'u_0} &= -\frac{t}{k}\overline{W}(z) \\
\frac{\tau'_{23}{}^{c}}{G'u_0} &= 2\frac{t}{f}\cos\theta\,\overline{W}(z)
\end{aligned}\right\} \quad (D43)$$

where

$$\overline{W}(z) = \hat{\gamma}_1^D \frac{B_1^*}{u_0}\hat{R}_1 \cosh\frac{\hat{R}_1 z}{c} + \hat{\gamma}_3^D \frac{B_3^*}{u_0}\hat{R}_3 \cosh\frac{\hat{R}_3 z}{c} \quad (D44)$$

The frame bending moments and associated extreme fiber bending stresses are zero at stations ⓪ , ① , ④ and ⑤ . From the first of equations (E38) of reference 1, one obtains the following dimensionless expression for the extreme fiber transverse bending stresses $\sigma'_{②}$ along junction line ② :

$$\frac{\sigma'_{②}{}^{c}}{Eu_0} = \frac{3}{1-\nu^2}\frac{c}{k}\frac{t}{f}\frac{1 + 2\frac{k}{f}\cos\theta}{1 + 2\frac{k}{f}}\frac{v_2(z)}{u_0} \quad (D45)$$

REFERENCES

1. Lin. C. J.; and Libove, C.: Theoretical Study of Corrugated Plates: Shearing of a Trapezoidally Corrugated Plate With Trough Lines Held Straight. Syracuse University Research Institute; Department of Mechanical and Aerospace Engineering, Report No. MAE 1833-T1, May 1970. (Report prepared under NASA Grant NGR-33-022-115.)

2. Rothwell, A.: The Shear Stiffness of Flat-sided Corrugated Webs. The Aeronautical Quarterly, Aug. 1968, pp. 224-234.

3. Argyris, J. H.; and Kelsey, S.: Energy Theorems and Structural Analysis. Butterworths (London), 1960.

4. Timoshenko, S. P.; and Goodier, J. N.: Theory of Elasticity. Second ed., McGraw-Hill Book Co., Inc., 1951, p. 273.

5. Bryan, E. R.; and El-Dakhakhni, W. M.: Shear Flexibility and Strength of Corrugated Decks. J. of the Structural Division, Proc. ASCE, vol. 94, no. ST 11, Nov. 1968, pp. 2549-2580.

6. McKenzie, K. I.: The Shear Stiffness of a Corrugated Web. R. & M. No. 3342, British A.R.C., 1963.

7. Bryan, E. R.; and Jackson, P.: The Shear Behavior of Corrugated Steel Sheeting. In "Thin Walled Steel Structures: their design and use in buildings," K.C. Rockey and H.V. Hill, eds., Crosby Lockwood (London), Gordon and Breach (New York), 1969 (Proceedings of a symposium held in Sept. 1967).

8. Horsfall, J. R.: The Buckling of Corrugated Webs in Shear. Thesis submitted for the award of DCAe, The College of Aeronautics, 1964.

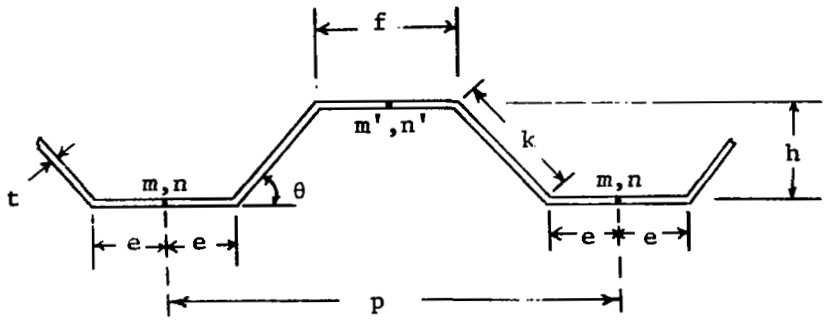

(a) Cross section

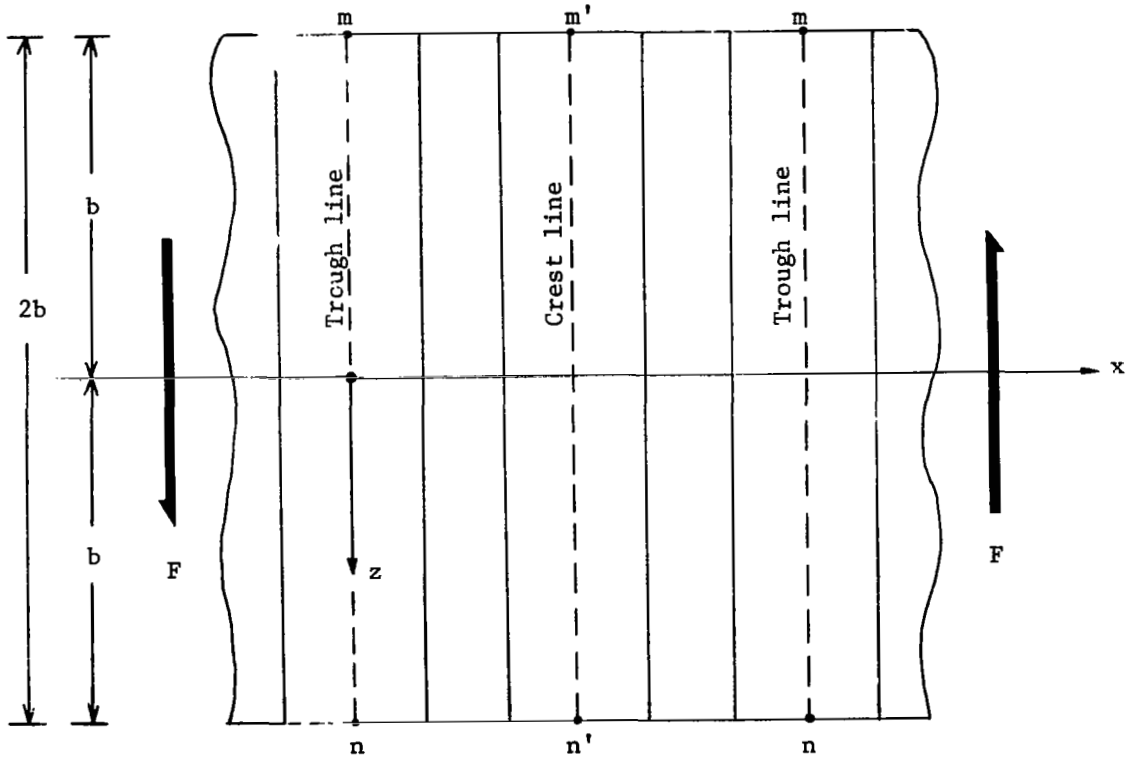

(b) Plan view

Figure 1. - Configuration of trapezoidally corrugated plate considered in the present analysis.

(a) Point attachment at the ends of the trough lines.

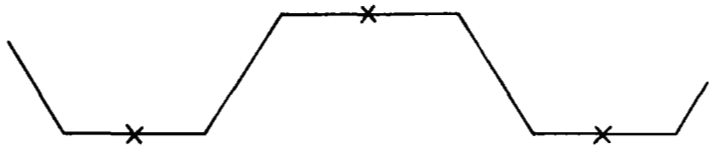

(b) Point attachment at the ends of the trough lines and crest lines.

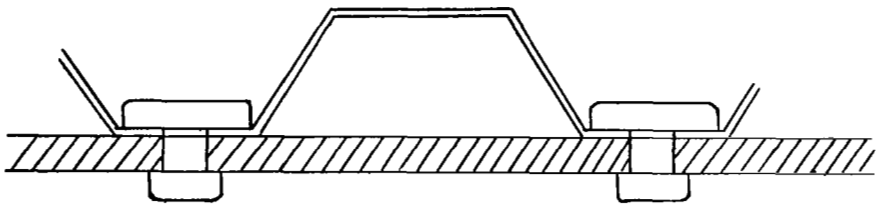

(c) Wide attachment at ends of trough lines only.

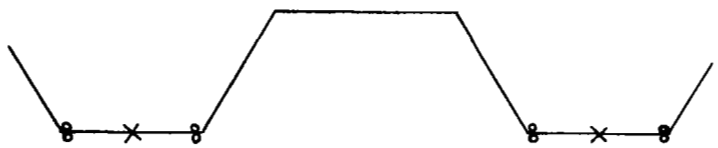

(d) Idealization of (c) used in the analysis: Point attachments at the ends of the trough lines, and point attachments permitting longitudinal sliding at the junctions of the trough plate elements and the inclined plate elements.

Figure 2. - Types of attachment considered at the ends of the corrugations.

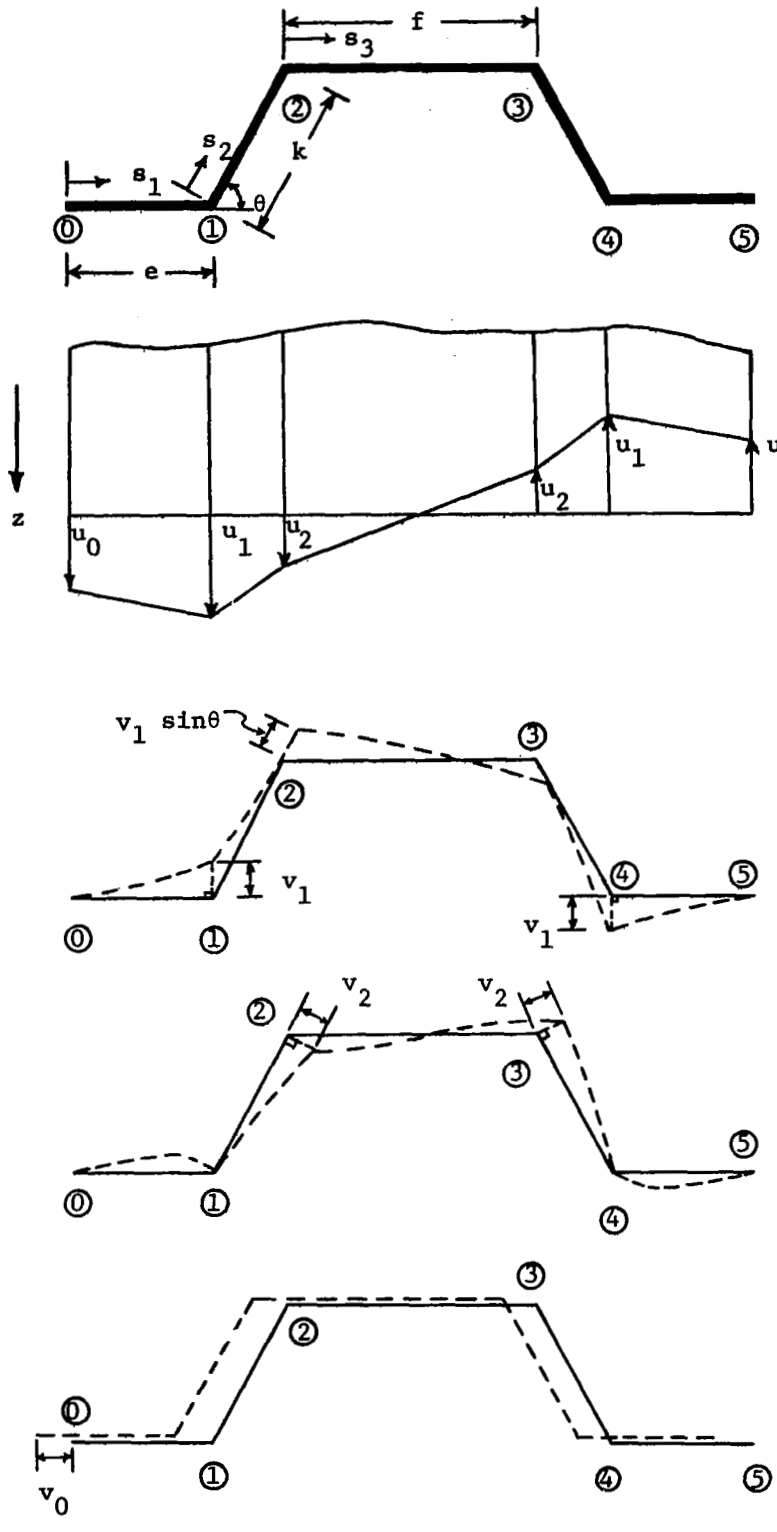

(a) Diagram of cross section.

(b) Assumption regarding longitudinal displacements.

(c) Component displacement modes for displacements in the plane of the cross section

Figure 3. - Diagrammatic representation of assumptions regarding displacements.

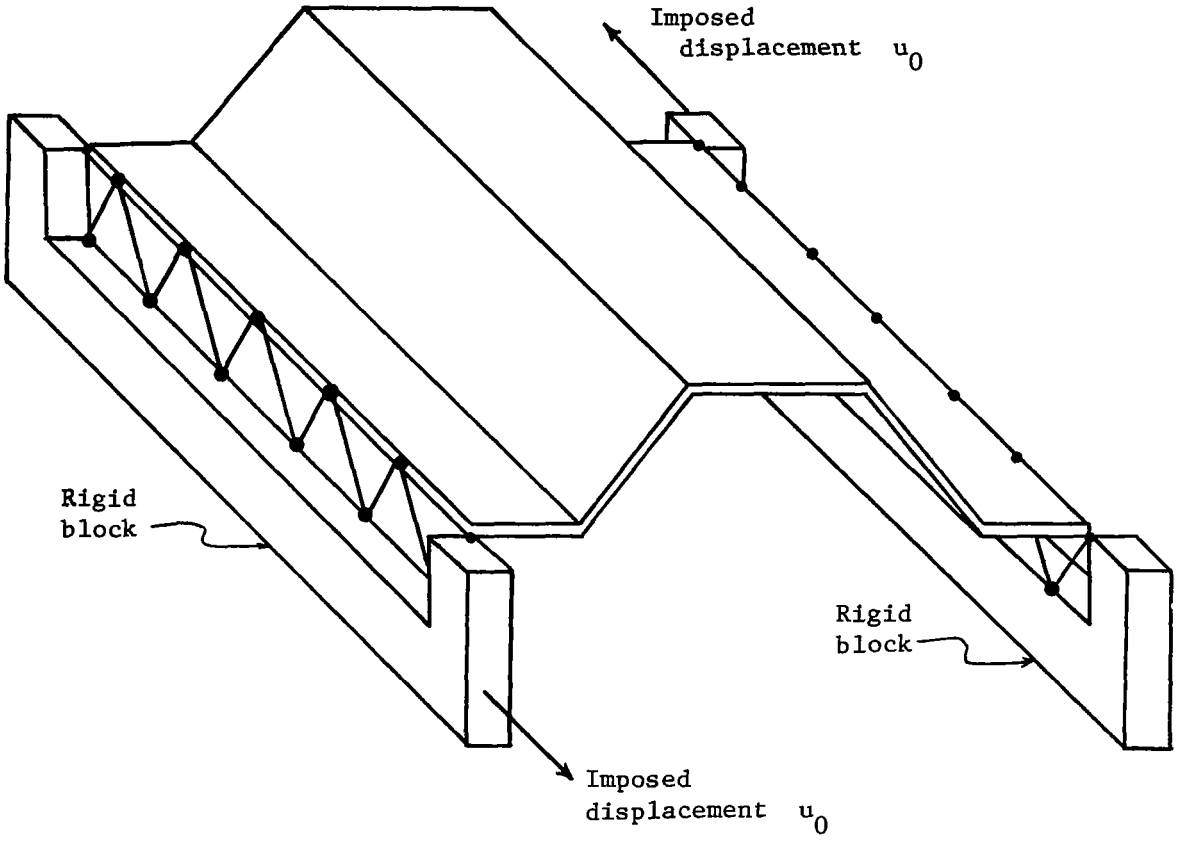

Figure 4. - Schematic representation of a single corrugation.

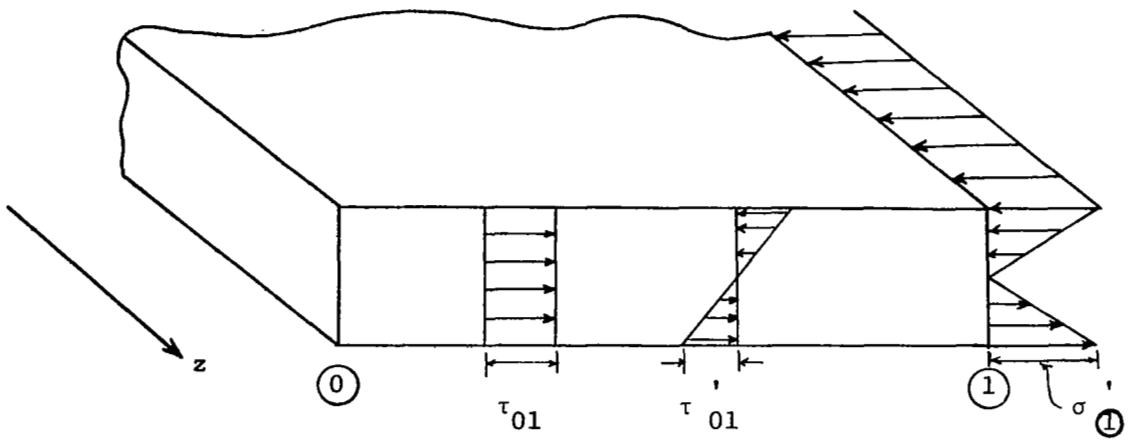

Figure 5. - Sign convention for τ_{01}, τ'_{01} and σ'_1.

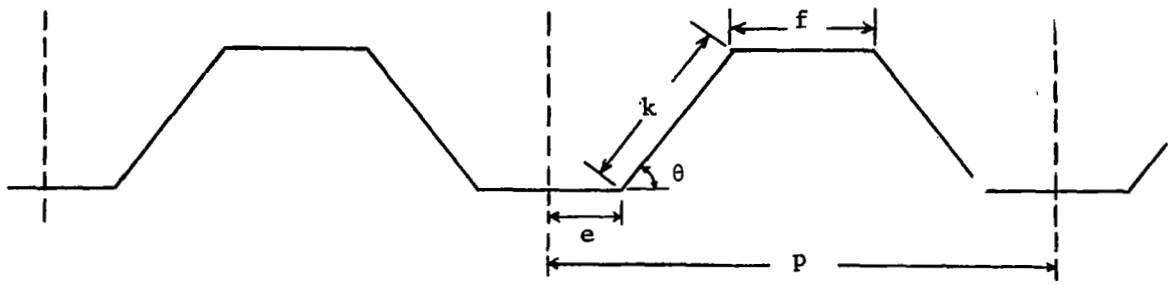

(a) General case

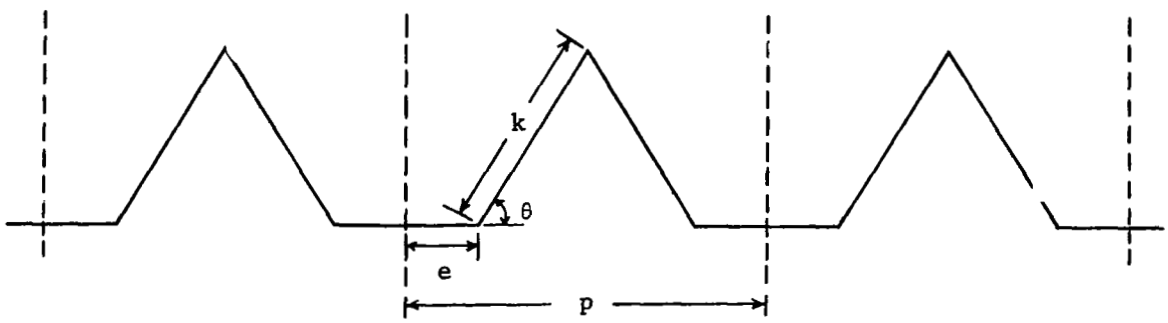

(b) Special case f = 0

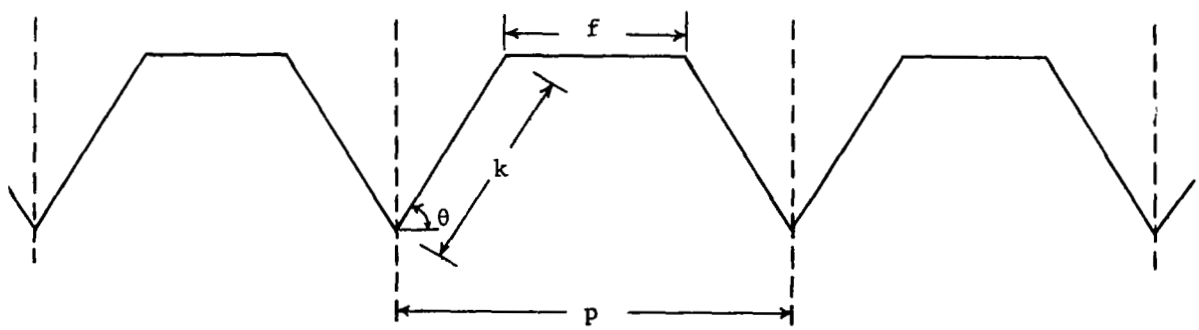

(c) Special case e = 0

Figure 6. - General and special cross-sectional geometries considered in the analyses.

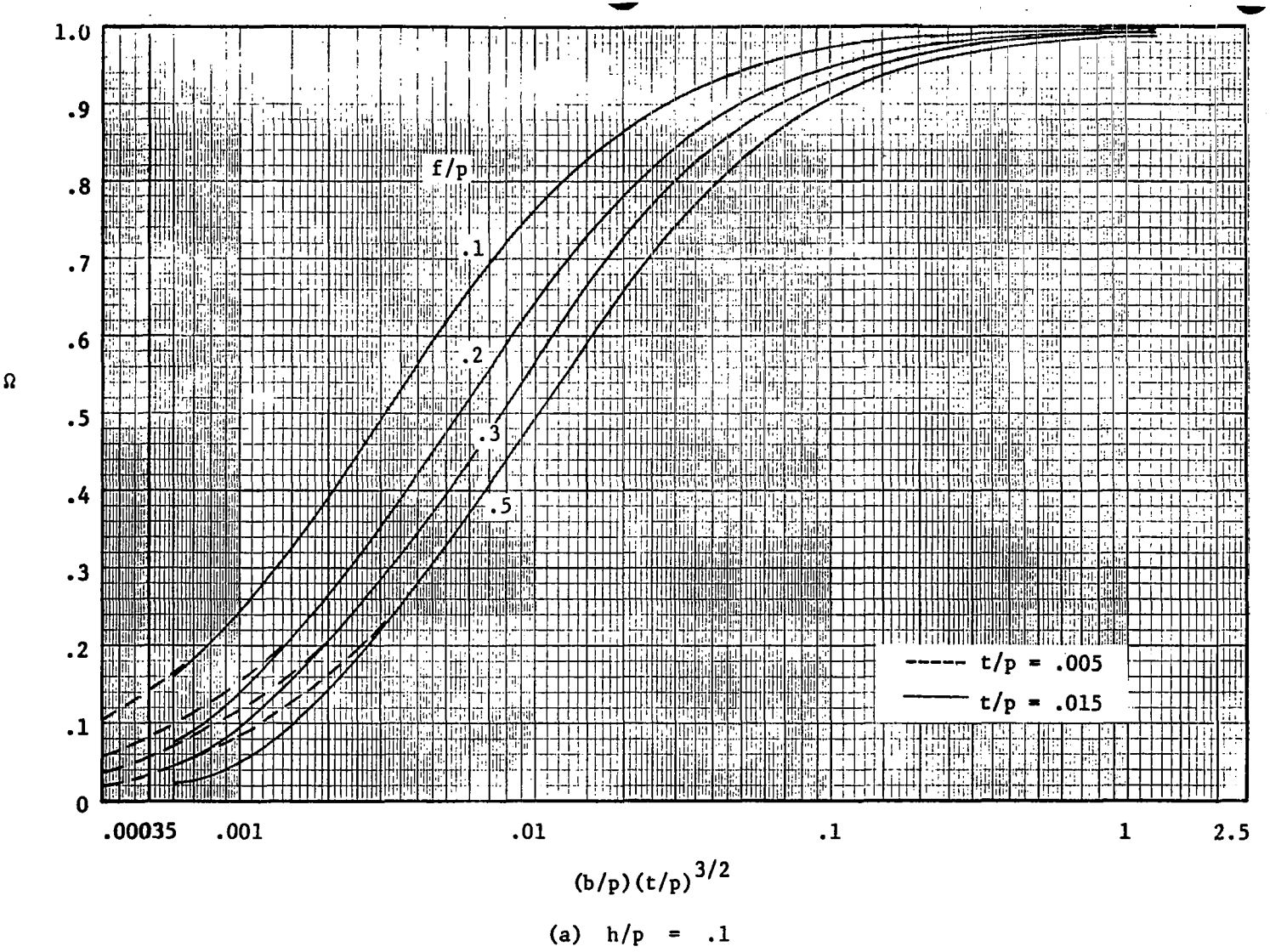

(a) h/p = .1

Figure 7. - Relative shear stiffness for the case of point attachments at the ends of trough line only.

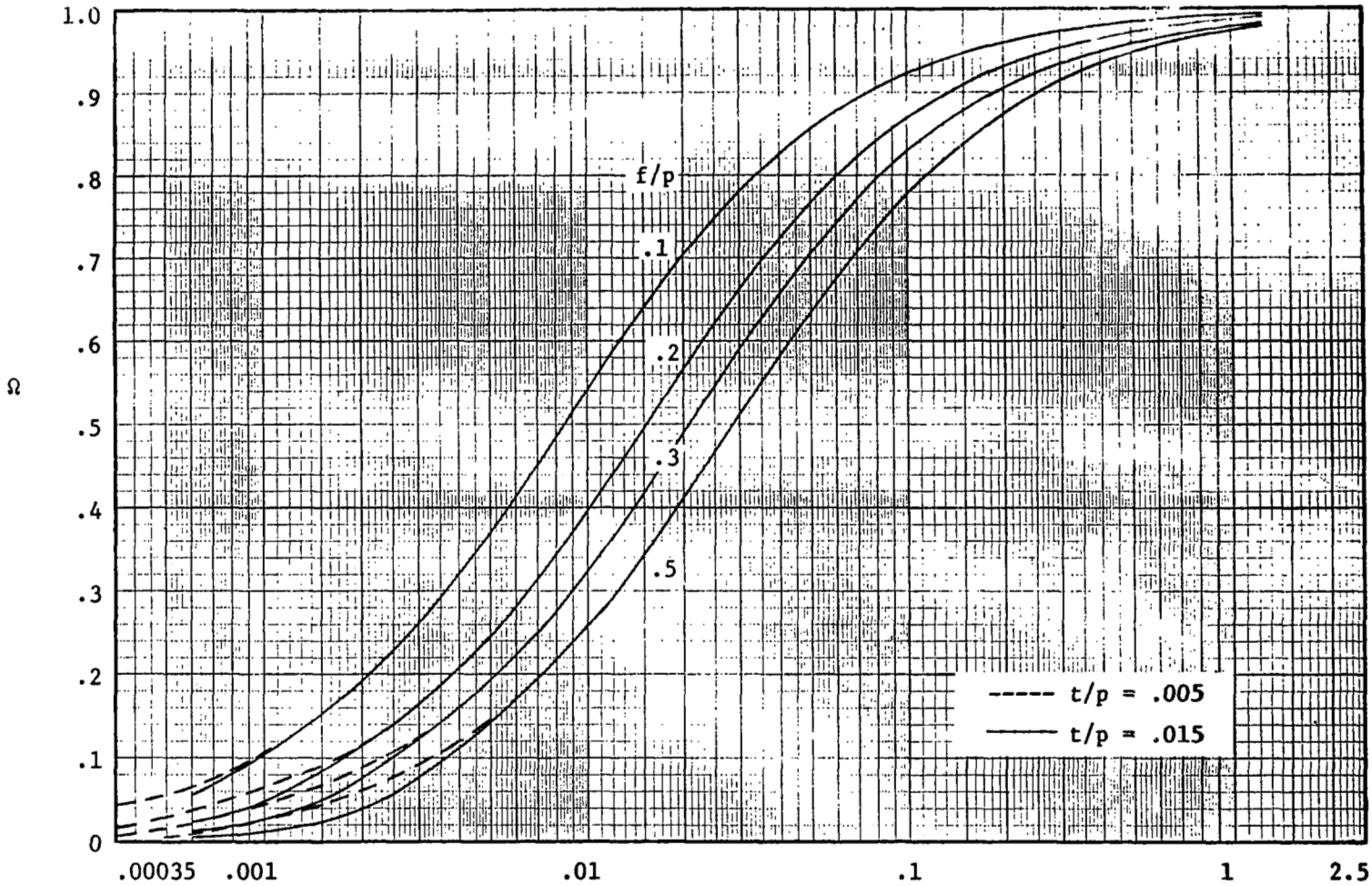

(b) h/p = .2

Figure 7. - Continued.

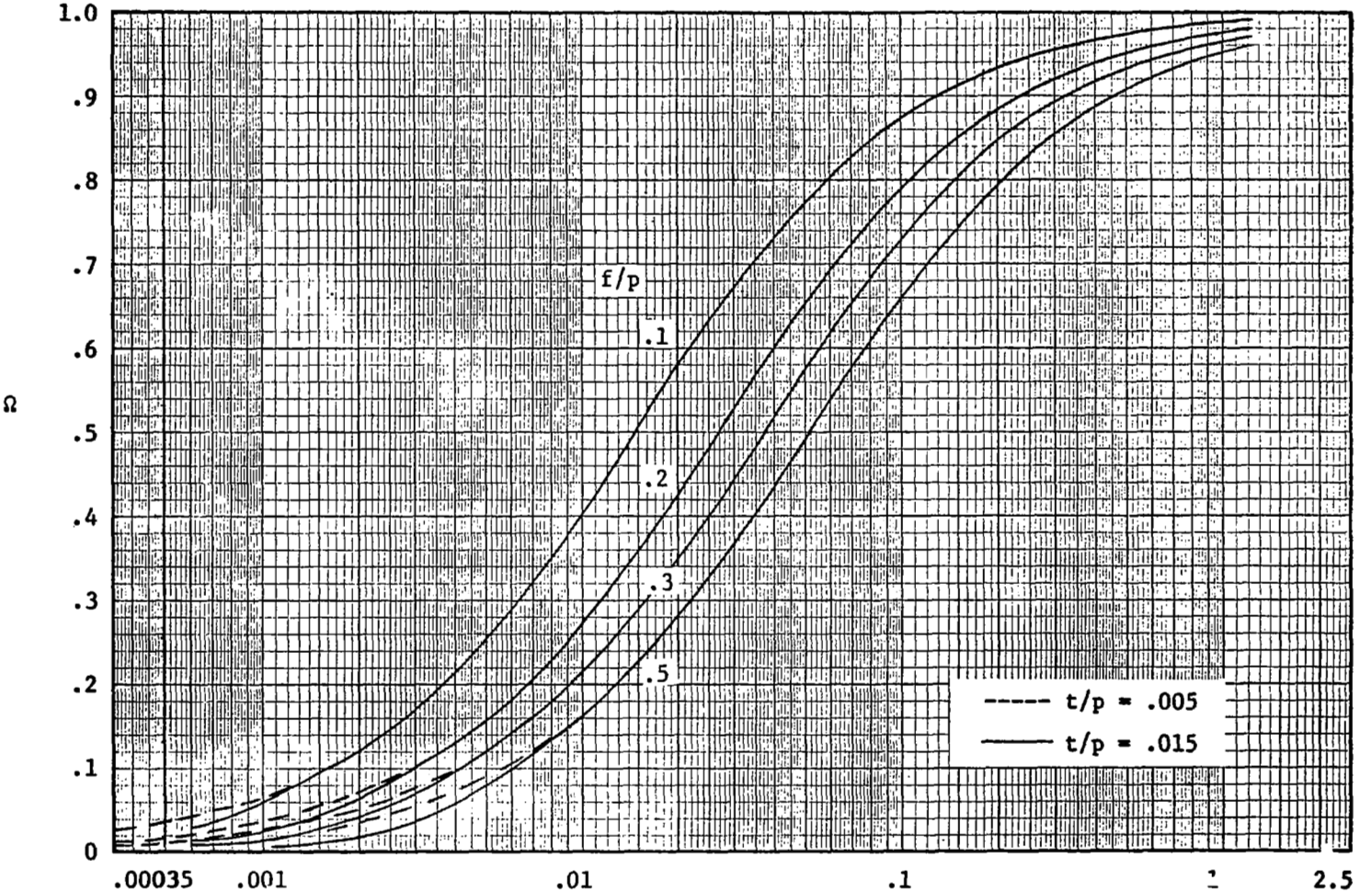

(c) h/p = .3

Figure 7. - Continued.

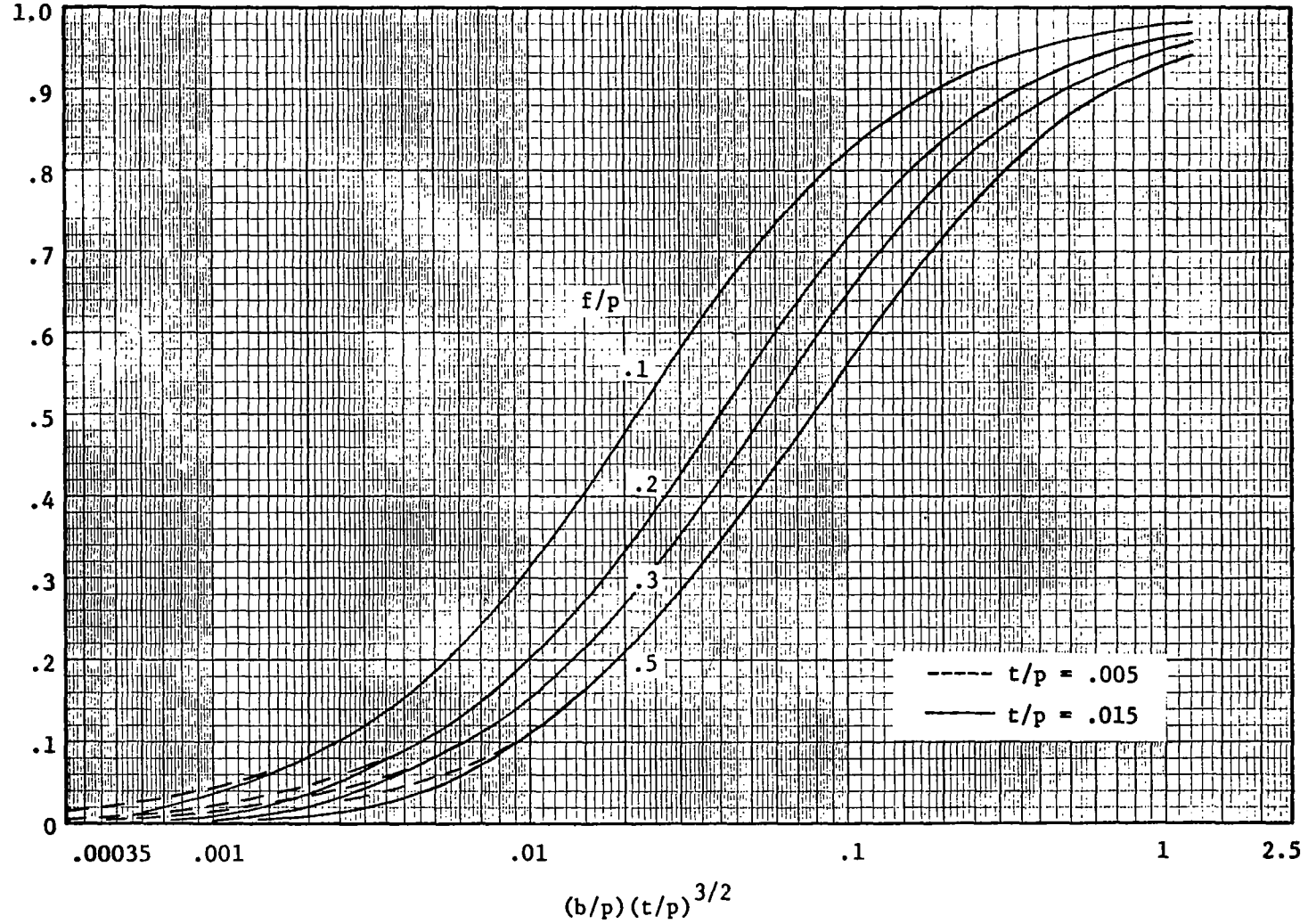

(d) h/p = .4

Figure 7. - Continued.

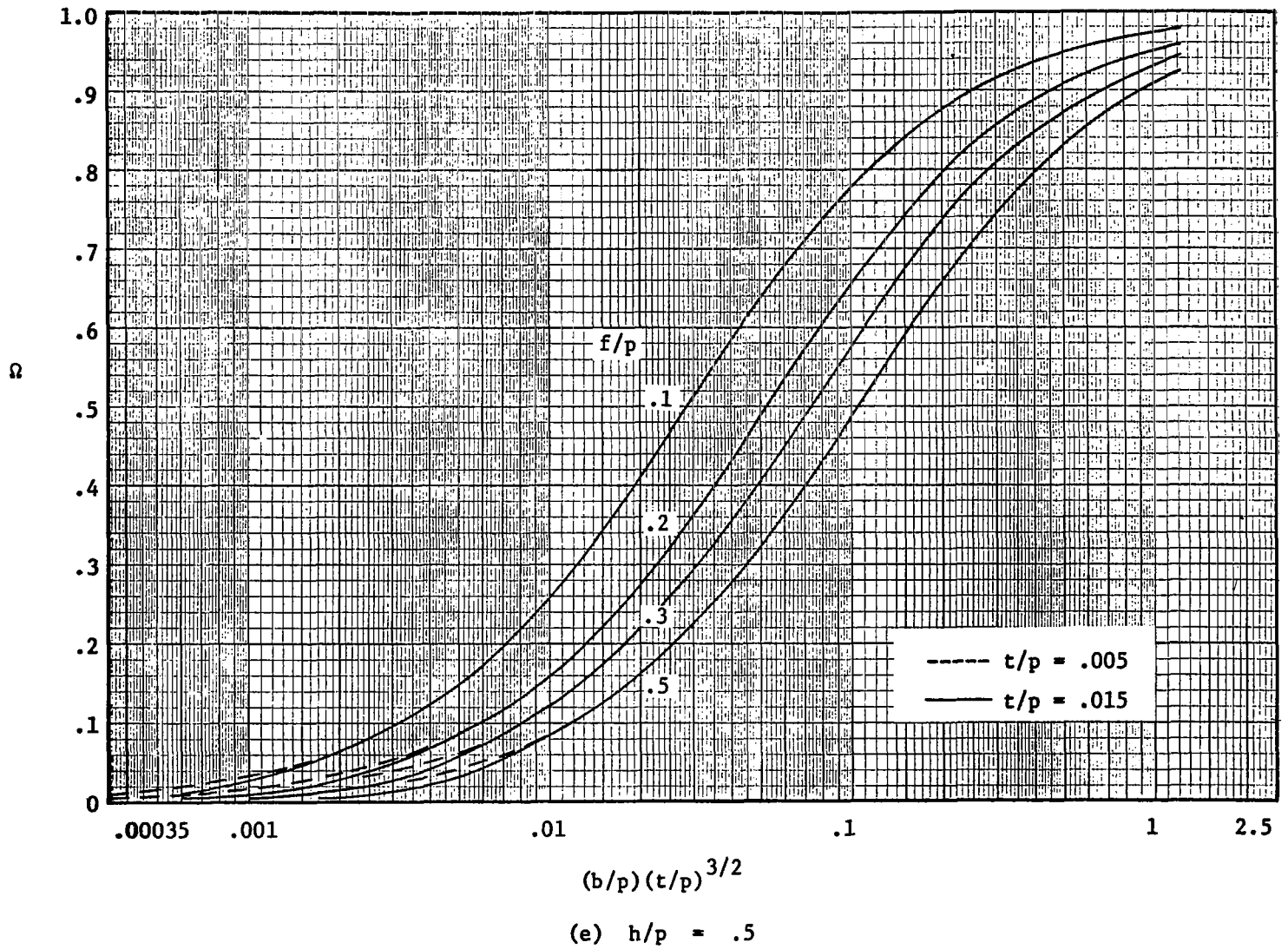

(e) h/p = .5

Figure 7. - Concluded.

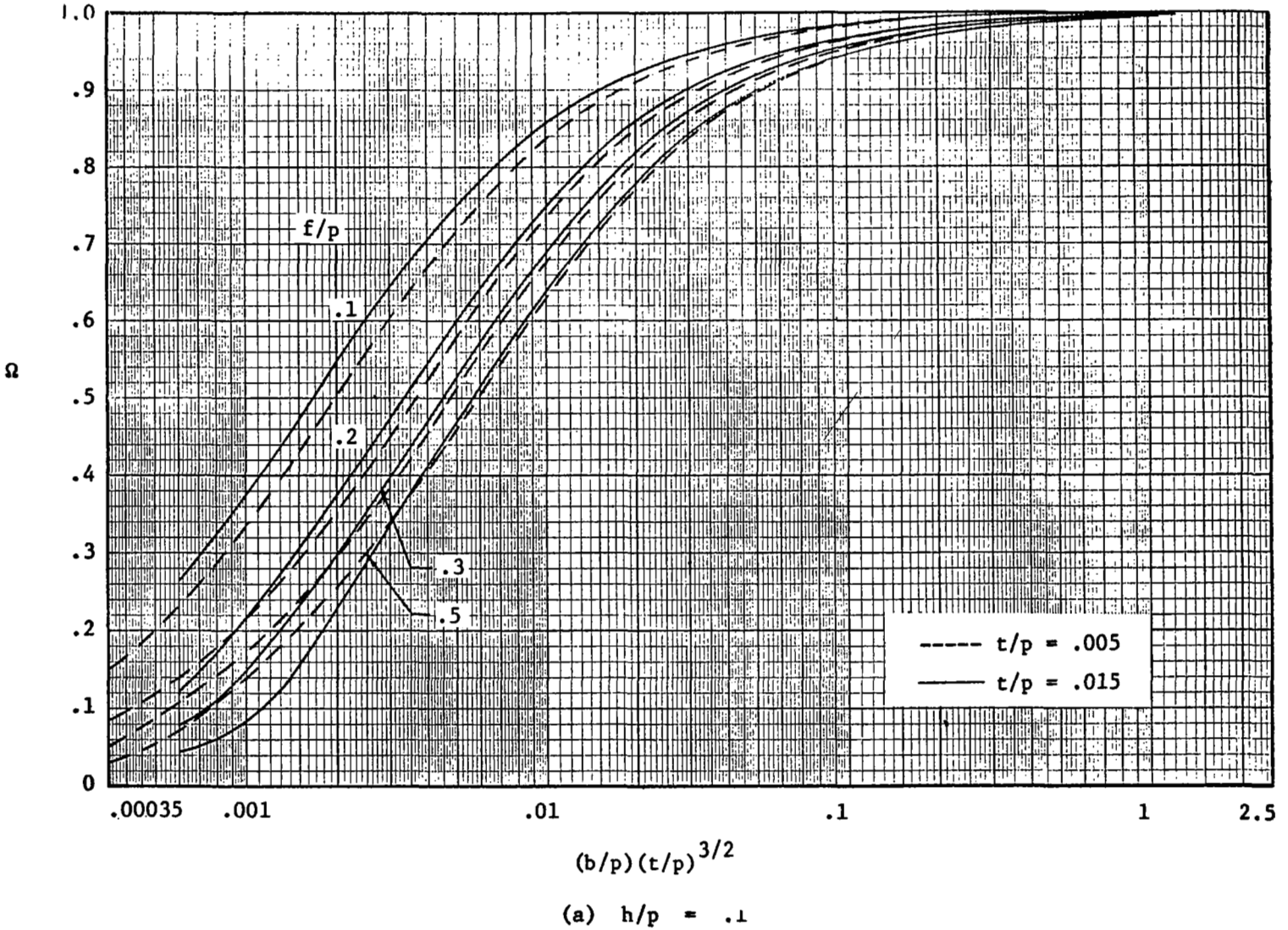

Figure 8. - Relative shear stiffness for the case of point attachments at the ends of both the trough lines and the crest lines.

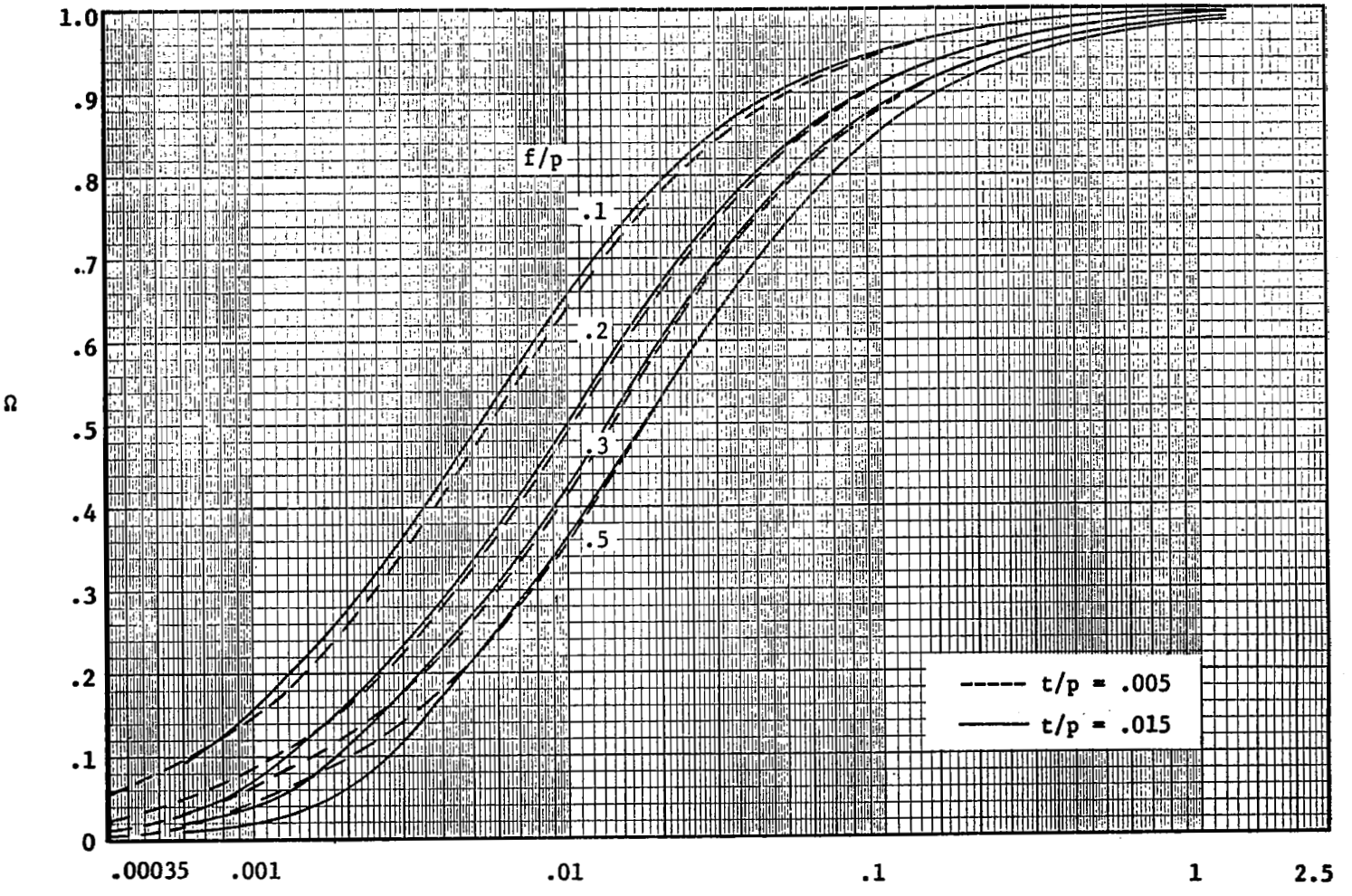

(b) h/p = .2

Figure 8. - Continued.

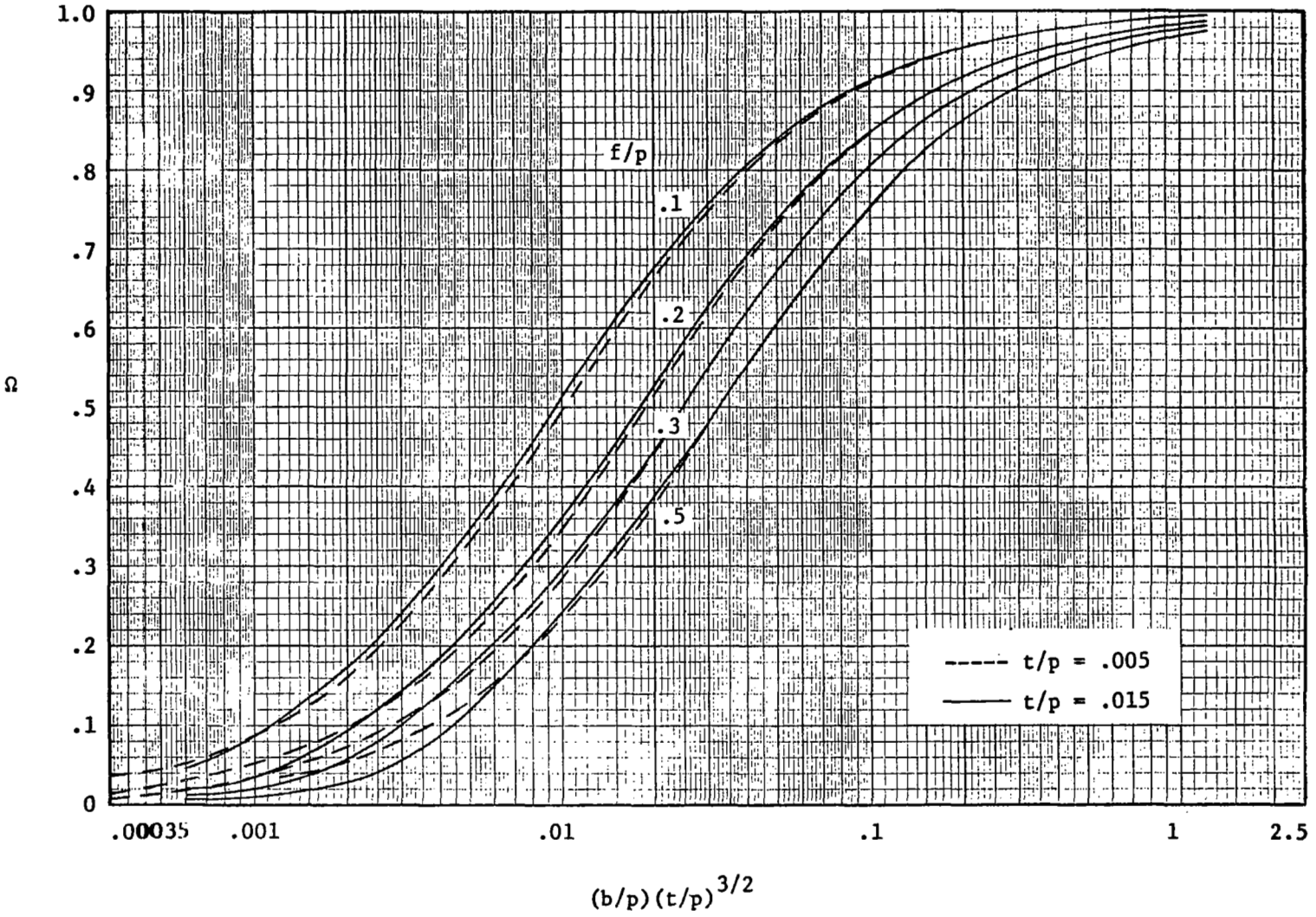

(c) h/p = .3

Figure 8. - Continued.

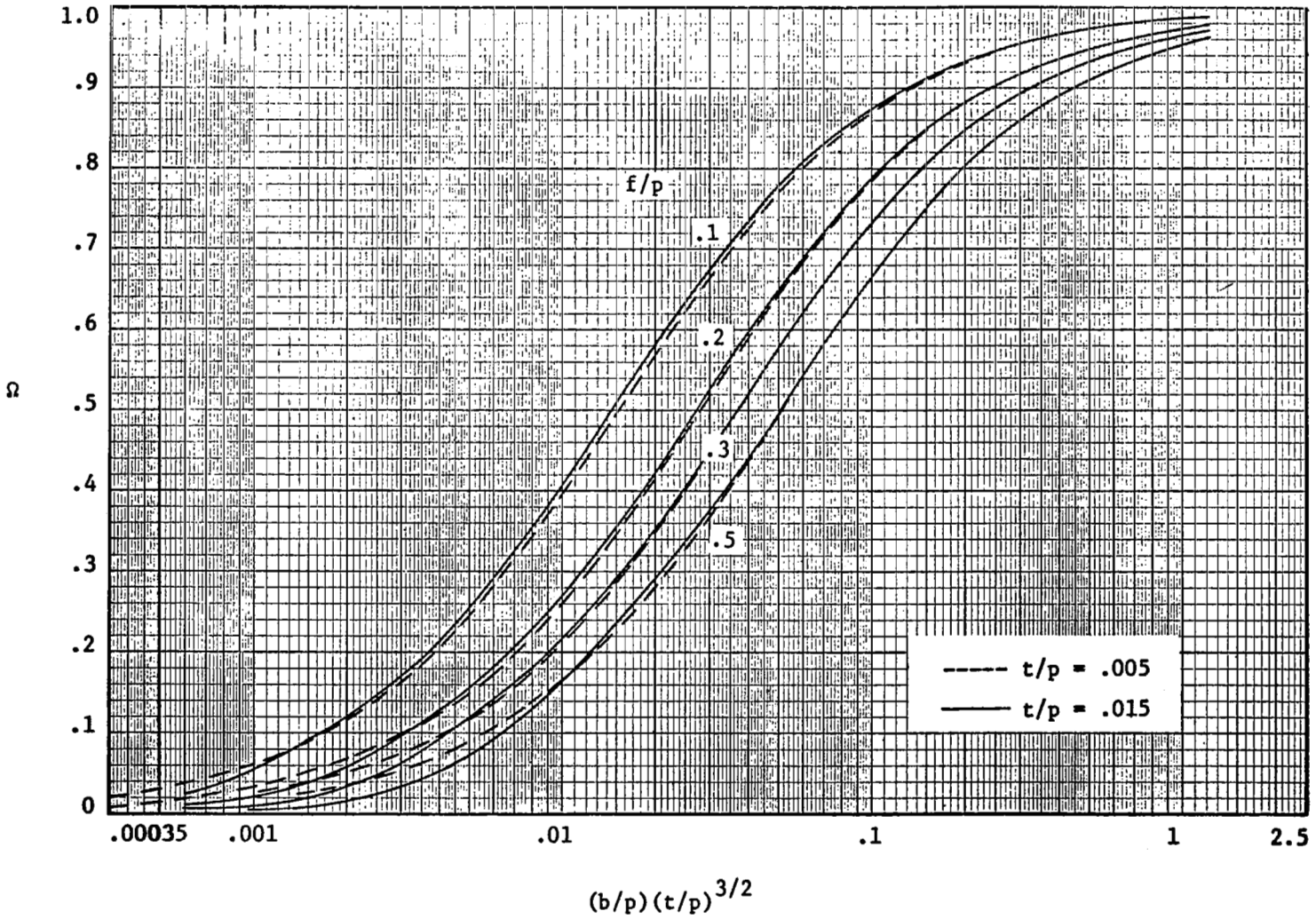

(d) h/p = .4

Figure 8. - Continued.

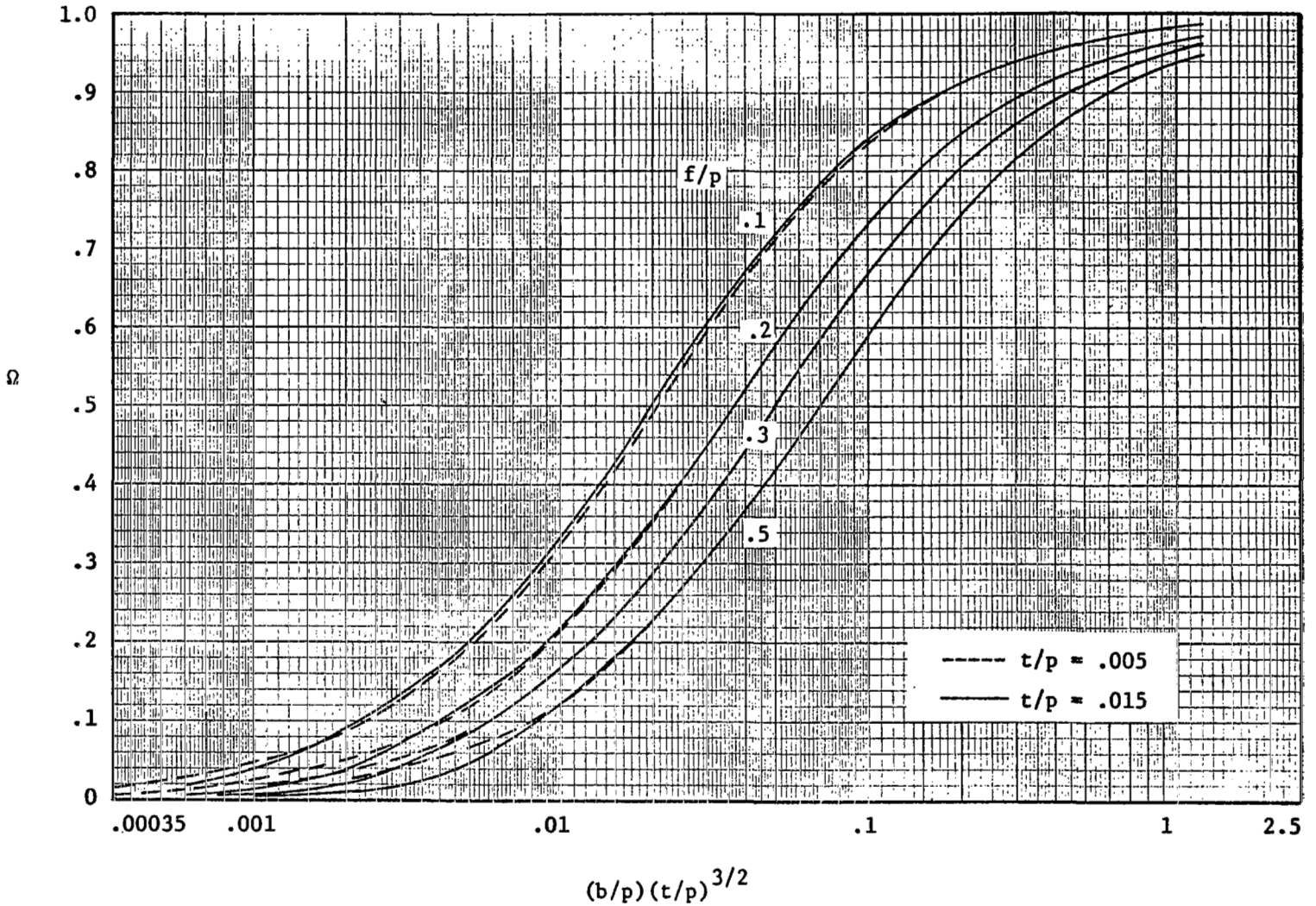

(e) h/p = .5

Figure 8. - Concluded.

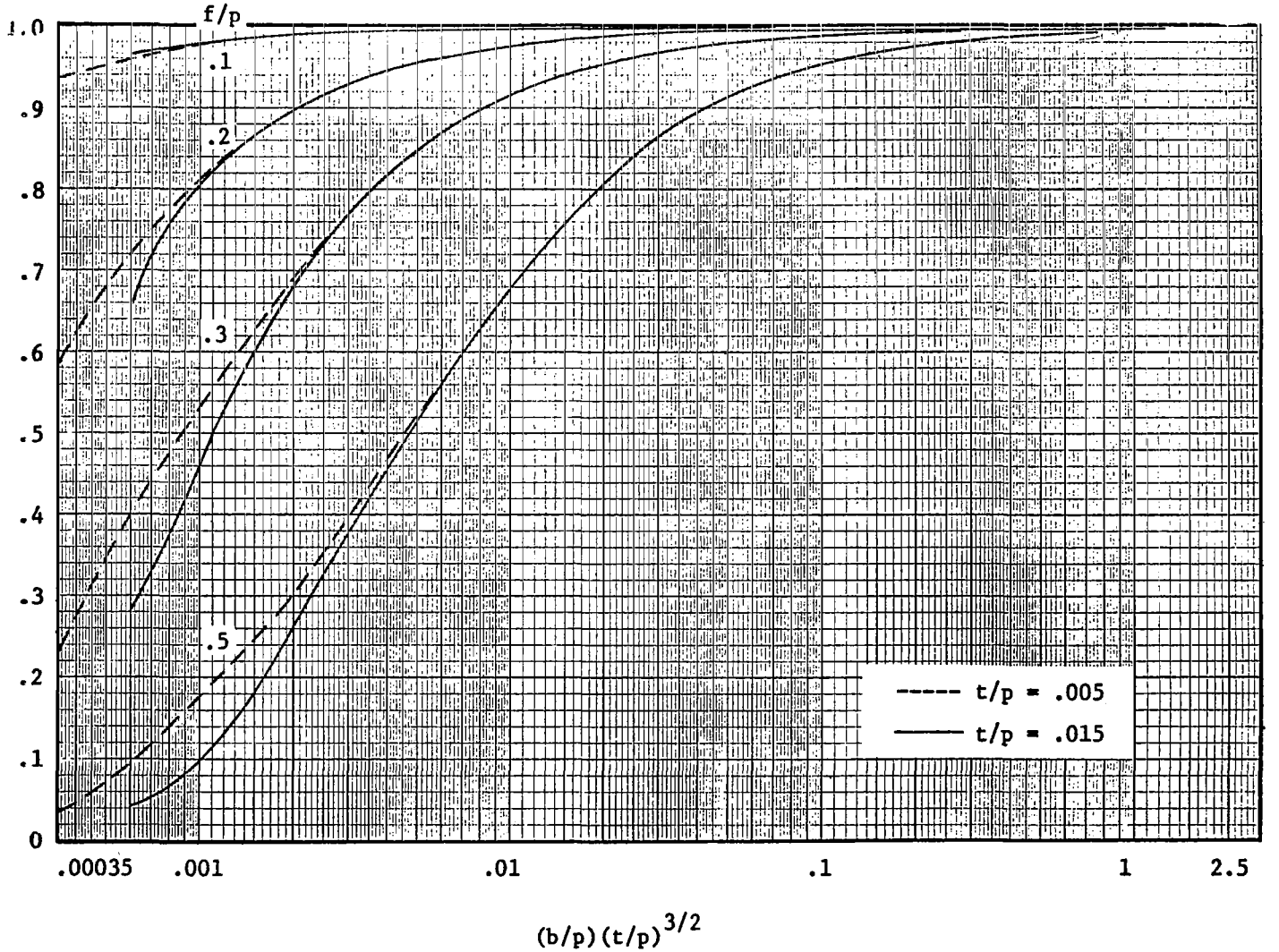

(a) h/p = .1

Figure 9. - Relative shear stiffness for the case of wide attachments at the ends of the trough lines.

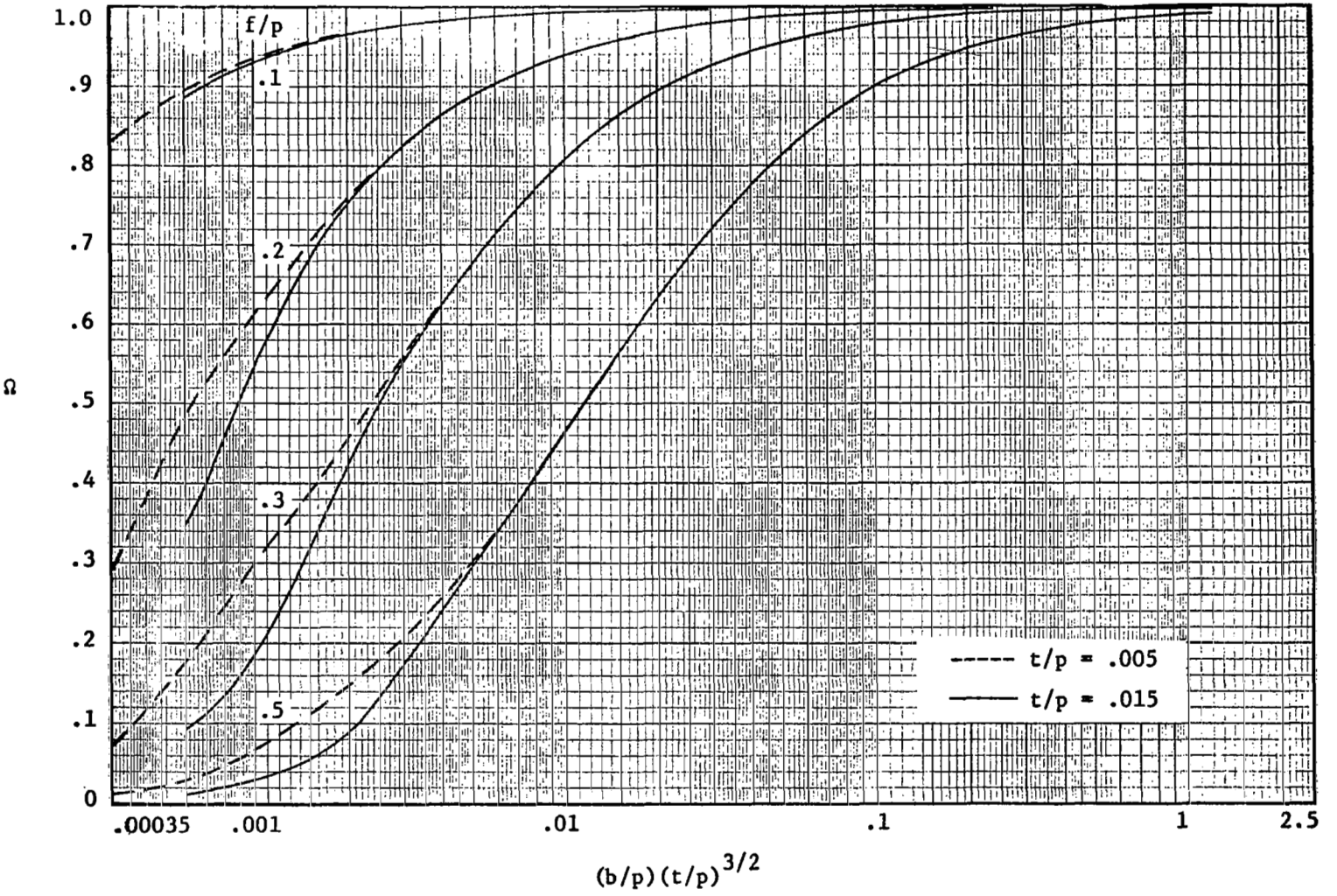

(b) h/p = .2

Figure 9. - Continued

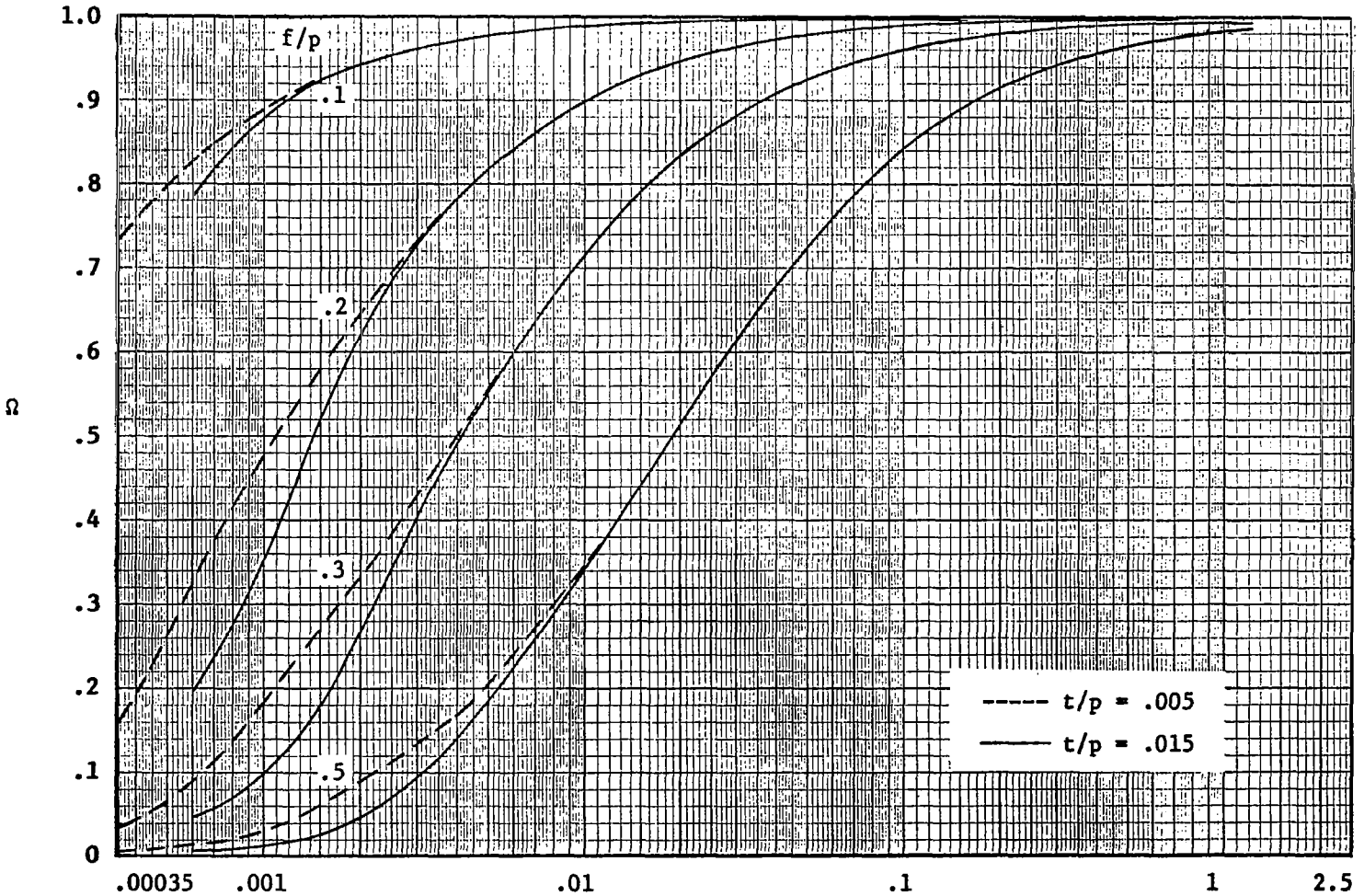

(c) h/p = .3

Figure 9. - Continued.

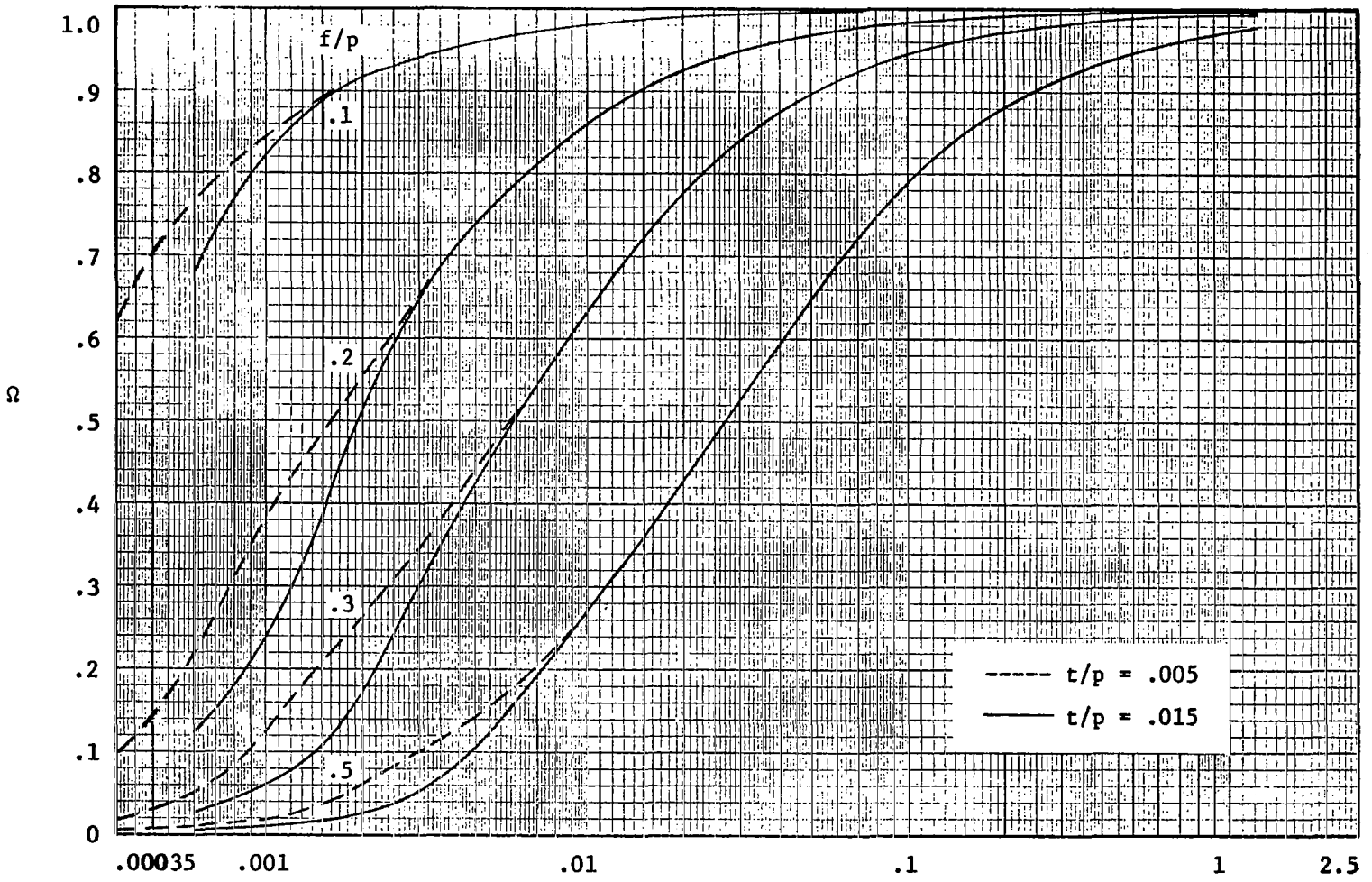

(d) h/p = .4

Figure 9. - Continued.

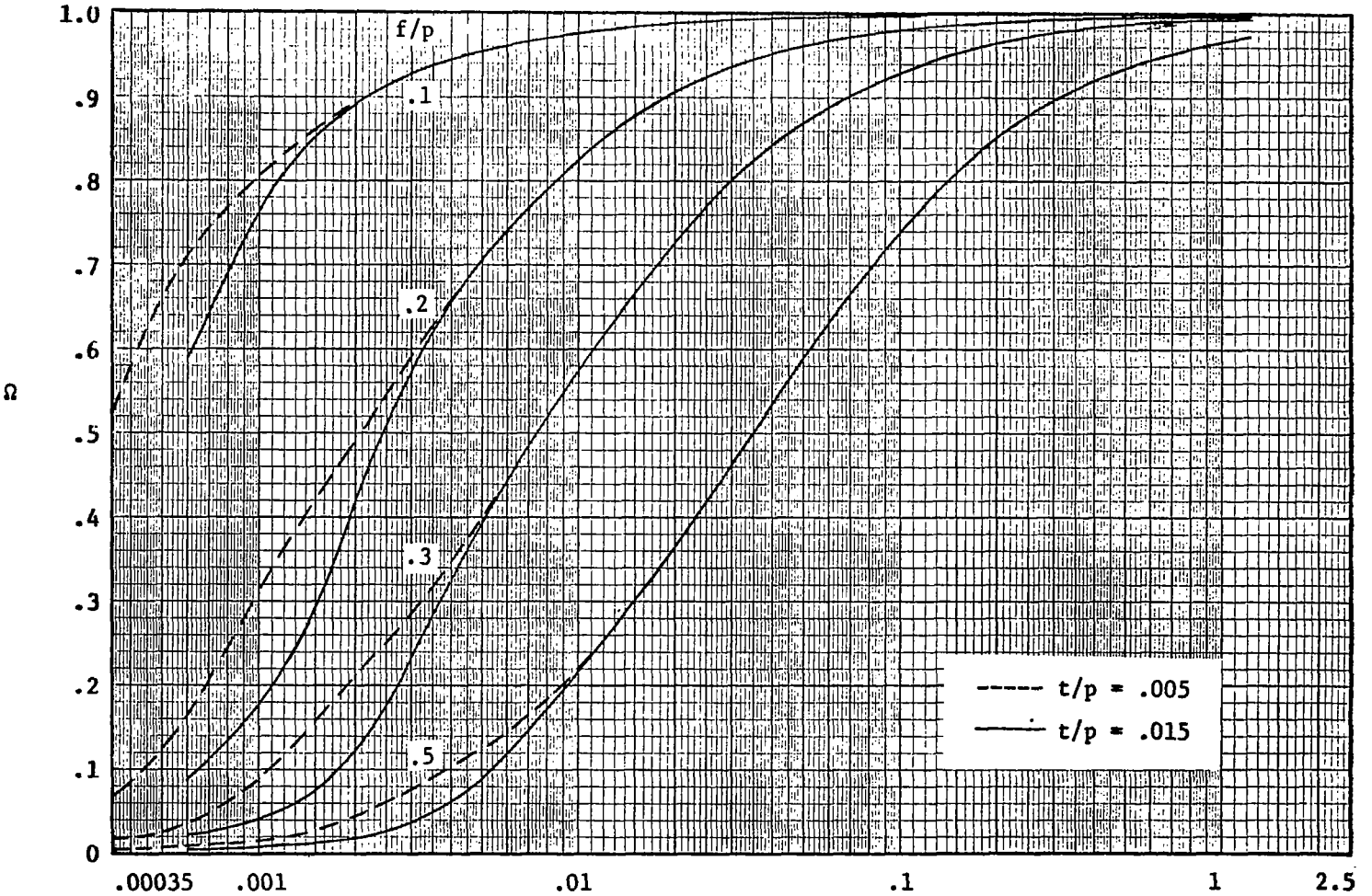

(e) h/p = .5

Figure 9. - Concluded.

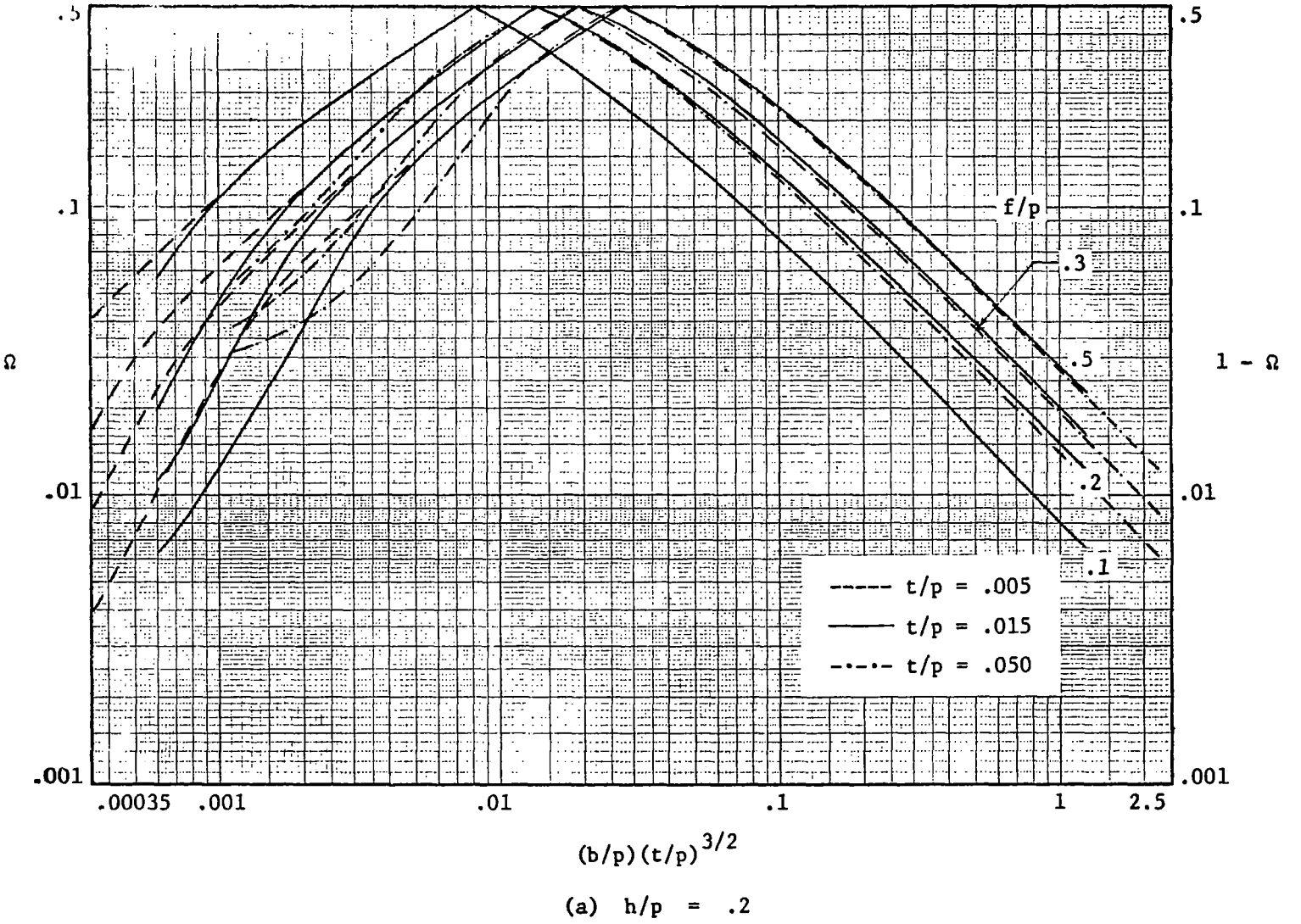

(a) h/p = .2

Figure 10. - Special log-log plot of relative shear stiffness data for the case of point attachments at the ends of the trough lines only.

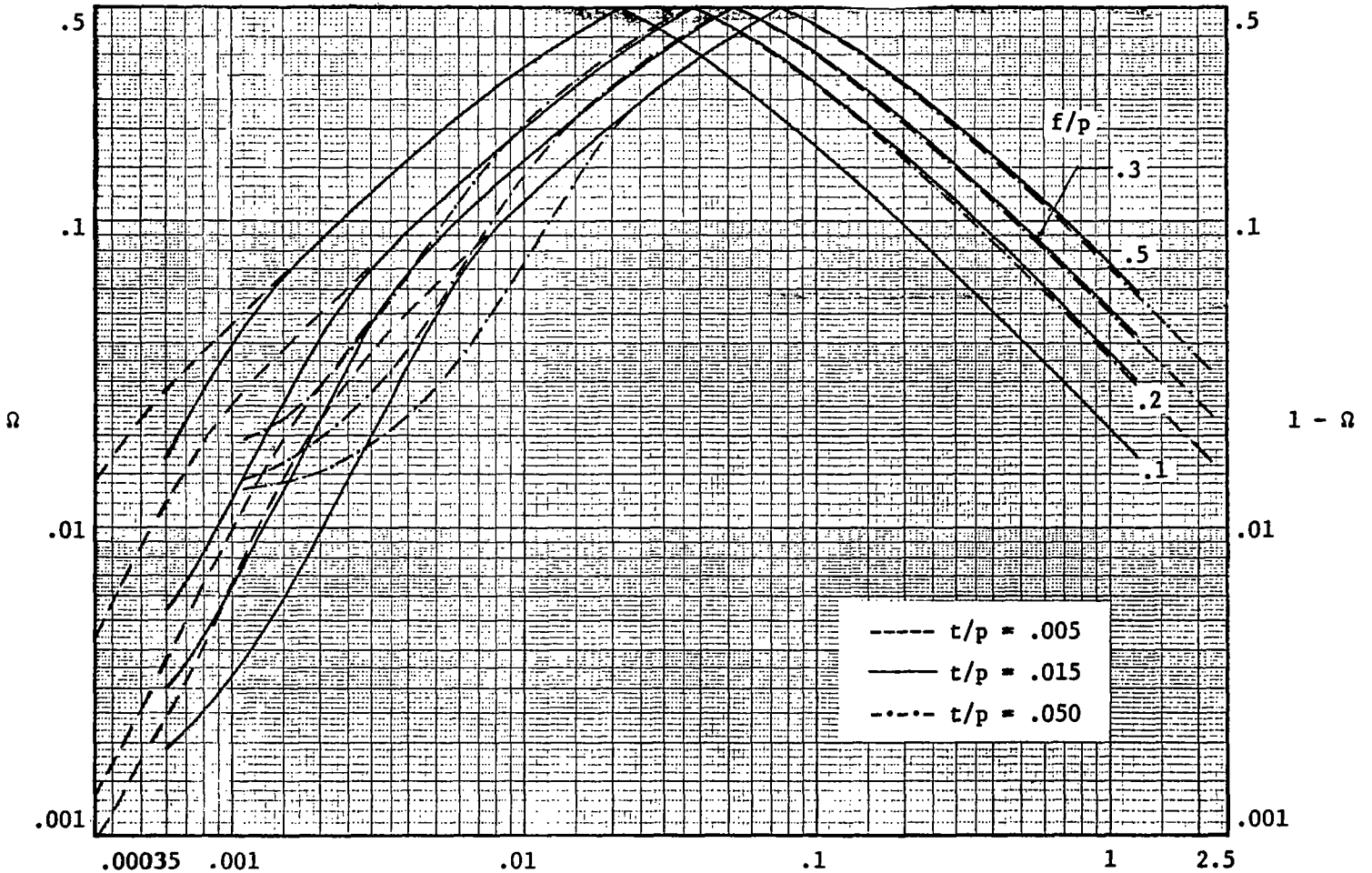

(b) h/p = .4

Figure 10. - Concluded.

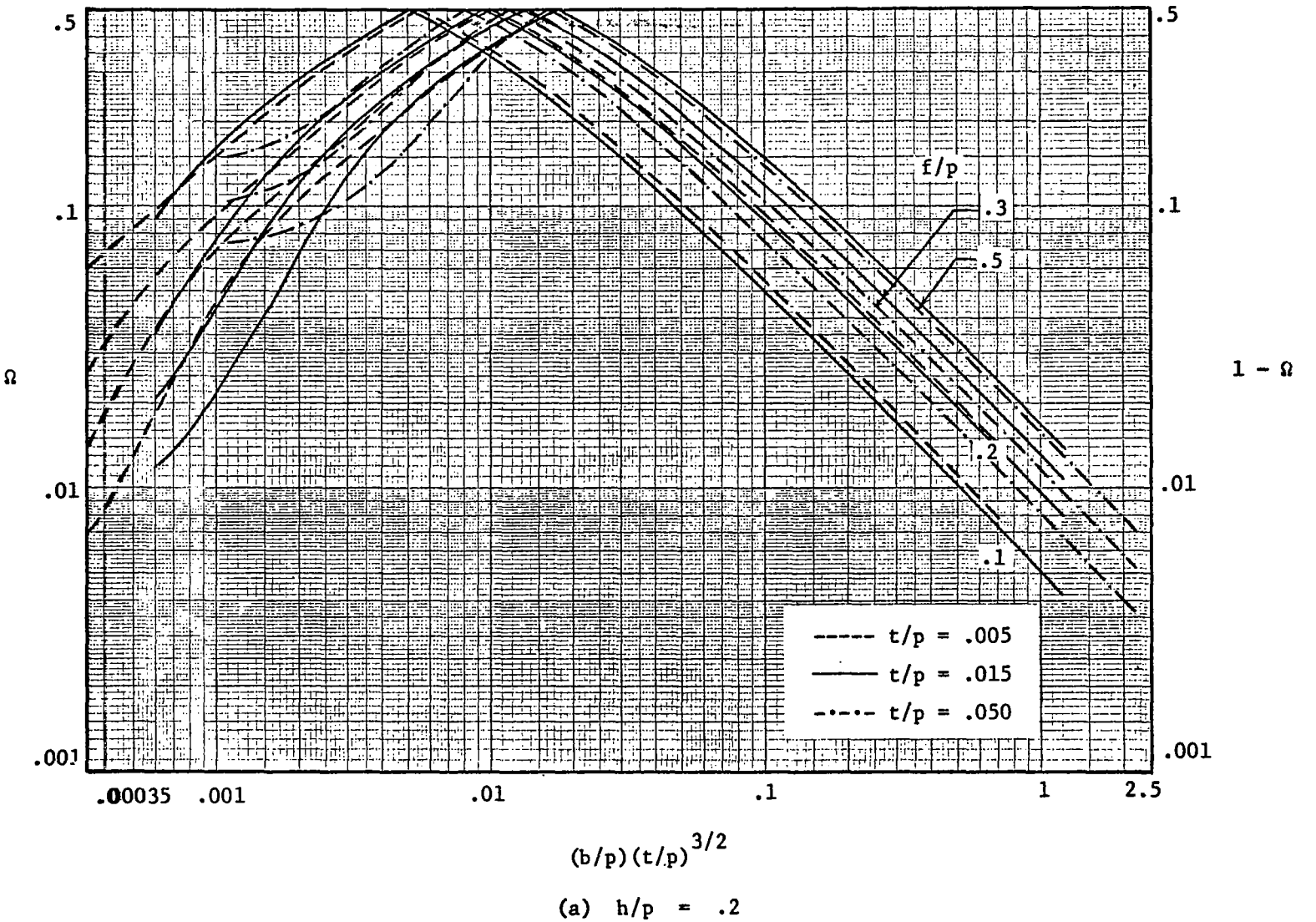

(a) h/p = .2

Figure 11. - Special log-log plot of relative shear stiffness data for the case of point attachments at the ends of both the trough lines and the crest lines.

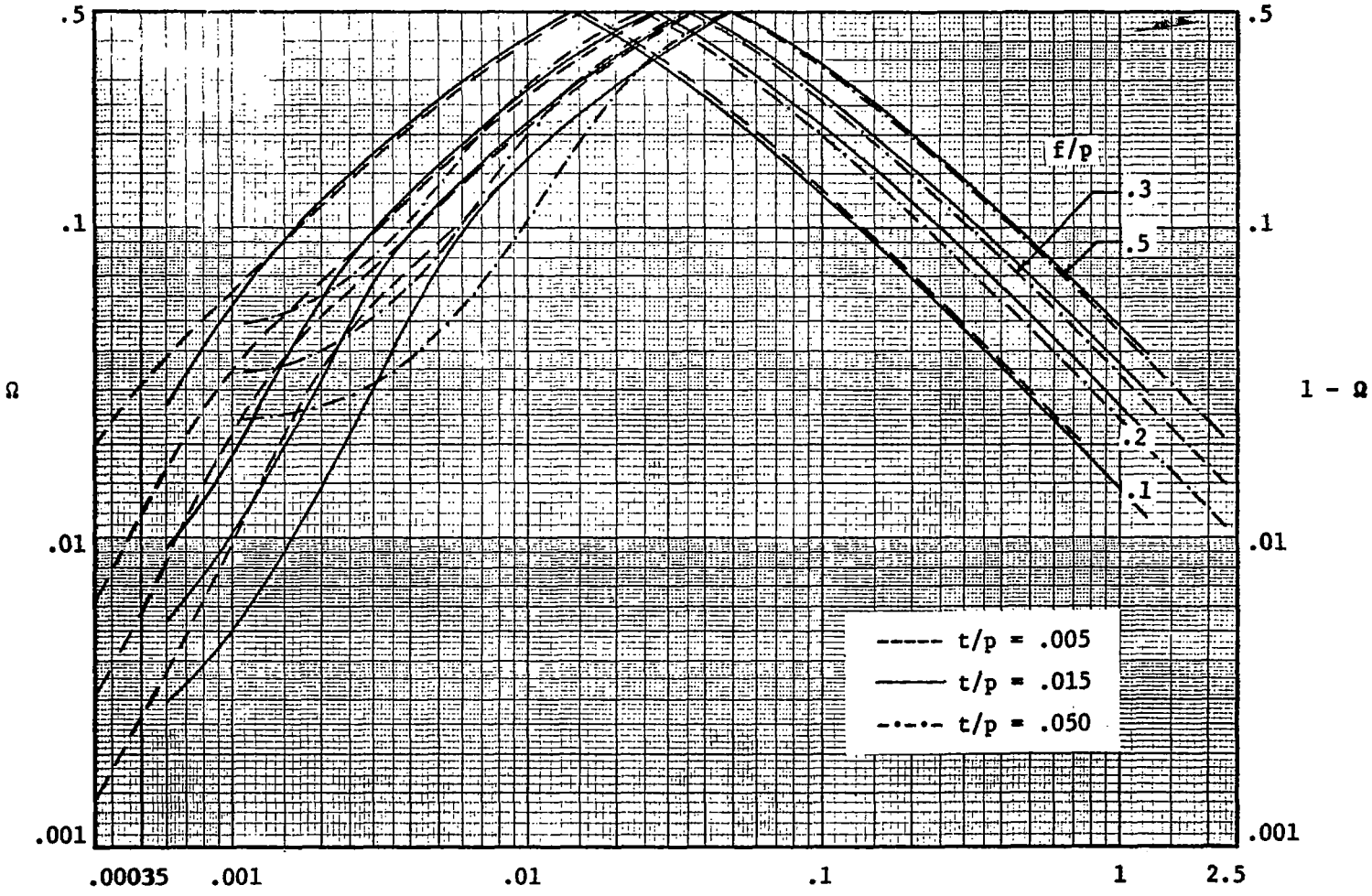

(b) h/p = .4

Figure 11. - Concluded.

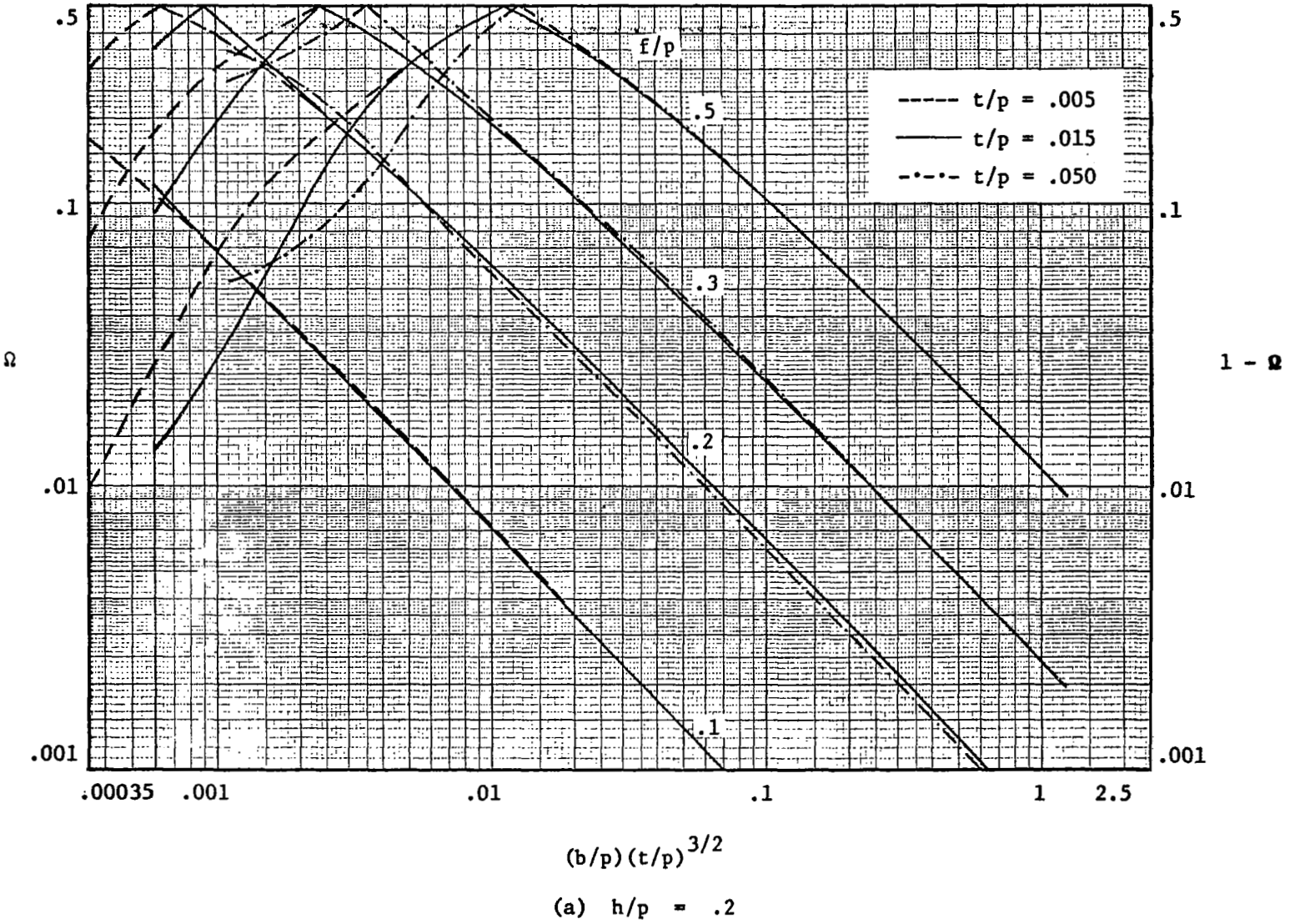

(a) h/p = .2

Figure 12. - Special log-log plot of relative shear stiffness data for the case of wide attachments at the ends of the trough lines.

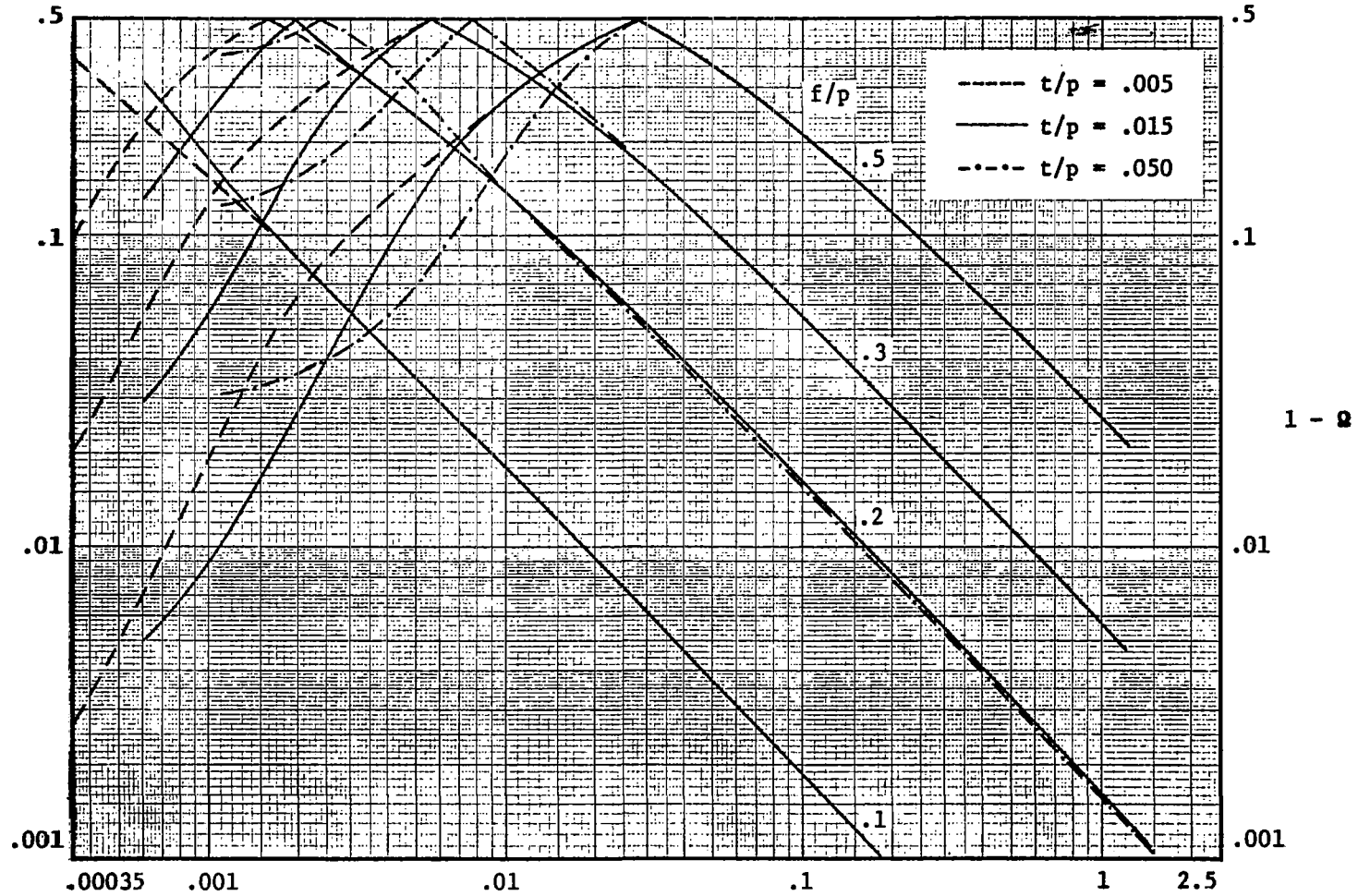

(b) h/p = .4

Figure 12. - Concluded.

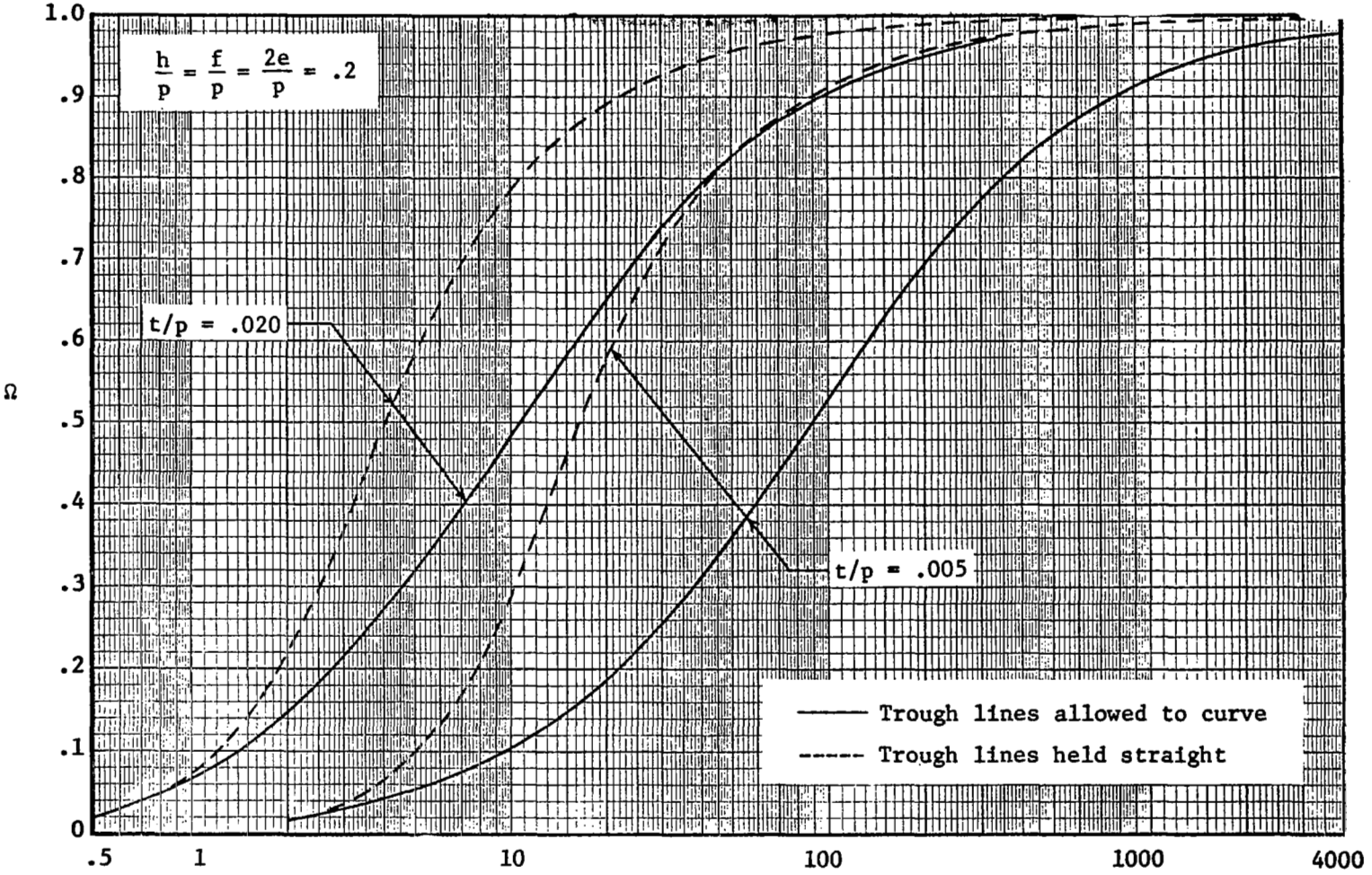

Figure 13. - Comparison of shear stiffness for trough lines held straight (ref. 1) and trough lines permitted to curve (present analysis), for the case of point attachments at the ends of the trough lines only.

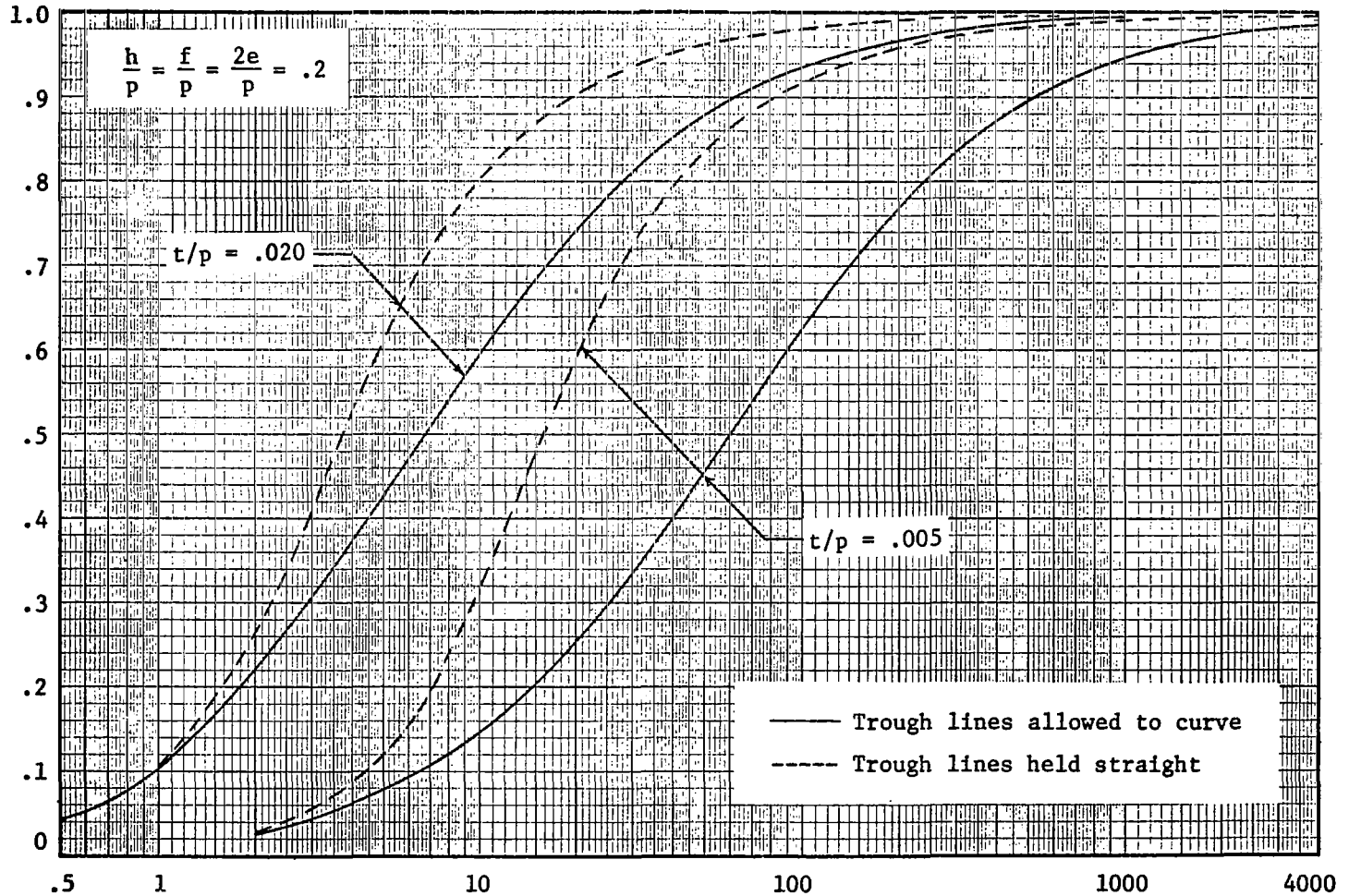

Figure 14. - Comparison of shear stiffness for trough lines held straight (ref. 1) and trough lines permitted to curve (present analysis), for the case of point attachments at the ends of both the trough lines and the crest lines.

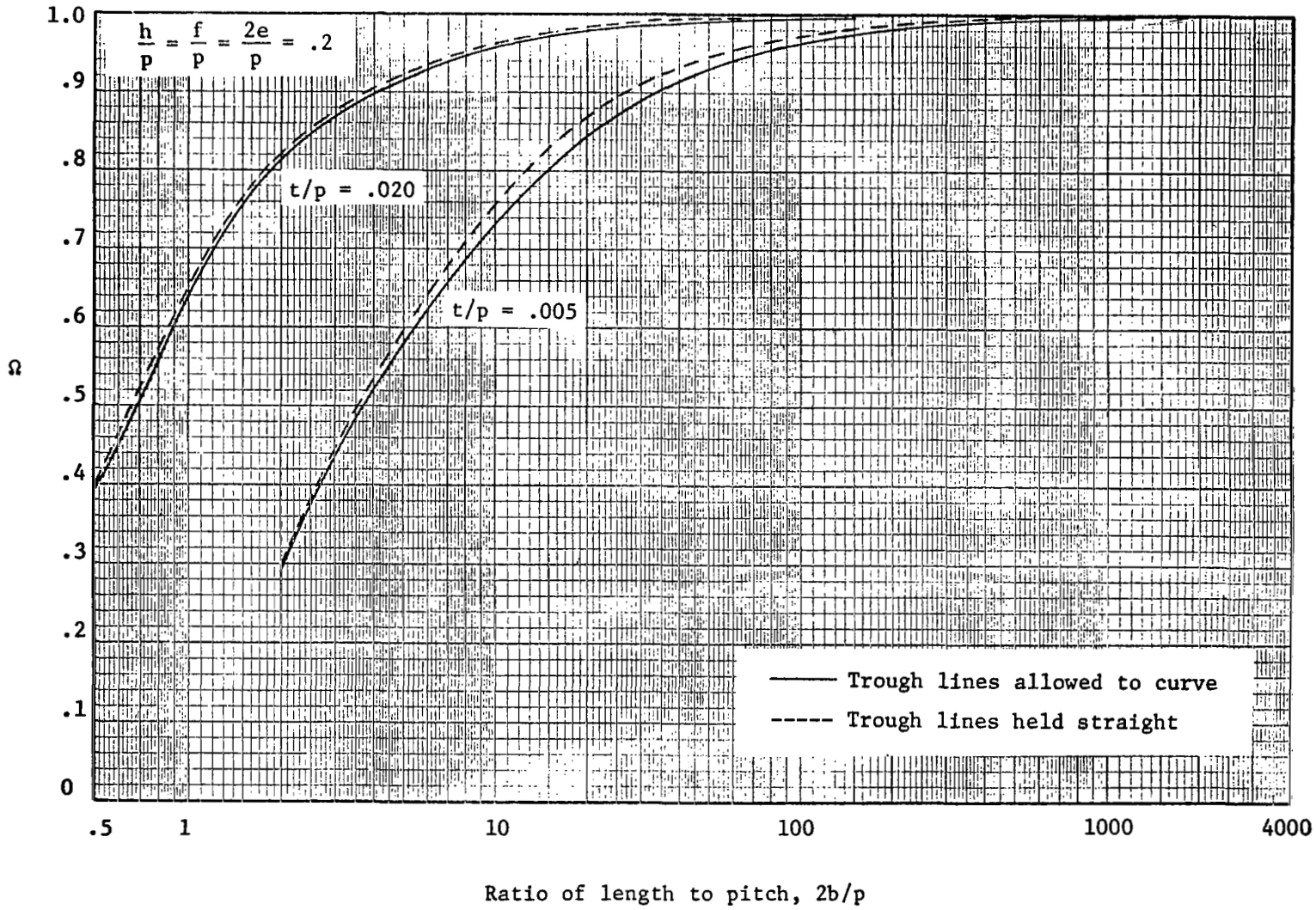

Figure 15. - Comparison of shear stiffness for trough lines held straight (ref. 1) and trough lines permitted to curve (present analysis), for the case of wide attachments at the ends of the trough lines.

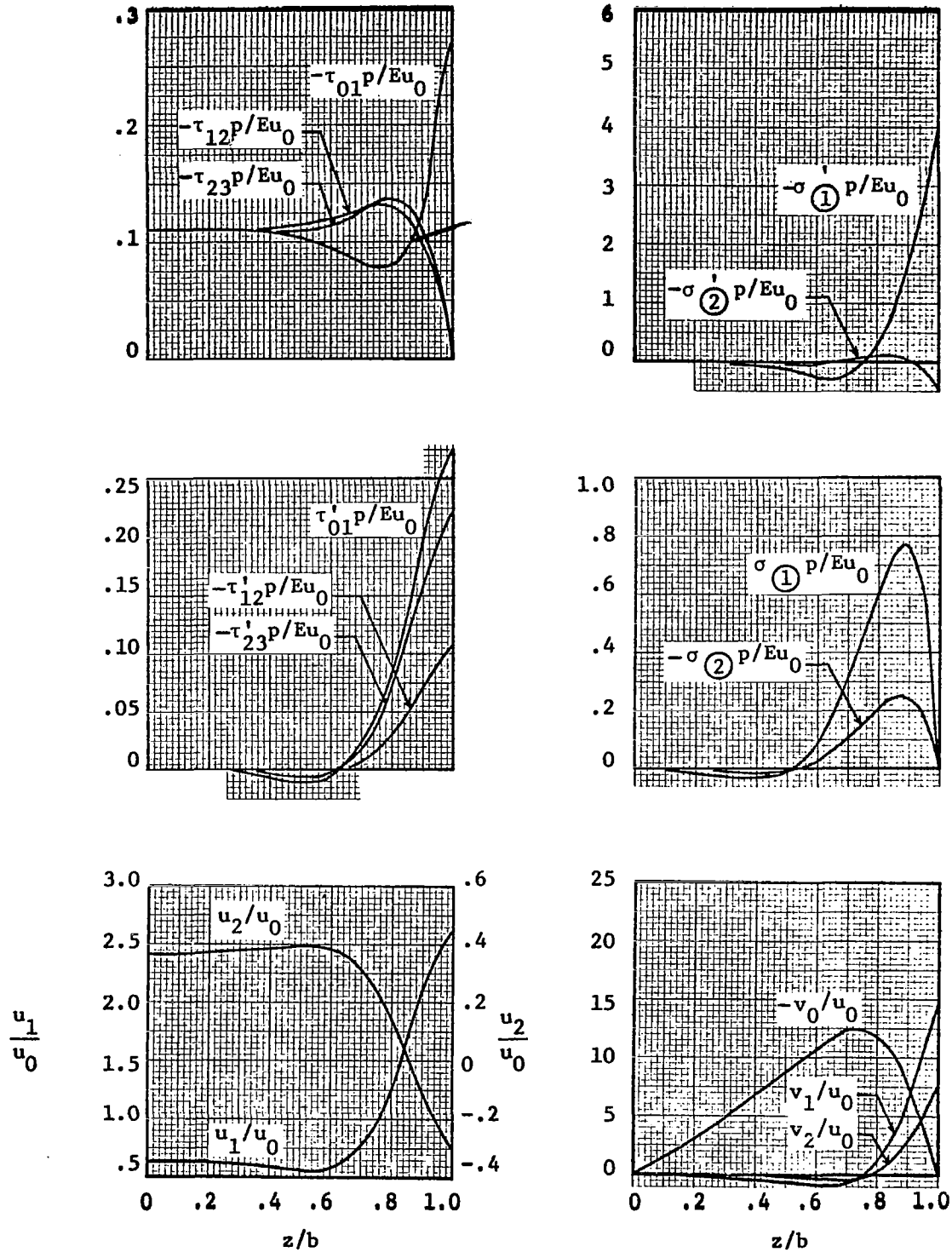

Figure 16. - Variation of stresses and displacements along the length of the corrugation for a particular geometry with point attachments at the ends of the trough lines only.

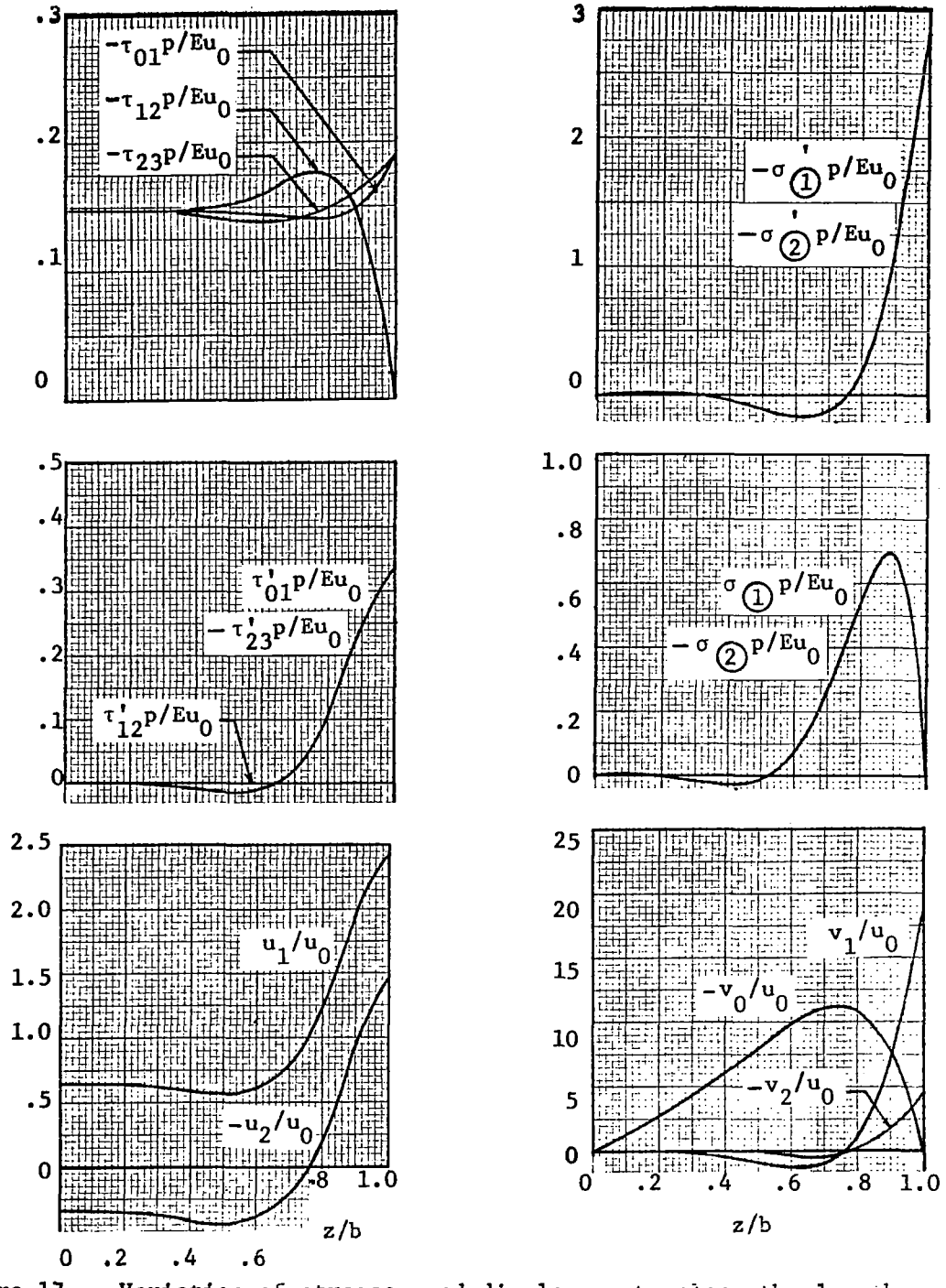

Figure 17. - Variation of stresses and displacements along the length of the corrugation for a particular geometry with point attachments at the ends of both the trough lines and the crest lines.

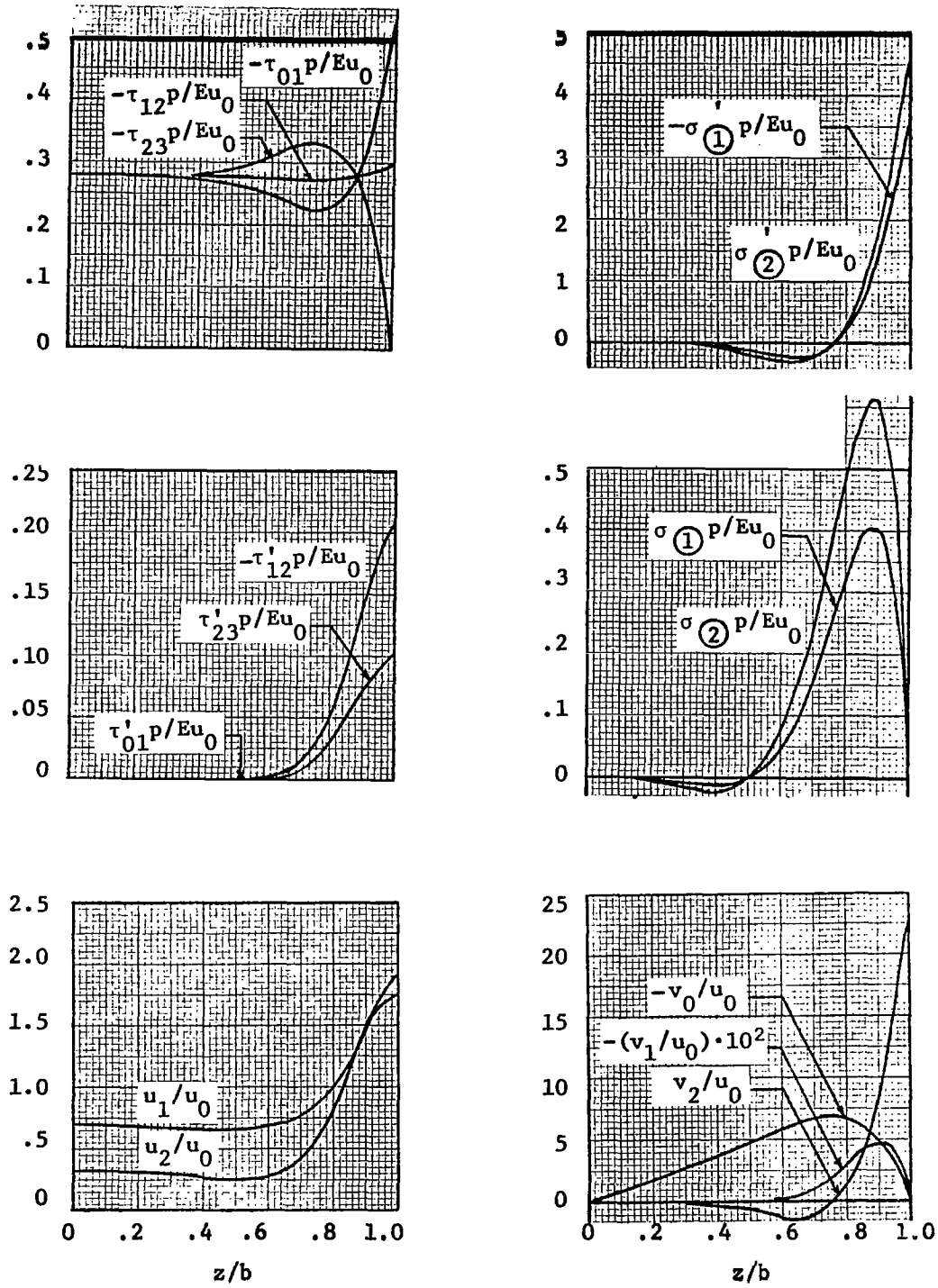

Figure 18. - Variation of stresses and displacements along the length of the corrugation for a particular geometry with wide attachments at the ends of the trough lines.

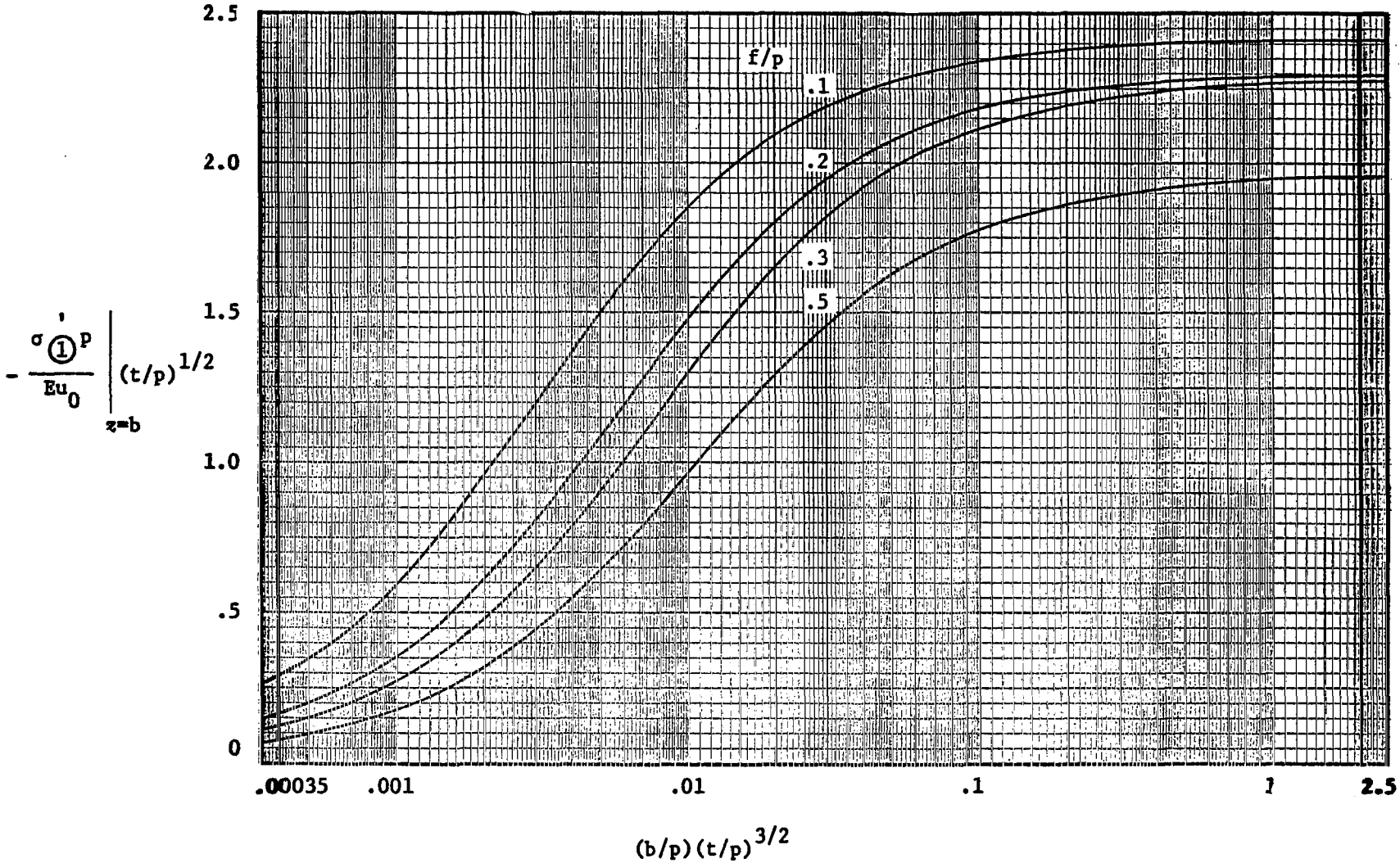

(a·I) Frame bending stress for h/p = .1

Figure 19. - Dimensionless maximum-stress parameters for the case of point attachments at the ends of the trough lines only.

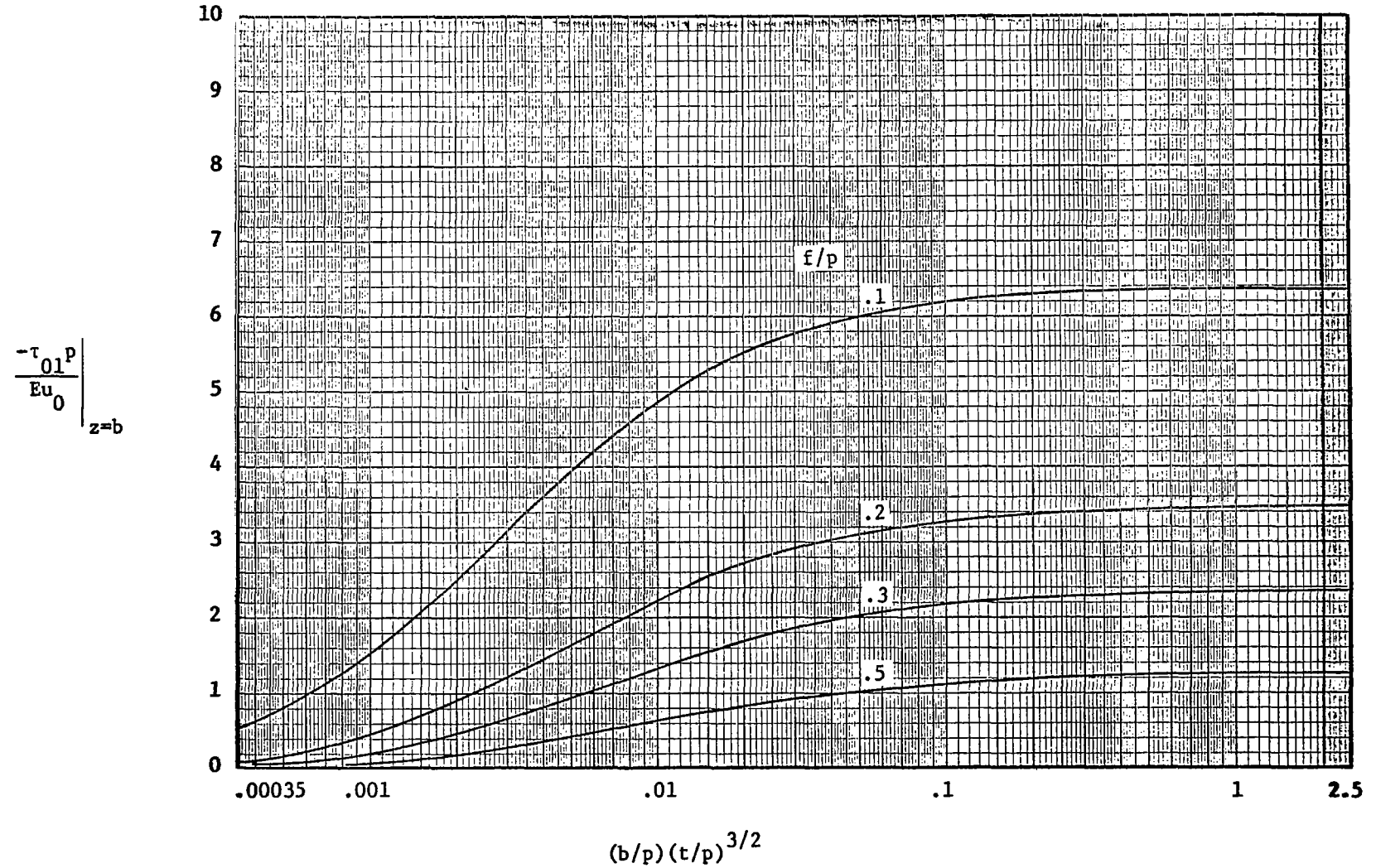

(a·II) Middle-surface shear stress for h/p = .1

Figure 19. - Continued.

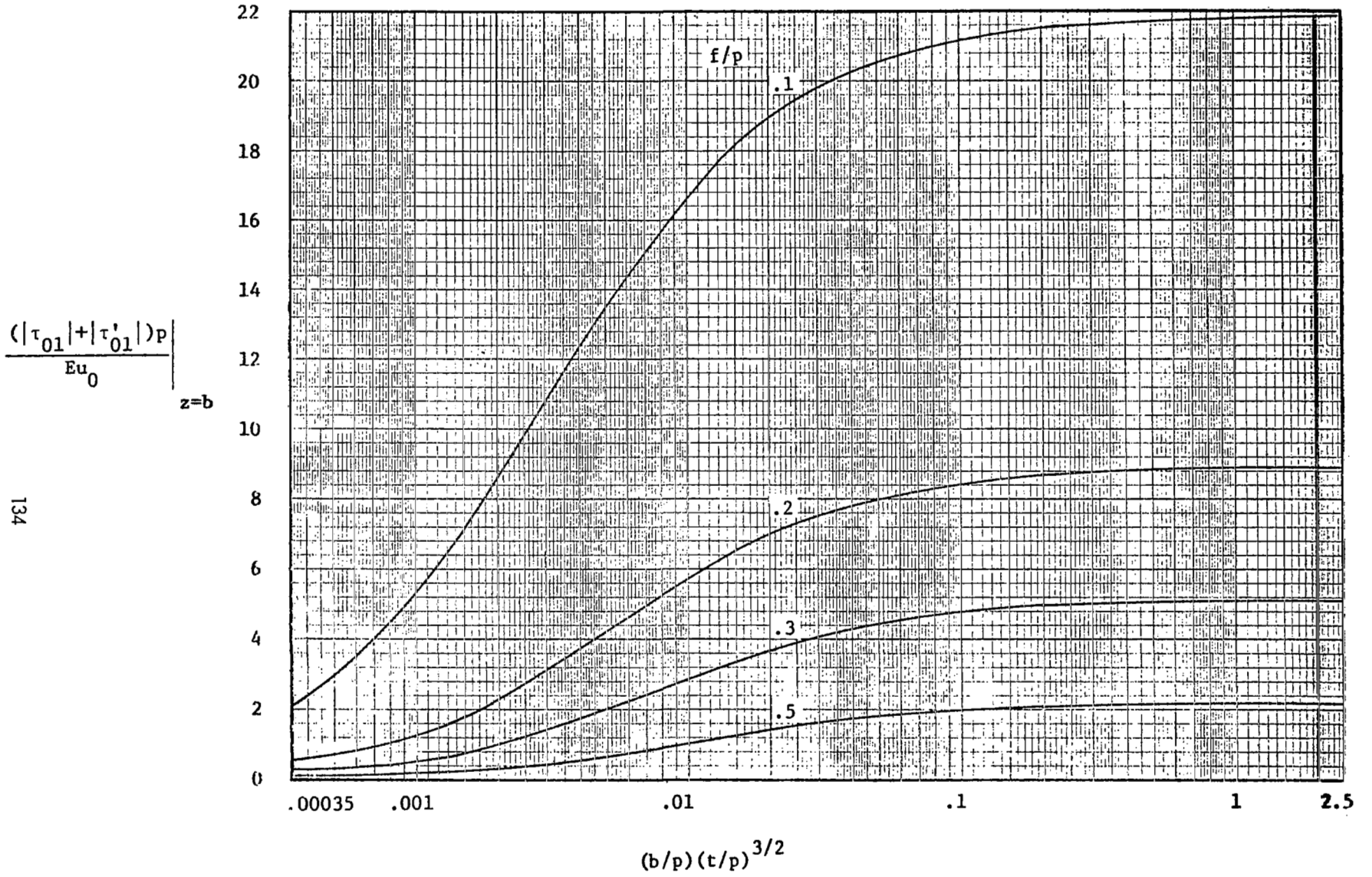

(a·III) Extreme-fiber shear stress for h/p = .1

Figure 19. - Continued.

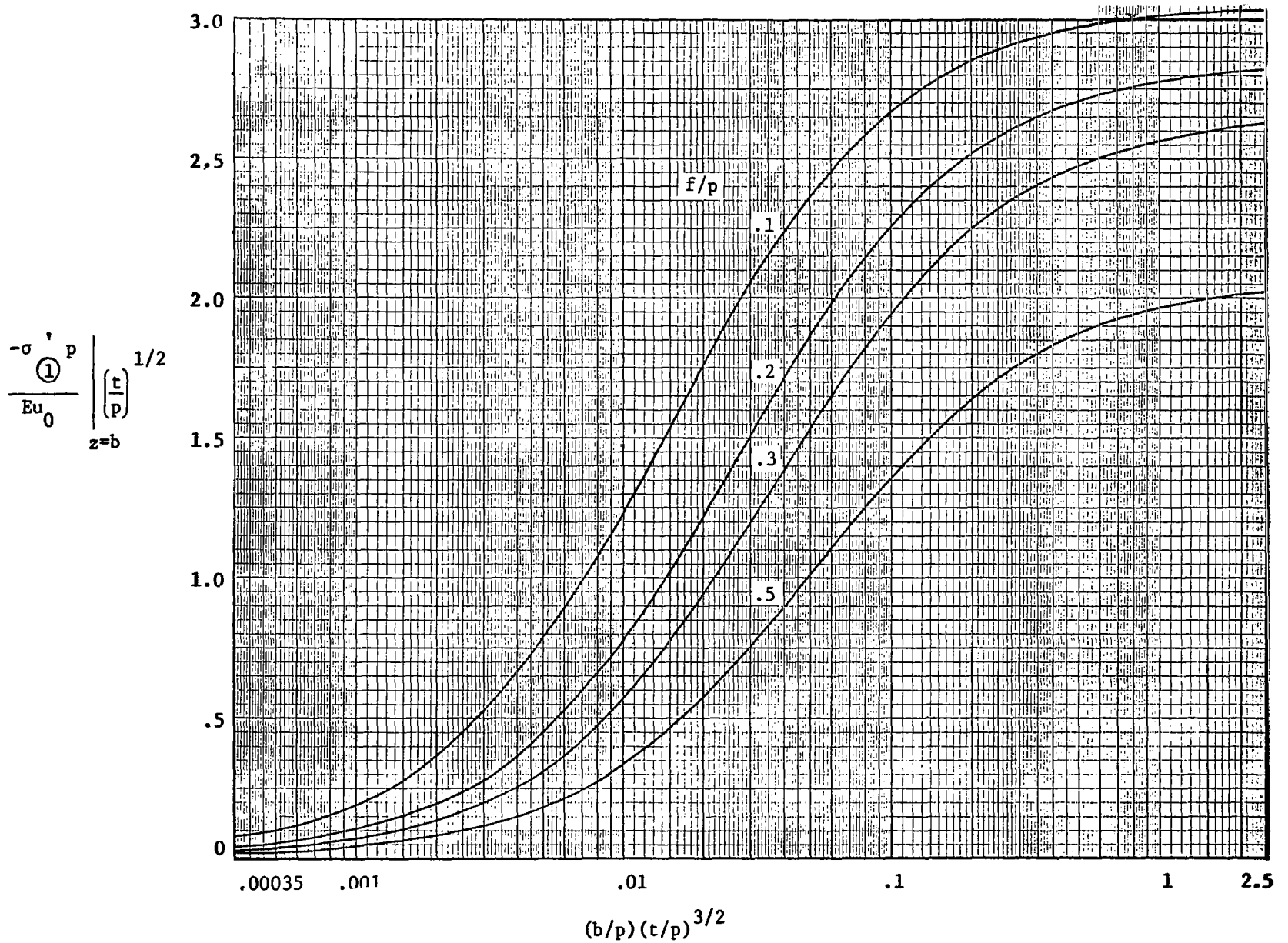

(b·I) Frame bending stress for h/p = .3

Figure 19. - Continued.

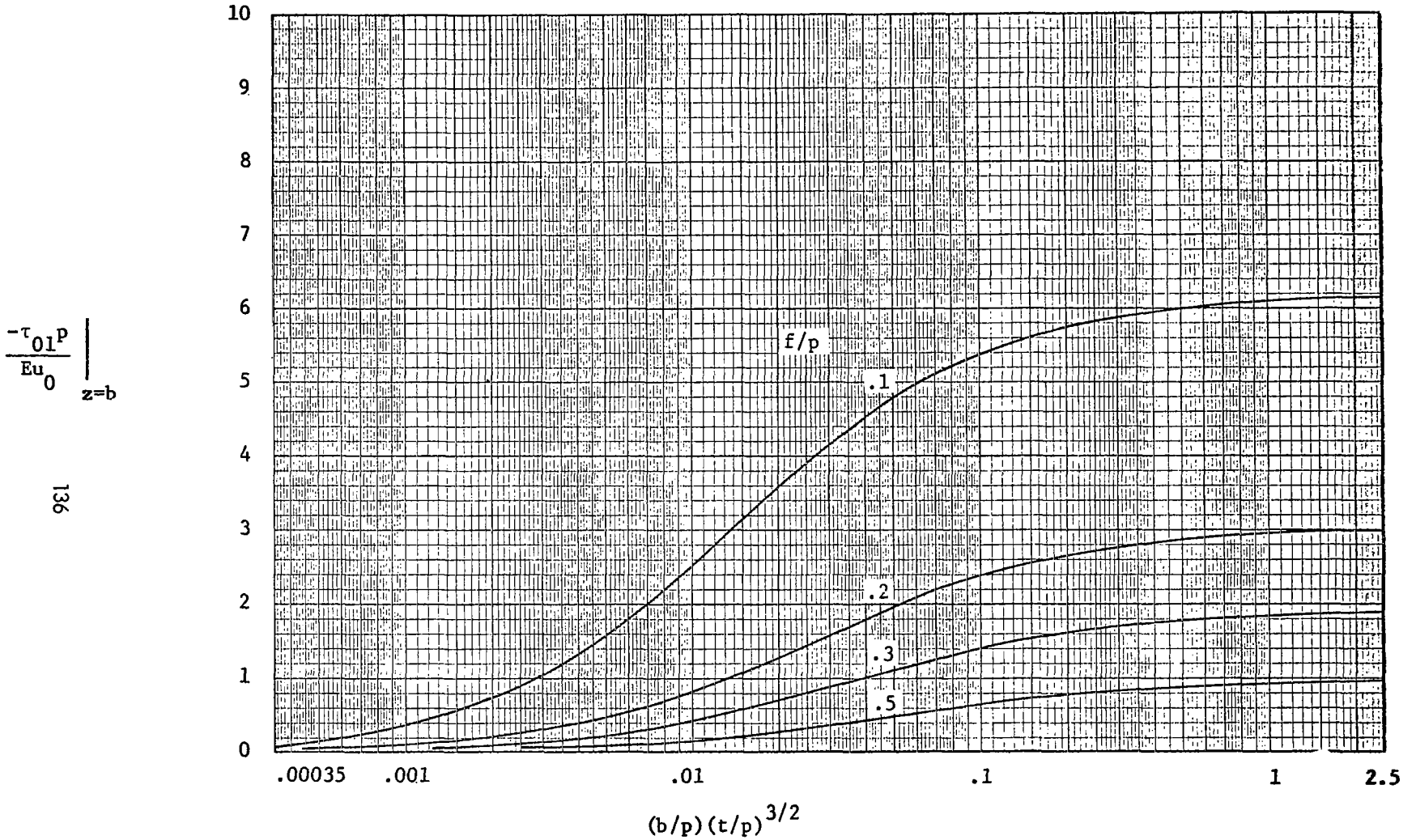

(b·II) Middle-surface shear stress for h/p = .3

Figure 19. - Continued.

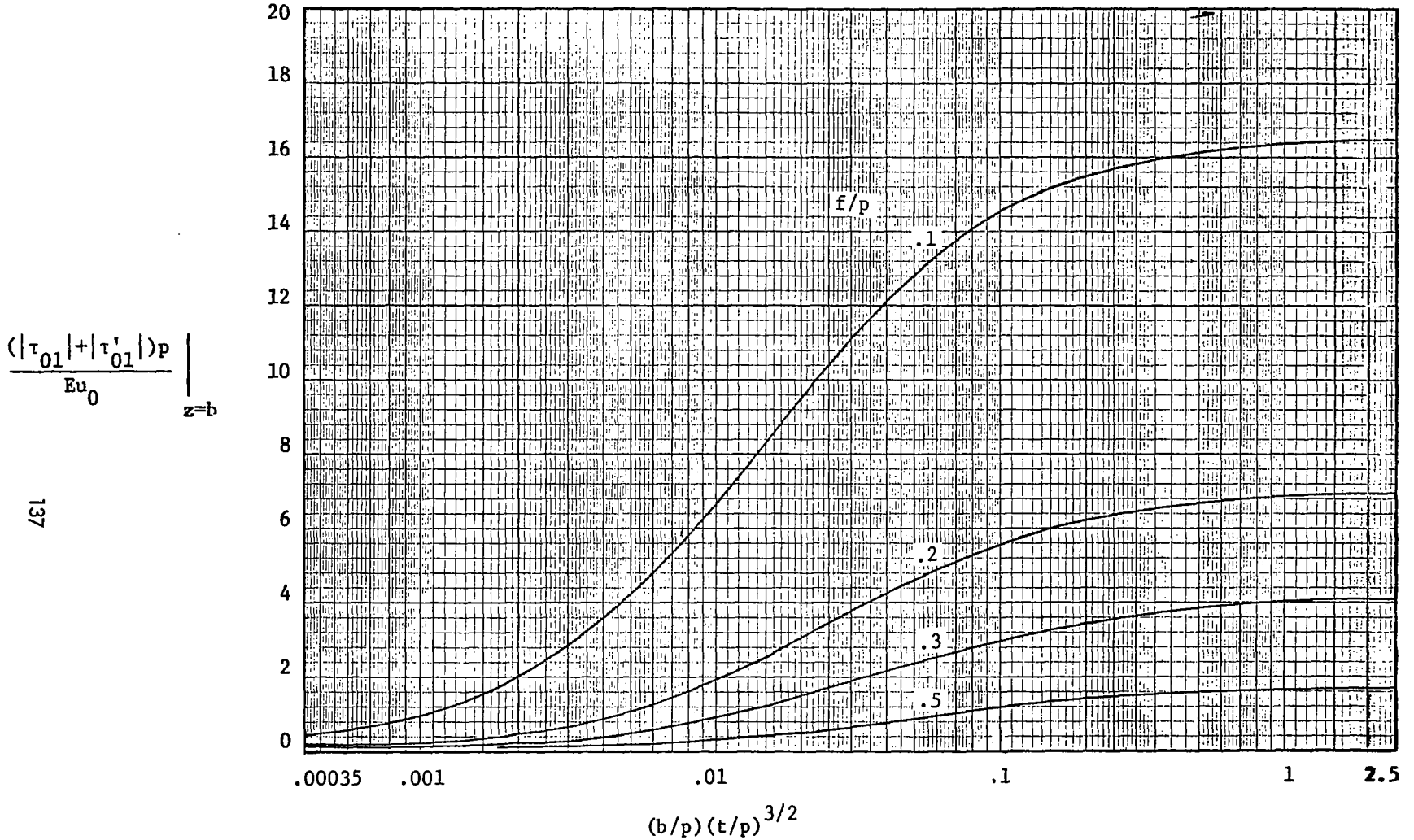

(b·III) Extreme-fiber shear stress for h/p = .3

Figure 19. - Continued.

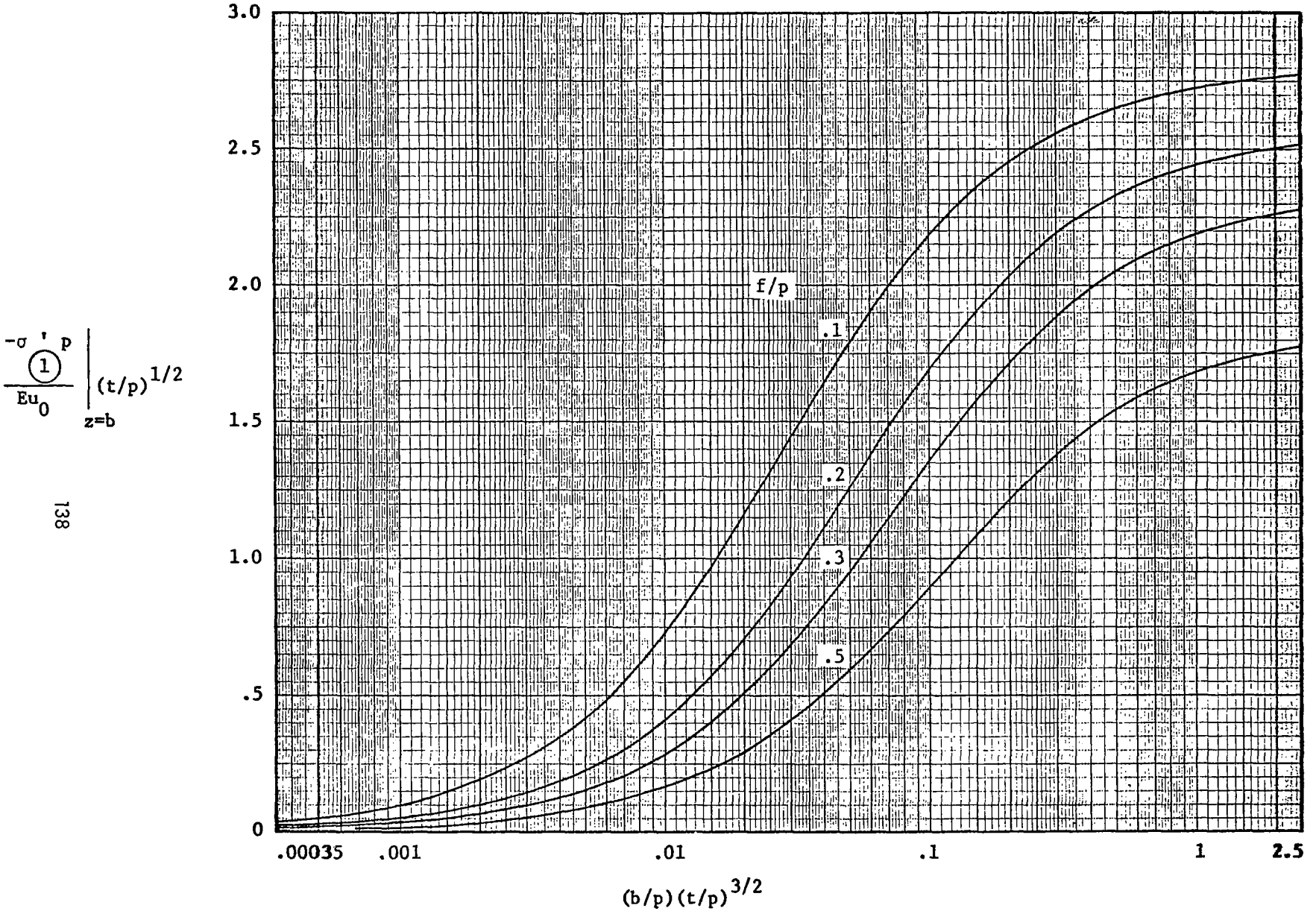

(c·I) Frame bending stress for h/p = .5

Figure 19. Continued.

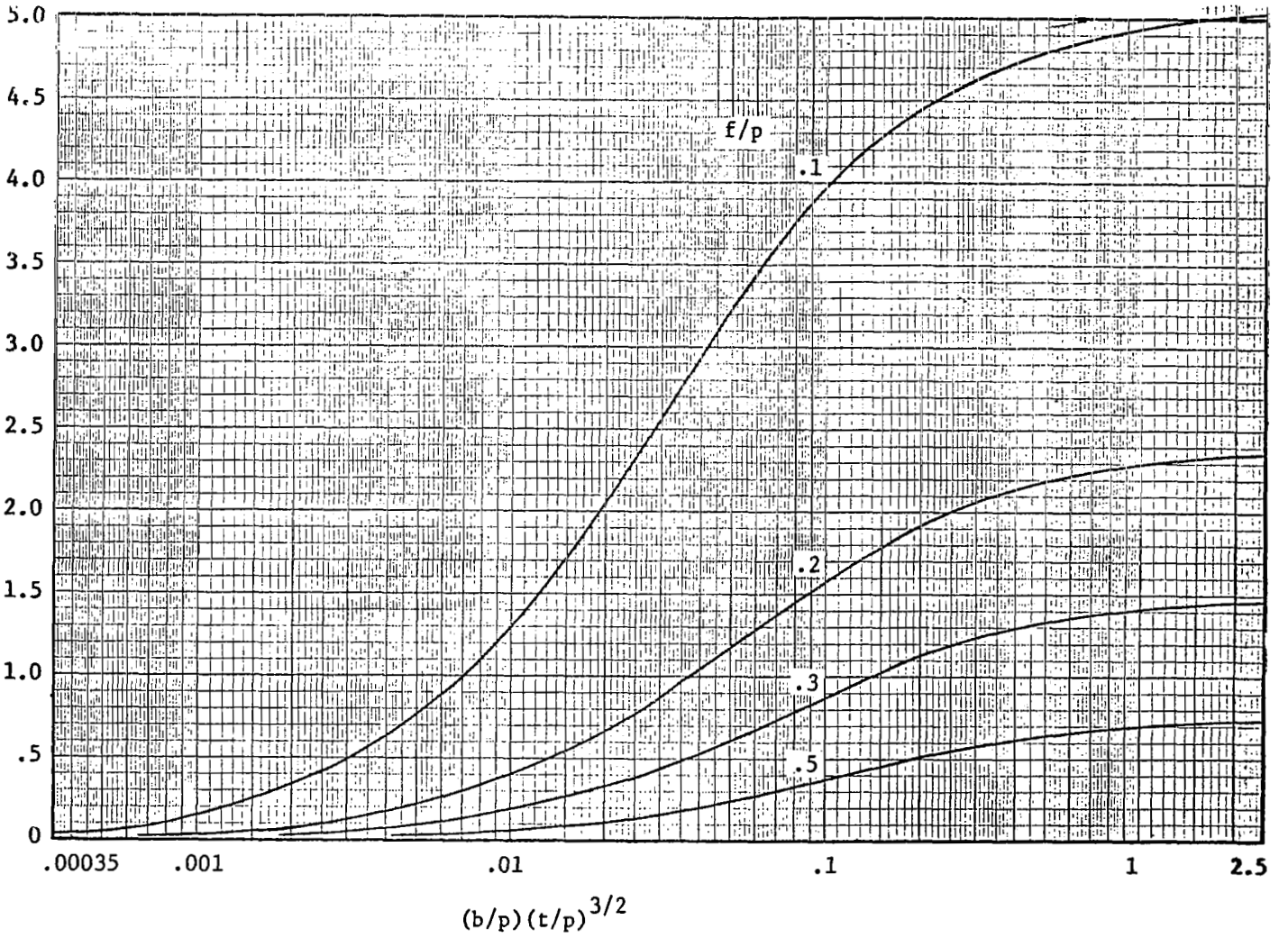

(c·II) Middle-surface shear stress for h/p = .5

Figure 19. - Continued.

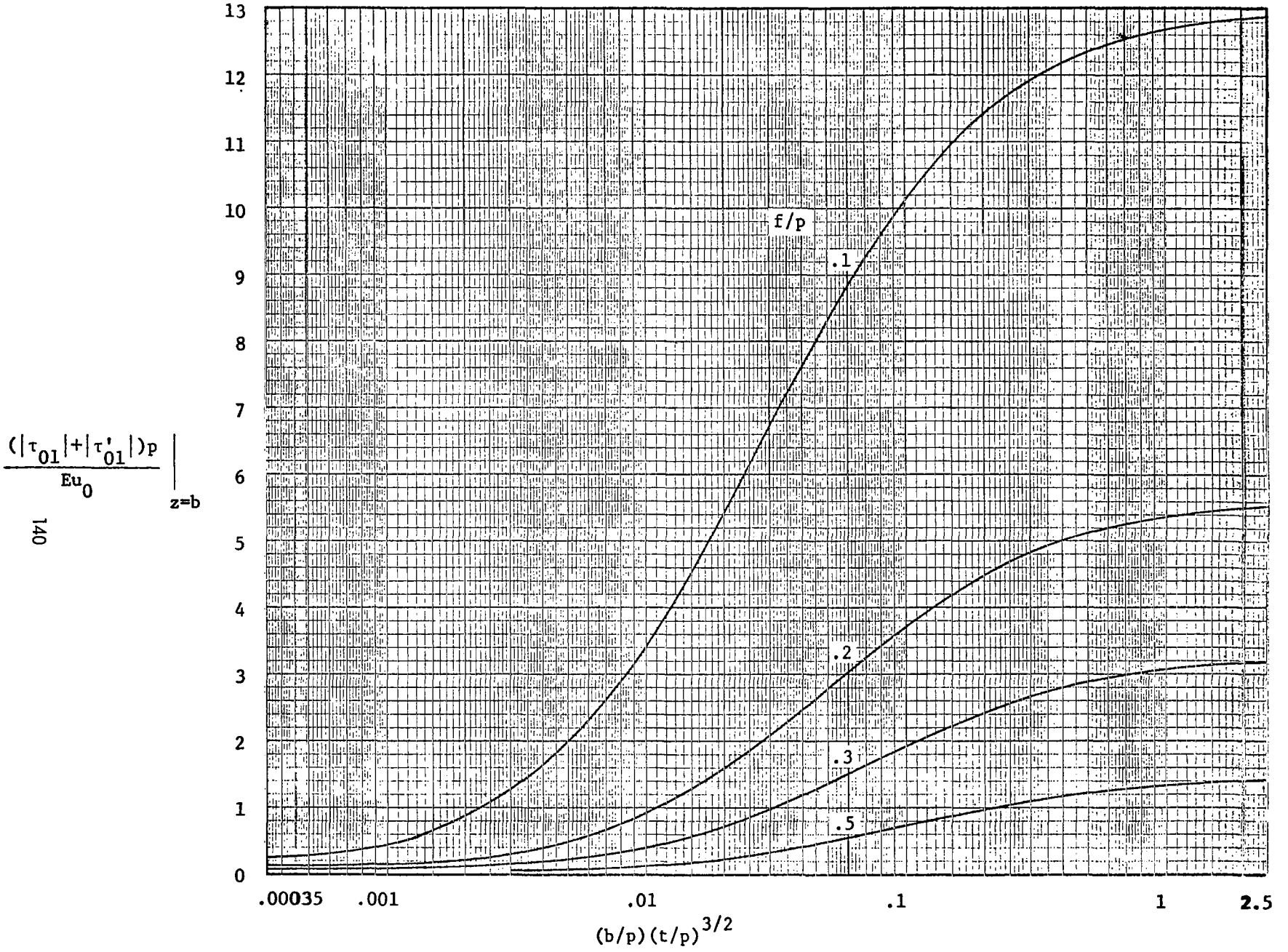

(c·III) Extreme-fiber shear stress for h/p = .5

Figure 19. - Concluded.

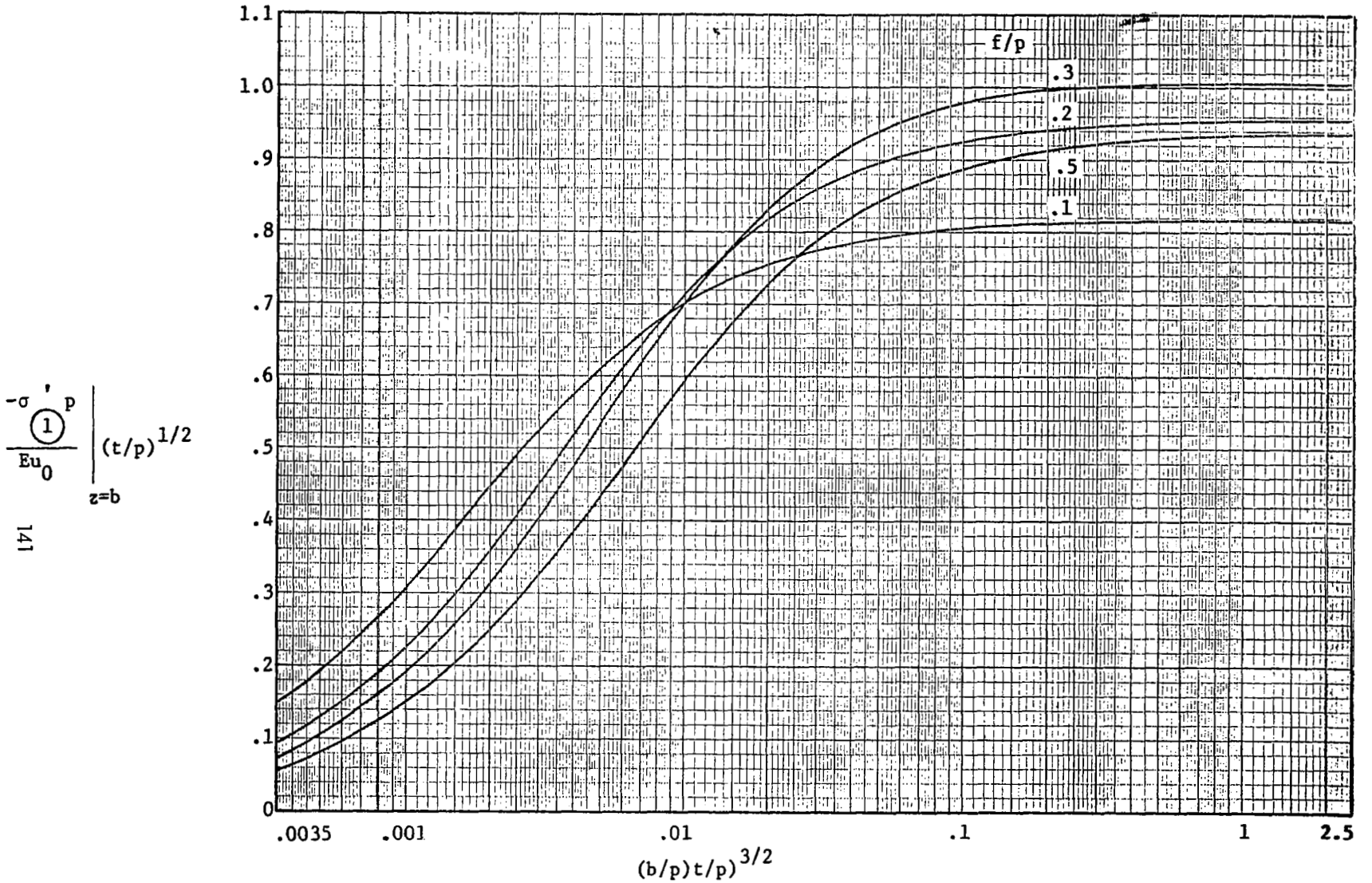

(a·I) Frame bending stress for h/p = .1

Figure 20. - Dimensionless maximum-stress parameters for the case of point attachments at the ends of both the trough lines and the crest lines.

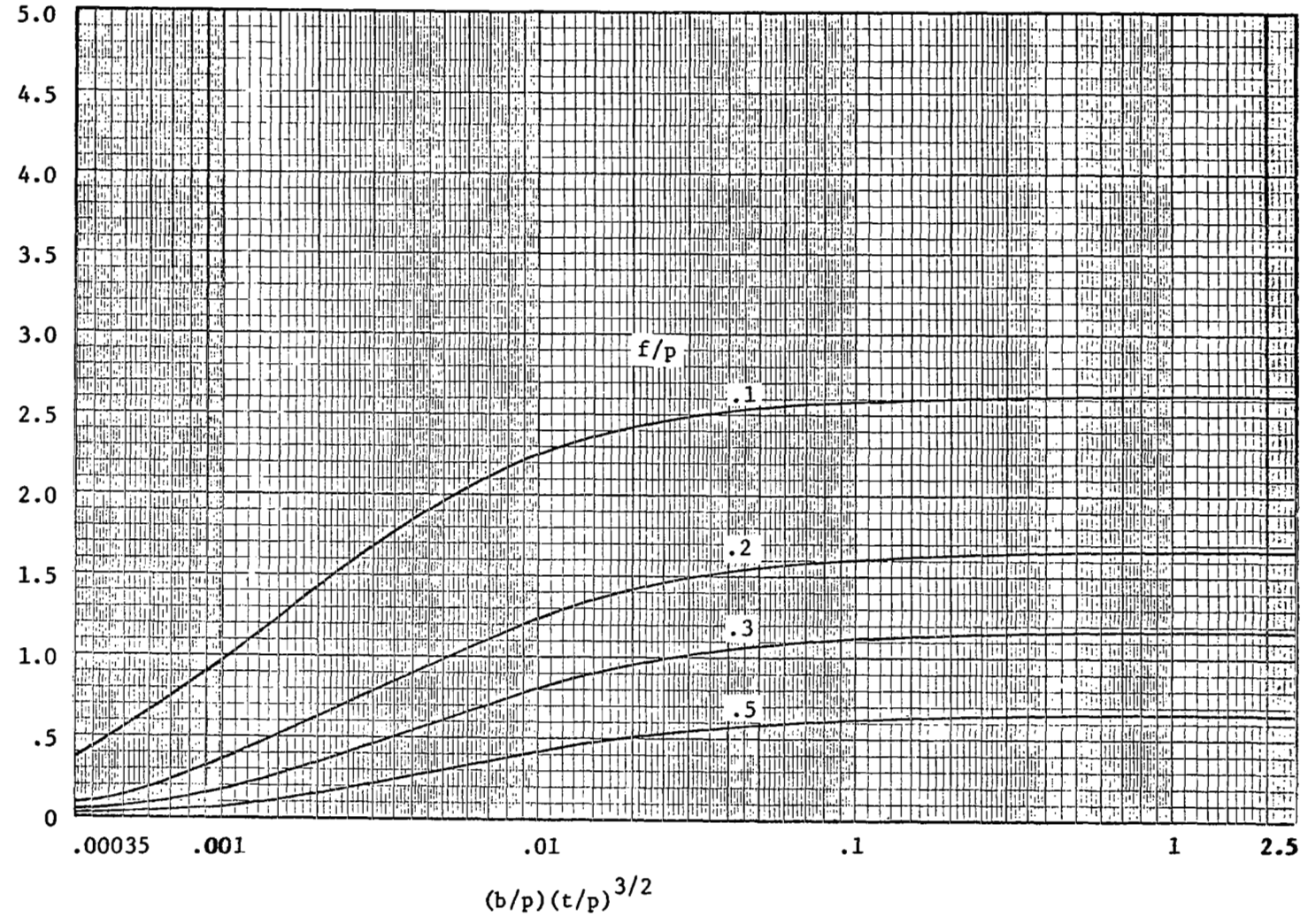

(a·II) Middle-surface shear stress for h/p = .1

Figure 20. - Continued.

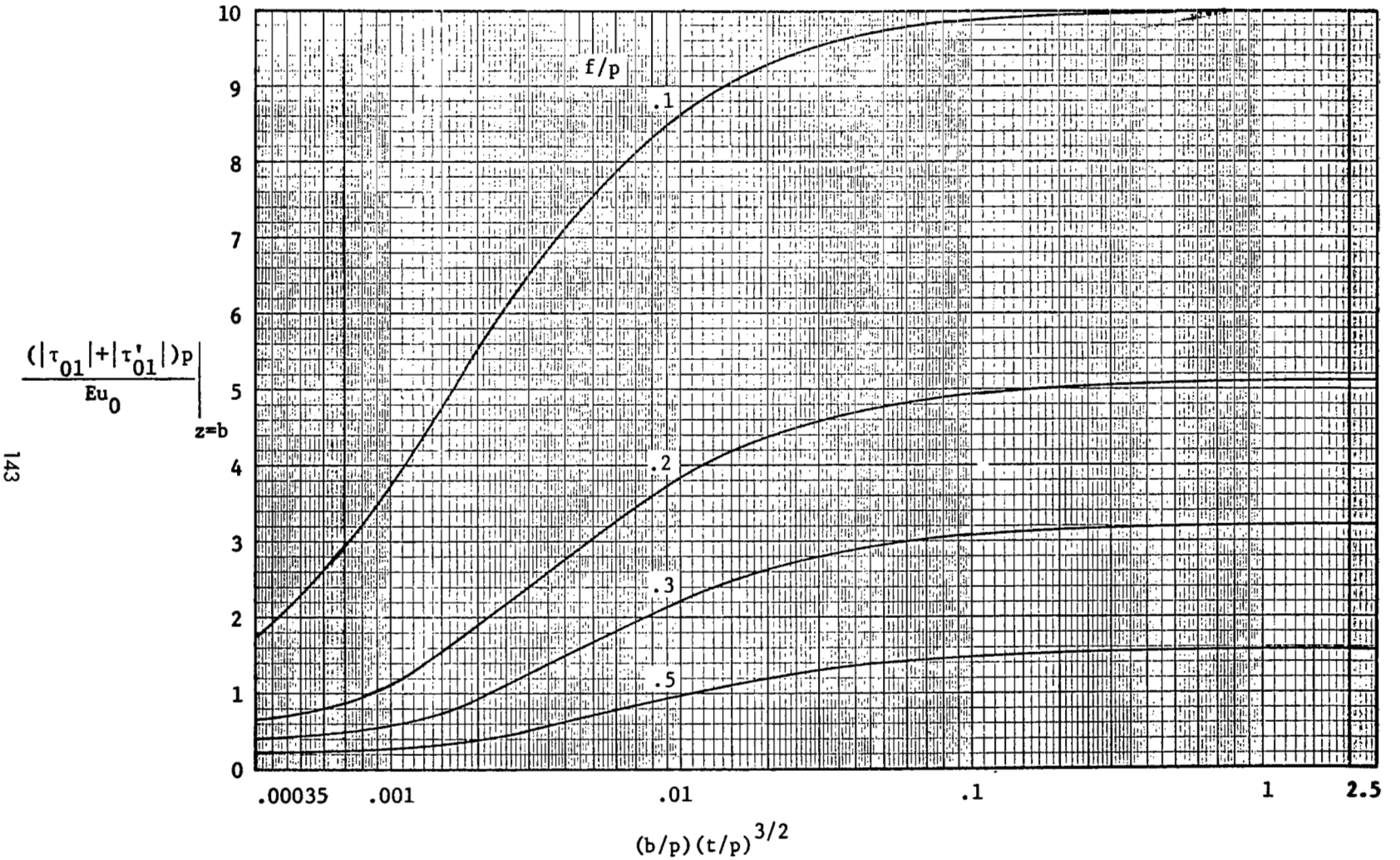

(a·III) Extreme-fiber shear stress for h/p = .1

Figure 20. - Continued.

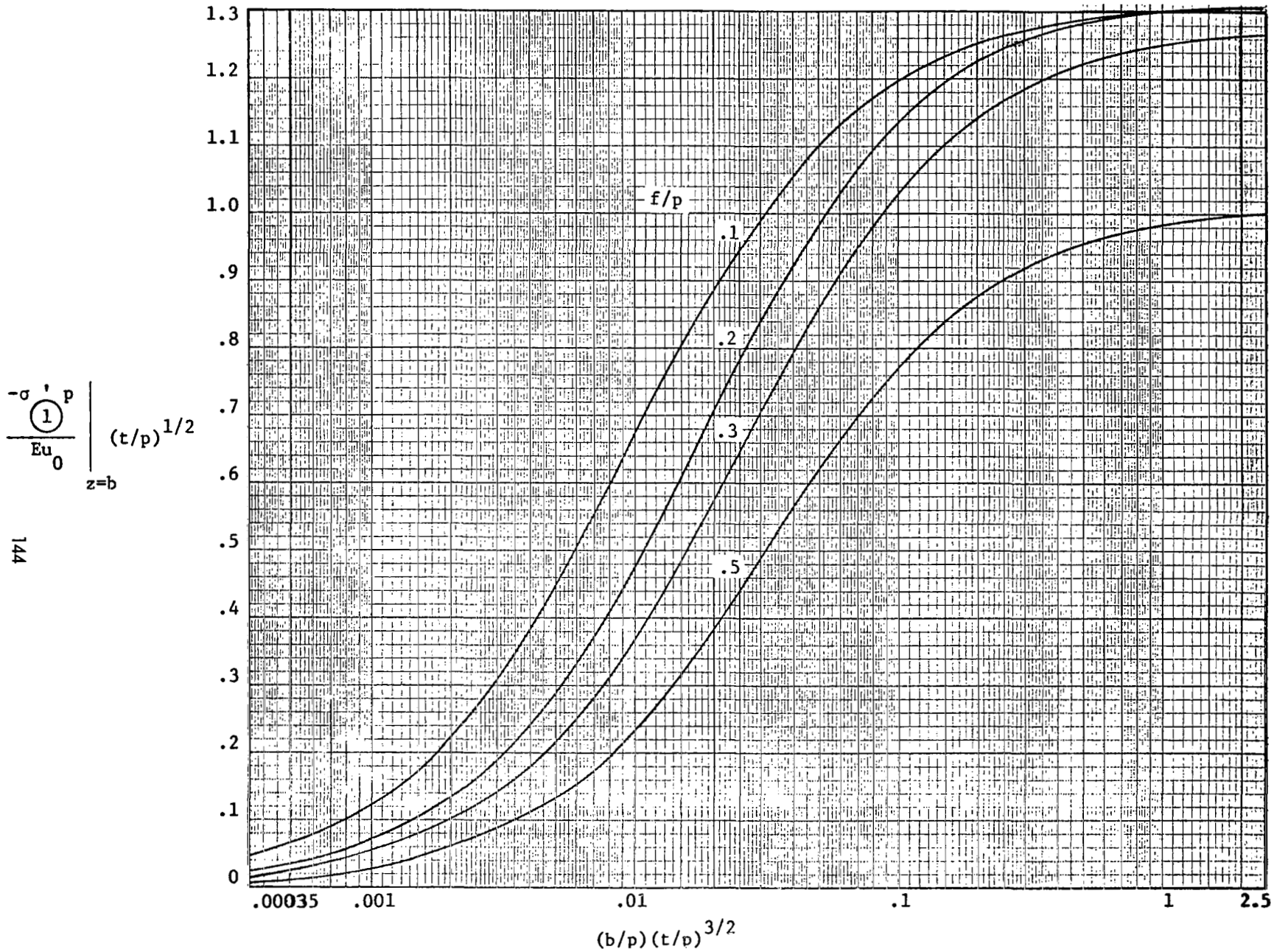

(b·I) Frame bending stress for h/p = .3

Figure 20. - Continued.

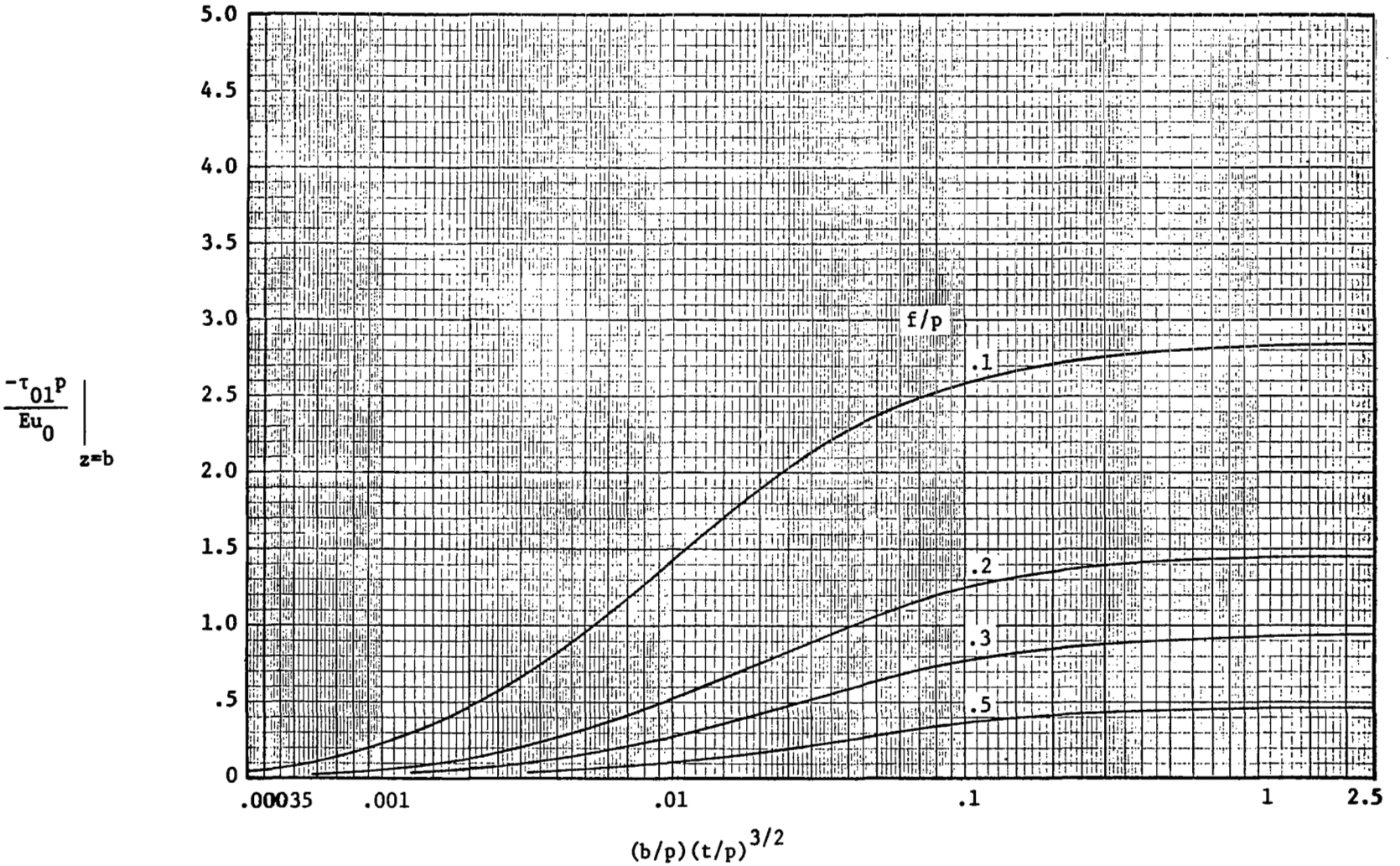

(b·II) Middle-surface shear stress for h/p = .3

Figure 20. - Continued.

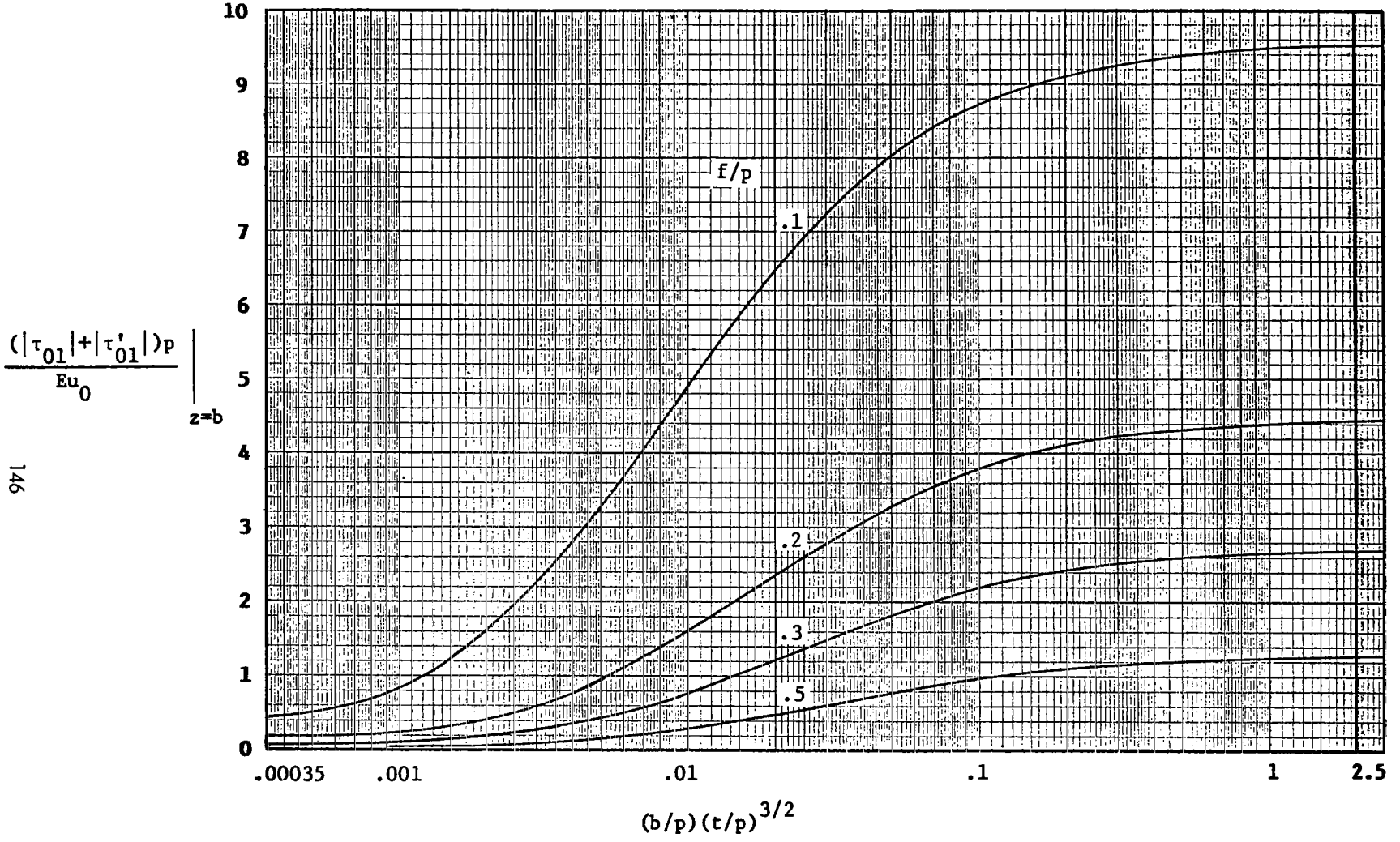

(b·III) Extreme-fiber shear stress for h/p = .3

Figure 20. - Continued.

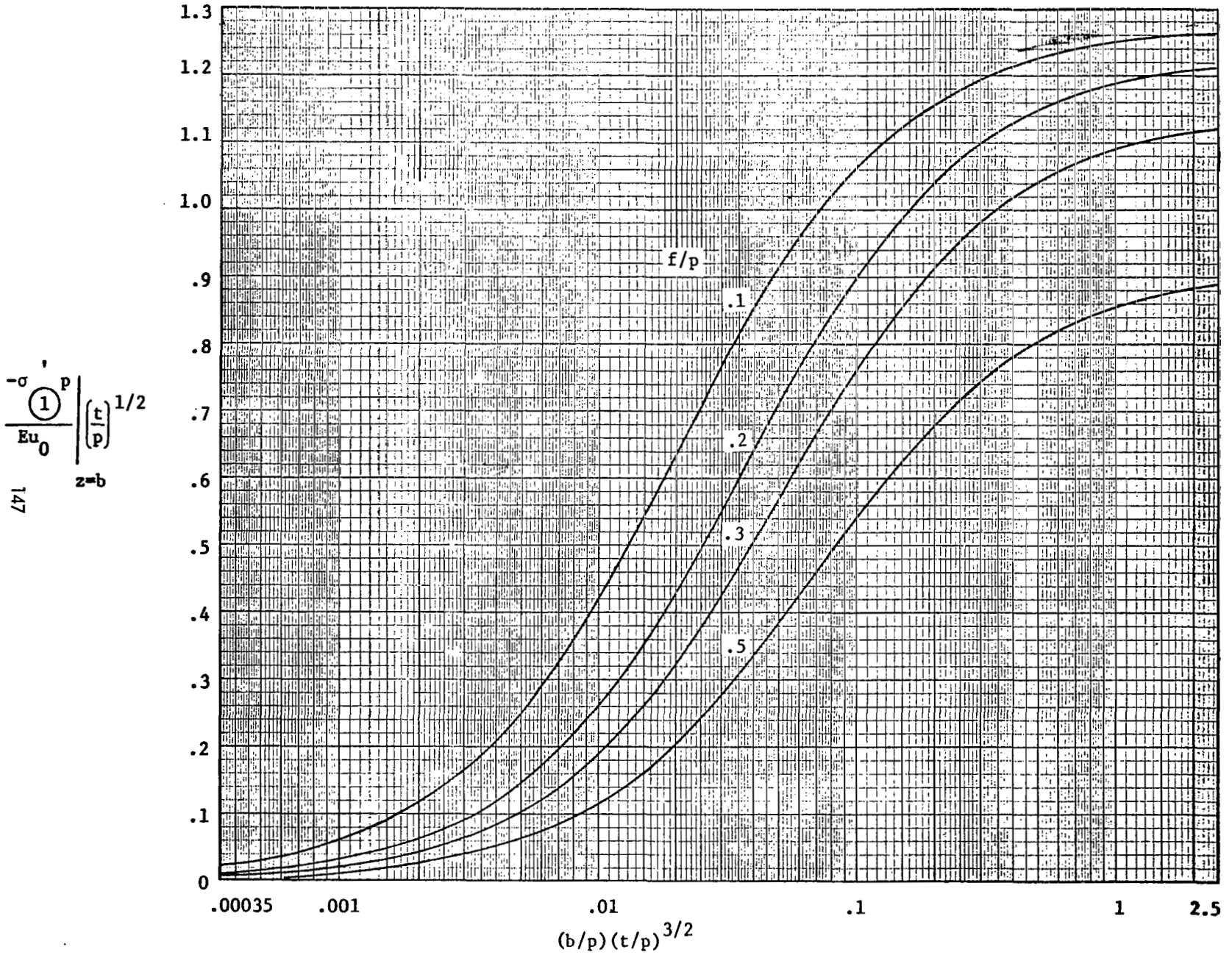

(c•1) Frame bending stress for h/p = .5

Figure 20. - Continued.

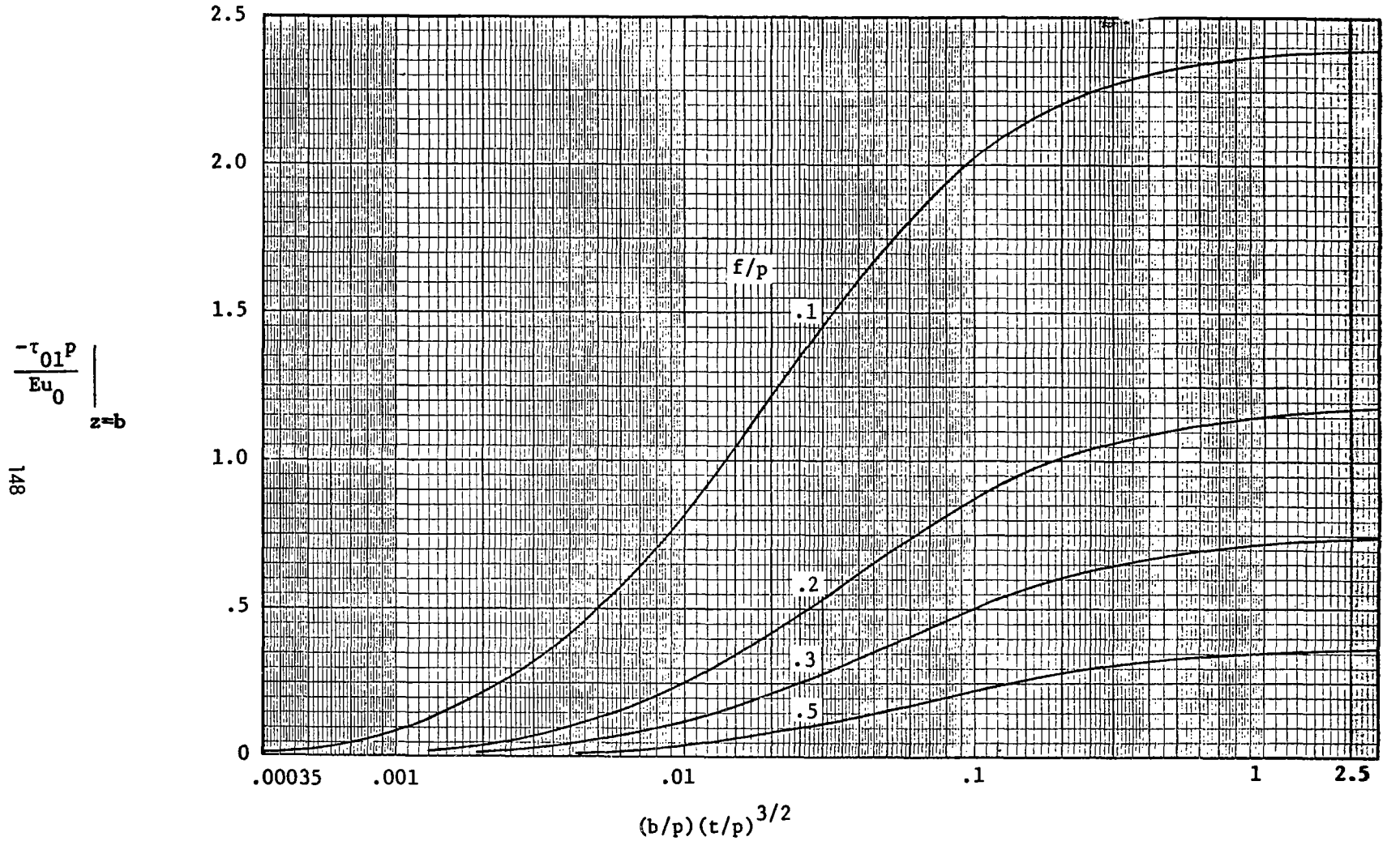

(c·II) Middle-surface shear stress for h/p = .5

Figure 20. - Continued.

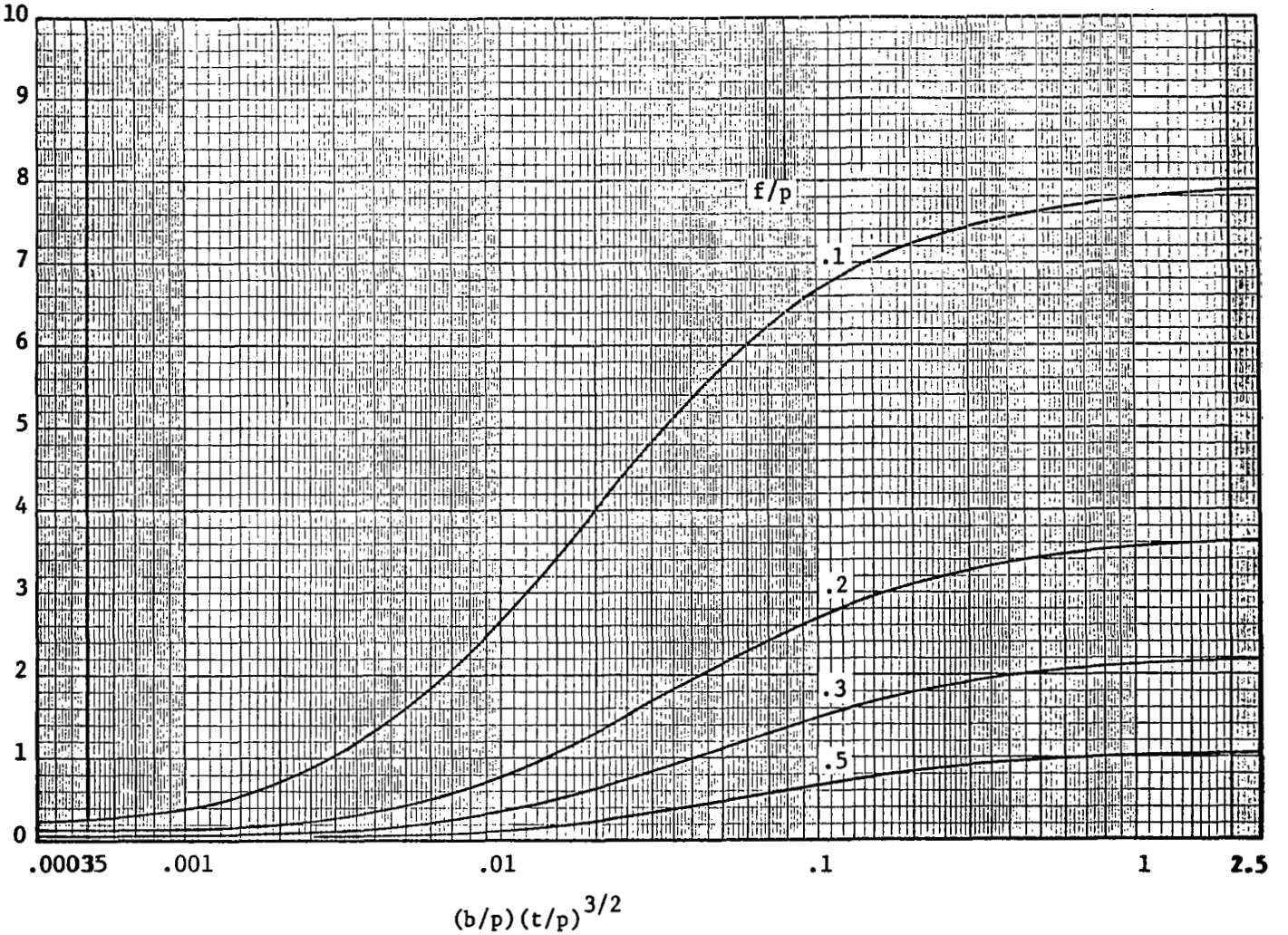

(c·III) Extreme-fiber shear stress for h/p = .5

Figure 20. - Concluded.

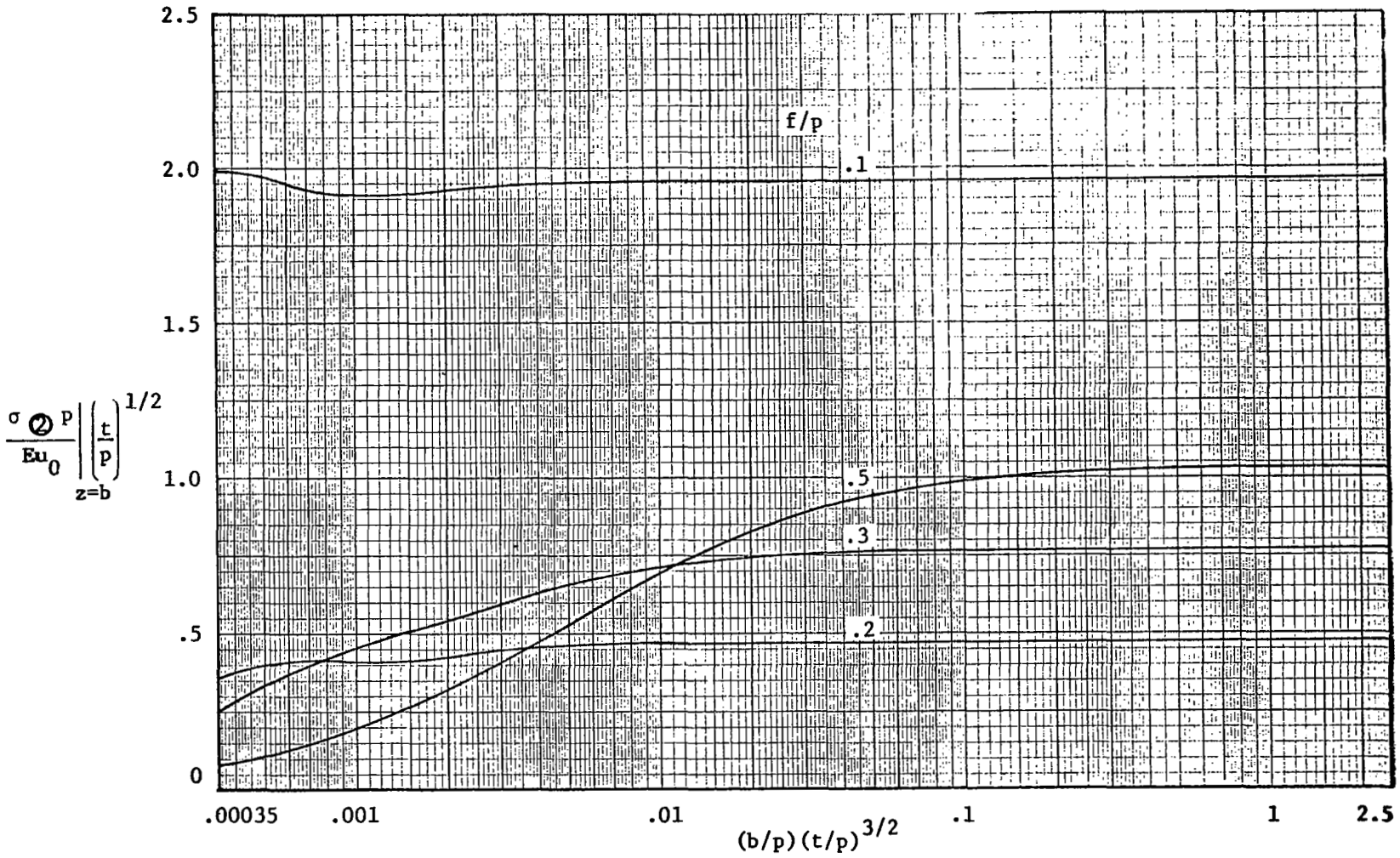

(a·I) Frame bending stress for h/p = .1

Figure 21. - Dimensionless maximum-stress parameters for the case of wide attachments at the ends of the trough lines.

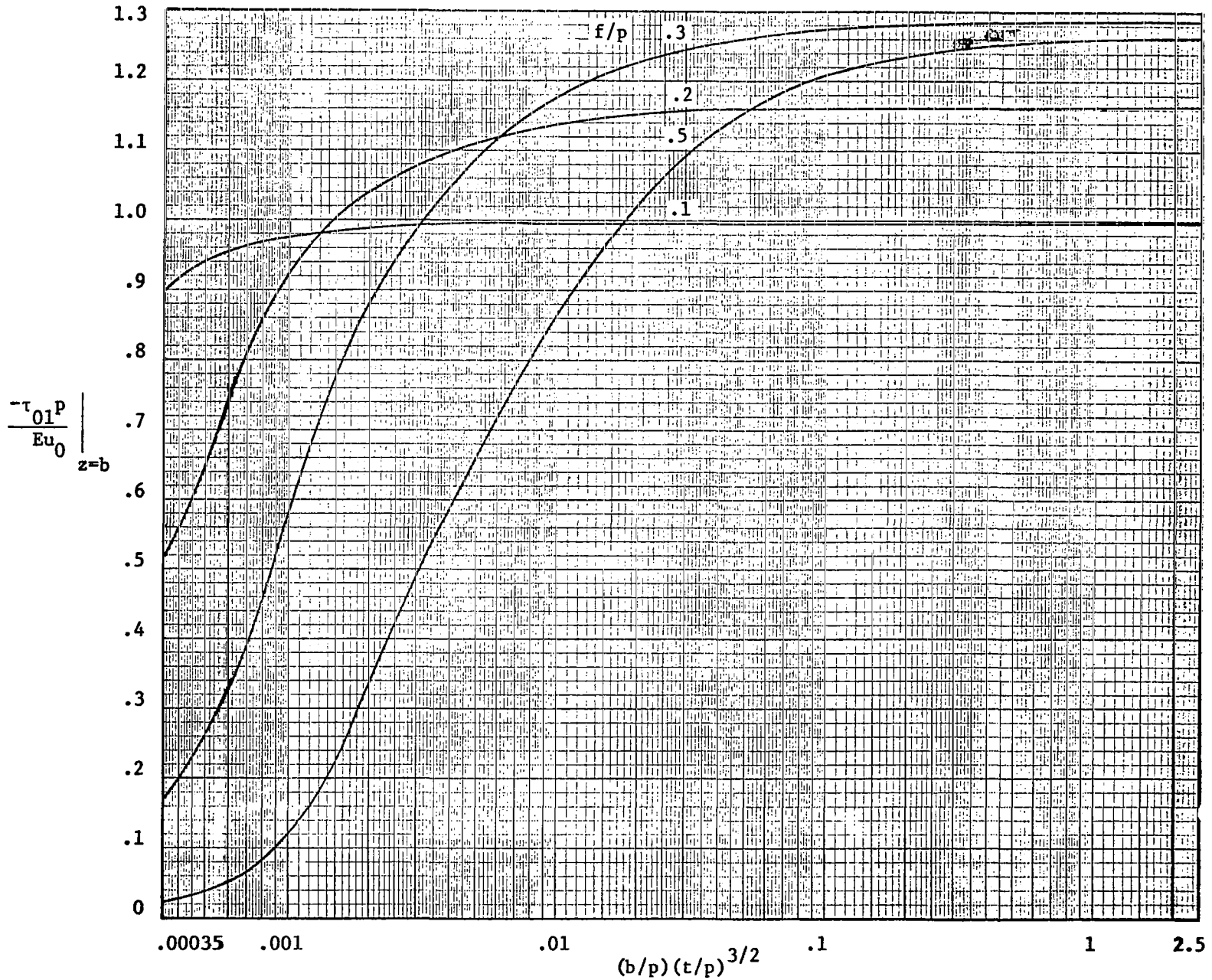

(a·II) Middle-surface shear stress for h/p = .1

Figure 21. - Continued.

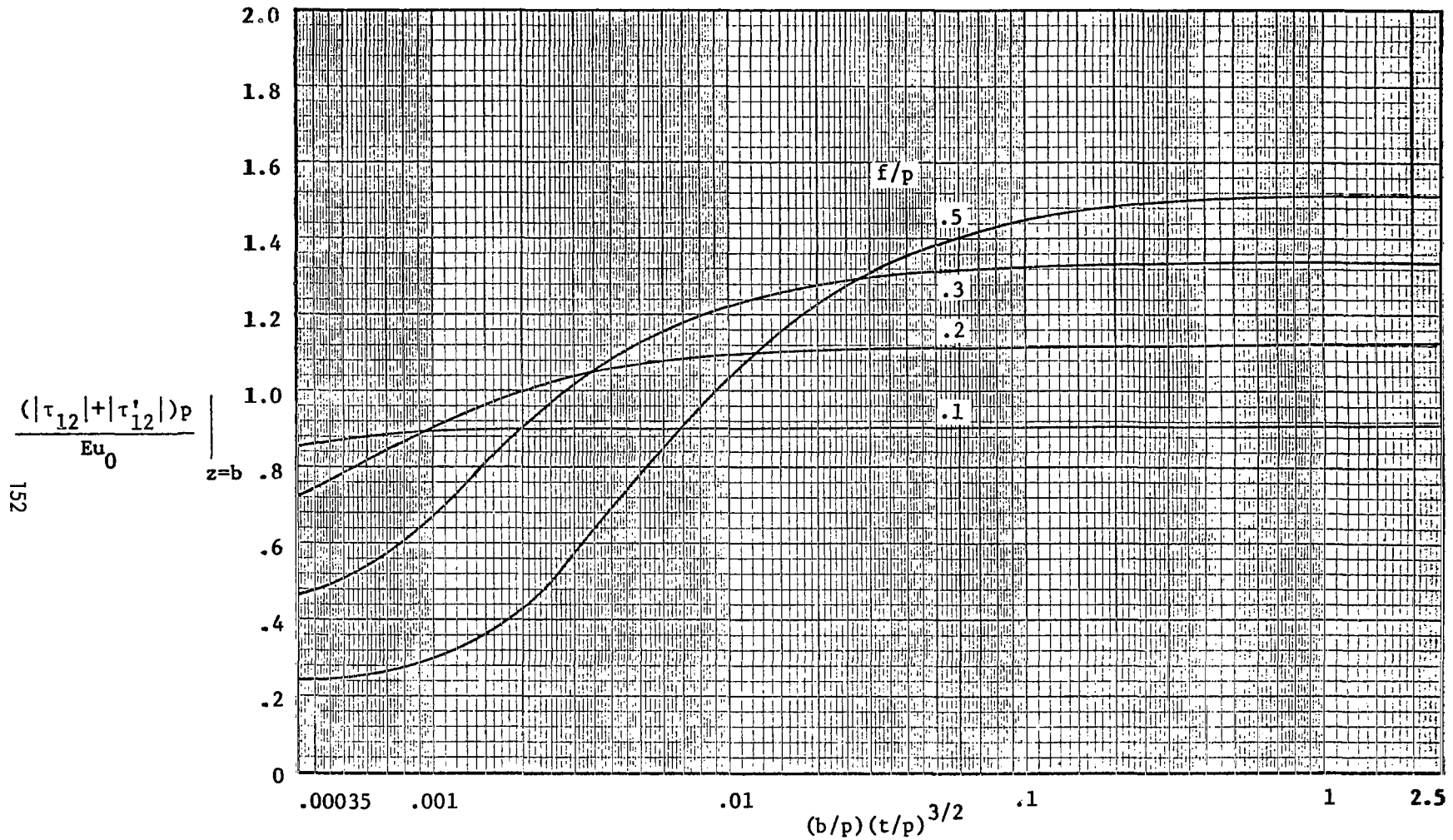

(a·III) Extreme-fiber shear stress for h/p = .1

Figure 21. - Continued.

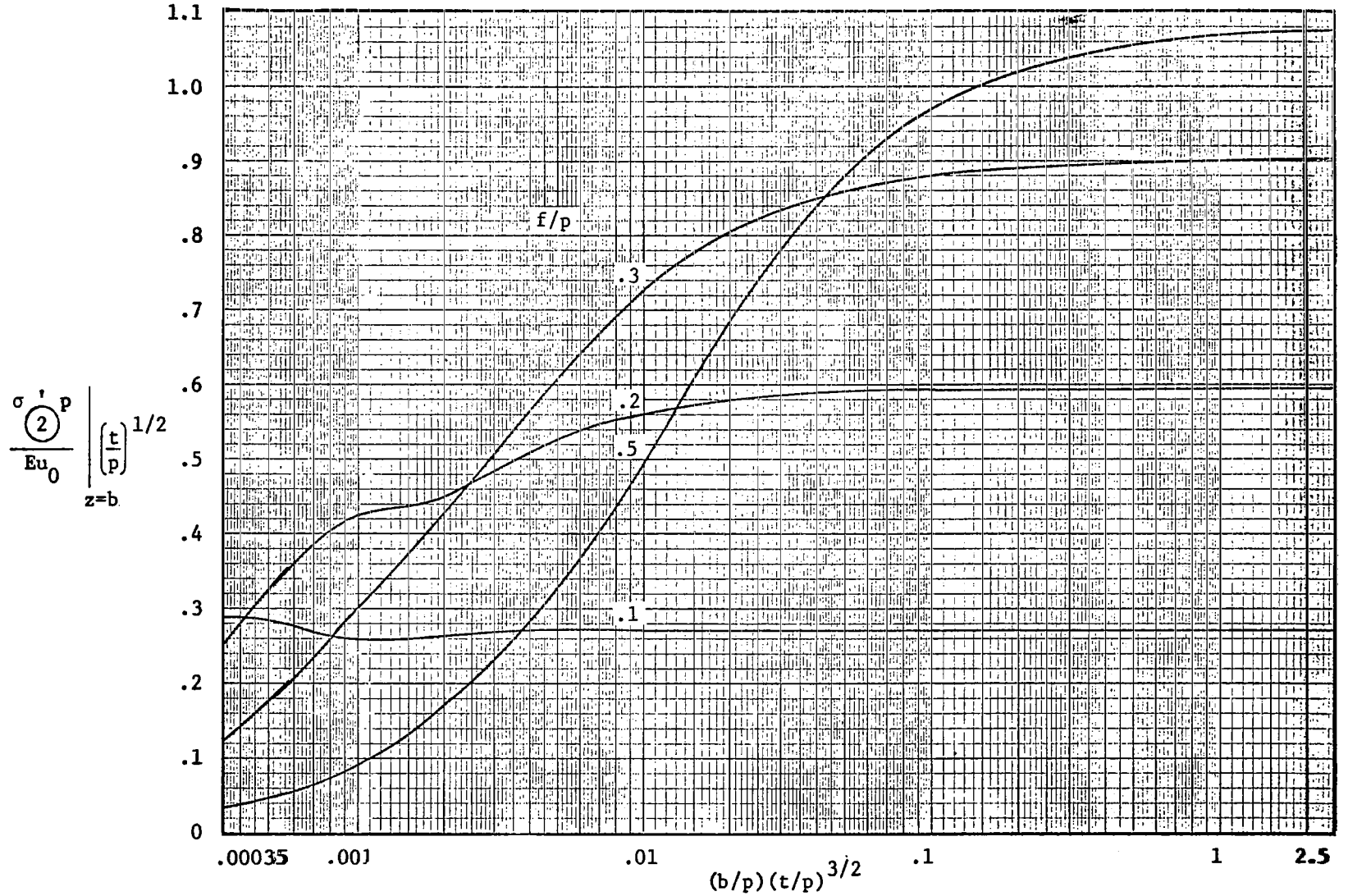

(b·I) Frame bending stress for h/p = .2

Figure 21. - Continued.

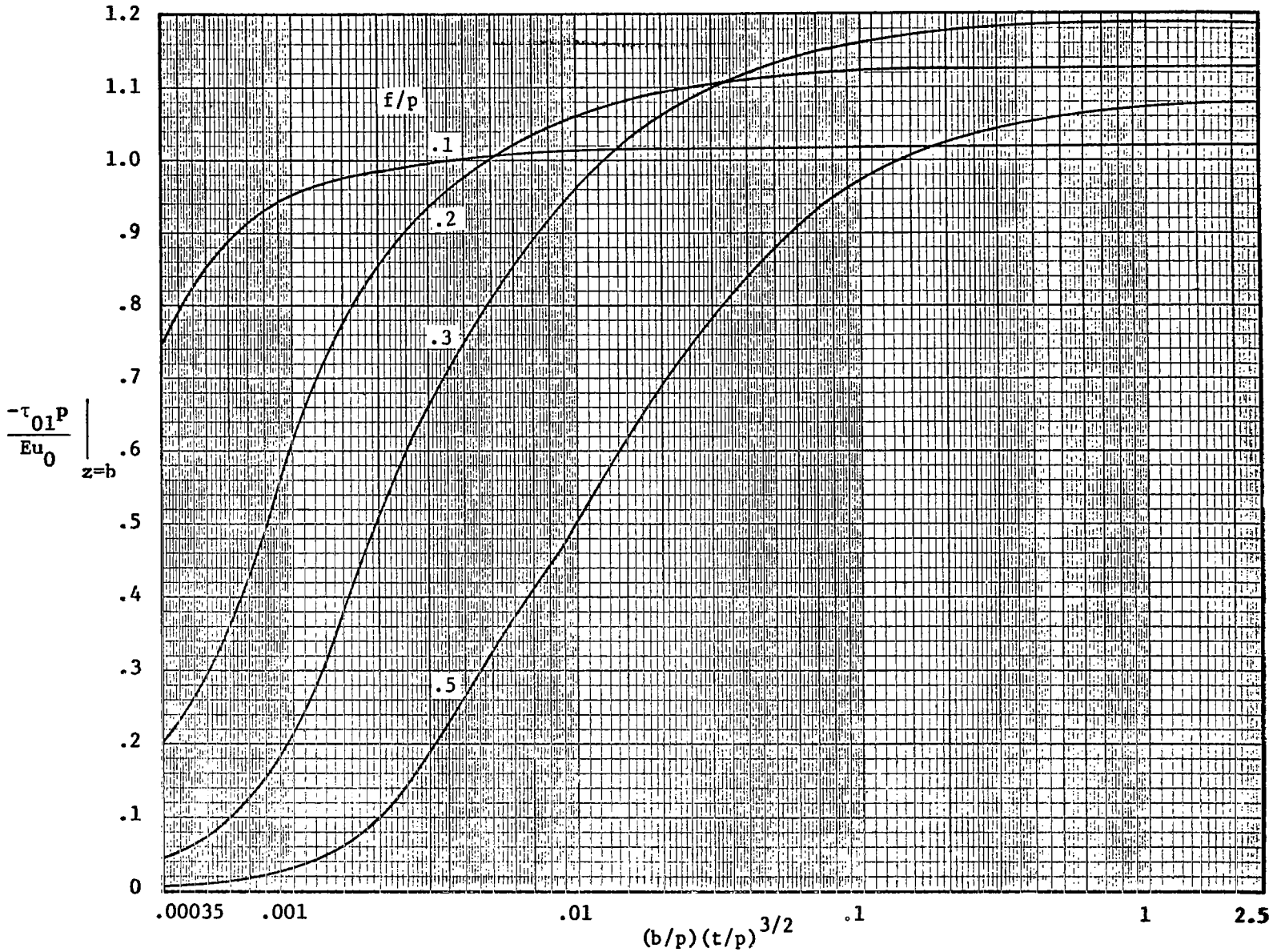

(b·II) Middle-surface shear stress for h/p = .2

Figure 21. - Continued.

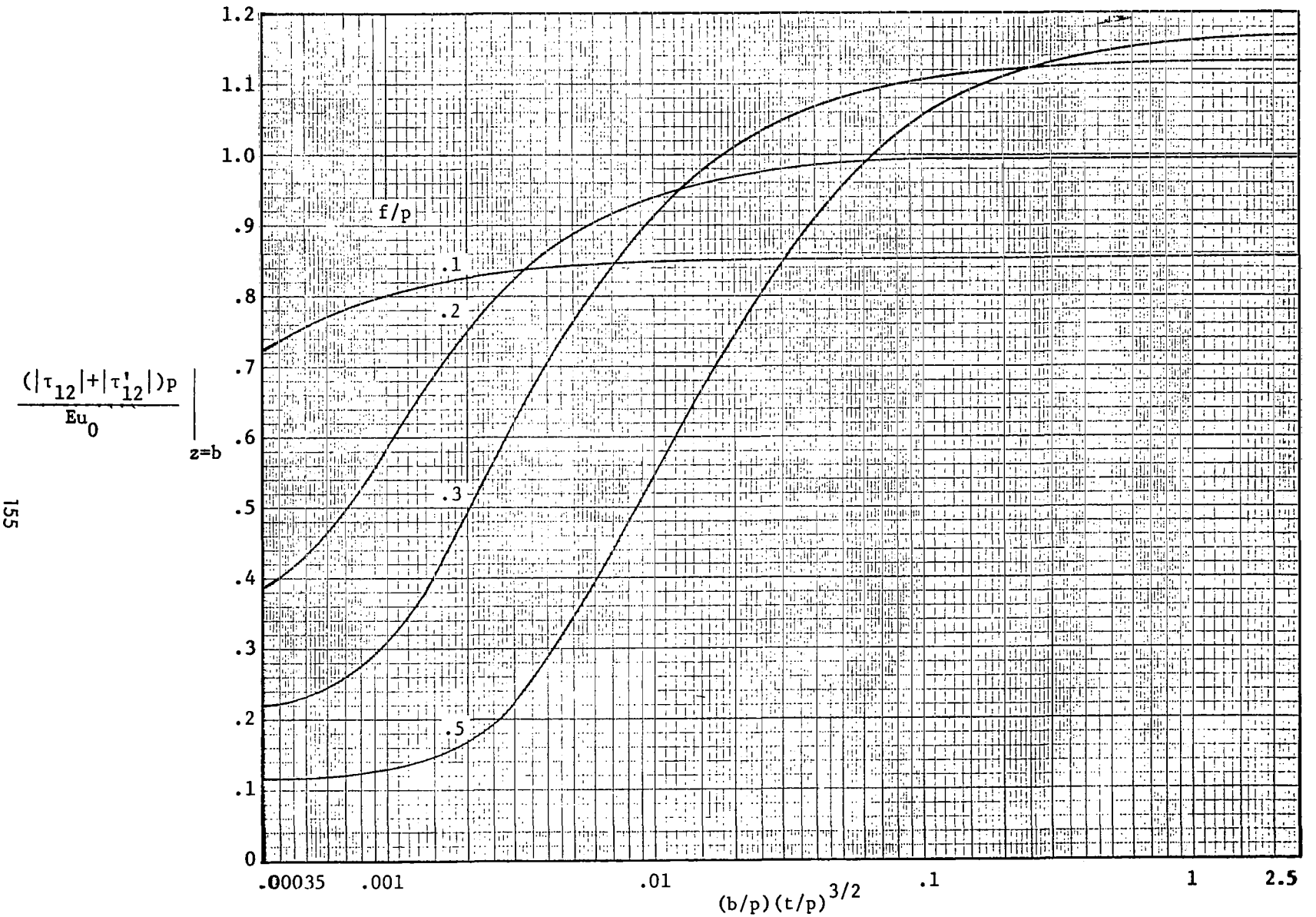

(b·III) Extreme-fiber shear stress for h/p = .2

Figure 21. - Continued.

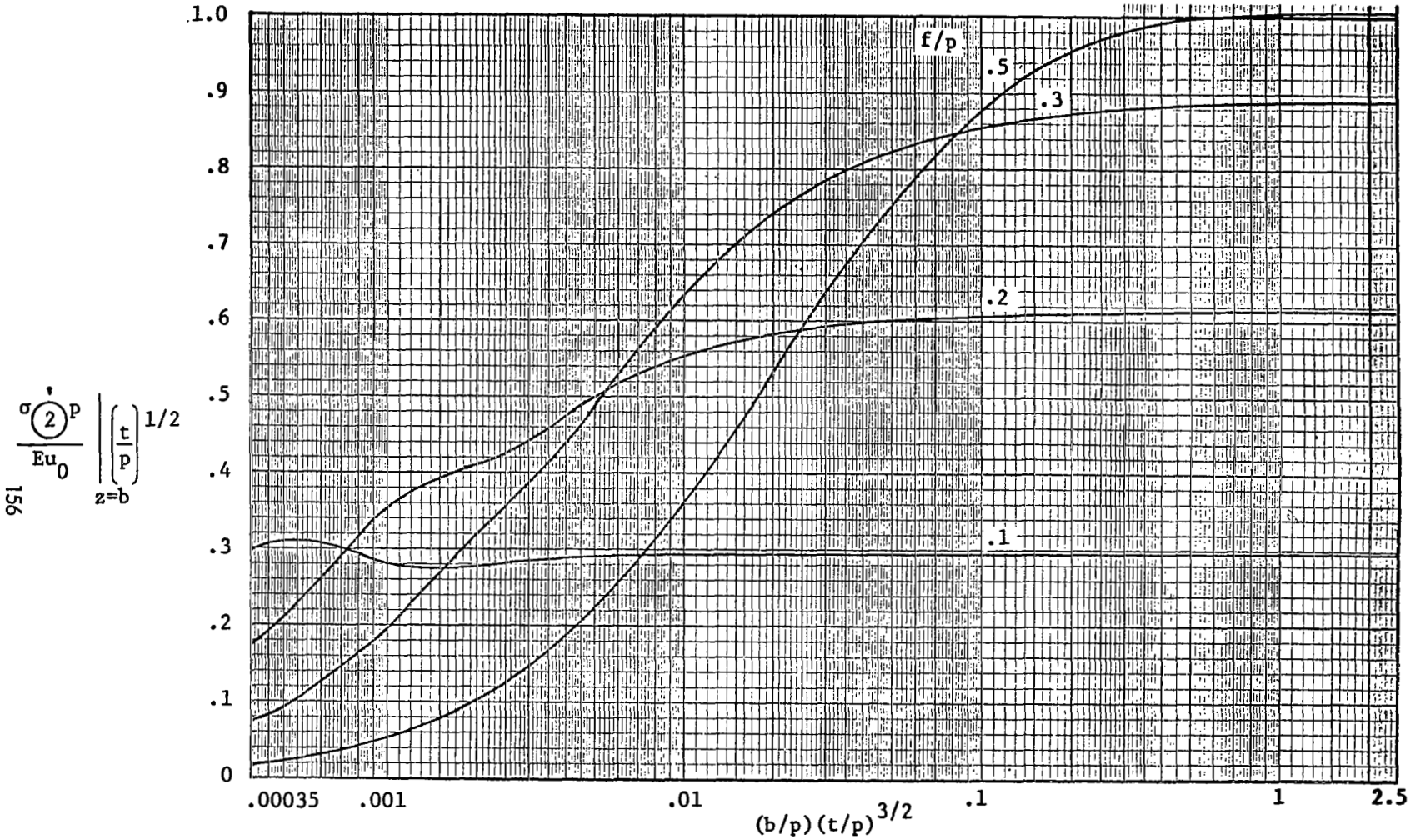

(c·I) Frame bending stress for h/p = .3

Figure 21. - Continued.

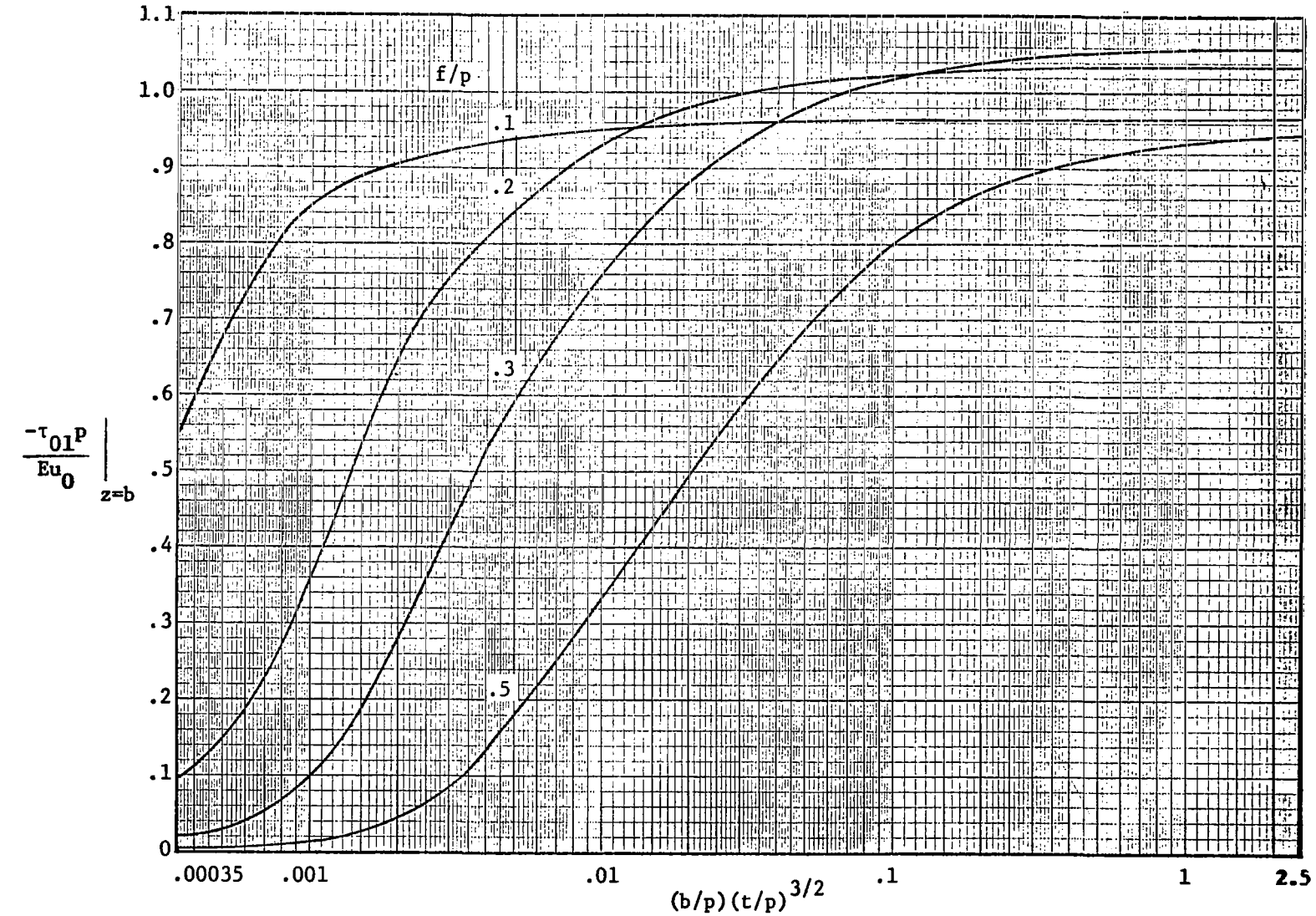

(c·II) Middle-surface shear stress for h/p = .3

Figure 21. - Continued.

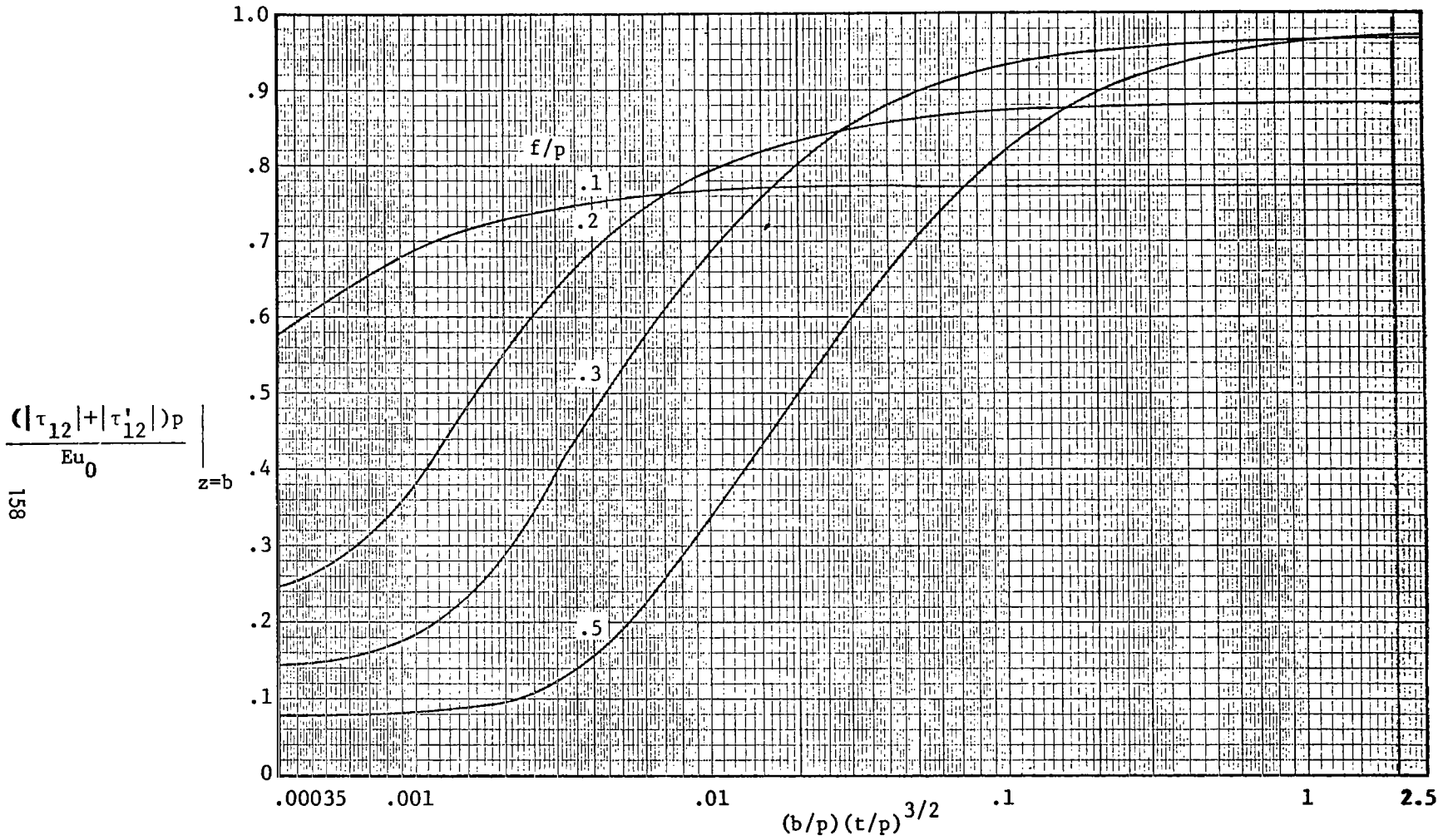

(c·III) Extreme-fiber shear stress for h/p = .3

Figure 21. - Continued.

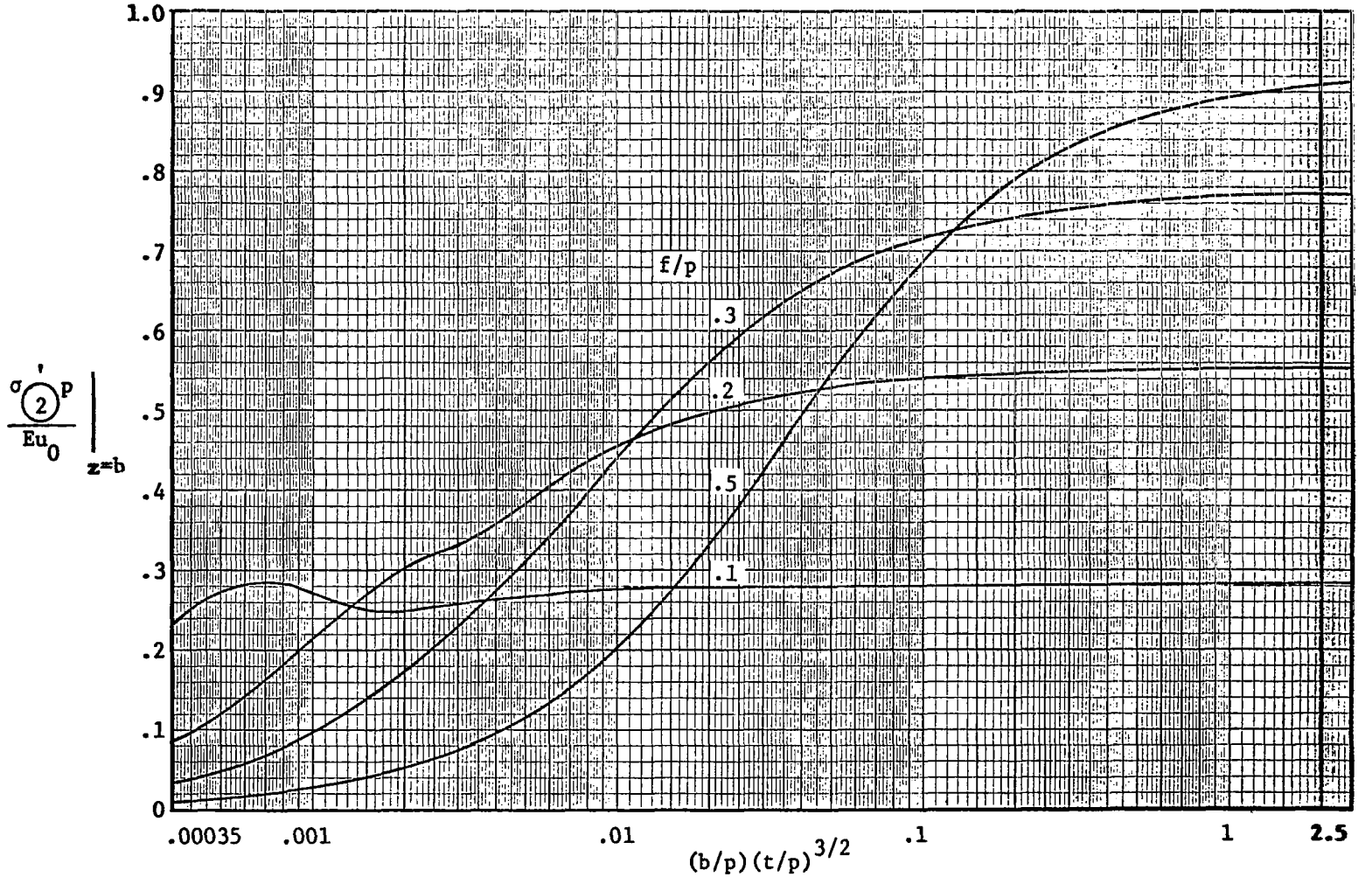

(d·I) Frame bending stress for h/p = .5

Figure 21. - Continued.

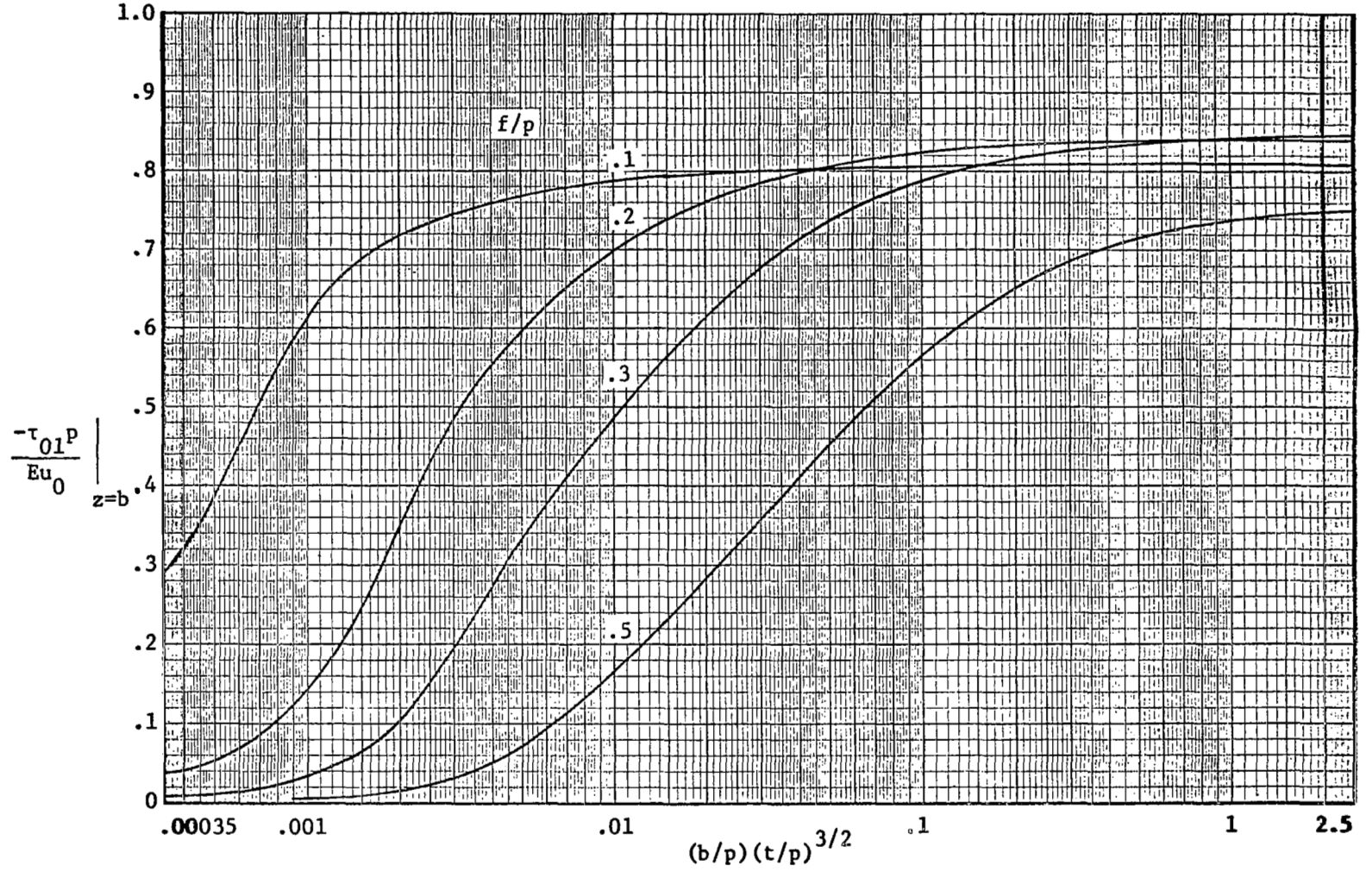

(d·II) Middle-surface shear stress for h/p = .5

Figure 21. - Continued.

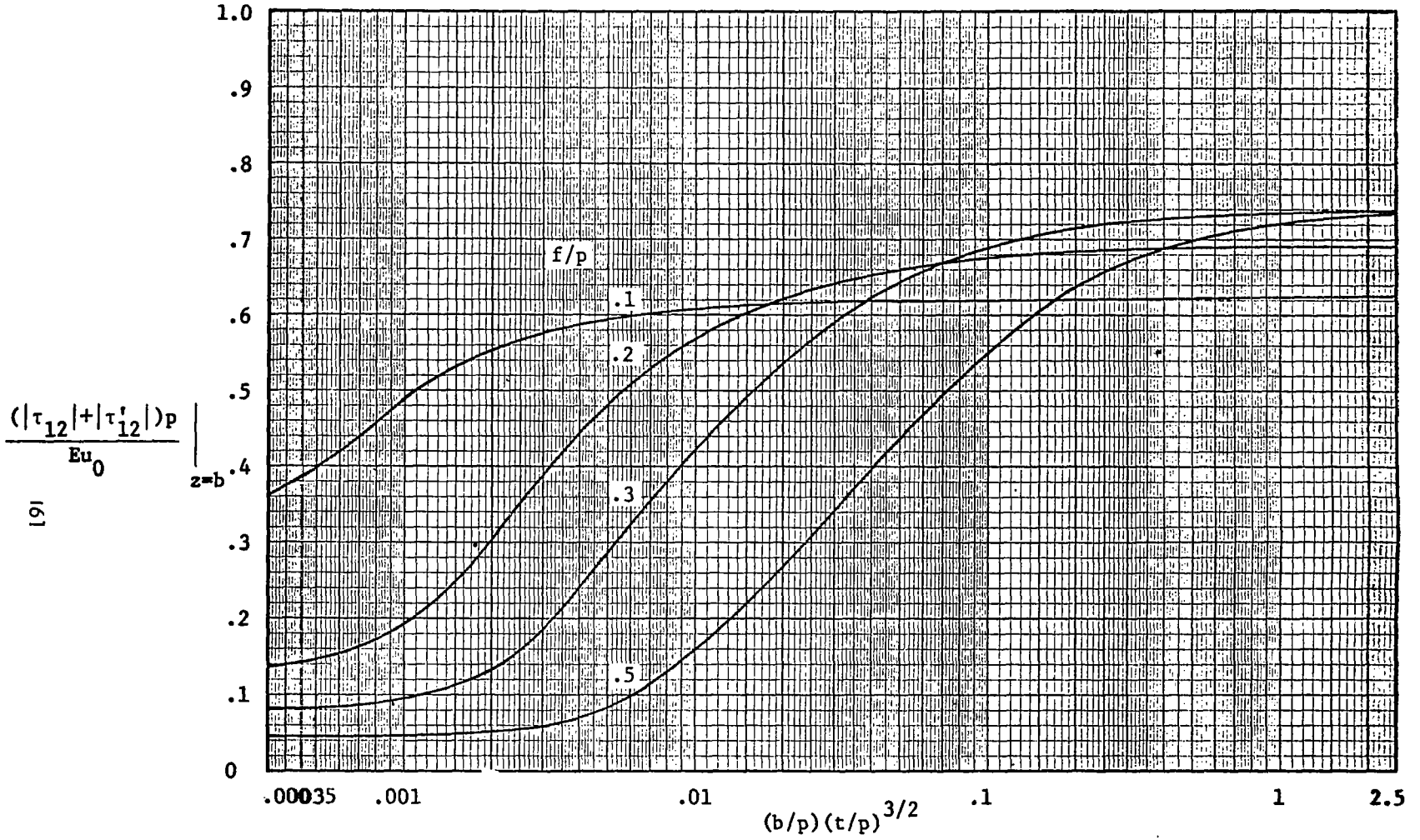

[61]

(d·III) Extreme-fiber shear stress for h/p = .5

Figure 21. - Concluded.

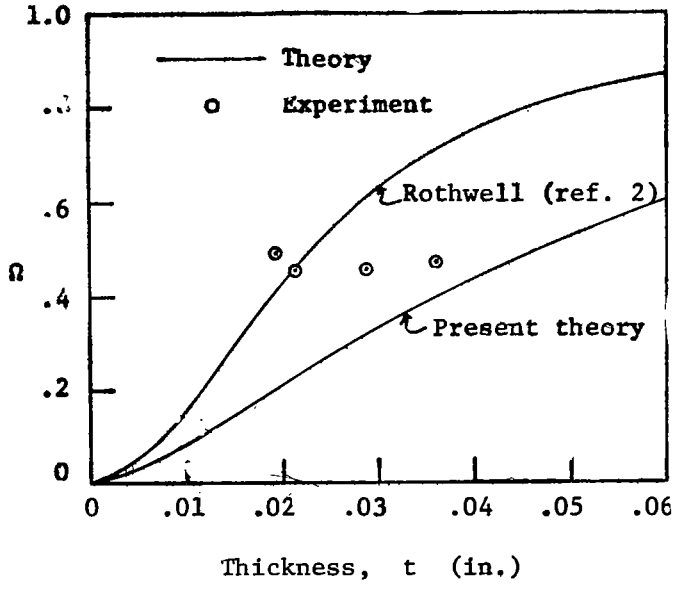

Figure 22. - Comparison of experimental data of reference 8 (as cited in ref. 2), present theory, and the theory of reference 2.